Biological Solutions to 3-Isobutyl-2-Methoxypyrazine Remediation in Wine

Jin-Chen Li

A dissertation submitted to the degree of Doctor of Philosophy

School of Agriculture, Food and Wine

Faculty of Sciences

The University of Adelaide

THE UNIVERSITY of ADELAIDE

July 2021

Table of Contents

Declaration

I certify that this work contains no material which has been accepted for the award of any other degree or diploma in my name, in any university or other tertiary institution and, to the best of my knowledge and belief, contains no material previously published or written by another person, except where due reference has been made in the text. In addition, I certify that no part of this work will, in the future, be used in a submission in my name, for any other degree or diploma in any university or other tertiary institution without the prior approval of the University of Adelaide and where applicable, any partner institution responsible for the joint-award of this degree.

The author acknowledges that copyright of published works contained within the thesis resides with the copyright holder(s) of those works.

I also give permission for the digital version of my thesis to be made available on the web, via the University's digital research repository, the Library Search and also through web search engines, unless permission has been granted by the University to restrict access for a period of time.

I acknowledge the support I have received for my research through the provision of an Australian Government Research Training Program Scholarship.

7/7/2021

Jin-Chen Li Date

Acknowledgements

First and foremost, I would like to thank my principal supervisor, Professor Vladimir Jiranek, for offering me with the PhD opportunity to work on such an interesting and challenging project, and for guiding and supporting me throughout my studies with his vast knowledge, enthusiasm and patience. I'm also extremely grateful to Vlad for his time reviewing and helping with editing my thesis.

I would also like to thank my co-supervisors, Assoc. Professor Christopher Ford and Professor Kerry Wilkinson, for providing me with their supports and expertise that broadened the scope of this project. And I sincerely appreciate their time and efforts in reviewing my thesis.

Additionally, a big thank you to my independent advisor, Dr. Paul Boss, for his valuable suggestions in experimental design, and for offering me access to the GC instruments at CSIRO for IBMP analysis. And I would also like to thank him for generously providing me with the *VvOMT3* gene which was the basis for my Chapter 4. A special mention to Sue Maffei from CSIRO, for her technical support in IBMP analysis, and especially for her kind help in doing the analysis for me during COVID-19 shutdown period.

Next, I would like to thank all of the current and past members of Wine Microbiology Group- it is such a wonderful and friendly research group to work with, from which I've obtained numerous help and valuable advice. Specifically, thank you to Nick van Holst for technical supports. And I would like to acknowledge the helps I received from other research groups and people including Dr. Renata Ristic for sensory study, Carolyn Puglisi and Xingchen Wang for GC-MS analysis, Eva Sui for SDS-PAGE and Ross Sanders for IBHP samples. Additionally, a special thank you goes to Kilikanoon winery and Mr. Andrew Todd for their generosity of providing grapes for my experiments.

I would also like to thank China Scholarship Council and the University of Adelaide for the joint scholarship, and School of Agriculture, Food and Wine for the research funding. And a special thank-you goes to the University of Adelaide for providing me with a 3-month tuition

fee waiver during my candidature extension due to COVID-19 pandemic. And thank you Vlad, Chris and Kerry for supporting and helping me with the application for extension.

A special mention to my previous and current house mates: Bo Zheng, Jiao Jiang and Xueying Feng. Thank you for being such friendly, helpful and thoughtful house mates as well as friends, and these precious memories will always be missed. Moreover, I'd like to thank my other friends, Han Wang, Hua Luo, Jin Zhang, Maddy Jiang, Wen Ben, Yiming Huo, Yingxin Liu and Zhiheng He, for hanging out and sharing delicious foods together. A big thank you to my remote best friend Jingyang Chu, for being my emotional trashcan without any complaints (might be a few though), and for supporting me unconditionally. It has been a great pleasure to get to know all of you guys.

I would like to express my most sincere appreciation to hot pots and my hot pot mates: Xueying Feng, Bo Zheng, Hua Luo, Jin Zhang and Yiming Huo. Thank you for sharing hot pot with me, and thank you, hot pot, for being such a wonderful soul food whenever I'm worried or anxious. Musical artists are respected as well, especially Mayday for creating encouraging and healing songs that acted as the best background music throughout my PhD.

Last but not least, my greatest gratitude goes to my awesome parents. Thank you for your valuable guidance and being so supportive all the time. Thank you so much, and hopefully, see you soon!

Abstract

3-Isobutyl-2-methoxypyrazine (IBMP) is a naturally occurring volatile compound with a potent aroma reminiscent of green capsicum. It occurs in a diverse range of organisms, including wine grapes. It is present at trace levels (ng/L) and contributes varietal characters and aroma complexity to grape cultivars such as Cabernet Sauvignon and Sauvignon Blanc, but can mask wine aroma bouquet and even reduce wine quality at elevated concentrations. IBMP concentrations evolve during grape development such that less IBMP is found in fully ripe grapes, whereas early harvested grapes (e.g. picked to produce lower alcohol wines) or grapes from cool climate regions may contain higher levels of IBMP, which may indicate poor quality and are undesirable. IBMP managements in grapes and wines are therefore crucial for quality improvement. Vineyard solutions have been investigated extensively and include canopy management and irrigation control. However, options for postharvest remediation are so far limited in their effectiveness and/or specificity. A solution is needed. The aim of this project is to discover/develop biological methods for remediation of undesirably high levels of IBMP in grapes or wines. Specifically, this project focused on microbiological and enzymatic approaches.

Based on the fact that little is known about the biological degradation of IBMP by any organisms or enzymes, this project took an exploratory approach to seeking potential IBMP remediation solutions. From a microbiological perspective, 11 wine-related non-*Saccharomyces* yeast strains were trialled in sequential inoculation with a commercial *Saccharomyces cerevisiae* strain (EC1118, Lallemand) in Sauvignon Blanc fermentation spiked with IBMP. According to the instrumental and sensorial analysis of the final wine, IBMP levels did not significantly alter, neither among the various yeast treatments nor during alcoholic fermentation for any single treatment. Nevertheless, sensory studies suggested otherwise, with wines fermented with several strains being evaluated as more pronounced in fruity rather than green characters. This implies a masking of IBMP characters and may prove to be a feasible approach in Sauvignon Blanc winemaking to produce wines with organoleptically less greenness. It should be acknowledged that this result is variety-dependent, and yeasts perform differently in different grape juices (likely with different aroma precursors). Therefore, more trials are required to map the complete profile of yeast and variety interactions for masking green character.

A large-scale microbial screen was performed with IBMP provided as a putative sole or key nutrient with the aim of identifying IBMP-degrading microbes. Alternative substrates with similar structures with IBMP were also used for screening due to the fact that rapid and inexpensive determination of IBMP consumption was not available to this project. Results indicated that, unfortunately, no microbes appeared able to significantly degrade IBMP under the screening conditions. Nevertheless, two fungal strains, *Rhodotorula mucilaginosa* and *Rhodotorula glutinis*, were shown to degrade one of the alternative substrates, methyl violet. Further investigation of these two strains are needed to study their metabolic abilities against other wine-related compounds.

Enzyme engineering was also explored as a potential method for enzymatic remediation. VvOMT3, the *O*-methyltransferase catalysing the synthesis of IBMP in grapes was selected as the target protein for enzyme engineering due to its presumed structural specificity for substrate binding and catalytic activity. Random mutation was applied on this enzyme with error-prone PCR in the hope that the reaction may be reversed. Heterologous expression of mutant genes in *E. coli* BL21 was achieved and crude protein extracts were used for enzymatic assay. Unfortunately, no positive mutants were obtained from random mutation process. Nevertheless, some experimental findings and computational analysis, lead to predictions of key structural features relating to enzymatic functions. This data may support vine modification or selective breeding programs to reduce synthesis of IBMP.

As part of a commencement of a new line of investigation, a review of recent literature pertaining to demethylases was completed. New strategies and candidate enzymes and organism are being considered for work that could follow on from this PhD.

While this project did not yield a definitive IBMP modulation strategy, the findings provided important fundamental knowledge, as well as guidance for future work. Opportunities to utilise novel yeasts to, at least, mask the sensory impacts of IBMP may prove to be particularly fruitful.

List of Abbreviations

16S rRNA	16S ribosomal ribonucleic acid
2-MP	2-Methoxypyrazine
AGRF	Australian Genome Research Facility
A/Ala	Alanine
cDNA	complementary DNA
COMT	*Medicago sativa* caffeic acid *O*-methyltransferase
DNA	Deoxyribonucleic acid
DTT	Dithiothreitol
EP-PCR	Error-prone polymerase chain reaction
G/Gly	Glycine
HPLC-MS	High performance liquid chromatography-mass spectrometry
HS-SPME-GC-MS	Headspace solid-phase microextraction coupled to gas chromatography-mass spectrometry
I/Ile	Isoleucine
IBMP	3-isobutyl-2-methoxypyrazine
IEP-PCR	Iterative error-prone polymerase chain reaction
IPMP	3-isopropyl-2-methoxypyrazine
ITS	Internal transcribed spacer
L/Leu	Leucine
LB medium	Luria-Bertani medium
M/Met	Methionine
MJT	Mean January temperature
MP	Methoxypyrazine
MRSAJ medium	De Man, Rogosa and Sharpe apple juice medium
MsIOMT	*Medicago sativa* isoflavone *O*-methyltransferase
$NADP^+$	Nicotinamide adenine dinucleotide phosphate
PBS	Phosphate buffered saline
PCA	Principal component regression
PCR	Polymerase chain reaction
PLS-R	Partial least squares regression
Q/Gln	Glutamine

RATA	Rate all that apply
S/Ser	Serine
*s*BMP	3-*sec*-butyl-2-methoxypyrazine
SDS-PAGE	Sodium dodecyl sulfate-polyacrylamide gel electrophoresis
SAH	S-adenosyl-L-homocysteine
SAM	S-adenosyl-L-methionine
T/Thr	Threonine
TAE	Tris acetate EDTA
Tris	Tris(hydroxymethyl)aminomethane
TSS	Total soluble solids
UV-Vis	Ultraviolet visible
V/Val	Valine
v/v	Volume per volume
VvOMT	*Vitis vinifera O*-methyltransferase
W/Trp	Tryptophan
w/v	Weight per volume
YAN	Yeast assimilable nitrogen
YPD/YEPD	Yeast extract peptone dextrose

Chapter 1 Literature Review and Thesis Outline

1 Methoxypyrazines in grapes and wine

Pyrazines are naturally occurring heterocyclic compounds containing nitrogen atoms. They are widely studied in the food industry due to their significant contributions to food quality, especially aroma and flavour (Vernin and Vernin, 1982), and are categorised into four groups by origin: heat treatment-derived, micro-organism-derived, animal-derived and plant-derived (Müller and Rappert, 2010). Pyrazines are known to form during cooking processes due to the Maillard reaction (Fors and Olofsson, 1986), and have been found in heated foods, including cocoa products, roasted peanuts, popcorn, coffee, potato chips, roasted barley, rye crisp bread, beef products, roasted pecans and roasted filberts (Maga and Sizer, 1973). Among some plants and animals, pyrazines function as chemical signals to deter attack or attract others, without being harmful or advantageous to the plant or animal (Woolfson and Rothschild, 1990). Owing to their low vapor pressure, pyrazines evaporate easily and typically have an intense smell, which can contribute greatly to food aroma and flavour.

Methoxypyrazines (MPs), as a major sub-group of pyrazines, are recognised as having distinctive vegetative or earthy smells. Generally speaking, MPs that are commonly present in food include 2-methoxypyrazine, 2-methoxy-3-methylpyrazine, 2-methoxy-3-ethylpyrazine, 2-methoxy-3-hexylpyrazine, 2-methoxy-3-isobutylpyrazine (IBMP), 2-methoxy-3-isopropylpyrazine (IPMP) and 2-methoxy-3-*sec*-butylpyrazine (*s*-BMP) (Fig. 1). Among these MPs, IBMP, IPMP and *s*-BMP have been extensively studied by wine scientists due to their distribution and aromatic contributions to wines of selected varieties. IBMP was first identified in *Capsicum annuum var. grossum* in 1969 and is responsible for the characteristic aroma of green bell pepper or capsicum (Buttery et al., 1969). Since then, researchers have revealed the common occurrence of IBMP, IPMP and *s*-BMP in the plant kingdom. Their odour descriptions and thresholds in different media (water, wine and synthetic wine) have been reported (Table 1).

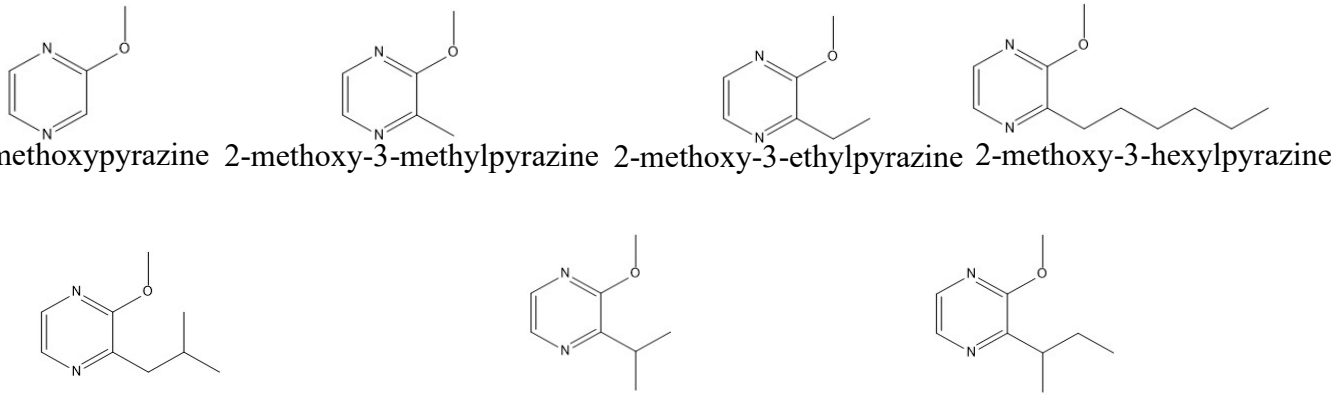

Figure 1 Chemical structures of seven common 2-methoxy-3-alkylpyrazines

The first MP identified in wine grapes was IBMP in *Vitis vinifera* L. *cv*. Cabernet Sauvignon and was described as presenting a 'green bell pepper and herbaceous' aroma, which is a varietal characteristic of Cabernet Sauvignon wine (Roujou de Boubée, 2003). Several other *V. vinifera* varieties exhibit this 'herbaceous' smell due to MPs, including Sauvignon Blanc, Cabernet Franc, Merlot and Carmenere (Augustyn and Rapp, 1982; Augustyn et al., 1982; Allen et al., 1991; 1994; Marais, 1994; Kotseridis et al., 1998; Lopez et al., 1999; Roujou de Boubée et al., 2000; Sala et al., 2002; Belancic and Agosin, 2007; Blake et al., 2009), as well as some varieties unique to Spain and Uruguay (Campo et al., 2005; Escudero, 2007). Occurring naturally, the concentrations of MPs typically decrease during grape berry development (Allen and Lacey, 1993; Hashizume and Samuta, 1999). At low levels, these highly potent aroma compounds can positively impact wine quality, but can be unpleasant and overpowering at higher concentrations, and can indicate that a wine was produced in a cool-climate region or made from grapes of sub-optimal ripeness or low quality (Lacey et al., 1991; Kotseridis et al., 1998; Chapman et al., 2004). Since intense vegetative notes are generally considered to be detrimental to wine quality, remediation of 'green' characters in grapes/wine is required to improve overall quality, and MP metabolism is therefore of particular research interest.

IBMP is the major MP in wine and is believed to impart the greatest influence on wine aroma profiles due to its occurrence at concentrations well above its sensory threshold in wine matrices (Harris et al., 1987; Maga, 1990; Allen et al., 1991; Kotseridis et al., 1998; Roujou de Boubée et al., 2000). The highest IBMP concentrations in grapes and wine ever reported were 307 ng/L and 56.3 ng/L, respectively (Sala et al., 2005). Researchers have shown that

the intensity of the varietal 'herbaceous' character in Cabernet Sauvignon wines is positively correlated with IBMP concentrations (Allen et al., 1991; Rajchl et al., 2009). Although some researchers have suggested that IPMP has a lower odour threshold and is the dominant MP in wine (Pickering et al., 2008), IPMP is generally considered as less potent than IBMP, and imparts a galbanum, earthy, green pea and/or leaf aromas (Boelens and Gemert, 1995; Seifert et al., 1970; Maga, 1990; Allen et al., 1991; 1994; Blake et al., 2009). According to the literature, IPMP can occur in grapes and wine at concentrations up to 48.7 ng/L and 4.5 ng/L, respectively (Sala et al., 2005). IPMP has been associated with vineyard pests such as the multi-coloured Asian Lady Beetle (*Harmonia axyridis*) and Seven-spot Lady Beetle (*Coccinella septempunctata*) (Pickering et al., 2008; Kögel et al., 2012). IPMP concentrations tend to increase alongside pest populations in the vineyard. (Sidhu et al., 2015; Kögel et al., 2015).

This literature review aims to discuss research related to IBMP in grapes and wine, mainly involved in the wine industry. Additionally, IBMP biosynthesis and proposed metabolism pathways in grapes and other organisms will be discussed.

Table 1 The occurrences, odour descriptors and thresholds of three major 2-methoxy-3-alkylpyrazines

MP	Occurrence	Matrix	Threshold (ng/L)	Odour description	References
2-Methoxy-3-isobutylpyrazine (IBMP)	French beans; broad beans; beetroot; lettuce; nasturtium; garden pea; green bell pepper; red or chilli pepper; potato	Water	10	Bell pepper, earthy, musty, green	Murray and Whitfield, 1975; Boelens and Gemert, 1995
		Water	2	Bell pepper, green	Murray and Whitfield, 1975; Seifert et al., 1970; Buttery et al., 1969; Parliment and Epstein, 1973
		Water	0.5	Green pepper	Kotseridis et al., 1998
		Water	16	Strongly green bell pepper like	Takken et al., 1975
		Red wine	15,10	Green bell pepper	Roujou-de-Boubée et al., 2000; Kotseridis et al., 1998
		White wine	1	Vegetative, herbaceous, grassy, green	Allen et al., 1991
		Synthetic wine	2	Musty, green pepper	Maga, 1990
2-Methoxy-3-isopropylpyrazine (IPMP)	Asparagus; French beans; broad beans; beetroot; carrot; cucumber; lettuce; nasturtium; garden pea; sweet bell pepper; red or chilli pepper; thistle, milk or cow	Water	2	Strong galbanum-like, earthy, musty, potato bin, green pepper, roasted	Boelens and Gemert, 1995; Seifert et al., 1970;
		Red wine	2	leafy	Maga, 1990
		White wine	2	Green pea; earthy	Allen et al., 1991; Blake et al., 2009
		Synthetic wine	2	Musty, earthy, leafy	Maga, 1990
3-*sec*-Butyl-2-methoxypyrazine (*s*-BMP)	French beans; broad beans; beetroot; seakale beet, chard, silver-beet; carrot; lettuce; nasturtium; parsnip; garden pea; sweet bell pepper; red or chilli pepper	Water	0.04, 2	Green (peas, bell pepper, galbanum),	Mihara and Masuda, 1988; Boelens and Gemert, 1995

2 MP biosynthesis

2.1 IBMP biosynthesis in grapes

This section reviews the discoveries and hypotheses related to MP biosynthesis patterns in grapes, and microbial species such as bacteria. The first synthesis pathway for IBMP, inspired by hydroxypyrazine synthesis (Jones, 1949), was achieved chemically using amino acids acting as the primary substrates (Buttery et al., 1969). Specifically, leucine, isoleucine and valine were identified as likely precursors to 3-isobutyl, *sec*-butyl and 3-isopropyl-2-methoxypyrazines, given their structural resemblance in the alkyl moiety (Murray and Whitfield, 1975). A biosynthesis route was initially proposed in which reactions between α-amino acids and α, β-dicarbonyl compounds to initiate the subsequent steps (a detailed description can be found in Chapter 4; Murray et al., 1970; Gallois et al., 1988). However, this scheme was later questioned, based on the fact that amides of common α-amino acids and glyoxals are rarely found in nature (Nursten and Sheen, 1974). The complete biosynthesis pathways for IBMP (in any organism) remains unknown, with the exception of some key steps that have been elucidated in wine grapes (*Vitis vinifera*), that will be introduced below.

The final step of IBMP biosynthesis in grapes has been identified, which involves the methylation of 2-hydroxy-3-isobutylpyrazine (IBHP) to produce IBMP. The enzyme involved in this step is believed to be an *O*-methyltransferases (OMT; Hashizume et al., 2001). This group of enzymes catalyse methylation, which transfers the methyl group from the donor, *S*-adenosyl-L-methionine (SAM) to the acceptor's hydroxyl group yielding methyl ester derivatives and *S*-adenosyl-*L*-homocysteine. Several *O*-methyltransferases (VvOMT1, VvOMT2, VvOMT3 and VvOMT4) were isolated from *V. vinifera* L. *cv*. Cabernet Sauvignon and shown to catalyse the methylation of 2-hydroxy-3-isopropylpyrazine (IPHP) and IBHP to IPMP and IBMP, respectively (Hashizume et al., 2001; Dunlevy et al., 2010; Dunlevy et al., 2013a; Guillaumie et al., 2013). The substrate specificity of these enzymes was also studied, and results suggested that VvOMT1 and VvOMT2 also acted on other substrates such as caffeic acid (Dunlevy et al., 2010). However, their N-terminal amino acid sequences were different from those of caffeic acid OMTs, or other stress-induced multifunctional OMTs showing strong catalytic activity for caffeic acid (Hashizume et al., 2001; Chiron et al., 2000). Compared with other VvOMTs identified, studies suggested that VvOMT3 exhibited higher specificity and greater catalytic efficiency for the methylation of

IBHP (Guillaumie et al., 2013), while both VvOMT1 and VvOMT2 showed the greatest activity against the flavonol quercetin.

Full-length cDNAs (*VvOMT1*, *VvOMT2*, *VvOMT3* and *VvOMT4*) encoding grape *O*-methyltransferases were successfully isolated from Cabernet Sauvignon and all enzymes were shown to catalyse the methylation of IBHP to IBMP and IPHP to IPMP *in vitro* (Dunlevy et al., 2010; Guillaumie et al., 2013). Enzymatic affinity and catalytic efficiency studies were performed on VvOMT1-4 with purified recombinant proteins heterologously expressed in *Escherichia coli*. Pairwise study of VvOMT1 and VvOMT2 suggested that VvOMT1 had similar affinity (K_m value) for both IBHP and IPHP, while a higher turnover number (k_{cat}) for IBHP than IPHP led to greater overall catalytic activity (k_{cat}/K_m) for IBHP. On the other hand, VvOMT2 exhibited a higher affinity but lower turnover number for IBHP than with IPHP yielding similar catalytic efficiencies for both substrates. VvOMT3 exhibited much higher catalytic activity for IBHP than any other VvOMTs (Dunlevy et al., 2013a).

Quantitative trait loci (QTL) analysis and real-time PCR of these enzymes were performed within grape varieties producing various levels of IBMP (Guillaumie et al., 2013). Results indicated that expression levels of *VvOMT3* and *VvOMT4* differed greatly between Cabernet Sauvignon, a high IBMP-producer and Petit Verdot, a low IBMP-producer, especially at the bunch closure stage, when MPs increase greatly in Cabernet Sauvignon berries. On the contrary, no significant difference in expression patterns of *VvOMT1* and *VvOMTt2* were observed between these two varieties. Therefore, it was proposed that VvOMT3 and, to a lesser extent, VvOMT4 are the key methyltransferases of IBMP biosynthesis in grapes.

Phylogenetic analysis indicated that VvOMT1 and VvOMT2 shared highest sequence identity similarity with VvOMT3 and VvOMT4, and all these OMTs belong to class II of the plant OMT family (Dunlevy et al., 2010; Dunlevy et al., 2013a); members of which show activity against flavonoids, orcinol, eugenol, chavicol, isoflavonoids and resveratrol (Christensen et al., 1998; Lavid et al., 2002; Gang et al., 2002; Akashi et al., 2003; Schmidlin et al., 2008).

The structural and functional relationship within these enzymes has also been proposed (Vallarino et al., 2011; Guillaumie et al., 2013). For example, H272 was predicted to be the catalytic residue for VvOMT1 (Zubieta et al., 2001). Furthermore, for VvOMT1 and

VvOMT2, a hydrogen bond network between H272 and substrates was needed, which can promote the transfer of a methyl group from SAM to the substrate (Vallarino et al., 2011). A modelling study suggested that the active site was formed mainly by hydrophobic interactions between the enzyme and substrates (Vallarino et al., 2011), and the greater affinity for IBHP observed in VvOMT1 was due to the higher numbers of aliphatic carbons in IBHP resulting in greater hydrophobicity (Vallarino et al., 2011). For VvOMT2, a mutation led to a less hydrophobic cavity in two crucial residues (L319 and V322) in the active site. This microenvironment resulted in an interaction between the aliphatic chains of substrates and H272, which impeded the generation of hydrogen bonds. This subsequently decreased the probability for substrates to reach the conformation required for forming the transition state (Vallarino et al., 2011). Structural comparisons of VvOMT3 and VvOMT1 revealed the similarity in the general structures of the active site (Guillaumie et al., 2013), however, the distances between the methyl group of SAM and the oxygen atom of IBHP are different. Therefore, the greater efficiency for IBHP methylation with VvOMT3 was proposed to be due to the more flexible catalytic environment.

One of the early steps involved in IBMP biosynthesis in grapes has been proposed, with L-leucine (L-Leu) and 2-amino-4-methylpentanamide (AMPA) being speculated as the key intermediates (Lei et al., 2019). These two compounds were incorporated into grapevines *in situ* before veraison, and berry samples were collected at intervals during fruit development. IBMP analysis suggested that both L-leu and AMPA treatment groups showed significantly higher levels of IBMP than control groups at each sampling time during berry development. Expression levels of *VvOMT1*, *3* and *4* were also investigated, but no significant differences between treatments and controls were observed in pre-veraison samples. However, post-veraison samples indicated otherwise; *VvOMT3* was the only gene that showed a significant increase in expression levels in treatment groups compared to controls, whereas the patterns for *VvOMT1* were not consistent in the two treatments. Additionally, the expression levels for *VvOMT4* were significantly lower when compared to the controls. This study, though preliminary, provided a possible insight into further study on IBMP biosynthesis pathway in *V. vinifera*.

Several investigations into IBMP biosynthesis in grapes have been undertaken. Hashizume (1997) and Roujou de Boubée (2003) proposed that IBMP is synthesised in grapevine leaves and berries. Roujou de Boubée suggested that some IBMP is transported via phloem from

leaves to berries, rather than being synthesised *in situ*, based on a study into the distribution of deuterated IBMP (3-isobutyl-2($^2H_3$)- methoxypyrazine) observed after application to leaves as an aqueous solution. However, Koch et al. (2009; 2010) argued that leaves and berries synthesise IBMP separately, and that synthesis was genotype-dependent, according to results from a grafting experiment, whereby a high IBMP-producing variety (Cabernet Sauvignon) and a non-IBMP-producing variety (Muscat blanc; syn, Moscato bianco, Muscat de Frontignan) were grafted onto each other. More recently, Dunlevy et al. (2013b) investigated the location of biosynthesis within a single berry by measuring the amounts of IBMP in different parts in a berry, as well as the expression level of *VvOMT3*. The greatest abundance of IBMP was in berry pulp during pre-véraison developmental stages, in accordance with the peak expression level of *VvOMT3*. Nevertheless, berry skin contributed the most to IBMP accumulation during berry development, which may suggest that IBMP is synthesised in the pulp before being diffused or transported into the skin.

In the grafting study (Koch et al., 2010) involving Cabernet Sauvignon, a high IBMP-producer, and Muscat Blanc vines, a low IBMP-producer, the IBMP concentration of berries was determined after the shoot bearing fruit was replaced (above the bunch position) via grafting of a shoot of the other variety. The approach grafting occurred prior to anthesis and sampling of berries occurred at harvest. IBMP was detected in Cabernet Sauvignon berries irrespective of the shoot variety, indicating the IBMP was grape-derived, and depended on the fruit genotype; i.e. IBMP was synthesised locally and not translocated from shoots.

2.2 MP biosynthesis in micro-organisms

Microbial production of MPs has also been investigated (Table 2). Among them, *Pseudomonas* sp. and *Pseudomonas taetrolens* were shown to produce IPMP (MillerIII et al., 1973; Gallois et al., 1988; Gallois and Grimont, 1985), with a synthetic pathway postulated (Fig. 3). However, little is known about the enzymes responsible for MP biosynthesis thus far.

Table 2 Major pyrazines and their respective producing micro-organisms

Pyrazine	Microbial Species	References
3-Isopropyl-2-methoxypyrazine (IPMP)	*Pseudomonas perolens*	Cheng et al., 1991
3-sec-Butyl-2-methoxypyrazine (*s*-BMP)		
3-Isopropyl-2-methoxy-5-methylpyrazine	*Serratia oderifera*	Gallois and Grimont,
3-Isopropyl-2-methoxy-methylpyrazine	*Serratia ficaria*	1985
3-Isobutyl-2-methoxypyrazine	*Serratia rubidea*	
3-sec-Butyl-2-methoxy-5-methylpyrazine	*Cedaceae davisae*	

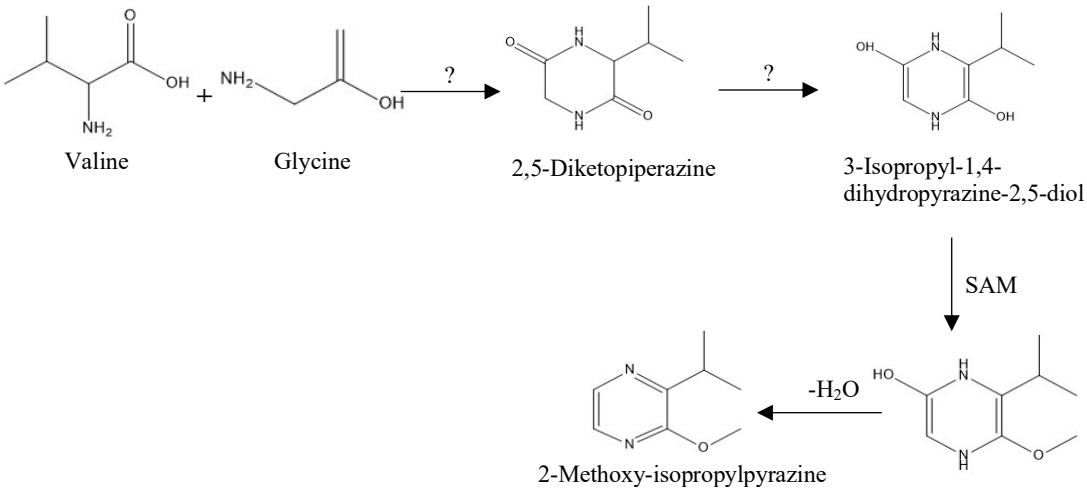

Figure 3 Putative biosynthesis pathway of IPMP from leucine by *Pseudomonas perolens* (Cheng et al., 1991; Rajini et al., 2011). Abbreviations: SAM, S-adenosyl methionine; ?, reaction mechanisms not determined.

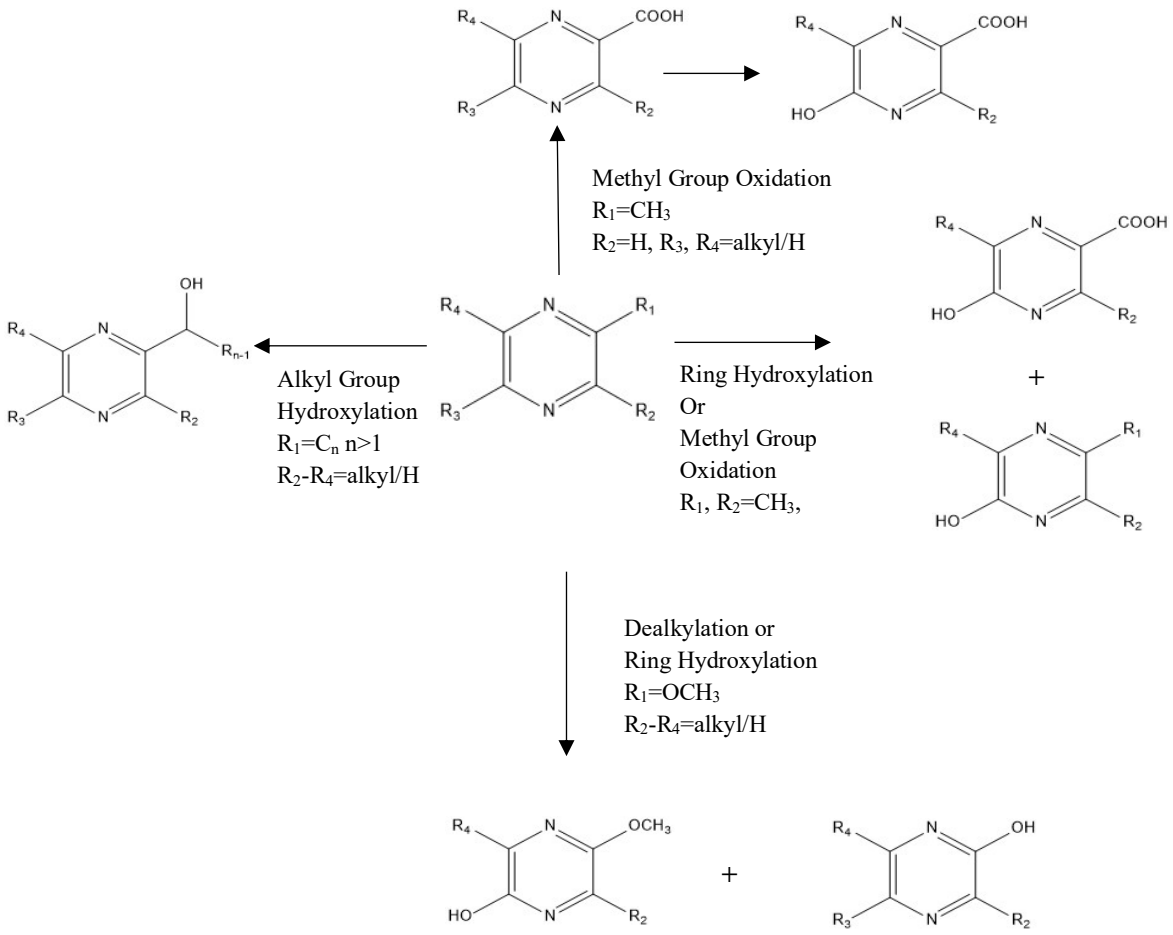

Figure 4 Proposed metabolic pathways for pyrazine derivatives (Adapted from Adams et al., 2002)

2.3 Pyrazine degradation

No information is currently available for MP degradation mechanisms in either grapes or microbes. However, degradation patterns for other pyrazines with similar chemical structures are discussed below, acting as a reference for studying MP degradation.

2.3.1 Pyrazine metabolism in animals

Researchers have identified two fundamental reaction patterns for pyrazine conversion in animals. The first involves the oxidation of the alkyl group by a Cytochrome P450 (CYP450) type enzyme yielding a carboxylic acid or alcohol, while the other involves ring hydroxylation by molybdenum-containing oxidases (Hawksworth and Scheline, 1975; Yamamoto et al., 1987; Whitehouse et al., 1987). The resulting carboxylic acids, alcohols and hydroxylated pyrazines can be excreted directly or as conjugates with glutathione or

glucuronic acid via the kidneys (Adams et al., 2002). Metabolic pathways for major pyrazines have therefore been proposed (Fig. 4).

Pyrazines with a ring-activating alkoxy side chain are proposed to be subject to nucleophilic attack by molybdenum-containing hydroxylases (Beedham, 1988), and are thus hydroxylated, with the methoxy-group being *O*-demethylated. According to rat-feeding experiments and metabolite analysis of the urine (Hawksworth and Scheline, 1975), 75% of 2-methoxypyrazine was ring hydroxylated, and 20% was *O*-demethylated. These results indicated that either the liver enzyme systems or the gastrointestinal microflora of rats were responsible for the hydroxylation and demethylation reactions, which can be further studied.

Pyrazines with a methyl side chain tend to be oxidised giving pyrazine-2-carboxylic acids. In Hawksworth and Scheline's experiment (1975), 89% of 2-methylpyrazine, 2,5-dimethylpyrazine or 2,6-dimethylpyrazine, underwent oxidation to produce pyrazine-2-carboxylic acid derivatives (Hawksworth and Scheline, 1975). Additionally, it was also found that the side chain of methylpyrazine derivatives could be oxidised to form the respective alcohols (Wallin et al., 1989; Knize et al., 1989; Sjödin et al., 1989; Turesky et al., 1988).

2.3.2 Pyrazine degradation in micro-organisms

The structural resemblance of pyrazines and methoxylated aromatic compounds with MPs makes it worthwhile reviewing the metabolism of these compounds to shed light on the possible degradation of IBMP. This information is discussed in detail in Chapter 2 and Section 1.2 of Chapter 3.

3 Studies on potential IBMP remediation in the wine industry

Compared to the studies concerning IBMP metabolism, significantly more studies have been carried out to investigate the potential for viticultural practices to be used as IBMP management strategies.

The location of IBMP in Cabernet Sauvignon bunches during berry development was determined (in ng/kg fresh material) and indicated that within grape bunches, IBMP is most abundant in rachis/stems (53.4%), followed by skins (31%) and seeds (15%), whereas pulp contains the least IBMP (0.6%) (Roujou de Boubée et al., 2002). These findings were in accordance with the results from a study which demonstrated that green characters could be

greatly diminished by destemming fruit (Roujou de Boubée et al., 2002). Distribution of IBMP within a grape bunch changes during fruit development. Specifically, the proportion found in grape skins increases from pre-véraison to harvest, whereas concentrations decrease in other grape bunch tissues (Roujou de Boubée et al., 2002).

The influence of environmental factors on IBMP levels in grapes has been thoroughly studied and various parameters were shown to impact IBMP concentration during berry development. Temperature is widely acknowledged to affect IBMP levels, and fruits from cooler regions generally show more intense green characters due to higher concentrations of IBMP (Heymann and Noble, 1987; Allen and Lacey, 1993). Seasonal variation as well as spring temperature were found to impact IBMP levels (Mendez-Costabel et al., 2013). Humidity and soil type have also been investigated and increased humidity pre-véraison can lead to high IBMP levels (Roujou de Boubée et al., 2000). Specifically, impacts of winter rainfall were investigated which suggested that less humidity in winter could yield less IBMP in ripened grapes (Mendez-Costabel et al., 2014). Additionally, nutrient-rich clay soils with high water-holding capacity can lead to high levels of IBMP as well (Roujou de Boubée et al., 2000). A study on vine nitrogen status revealed no significant effect of nitrogen nutrition on both IBMP level and the expression profiles of *VvOMT3* and *VvOMT4* (Helwi et al., 2015).

Sunlight, as one of the vital components for plant life, has also been studied as a factor affecting IBMP levels in grapes (Hashizume and Samuta, 1999). Berries were sampled 30, 50 and 70 days after anthesis and were exposed to artificial fluorescent light directly, with and without first being soaked in a saturated $CaCl_2$ solution to inhibit enzymatic reactions. Results suggested that IBMP (ng/kg) increased in samples collected at 30 days and 50 days post-anthesis but decreased in samples collected 70 days post-anthesis, which corresponded with véraison. In control samples, which did not receive any light exposure, decreases in IBMP concentrations were observed. The IBMP levels in light-treated berries that were pre-treated with $CaCl_2$ decreased exponentially compared to control samples, irrespective of sampling time. The authors hypothesised that light exposure influenced IBMP concentrations in grapes in opposing ways, depending on the stage of berry growth. Specifically, IBMP synthesis was favoured during berry developmental stages, whereas photodecomposition occurred in ripening fruits. However, further *in vivo* studies are required to confirm these results. Other light-related research mainly focused on the effects of sunlight exposure during grape development on IBMP concentrations in grapes and wine. Several studies conducted in

different regions around the world have suggested that increased sunlight exposure leads to reduced IBMP accumulation at pre-véraison stages (Noble et al., 1995; Marais et al., 1999; Sala et al., 2004). On the other hand, one study found no correlation between increased sunlight exposure and IBMP degradation post-véraison (Ryona et al., 2008). Taken through to a wine outcome suggested that while increased sunlight exposure did not significantly influence IBMP levels in grapes during ripening, grapes that received less light exposure contained lower levels of IBMP during maceration (Koch et al., 2012).

Given the large numbers of studies with conflicting results, genetic explanations were required. Dunlevy and colleagues (2013b) explored how sunlight exposure and crop level affect IBMP levels in grapes. Results suggested that greater sunlight exposure led to reduced expression levels of *VvOMT3* and therefore lower concentrations of IBHP, both of which resulted in less IBMP in ripened fruits. In contrast, reduced crop levels did not significantly influence either IBHP concentrations or *VvOMT3* expression, despite a significant increase in IBMP concentrations, which might be explained by differences in berry size.

Studies concerning IBMP remediation via post-harvest practices are fairly limited and tend to focus on amelioration using adsorption. Pickering and colleagues (2006) evaluated the IPMP remediation efficacy of several adsorption agents including activated charcoal, bentonite, oak chips and deodorised oak chips, as well as light exposure (both ultraviolet and visible) in wine. Significantly lower concentrations of IPMP were observed following treatment of white wine with activated charcoal and red wine with deodorised oak chips, and the intensity of IPMP-related sensory attributes was diminished in wine treated with oak chips (Pickering et al., 2006). Nevertheless, further investigations into the effects of adsorbents on wine chemical and sensory properties are required. The addition of other adsorbents including silicone, polyethylene-based polymers, polypropylene-based polymers, polylactic acid-based polymers have also been evaluated during red, white and rosé wine making (Ryona et al., 2012; Pickering et al., 2014; Botezatu et al., 2016). Removal of MPs to varying degrees was observed under different winemaking conditions. However, the selectivity of adsorbents is worth future research. In comparison, a putative imprinted magnetic polymer (PIMP) was trialled for use during red winemaking (Liang et al., 2018) with a polylactic acid-based film as control. IBMP removal was observed for wine used with PIMP, with no apparent negative impact on overall aroma, which suggests this approach as a potential post-harvest remediation strategy for the wine industry.

4 Thesis outline

Despite the progress mentioned above in potential IBMP amelioration methods, remediation strategies are still needed. Based on this literature review, highly specific remediation options (i.e., biological remediation) are not available, and therefore the major research gap is summarised as the absence of any IBMP-degrading microbes or enzymes that can be utilised by winemakers for this purpose.

Hence, the research described in this thesis aims to discover/develop biological methods for remediation of undesirable IBMP in grapes and wines, mainly focused on microbiological and enzymatic approaches. Strategies and potential enzymes and microbes are discussed and considered for work in this project as well as any follow-up research. Based on the fact that little is known on the biological degradation of IBMP, this research was therefore initiated by an exploratory experiment, in which effects of different non-*Saccharomyces* yeast strains on IBMP levels during fermentation were investigated (Chapter 2). Both chemical and sensorial analysis on wine yielded from different yeast treatments were included, aiming for a more comprehensive evaluation. To further explore the potential IBMP-degrading microbes, a large-scale microbial screen was performed with IBMP acted as a putative sole or key nutrient (Chapter 3). Compounds with similar chemical structures with IBMP were used as alternative substrates for higher screening efficiency. On the other hand, enzymatic remediation was also included for investigation in this research (Chapter 4). VvOMT3 was selected as the target enzyme for protein engineering in the hope that this reaction may be reversed. Random mutagenesis was performed followed by activity screening with mutants heterologously expressed in *E. coli*. Ultimately, given the mild success of work until this point, options for a new approach based on potential microbial demethylases was explored through a review on these enzymes and their biotechnological application (Chapter 5).

In summary, this research aims to define a potential biological approach to degrade/remediate undesirably high levels of IBMP in grapes and wine. The findings obtained from this research can potentially provide important fundamental knowledge and guidance for future work.

Chapter 2 Paper manuscript

Effects of Non-*Saccharomyces* Yeast Strains on IBMP Levels and Aroma Properties in Sauvignon Blanc Wines during Fermentation

Jin-Chen Li, Kerry L. Wilkinson, Christopher M. Ford, Vladimir Jiranek*

School of Agriculture, Food and Wine, Waite Campus, The University of Adelaide, PMB 1, Glen Osmond, South Australia 5064, Australia
* Corresponding author. E-mail address: vladimir.jiranek@adelaide.edu.au

Abstract

3-Isobutyl-2-methoxypyrazine (IBMP), is a grape-derived aroma compound reminiscent of green capsicum and is found in many wine grape varieties such as Cabernet Sauvignon and Sauvignon Blanc. High levels in grapes can lead to excessive greenness in final wine products thus reducing quality. A fermentation trial with 11 non-*Saccharomyces* yeast strains was conducted in this study as a potential post-harvest remediation strategy. Wines fermented with *Kazachstania servazzii, Metschnikowia pulcherrima, K. aerobia, Hanseniaspora uvarum, Meyerozyma guillermondii* and *Candida krusei* were rated with higher levels of fruitiness and less greenness in the sensory study, though no significant differences were observed among yeast treatments for IBMP concentrations. A masking effect is therefore proposed, and usage of these strains may prove to be a feasible approach for Sauvignon Blanc winemaking to mitigate the perception of greenness.

Key words

Fermentation, non-*Saccharomyces*, *Saccharomyces cerevisiae*, sequential inoculation, IBMP, aroma matrix, GC-MS, aroma masking effect

Statement of Authorship

Title of Paper	Effects of non-*Saccharomyces* yeast strains on IBMP levels and aroma properties in Sauvignon Blanc wines during fermentation
Publication Status	☐ Published ☐ Accepted for Publication ☐ Submitted for Publication ☒ Unpublished and Unsubmitted work written in manuscript style
Publication Details	

Principal Author

Name of Principal Author (Candidate)	Jin-Chen Li
Contribution to the Paper	Conception of ideas for the experiment, conduction of the experiment, manuscript preparation and editing.
Overall percentage (%)	80%
Certification:	This paper reports on original research I conducted during the period of my Higher Degree by Research candidature and is not subject to any obligations or contractual agreements with a third party that would constrain its inclusion in this thesis. I am the primary author of this paper.
Signature	Date 15/2/2021

Co-Author Contributions

By signing the Statement of Authorship, each author certifies that:

i. the candidate's stated contribution to the publication is accurate (as detailed above);

ii. permission is granted for the candidate in include the publication in the thesis; and

iii. the sum of all co-author contributions is equal to 100% less the candidate's stated contribution.

Name of Co-Author	Kerry L. Wilkinson
Contribution to the Paper	Conception of ideas for the experiment, supervision of the research, and manuscript editing.
Signature	Date 15/2/2021

Name of Co-Author	Christopher M. Ford
Contribution to the Paper	Conception of ideas for the experiment, supervision of the research and manuscript editing.
Signature	Date 15-Feb-21

Name of Co-Author	Vladimir Jiranek		
Contribution to the Paper	Conception of ideas for the experiment, supervision of the research, manuscript editing, and acted as corresponding author.		
Signature		Date	15.2.21

1 Introduction

Winemaking, specifically, grape juice fermentation, is a complicated biochemical process involving the conversion of sugar to alcohol and the production of various secondary metabolites, in which wine yeast play significant roles and are one of the key factors determining wine quality and style. Specifically, they are responsible for generating yeast-derived volatiles recognised as secondary aromas, which either enhance aroma complexity and add distinctiveness to certain types of wine or else impart undesired aromas and flavours. The first property is well researched and extensively applied in winemaking in order to bring out the full potential of various grape varieties. Many of the enzymatic mechanisms (both desirable and undesirable) have been elucidated, and this knowledge has been used in the exploration for potentially useful yeasts (i.e., β-glucosidase, *Hanseniaspora uvarum*; Mateo and Di Stefano, 1997), including those that do not produce undesirable compounds or in fact eliminate them (e.g. pectinase, *Metschnikowia pulcherrima*; Fernández et al., 2000). 3-Isobutyl-2-methoxypyrazine (IBMP), a potent aroma compound present naturally in wine grapes, can be undesirable at high levels, thereby requiring remediation, ideally with a high degree of specificity. Amelioration of high concentrations of IBMP has been mostly achieved through viticultural practices (Noble et al., 1995; Marais et al., 1994; Sala et al., 2004). In comparison, the available oenological methods are limited and non-specific (Ryona et al., 2012; Pickering et al., 2006; 2014; Botezatu et al., 2016). Wine yeasts, as a dominant factor determining wine quality, as well as harbouring diverse enzymes with versatile metabolic activities, that could potentially contribute to IBMP remediation. Yet little research has been undertaken to investigate the potential impacts of various species of wine yeasts on IBMP levels and the resultant sensory profiles, so this remains worthy of investigation.

The work of Louis Pasteur revealed *Saccharomyces cerevisiae* as the basis for the mysterious bioconversion of grape juice to wine and led to the wide recognition of this as the primary wine yeast. Apart from the basic job of producing alcohol from sugar, *S. cerevisiae* has been thoroughly studied in terms of its ecology, physiology, biochemistry and molecular biology and how these are involved in wine production to influence wine chemistry and sensory properties (Ribéreau-Gayon et al, 2006; Pretorius et al., 1999; Fleet 2003).
However, it has gradually been acknowledged that fermenting grape must contains a mixture of yeast species and that ‘wild’ non-*Saccharomyces* yeasts and their impacts are typically numerous. For a long time, most non-*Saccharomyces* present in wine production were

referred to as spoilage yeasts as they were often isolated from spoiled wines (van der Walt and van Kerken, 1959; Rankine, 1972). Even though there were some early reports on the positive aspects of these yeasts due to their production of quality-enhancing metabolites during fermentation, negative influences such as high volatile acid production were noted more often (Jolly et al., 2014).

In contrast, spontaneous fermentations which are ferments conducted by mixed cultures of yeasts undergoing sequential dominance, have long been recognised for the crucial part indigenous yeasts play in bringing out the desired characteristics unique to a region (Comitini et al., 2017). Though exposed to a higher risk of spoilage, wines made in such manner are generally reported to have improved quality such as better flavour integration and more complexity (Heard and Fleet, 1985; Gil et al., 1996; Lema et al., 1996; Soden et al., 2000; Varela et al., 2009; Izquierdo Canas et al., 2011). This has led to a re-evaluation of the roles of non-*Saccharomyces* during fermentation, with selected strains being used to impart positive effects on wine quality. Beyond the contribution from non-*Saccharomyces* yeasts to improved aroma and flavour complexity, some yeast species have shown abilities to address some modern winemaking issues such as excessive ethanol yields (Ciani et al., 2016).

Deliberate inoculation of non-*Saccharomyces* strains during fermentation has been reported for species including *Torulaspora*, *Metschnikowia*, *Hanseniaspora*, *Lachancea*, *Pichia* and *Candida* (Jolly et al., 2013). *S. cerevisiae* is normally used to complete the alcoholic fermentation, as very few of the non-*Saccharomyces* ferment well, and most typically cannot finish fermentation. Therefore, the common practice of sequential inoculation is used, whereby one or more non-*Saccharomyces* strains are inoculated into the musts to initiate the fermentation, with durations of different fermentation periods (ranging from one hour to 15 days) are allowed before *S. cerevisiae* is inoculated to complete the fermentation (Ciani and Ferraro, 1998; Ferraro et al., 2000; Jolly et al., 2003).

1.1 Improvement of wine aroma and flavour profile with non-*Saccharomyces*

1.1.1 *Metschnikowia pulcherrima*

Metschnikowia pulcherrima, was one of the first released commercial non-*Saacharomyces* yeast and it offers enzyme activities during fermentation that help enhance certain varietal aromas. The commercial strain is reported to influence varietal aroma through an α-L-

arabinofuranosidase release of terpenes, as well as to enhance formation of volatile thiols when used in sequential inoculation (Lallemand, 2014). Moreover, some strains are reported to produce high levels of esters that could contribute aroma complexity to wine (Clemente-Jimenez et al., 2004; Rodriguez, et al., 2010; Sadoudi et al., 2012). Wines, especially white varieties such as Sauvignon Blanc and Chenin Blanc, when made using sequential inoculation with these species, are generally awarded higher quality scores because they exhibit more intense aromas and flavours than control wines (made with *S. cerevisiae* only) (Jolly et al., 2003; Parapouli et al., 2010; Rodriguez, et al., 2010). However, opposing results were observed where a Chardonnay wine made with a *M. pulcherrima* strain and *S. cerevisiae* using sequential inoculation manner was rated as inferior to the corresponding control (Jolly et al., 2003), suggesting that the performance of this species may be variety/juice/strain dependent.

1.1.2 *Lachancea thermotolerans*

Lachancea thermotolerans, formerly known as *Kluyveromyces thermotolerans* (Kurtzman, 2003), is known to produce L-lactic acid during alcoholic fermentation (Jolly et al., 2014). The metabolic pathway for conversion of sugar to L-lactic acid, though not completely understood, suggests a possible reduction to alcohol yield in final wines, with up to a 1% (v/v) of decrease in alcohol content being reported (Gobbi et al., 2013). Increased concentrations of glycerol and 2-phenylethanol, and decreased levels of volatile acidity during mixed fermentation, which are desirable, were also observed (Kapsopoulou et al., 2006; Comitini et al., 2011; Gobbi et al., 2013). It has been proposed that the timing of inoculation with *S. cerevisiae* played a crucial role in determining the effect of *L. thermotolerans* on wine composition, and thus wine flavours and structure (Kapsopoulou et al., 2006; Gobbi et al., 2013; Hranilovic et al., 2021).

1.1.3 *Hanseniaspora* species

Among *Hanseniaspora* species, *H. uvarum* is the most abundant non-*Saccharomyces* yeast found in grape must (Jolly et al., 2014), thus theoretically being the major contributor among non-*Saccharomyces* yeasts to wine quality. However, this genus is proposed to be a double-edged sword when it comes to impacting wine quality. For example, *H. guilliermondii* was complimented for being a strong producer of 2-phenylethyl acetate which is associated with ‘fruity’, ‘flowery’ and ‘rosy’ notes in monoculture wines (Rojas et al., 2003; Lambrechts and Pretorius, 2000), but it can also produce aromas perceived as unpleasant in mixed

fermentations with *S. cerevisiae*, including 3- (ethylthio)-1-propanol ('rancid' and 'sweaty'), trans-2-methyltetrahydrothiophen-3-ol ('onion' and 'chive-garlic') and other odorous sulfur compounds (Moreira et al., 2008, 2010).

H. uvarum, is reported to show an increased production of desirable compounds including higher alcohols, ethyl esters and medium-chain fatty acids in mixed fermentations with *S. cerevisiae*, but also produces acetic acid at well above admissible levels (Andorra et al., 2010). In another mixed fermentation trial, co-fermentation of *H.uvarum* and *S. cerevisiae* produced lower levels of methional and 2-(methylthio)ethanol and 2-methyltetrahydrothiophen-3-one, which are undesirable heavy sulfur compounds presenting off-odours not produced in the *S. cerevisiae* monoculture (Moreira et al., 2008).

1.1.4 *Candida stellata*

Candida stellata is famous for producing high levels of glycerol in wine, i.e. concentrations up to 15.9 g/L compared to levels at 4-6.3 g/L for *S. cerevisiae* (Radler and Schütz, 1982; Ciani and Ferraro, 1998), which is favourable given glycerol is considered sweet at concentrations above 5.2 g/L in white wine and to contribute to wine body and complexity at higher levels (Noble and Bursick, 1984; Scanes et al., 1998). Another notable advantage of *C. stellata* is that it is fructophilic, thereby shortening fermentation times when co-fermenting with glucophilic *S. cerevisiae*, which sometimes become stuck due to high residual fructose contents (Magyar and Tóth, 2011). The effects of this species on wine flavour and aroma profiles are variety/strain-dependent and difficult to predict. Mixed fermentation with *S. cerevisiae* in Sauvignon Blanc exhibited significantly higher levels of terpenols (Sadoudi et al., 2012), yet both co-inoculation and sequential inoculation in Chardonnay produced wines with lower intensities for 'desirable' characters and higher intensities for 'undesirable' attributes (Soden et al., 2000). Similar results were obtained by others (Jolly et al., 2003) in Chardonnay wines produced with sequential inoculation of *C. stellate* and *S. cerevisiae*. These wines were judged to be of lower quality than control *S. cerevisiae* wines, even though higher concentrations of total esters were produced in the mixed fermentation.

1.1.5 *Torulaspora delbrueckii*

This commercially available non-*Saccharomyces* yeast was formerly used to ferment musts with low levels of sugar and acid (Castelli, 1955). However, subsequent research with pure cultures revealed its ability to produce lower levels of volatile acids than *S. cerevisiae* and

thus its suitability for use with botrytised grapes or musts with high sugar contents (Moreno et al., 1991; Bely et al., 2008; Renault et al., 2009). A specific strain was reported to produce linalool, a volatile monoterpene alcohol that adds varietal aromatic character to Muscat varieties (King and Dickinson, 2000). Sensory studies confirmed the higher quality of wines fermented with *T. delbrueckii* compared to traditional *S. cerevisiae* monoculture. Specifically, sequential inoculation with *T. delbruckii* and *S. cerevisiae* in Amarone wines produced increased aroma intensity, increased sweetness and astringency, and decreased vegetal attributes (Azzolini et al., 2012). Unfortunately, this research did not quantitatively dissect the vegetal character, which might be worth further investigation.

1.1.6 *Wickerhamomyces anomalus*

Though frequently associated with over-production of ethyl acetate, which could be a drawback for use in fermentation, *Wickerhamomyces anomalus* is recognised for its importance in exhibiting enzymatic activities and physiological characteristics potentially useful to winemaking (Padilla et al., 2018). Details will be introduced in following sections.

1.2 Enzymatic activities of non-*Saccharomyces* yeasts of potential value in winemaking

Enzymes are helpful in winemaking to improve the fermentation process, enhance wine quality and address problems such as wine haze (Jolly et al., 2014). Most commercially available preparations are derived from bacteria, filamentous fungi, and less defined microbial blends. Non-*Saccharomyces* yeasts, while being fermentation performers, are also recognised as an enormous library of enzymatic activities with the possibility that their metabolic heterogeneity offers the potential to both optimise and innovate fermentation processes. It is therefore important to ascertain the potential of wine yeasts for extracellular enzymes of oenological interest, in order to specifically choose desired enzymatic activities to enhance wine quality. Of the many potential enzymes relevant to winemaking, some are already being studied extensively, such as polygalacturonases, proteases, cellulases, glycosidases and lyases and examples of their opportunities are discussed below.

1.2.1 Juice and wine clarification

Pectinolytic enzymes (mainly polygalacturonases) are polysaccharidases able to degrade pectin, which is a group of complex structural polysaccharides mainly present in the middle lamella and primary cell wall of higher plants (Blanco et al., 1999). Pectinases are widely adapted in wine production to help break down the grape tissues and thus improve juice yield,

colour and flavour extraction and clarification (Fleet, 2008). Pectinases are produced by bacteria and filamentous fungi mainly for phytopathogenic purposes and are sources for producing commercial pectinase preparations. However, some undesirable enzyme contaminants, for instance pectinesterases, can negatively influence wine quality (Alimardani-Theuil et al., 2011). As a preferred pectinase source, wine yeasts have been studied extensively with many exhibiting polygalacturonase activity. Species showing promise include *M. pulcherrima*, *L. thermotolerans*, *W. anomalus*, *C. stellata*, *S. cerevisiae*, *Aureobasidium pullulans*, *Rhodotorula dairenensis* and *Cryptococcus saitoi* (Fernández et al., 2000; Fernández-González et al., 2004; Merín et al., 2015). A selected strain of *R. dairenensis* has been reported to perform satisfactorily in wine-like environments, be resistant to SO_2 (to 120 mg/L) and ethanol (to 15% v/v), making it an ideal candidate for pectinolytic yeast selection (Merín et al., 2015).

Protein, another component contributing to turbidity, can be problematic in finished white wines. The removal of protein is traditionally achieved by the addition of fining agents such as bentonite. However, due to the lack of selectivity, use of bentonite can adversely affect wine aroma and flavour profiles, thus making protease a potentially better solution. A wide selection of yeasts exhibit protease activity, including *Rhodotorula sp*., *Aureobasidium pullulans*, *Rhodosporidium toruloides*, *Metschnikowia sp*., *W. anomalus*, *Hansensiaspora sp*., whereas no activity was detected for several strains of *S. cerevisiae* (Chomsri, 2008; Belda et al., 2016).

1.2.2 Wine aroma enhancement

Non-*Saccharomyces* yeasts have long been regarded as a useful tool for enhancing varietal aroma profiles, in which most of the characteristic aroma compounds are found as odourless conjugated precursors in certain grape varieties (Tominaga et al., 1998). Terpenes and volatiles such as cyclic and straight-chain alcohols are present at trace levels in their free forms or bound to sugar molecules to form odourless, stable glycosidic complexes in grapes (Baumes., 2009). Similarly, volatile thiols are almost undetectable in grapes where they are present as cysteine-bound conjugates, only being released during the alcoholic fermentation. Later research revealed the releasing mechanisms of these conjugated precursors, namely, hydrolytic activities from glycosidases and C-S lyases, to free terpenes and thiols, respectively (Tominaga et al., 1995; Mateo and Di Stefano, 1997).

Among glycosidases, β-glucosidase is the most thoroughly studied, with many yeasts including *S. cerevisiae*, *Hanseniaspora spp*., *Torulaspora delbrueckii* and *Wickerhamomyces anomalus* reported to exhibit such activity (Mateo and Di Stefano, 1997; Mateo et al., 2010). Some strains of *H. uvarum* produce a β-glucosidase with relatively stable activity at a wide range of pH values (Belda et al., 2016). Additionally, the highest β-glucosidase activity was observed at pH 3.2 for *H. uvarum* and *W. anomalus* strains, and the activity of the latter one was not inhibited by glucose (Mateo et al., 2011), whereas *S. cerevisiae* and some other non-*Saccharomyces* yeasts are reported to show notable loss of activity under such wine-like pHs (Delcroix et al., 1994; Rosi et al., 1994).

β-Lyase, an enzyme involved in the direct release of thiols, has been studied in depth in *S. cerevisiae*, and is reported in some non-*Saccharomyces* species, including *T. delbrueckii*, *Kluyveromyces marxianus* and *Meyerozyma guilliermondii* (Belda et al., 2016). The activity in both *S. cerevisiae* and non-*Saccharomyces* yeasts is strain-specific, with great intraspecific variability being observed (Zott et al., 2011; Roncoroni et al., 2011; Belda et al., 2016). For example, some *M. pulcherrima* and *L. thermotolerans* strains can release thiols in Sauvignon Blanc fermentations, while in other studies few strains showed this activity (Zott et al., 2011; Belda et al., 2016).

The enzymatic activities discovered so far in non-*Saccharomyces* yeasts are still just the tip of the iceberg, and more are waiting to be identified to ideally cater for various oenological demands and allow adjustment of wine quality.

1.3 Aim of this study

IBMP, as a grape-derived odorous compound, can influence wine aroma profiles at different levels and is especially undesirable at high concentrations. Various remediation methods have been trialled, but little is known about the effects of winemaking practices such as yeast selection on wine *vs* juice IBMP content. In a preliminary study, Treloar and Howell (2006) reported the capacity of several commercial *S. cerevisiae* yeast strains to affect IBMP concentrations during fermentation and observed a statistically significant difference of 37% (1.53 ng/L) among different strains. However, the limited description of the experiments, namely analytical methods, makes it difficult to assess the quality and reliability of the findings. Nevertheless, the research was the first to investigate the association of wine-related

yeasts and IBMP levels in resultant wine. Given the great metabolic versatility of non-*Saccharomyces* yeasts, this project aims to investigate the possible effects of different non-*Saccharomyces* yeast strains in sequential inoculations on IBMP concentrations as well as the resulting overall wine aroma profile.

2 Materials and methods

2.1 Vinification methods

Sauvignon Blanc grapes (100 kg) were harvested from a vineyard located at Adelaide Hills wine region (34°59'S, 138° 47' E, 378 m) when the total soluble solids (TSS) reached 23°Brix and transferred directly to the University of Adelaide, Waite Campus. The Mean January Temperature (MJT), an indication of the hotness of a region during the growing season, was 21.5°C at this vineyard site with the highest temperature reaching 41°C, and 8 days of a maximum daily temperature exceeding 30°C. The average January rainfall is 33.5 mm (2010-2020) with the 2020 January rainfall being 42.8 mm. Grapes were crushed and pressed, with the addition of 30 ppm of SO_2 in the form of PMS (potassium metabisulphite). The juice (25 L) was then settled for 3 days at 4 °C before racking off of gross lees and spiking with 52 ng/L of IBMP which was confirmed by GC analysis as described in Section 2.4. Basic juice composition is detailed in Table 2.1. The juice (500 mL per replicate) was distributed into 1 L fermentation vessels and each strain treatment was performed in triplicate (36 vessels for 11 strain treatments and 1 control). Eleven non-*Saccharomyces* yeast strains were pre-cultured overnight in YEPD media at 28 °C and then sub-cultured at the inoculation rate of 1×10^6 cells/mL into starter medium (1:1 YEPD and Sauvignon Blanc juice, v/v) and incubated overnight at 23°C, before inoculation into the juice fermentations at an inoculation rate of 5×10^6 cells/mL. Ferments were initially kept at 20 °C for 5 days and then transferred to 16 °C after sequential inoculation with *Saccharomyces cerevisiae* (EC1118, Lallemand), and were sampled daily to monitor sugar consumption kinetics. Fermentations were deemed finished once the sugar levels were below 2.5 g/L, upon which 90 ppm of SO_2 in the form of PMS was added and wines from replicates were combined into one container with minimal headspace and cold stabilised at 4 °C for 14 days. Wines were subsequently bottled in 750 mL glass bottles sealed with screw caps, with the headspace filled with nitrogen to minimise oxidation and stored at 4 °C for sensory study. Samples from each replicate were collected at the following timepoints: a, after non-*Saccharomyces* inoculation; and b, on the completion

of fermentation, and were analysed for IBMP concentration by GC-MS/MS as described in Section 2.4.

Table 2.1 Physicochemical parameters of Sauvignon Blanc grape juice

Titratable Acidity (TA)	8.2 (g/L)
pH	3.51
TSS° Brix	23
TSS° BAUME	12.2
Yeast Assimilable Nitrogen (YAN)	245.9 (mg/L)
Malic Acid	3.54 (g/L)
Volatile Acid	0 (g/L)

2.2 Follow-up trials as 100 mL fermentation in sterile Sauvignon Blanc juice

Grape juice pressed from the same batch of Sauvignon Blanc juice was used for 100 mL fermentations. IBMP was spiked into grape juice at a concentration of 30 ng/L (confirmed by GC analysis). A lower level of IBMP was obtained in sterile juice compared to those used in Section 2.1 (50 ng/L), mainly due to the possible binding effects and volatilisation during juice sterilisation. However, differences *between* the trials are not important, since impact on IBMP concentrations were evaluated between treatments *within* each trial. Juice was sterilised (0.2 μm) before distribution into individual 250-mL flasks equipped with a fermentation lock and ports for aseptic sampling. Pre-cultivation of yeast strains was described in Section 2.1. Two different inoculation rates were applied for every strain tested, one of which was identical to the previous fermentation, and the other was 6-times the original dosage (i.e., 3×10^7 cells/mL), with each treatment conducted in triplicates. EC1118 was inoculated at 5×10^6 cells/mL into all treatment groups after 5 days of fermentation by the pure culture. All fermentations were incubated with shaking (120 rpm) at 16 °C. Fermentation kinetics were monitored by weighing each flask daily for CO_2 loss, and completion of alcoholic fermentation was confirmed by sugar analysis. Samples for IBMP analysis were collected at two timepoints, immediately after inoculation and at the end of fermentation.

2.3 Measurement of basic compositional features of the juice and wine

Titratable acidity and pH were measured by an InMotion™ Flex Autosampler connected with Mettler Toledo T50 titrator. Alcohol concentrations were determined by an Anton Paar®

DMA 4500 M density meter. Sulfur dioxide content of wine in both free and bound forms were analysed by the aspiration/titration method (Rankine and Pocock, 1970). Sugar concentrations were quantified by reacting with hexokinase/glucose-6-phosphate dehydrogenase (Megazyme, Deltagen Australia) and phosphoglucose isomerase (Megazyme, Deltagen Australia) in reaction buffers and measuring absorbances (340 nm) of the NADPH by-product from the reactions (Henniger and Mascaro Jr, 1985). Malic acid, acetic acid and glycerol were measured by HPLC analysis with undiluted final wine samples (Gardner et al., 2006). For HPLC analysis, samples were clarified by centrifugation (10, 000 × *g*, 3 min). HPLC analysis was conducted with an Aminex HPX-87H column (300 mm × 7.8 mm; Biorad), and a working temperature of 60 °C with 2.5 mM of H_2SO_4 at a flow rate of 0.5 mL/min. A RID-10A refractive index detector (Shimadzu, Kyoto, Japan) was used for peak detection, and compound determination and quantification was achieved by comparing with standards prepared in Chemically Defined Grape Juice Medium (CDGJM, Henschke and Jiranek, 1993; Mcbryde et al., 2006) using Delta integration software (DeltaWare Dataworks, Brisbane, Australia).

2.4 GC-MS/MS analysis of IBMP concentrations in juice and wine

IBMP determination followed the method of Dunlevy et al. (2010). Wine samples (5 mL) and Milli-Q water (5 mL) were added to a 20 mL brown-glass headspace vial with 3 g of NaCl added. The mixture was then spiked with 100 µL of 5 µg/L d_3-IBMP (CDN Isotopes, Quebec, Canada) as an internal standard. Samples were analysed immediately. SPME-GC-MS was performed on a 6890 Gas Chromatograph (Agilent, Santa Clara, CA, USA) with a Gerstel (Mülheim an der Ruhr, Germany) MP2 auto-sampler. A divinylbenzene-carboxen-polydimethylsiloxane fibre (2 cm, 23-Gauge, 50/30 Peak µm DVB-CAR-PDMS, Supelco, Bellefonte, PA, USA) was used with the auto-sampler for compound extraction. Samples were incubated at 40 °C for 5 min and extracted at the same temperature for 30 min with agitation. Analytes were partitioned in the injector at 250 °C for 2 min, and the purge was subsequently switched onto 20 mL/min. A ZB-Wax column (30 m length, 0.25 mm i.d., 0.25 µm film thickness) was used for chromatography, and helium was used as the carrier gas at a flow rate of 1.2 mL/min. A temperature gradient from 30 to 80 °C of 3 °C/min was applied after an initial hold at 30 °C for 2 min, and then an isothermic hold for 14 min was performed before another temperature gradient from 80 to 230 °C of 25 °C/min was performed, finishing with a 5 min hold at the final temperature. For mass spectrometry, a transfer line temperature of 250 °C, source temperature of 230 °C, quadrupole temperature of 150 °C, and

ionising potential of 70eV with selective ion monitoring were used. Mass channels for IBMP were *m/z* = 94, 124 and 151 after 25.5 min, and 95, 127 and 154 for d_3-IBMP with dwell times of 50 ms. IBMP was quantified using the 94 and 151 ions, while 95 and 154 were used for d_3-IBMP.

Peak detection and compound determination were achieved by a Hewlett-Packard 5973N Mass Spectrometer. IBMP quantification was performed by comparing ion peak areas with that of internal standards and calculating based on the standard curve generated.

2.5 Sensory analysis of finished wines

Differences in aromas amongst the first batch of wines (Section 2.1) including the intensity of 'greenness' were noticed; therefore a sensory study was performed to profile aroma characters of each wine using the 'Rate-All-That-Apply' (RATA) method (Ares et al., 2014). Since IBMP, a non-food grade chemical, was used for spiking during the winemaking process, the sensory study was constrained to evaluation of aroma attributes only. A pilot panel (n = 4) was hosted prior to the formal sensory trial to characterise each sample and generate aroma descriptors for use in the RATA survey (aroma attributes used in RATA survey described in Table 2.2). Participants (n = 50; 19 males and 31 females) convened from The University of Adelaide and the AWRI (Australian Wine Research Institute) were required to rate the perceivable aroma characters with a scale of seven levels ranging from extremely low to extremely high, and scores from 0 to 7 were obtained accordingly to quantify the results for data analysis. Specifically, different types of greenness related to IBMP were summarised from the panel discussion and such categories were designated as an imperative section for the evaluation instead of an optional selection as for other attributes based on the perception of each participant. This design enabled a full profile of green character evaluation to be depicted for each wine sample to comprehensively assess the outcomes of individual yeast treatments.

Wines were kept at 4 °C and were presented as 20-mL samples in four-digit coded, plastic lid-covered ISO standard wine glasses. Sensory evaluation was performed in isolated booths under sodium lights at 22-23 °C. Twelve wines were presented to each participant in random order generated by RedJade® software, which was also used as the survey tool during RATA test. Participants were required to rest for 30 s between samples and 2 min after every four

sampless to avoid sensory fatigue as well as to obtain higher evaluation accuracy. Data were collected by RedJade® software and analysed by XLSTAT® statistical software.

Table 2.2 Aroma attributes used for RATA survey generated from the pilot panel

Green characters	Other attributes
Vegetal	Overall aroma intensity
Green capsicum	Stone fruit
Grassy	Pome fruit
Leafy	Banana
Herbaceous	Floral
Cooked vegetables	Confectionary
Canned asparagus	Tropical
	Citrus
	Boxwood
	Smoky
	Mineral
	Solvent/alcohol

2.6 HS-SPME-GC-MS/MS analysis of major fermentation-derived aroma profiles

Wine samples were prepared in duplicate and spiked with 10 μL of internal standard mix solutions (Table 2.2) in 10 mL volumetric flasks, after which 10-fold dilution of wine samples was achieved by adding an aliquot of 0.5 mL of mixture to 4.5 mL of Milli-Q water in a 20 mL SPME vial (Supelco). Vials were then sealed for GC-MS analysis after adding 2 g of NaCl.

Table 2.2 Qualitative information for internal standards

Compound	RT (min)	Ions[a](*m*/*z*)	Spiked concentrations (mg/L)
d_4-3-methyl-1-butanol	16.317	**74**, 59, 42	0.1194
d_{13}-hexanol	24.191	**64**, 46, 78, 96	0.002532
d_3-hexyl acetate	19.954	**46**, 84, 64, 56	0.0012348
d_5-phenylethanol	54.626	**96**, 97, 127	0.0251024

[a] Ions in bold were used as the quantifier.

For GC-MS (Wang et al., 2016), sample analysis was achieved by a Gerstel selectable 1D/2D-GC-MS system (Lasersan Australasia Pty Ltd., Robina, QLD, Australia) using an Agilent 7890 GC equipped with a Gerstel MPS autosampler and low thermal mass (LTM)

series II external column modules coupled to a 5897 mass selective detector. For 1D separations, a deactivated SPME inlet liner (0.75 mm i.d., Supelco) and DB-Wax LTM column module (30 m, 0.25 mm i.d., 0.25 μm film thickness, Agilent J&W, Folsom, CA) were used. Carrier gas was provided at a constant flow of 1 mL/min with ultrapure helium (Coregas, Cavan, SA, Australia). The temperature program for LTM module began at 40 °C for 1 min, increasing to 135 °C at 2 °C/min, then to 212 °C at 5 °C/min, and finally to 250 °C at 15 °C/min, after which the temperature remained at 250 °C for 10 min, allowing a total run time of 76 min. The transfer line was programmed at 200 °C, and positive ion electron impact spectra were set at 70 eV for recording the scan runs with *m*/*z* ranging from 35-350.

For qualitative and quantitative analysis of major fermentation volatiles, samples were incubated at 50 °C with agitation (500 rpm) for 10 min, and then extracted with a DVB/CAR/PDMS SPME fibre (50/30 μm, 1 cm, 23 gauge) at the same temperature and agitation conditions. The injection mode was splitless with desorption at 240 °C for 10 min. New fibres were conditioned in the injection port for 1 h at 270 °C and pre-baked for 10 min before every samples to avoid carryover. Blank runs were performed routinely after every five samples. Compound was identified by the determination of retention indices for the DB-Wax column using a series of alkanes (C7-C40, Sigma-Aldrich), and with the help of mass spectral library matches (NBS 75K). Compound information (CAS number, retention time, quantifier/qualifier ions) is listed in Table 2.3.

Quantitative analysis of 27 volatiles was achieved with available reference standards. Calibration and validation were performed with a series of duplicate addition of authentic standards into model wine solution spiked with internal standard mixture. The internal standards were selected based on chemical similarity, retention time and coefficient of determination (R^2). There were 12 points (6 concentrations in duplicate) for each calibration function evenly spaced to cover 0-150% of the estimated analyte concentration in wine samples. Linearity of calibration curves was assessed from an inspection of residual plots and R^2 values.

Table 2.3 Qualitative information and method characteristics for volatile compounds determined by HS-SPME-GC-MS

Compound	CAS number	RT (min)	Ions[b] (*m*/*z*)	R^2	Aroma detection threshold[c] (μg/L)	Odour quality[q]
Ethyl butanoate†	105-54-4	8.485	**71**, 29, 88	0.9914	20[d]	Strawberry, lactic
Ethyl decanoate†	110-38-3	42.548	**88**, 101, 155	0.9902	200[e]	Flora, soap[r]
Ethyl hexanoate†	123-66-0	18.038	**88**, 99, 60	0.9920	14[e]	Apple peel, fruit
Ethyl lactate†	97-64-3	24.358	**45**, 29, 75	0.9929	146000[f]	Solvent[s]
Ethyl 2-phenylacetate‡	101-97-3	49.904	**91**, 65, 164	0.9927	650[g]	Fruit, sweet
Ethyl propanoate†	105-37-3	6.377	**57**, 75, 102	0.9934	1840[h]	Fruit
Ethyl 2-methylbutanoate§	7452-79-1	9.021	**57**, 85, 115	0.9926	1[d]	Fruity, anise, strawberry[r]
Ethyl isobutyrate§	97-62-1	6.381	**71**, 88, 116	0.9974	15[h]	Sweet, rubber
Ethyl isovalerate§	108-64-5	9.617	**88**, 57, 130	0.9943	3[d]	Fruit
Ethyl acetate†	141-78-6	4.789	**61**, 88	0.9969	15000[f]	VA, nail polish[j]
Isoamyl acetate†	123-92-2	12.205	**70**, 55, 87	0.9915	30[d]	Banana
Hexyl acetate§	142-92-7	20.214	**43**, 56, 69	0.9936	670[i]	Fruity, floral[i]
1-Butanol†	71-36-3	13.2	**56**, 41, 31	0.9913	500-4300[h]	Medicine, fruit, wine
1-Hexanol‡	111-27-3	25.002	**69**, 56, 84	0.9958	8000[d]	Green, grass[r]
1-Propanol‡	71-23-8	8.532	**31**, 42, 59	0.9937	500[j]	Alcohol, pungent
2-Ethyl-1-hexanol‡	104-76-7	33.7	**57**, 70, 98	0.9927	8000[k]	Citrus, green
2-Phenylethanol¤	60-12-8	54.731	**91**, 65, 122	0.9952	14000[e]	Floral, rose[j, s]
3-Methyl-1-butanol†	123-51-3	16.745	**55**, 42, 70	0.9938	30000[e]	Harsh, nail polish[j], fusel[r]
3-Octanol‡	589-98-0	27.577	**83**, 59, 101	0.9941	100000[l]	Nutty, musty
4-Methyl-2-pentanol†	108-11-2	14.31	**45**, 43, 41	0.9902	-	-
Benzyl alcohol¤	100-51-6	53.504	**108**, 107, 79	0.9983	900000[h]	Floral, rose
Isobutanol‡	78-83-1	11.507	**31**, 55, 74	0.9956	40000[e]	Wine, solvent, bitter
β-Damascenone¤	23696-85-7	51.772	**69**, 121, 190	0.9976	0.05[d]	Apple, rose, honey
1,8-Cineole‡	470-82-6	16.037	**108**, 81, 43	0.9903	0.00493[m]	Mint, sweet

3-Methylbutanoic acid‡	503-74-2	43.539	**60**, 43, 87	0.9904	700[h]	Sweat, acid, rancid
Butanoic acid‡	107-92-6	41.155	**60**, 73, 42	0.9918	173[n]	Rancid, cheese, vomit
Isobutyric acid‡	79-31-2	37.721	**73**, 88, 43	0.9918	1.5[o]	Rancid, butter, cheese
β-Ionone¤	127-41-3	55.677	**175**, 91, 43	0.9914	0.007[p]	Rose

[a] Internal standards for each compound in subscript symbols. †, d_4-3-methyl-1-butanol; ‡, d_{13}-hexanol; §, d_3-hexyl acetate; ¤, d_5-phenylethanol.

[b] Ions in bold were used as the quantifier.

[c] References given for each compound in superscript letters. Thresholds are indicated in aqueous ethanol except for Ferreira et al. (2000) and Swiegers et al. (2005), for which the matrix was wine.

[d] Guth (1997), [e] Ferreira et al. (2000), [f] Moyano et al. (2002), [g] Burdock (2009), [h] Miller (2019), [i] Peinado et al. (2004), [j] Swiegers et al. (2005), [k] Buttery et al. (1988), [l] Kamínsky et al. (1972), [m] Kirsch and Buettner (2013), [n] Francis (2012), [o] Chemical book website (https://www.chemicalbook.com/productindex_en.aspx), [p] Leffingwell & Associates website (http://www.leffingwell.com/chirality/chirality.htm), [q] reference from flavornet (http://www.flavornet.org) by Terry Acree and Heinrich Am, except where specified, [r] Ferreira et al. (2009), [s] Mayr et al. (2014).

2.7 Statistical analysis

Chemical and sensory data were processed with Microsoft Excel 2012. All data are presented as means with standard deviation from replicates. Sensory data and volatile data from GC analysis were processed by one-way ANOVA using the statistical add-in package XLSTAT (version 2020.5, AddinSoft SARL, Paris, France). Significantly different means were analysed for Pearson's type Principal Component Analysis (PCA), and for Partial Least Squares regression (PLS-R) analysis, using XLSTAT. The heatmap for sensory data was generated by GraphPad Prism (version 9.0.0, San Diego, US).

3 Results

3.1 Physicochemical parameters for grape juice and finished wines

Fermentation kinetics were monitored via sugar consumption (Fig. 3.1), revealing that yeasts consumed sugars at different rates and finished fermentation in the following order: *Saccharomycodes ludwigii* ≥ *Metschnikowia pulcherrima* ≥ *Wickerhamomyces anomalus* ≥

Kazachstania aerobic ≥ *Hanseniaspora uvarum* > *Meyerozyma guillermondii* ≥ *Candida krusei* ≥ EC1118 > *Kazachstania servazzii* > *Torulaspora delbrueckii* > *Lachancea thermotolerans* > *Aureobasidium pullulans*. It is interesting to note that a few non-*Saccharomyces* strains initially appeared to ferment more quickly with EC1118. The slowest strain, *Aureobasidium pullulans*, seemed particularly quick initially only to slow down markedly as fermentation progressed.

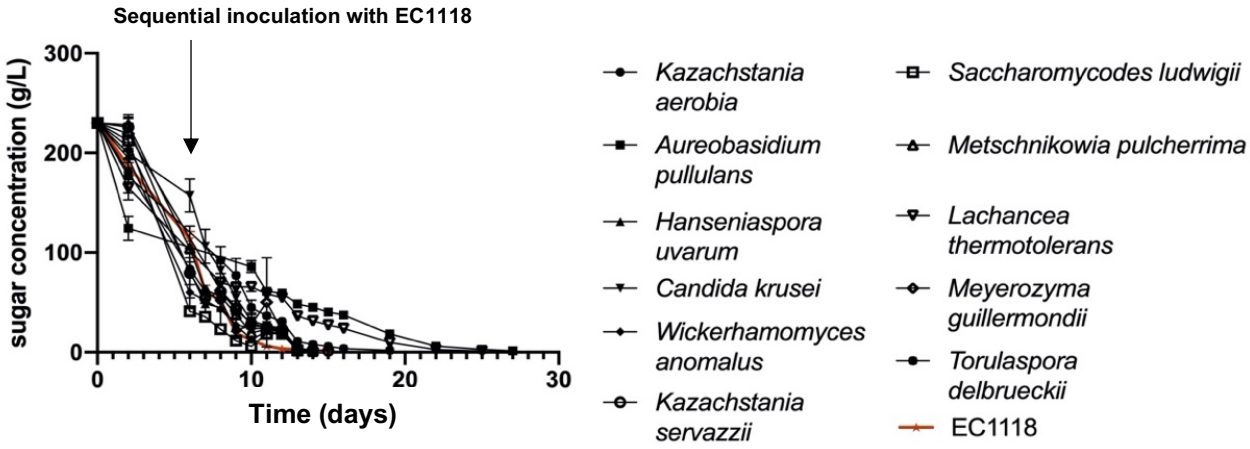

Figure 3.1 Fermentation kinetics of 12 yeast strains. The control group (EC1118) is highlighted in red. Sequential inoculation of treatments occurred 5 days after initial inoculation.

Some distinctive physicochemical parameters were recorded for each treatment group (Table 3.2). While alcohol yield was fairly consistent ranging from 14.13% to 14.47% (v/v), different yeasts yielded different wine acidity levels, with decreases in TA ranging from 1.63 to 2.33 g/L. pH levels were diverse, with both increases and decreases noted, and specifically, *H. uvarum* producing the lowest pH of 3.41, while *S. ludwigii* and *M. pulcherrima* produced wines with increased pH values of 3.67. Malic acid concentrations were at 3.4 g/L in the grape musts, with EC1118 consuming only 0.19 g/L, while *M. guillermondii* consumed 0.87 g/L.

Table 3.2 Composition of finished wines produced by co-fermentation of different non-*Saccharomyces* yeast strains and *S. cerevisiae* (EC1118), with single-yeast fermentation by EC1118 as the control.

Treatment	TA (g/L)	pH	Sulfur (mg/L)		Residual sugar (g/L)	Ethanol (%)	Malic acid (g/L)	Glycerol (g/L)	Acetic acid (g/L)
			Free	Total					
Kazachstania aerobia	6.35^{d}	3.52^{f}	nd	57.6^{d}	1.42^{de}	14.20^{g}	3.17^{d}	8.76^{b}	0.09^{ef}
Aureobasidium pullulans	5.87^{i}	3.64^{b}	nd	59.2^{c}	1.45^{d}	14.47^{ab}	2.70^{g}	7.34^{j}	0.15^{d}
Hanseniaspora uvarum	6.21^{e}	3.41^{h}	8^{a}	57.6^{d}	1.66^{c}	14.32^{e}	2.85^{f}	8.31^{c}	0.07^{f}
Candida krusei	6.08^{g}	3.48^{g}	nd	57.6^{d}	1.37^{e}	14.46^{bc}	3.33^{c}	7.44^{h}	0.18^{d}
Wickerhamomyces anomalus	6.44^{c}	3.66^{a}	0.8^{d}	63.2^{b}	1.28^{f}	14.13^{i}	3.34^{c}	7.39^{i}	0.43^{a}
Kazachstania servazzii	6.41^{c}	3.51^{f}	0.8^{d}	58.4^{d}	1.42^{de}	14.28^{f}	3.18^{d}	9.16^{a}	0.08^{f}
Saccharomycodes ludwigii	6.20^{ef}	3.67^{a}	4^{b}	40.8^{g}	1.99^{a}	14.43^{c}	3.50^{a}	7.01^{k}	0.13^{de}
Metschnikowia pulcherrima	6.57^{a}	3.67^{a}	0.8^{d}	57.6^{d}	1.08^{g}	14.25^{f}	3.46^{b}	7.90^{f}	0.07^{f}
Lachancea thermotolerans	6.16^{f}	3.61^{d}	0.8^{d}	52^{e}	1.31^{f}	14.40^{d}	2.57^{h}	7.61^{g}	0.18^{d}
Meyerozyma guillermondii	5.99^{h}	3.55^{e}	0.8^{d}	63.2^{b}	1.91^{b}	14.40^{d}	2.10^{i}	8.14^{d}	0.08^{f}
Torulaspora delbruckii	6.50^{b}	3.62^{cd}	1.6^{c}	42.4^{f}	1.86^{b}	14.17^{h}	3.08^{e}	7.32^{j}	0.40^{b}
EC1118	6.48^{b}	3.63^{bc}	1.6^{c}	84^{a}	1.12^{g}	14.49^{a}	3.34^{c}	7.93^{e}	0.29^{c}

Data for each parameter are presented as mean value (n = 3); superscripted letters indicate significant difference amongst different letters ($p < 0.05$) based on one-way ANOVA with least significant difference (LSD) pairwise comparison; nd, not detected.

3.2 IBMP concentrations during fermentation

IBMP concentrations were analysed by GC-MS/MS in samples collected from two time points during fermentations. Despite measurement of the initial concentration of IBMP in grape musts after spiking, concentrations differed in samples after the first inoculation. Changes in concentration within each treatment were therefore calculated and used for data analysis. No significant difference was observed between any treatment and the control (Table 3.3). Increased IBMP concentrations were observed in the finished wines in many cases, which was unexpected since some IBMP loss was anticipated through adsorption of

biomass. Possible explanations for this are discussed in Section 4.2. Follow-up fermentations at 100 mL scale were performed to confirm the above findings (see Section 3.3).

Table 3.3 IBMP concentrations (ng/L) in wine samples collected both at the beginning and end of alcoholic fermentation by non-*Saccharomyces* yeast over inoculated with *Saccharomyces cerevisiae* after 5 days. Delta concentrations ($Conc._{Day0}$- $Conc._{Finish}$) are used for a paired t-test comparison with EC1118[a].

Treatment	**Day 0**	**Finish**	**Delta**	***p*-value**
Kazachstania aerobia	47.80 ± 2.66	48.74 ± 0.40	-0.95 ± 2.95	0.9714
Aureobasidium pullulans	47.20 ± 1.68	48.93 ± 0.41	-1.73 ± 1.28	0.6590
Hanseniaspora uvarum	48.42 ± 1.39	49.40 ± 1.10	-0.98 ± 1.35	0.9621
Candida krusei	50.55 ± 0.78	51.61 ± 1.48	-1.06 ± 1.67	0.9982
Wickerhamomyces anomalus	47.57 ± 0.49	51.14 ± 0.66	-3.57 ± 1.11	0.3294
Kazachstania servazzii	50.57 ± 2.00	51.01 ± 2.02	-0.45 ± 3.97	0.1531
Saccharomycodes ludwigii	47.88 ± 0.47	50.79 ± 0.69	-3.17 ± 1.21	0.7732
Metschnikowia pulcherrima	47.25 ± 0.33	50.25 ± 0.24	-3.00 ± 0.39	0.4658
Lachancea thermotolerans	47.06 ± 3.83	50.19 ± 2.22	-3.14 ± 5.32	0.2456
Meyerozyma guillermondii	45.44 ± 1.53	51.36 ± 1.00	-5.92 ± 1.91	0.0621
Torulaspora delbrueckii	43.82 ± 3.54	51.18 ± 0.31	-7.36 ± 3.84	0.2521
EC1118	50.08 ± 2.20	51.15 ± 1.30	-1.07 ± 3.49	

[a]Data are presented as the mean of these replicates (n = 3) ± SD.

3.3 100-mL fermentations

Two non-*Saccharomyces* yeast strains (*W. anomalus* and *M. guillermondii*) were selected for the follow-up fermentations (100 mL) due to the statistically significant concentration increases of IBMP ($IBMP_{\text{initial conc.}}$ *vs* $IBMP_{\text{finish conc.}}$ within each treatment) observed for these two yeasts.

Fermentation kinetics were monitored via CO_2 loss (Fig. 3.2). Although each yeast fermented the juice to dryness (residual sugar < 1.1 g/L), the time required differed by strain. It took 33 days for the *W. anomalus* fermentations to finish alcoholic fermentation, while *M. guillermondii* took 21 days and EC1118 completed in just 6 days. IBMP concentrations (Table 3.4) were obtained using GC-MS/MS. Delta values (Table 3.5) were used for statistical analysis due to the variations in the initial concentrations. Even so, no significant

differences were obtained in pairwise comparisons between either treatment or treatment *vs* the control (Table 3.5).

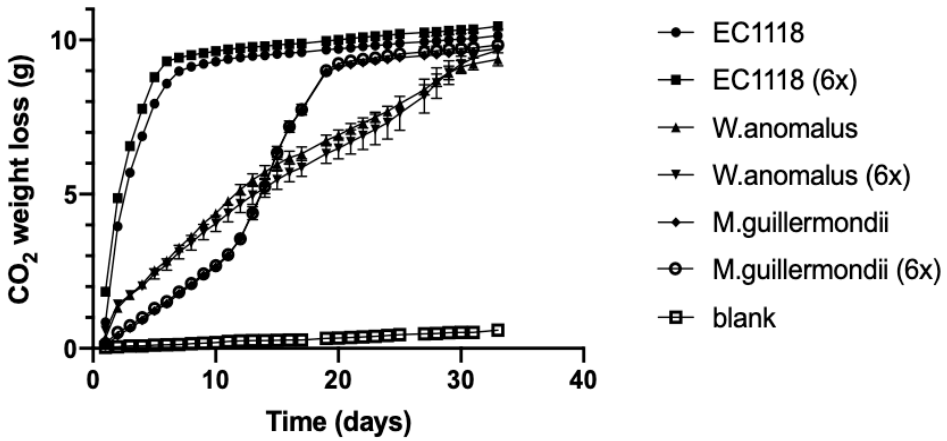

Figure 3.2 Fermentation kinetics of 3 yeast strains, determined by CO_2 weight loss. Sequential inoculation occurred 5 days after initial inoculation. 6×, the inoculation rates were 6 times the original dosage.

Table 3.4 IBMP concentrations (ng/L) in wine samples collected both at the beginning and end of alcoholic fermentation. Delta concentrations: $(Conc._{Day0} - Conc._{Finish})$[a].

Treatment	Day 0	Finish	Delta
EC1118	29.47 ± 0.67	19.51 ± 2.00	9.85 ± 2.92
EC1118 (6×)	29.14 ± 0.39	19.14 ± 1.09	10.00 ± 1.02
W. anomalus	30.34 ± 0.77	19.83 ± 0.80	10.79 ± 0.05
W. anomalus (6×)	30.17 ± 0.82	19.74 ± 0.38	10.42 ± 1.04
M. guillermondii	29.46 ± 0.81	18.70 ± 0.97	10.76 ± 0.23
M. guillermondii (6×)	29.33 ± 0.37	18.97 ± 0.99	10.37 ± 0.96
Blank	29.13 ± 1.19	19.23 ± 1.62	9.90 ± 2.64

[a]Data are presented as the mean ± SD (n = 3).

Table 3.5 *p*-Value obtained from Student's *t*-test for significance check between any two groups

	EC1118	EC1118 (6×)	*W. anomalus*	*W. anomalus* (6×)
W. anomalus	0.6960	0.3774		
W. anomalus (6×)	0.7626	0.6393		
M. guillermondii	0.6001	0.2771	0.8869	
M. guillermondii (6×)	0.7824	0.6724	0.6015	0.9475

3.4 Sensory analysis

Difference in aroma profiles were perceived in bench-top trials amongst the first batch of wines (Section 2.1, 3.1 and 3.2), therefore sensory analysis was performed to characterise wine aroma, including an evaluation of greenness for each wine using the RATA method. Even though statistical analysis performed on IBMP levels in finished wines indicated there were no significant differences, informal sensory assessment suggested differences between treatments in the perceptibility of IBMP-related aromas. As such wines were subject to detailed sensory analysis and promising results were obtained. Among the 19 aroma descriptors that were rated, significant differences were returned for 15 of them in the 12 wines examined (Table 3.6). Moreover, of seven IBMP-related attributes (i.e., vegetal, green capsicum, leafy, cooked vegetables, canned asparagus, grassy and herbaceous aromas), the first 5 were perceived as being significantly different. According to the principal component analysis (PCA) performed on the sensory data for the different yeast treatments, the first two factors accounted for 81.7% of the total variations, with groups with similar IBMP concentrations being differentiated along F1 and green characters clustering on the right-hand side of the plot and fruity attributes on the other (Fig. 3.3). *A. pullulans* and *K. aerobia*, which differed in IBMP concentration by only 0.19 ng/L, were positioned on opposite sides of the PCA biplot, due to opposing aroma profiles. Wines made with *A. pullulans* were associated with a strong 'cooked vegetable' character, and were more closely related to other green characters compared with wine made with *K. aerobia*, which was more closely associated with fruity and floral attributes. *W. anomalus* imparted potent solvent/alcohol aromas, which adversely affected the overall aroma intensity. EC1118, the popular commercial *S. cerevisiae* strain, gave wines with an aroma profile situated more at the high end of the scale for green character.

Generally speaking, 6 strains (*C. krusei*, *K. aerobia*, *H. uvarum*, *K. servazzii*, *M. guillermondii* and *M. pulcherrima*), gave Sauvignon Blanc wines with more desirable fruity and floral characters, which were consequently rated with less intense green attributes.

Table 3.6 Mean intensity ratings for aroma attributes evaluated in wine by Results of Rate-All-That-Apply (RATA) sensory analysis treatments

	Overall aroma intensity	Vegetal†	Green capsicum†	Grassy†	Leafy†	Herbaceous†	Cooked vegetables†	Canned asparagus†	Stone fruit	Pome fruit	Banana	Floral	Confectionary	Tropical	Citrus	Boxwood	Smoky	Mineral	Solvent/ alcohol
Meyerozyma guillermondii	4.68^{b}	2.74^{bcd}	3.16^{abced}	3.00^{ab}	2.80^{bcde}	3.02^{ab}	2.36^{b}	2.56^{bc}	2.40^{ab}	2.38^{abc}	2.62^{ab}	1.74^{abc}	2.40^{abc}	2.86^{ab}	2.34^{ab}	1.26^{c}	1.02^{abcd}	1.26^{ab}	2.78^{cde}
Aureobasidium pullulans	4.50^{bc}	3.36^{a}	3.62^{a}	3.06^{a}	3.16^{abc}	3.36^{a}	3.36^{a}	2.94^{ab}	1.92^{bc}	2.18^{bcd}	1.32^{d}	1.16^{d}	1.40^{f}	2.10^{cd}	2.10^{bc}	2.06^{a}	1.28^{a}	1.62^{a}	2.44^{def}
Saccharomycodes ludwigii	4.48^{bc}	3.46^{a}	3.34^{ab}	3.04^{a}	3.16^{abc}	3.18^{ab}	3.64^{a}	3.10^{a}	1.82^{c}	2.10^{cd}	1.32^{d}	1.20^{d}	1.78^{def}	2.06^{cd}	1.62^{c}	2.14^{a}	1.20^{ab}	1.52^{ab}	2.58^{def}
Lachancea thermotolerans	4.24^{c}	3.32^{a}	3.52^{a}	2.94^{abc}	3.64^{a}	2.82^{b}	3.54^{a}	3.08^{a}	1.84^{c}	2.00^{cd}	1.60^{cd}	1.44^{bcd}	1.72^{ef}	2.70^{ab}	2.26^{ab}	2.02^{a}	1.14^{abc}	1.44^{ab}	1.94^{f}
Kazachstania servazzii	4.54^{bc}	2.68^{bcd}	2.76^{cde}	2.64^{abcd}	2.84^{bcde}	2.98^{ab}	2.00^{b}	2.24^{cde}	2.48^{a}	2.76^{a}	2.48^{ab}	1.72^{abc}	2.08^{bcde}	2.72^{ab}	2.24^{ab}	1.38^{bc}	0.76^{cd}	1.36^{ab}	3.28^{bc}
EC1118	4.48^{bc}	3.20^{ab}	3.24^{abcd}	2.84^{abcd}	3.34^{ab}	3.14^{ab}	2.46^{b}	2.50^{bcd}	2.30^{abc}	2.10^{cd}	1.80^{cd}	1.52^{abcd}	1.58^{ef}	2.56^{abc}	2.08^{bc}	1.44^{bc}	0.94^{abcd}	1.34^{ab}	2.58^{def}
Metschnikowia pulcherrima	4.44^{bc}	2.92^{abc}	2.94^{bcde}	2.78^{abcd}	2.86^{bcde}	2.94^{ab}	1.98^{b}	2.02^{de}	2.54^{a}	2.30^{abcd}	2.68^{a}	1.80^{ab}	2.60^{ab}	2.50^{bcd}	2.64^{a}	1.28^{c}	0.86^{bcd}	1.28^{ab}	2.50^{def}
Hanseniaspora uvarum	4.50^{bc}	2.58^{cd}	2.82^{bcde}	2.48^{bcd}	2.76^{cde}	2.72^{b}	2.38^{b}	2.14^{cde}	2.40^{ab}	2.50^{abc}	2.66^{a}	1.90^{ab}	2.34^{abcd}	2.82^{ab}	2.02^{bc}	1.24^{c}	0.90^{abcd}	1.14^{b}	3.06^{bcd}
Torulaspora delbrueckii	4.34^{bc}	3.08^{abc}	3.28^{abc}	2.60^{abcd}	3.04^{bcd}	2.76^{b}	3.34^{a}	2.90^{ab}	2.08^{abc}	1.76^{d}	1.42^{cd}	1.26^{cd}	1.88^{cdef}	2.06^{cd}	2.10^{bc}	1.88^{ab}	0.94^{abcd}	1.40^{ab}	2.24^{ef}
Kazachstania aerobia	4.34^{bc}	2.74^{bcd}	2.70^{de}	2.38^{d}	2.78^{cde}	2.74^{b}	2.16^{b}	2.38^{cde}	2.44^{a}	$2..72^{ab}$	2.88^{a}	1.66^{abcd}	2.70^{a}	2.60^{abc}	1.84^{bc}	1.08^{c}	0.80^{bcd}	1.10^{b}	3.50^{b}
Candida krusei	4.48^{bc}	2.70^{bcd}	2.90^{bcde}	2.46^{cd}	2.42^{e}	2.90^{ab}	2.34^{b}	2.10^{cde}	2.32^{abc}	2.14^{cd}	2.48^{ab}	1.98^{a}	2.34^{abcd}	3.12^{a}	1.88^{bc}	1.18^{c}	0.68^{d}	1.10^{b}	2.58^{def}
Wickerhamomyces anomalus	5.44^{a}	2.34^{d}	2.66^{e}	2.58^{abcd}	2.56^{de}	2.86^{ab}	2.28^{b}	1.94^{e}	1.88^{c}	1.94^{cd}	2.02^{bc}	1.56^{abcd}	1.92^{cdef}	1.94^{d}	1.68^{c}	1.08^{c}	0.90^{abcd}	1.38^{ab}	5.54^{a}
Pr>F	<0.0001	0.000	0.002	0.094	0.001	0.306	<0.0001	<0.0001	0.014	0.014	<0.0001	0.015	<0.0001	0.000	0.012	<0.0001	0.140	0.424	<0.0001
Significant	**Yes**	**Yes**	**Yes**	No	**Yes**	No	**Yes**	**Yes**	**Yes**	**Yes**	**Yes**	**Yes**	**Yes**	**Yes**	**Yes**	**Yes**	No	No	**Yes**

Data for each attribute are presented as mean values (n = 50); superscripted letters indicate significant differences amongst intensity ratings (p<0.05) based on one-way ANOVA with least significant difference (LSD) pairwise comparison.

†indicates green characters related to IBMP.

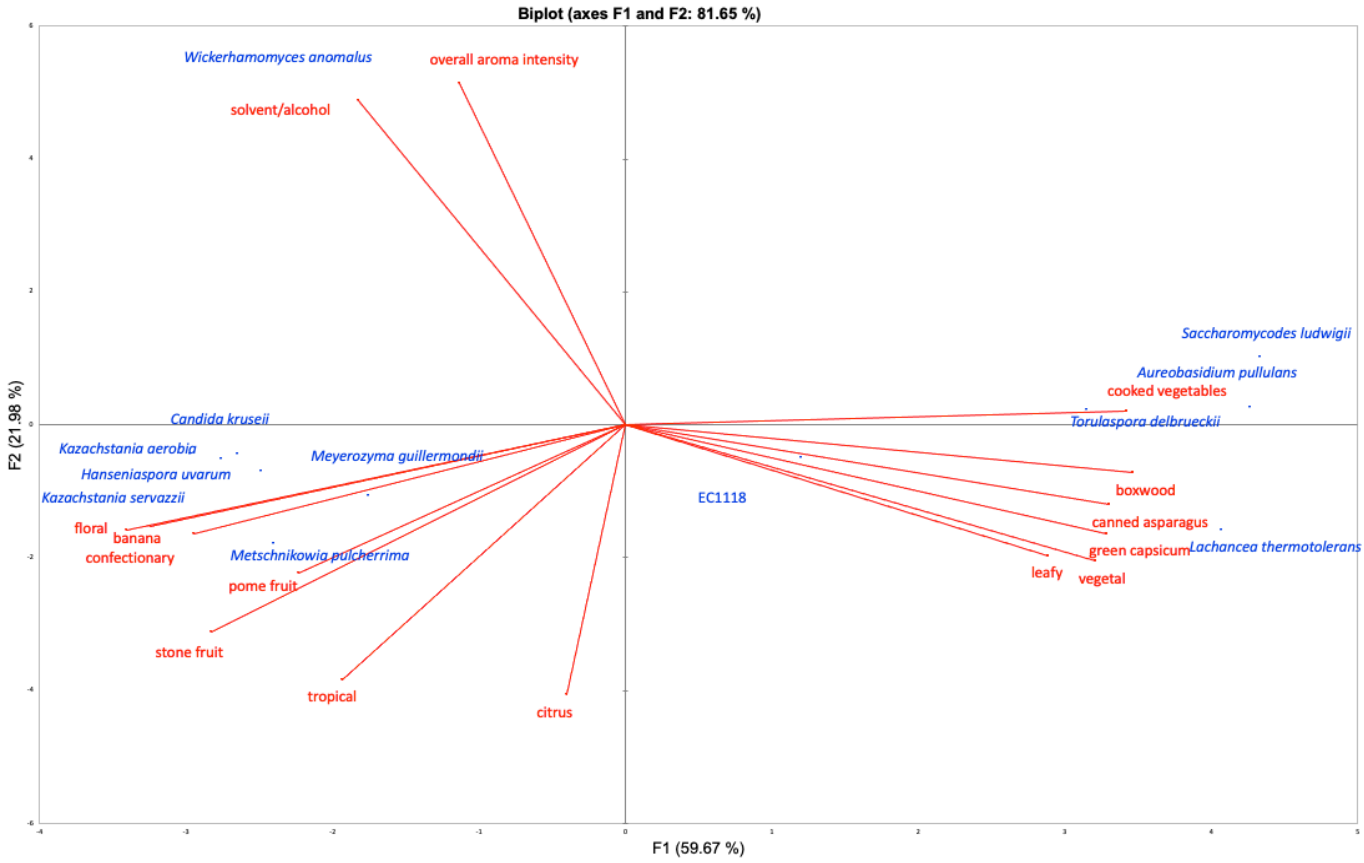

Figure 3.3 PCA biplot presenting scores and loadings of the standardised mean values for significant ($p < 0.05$) sensory attributes (red) and different treatments (blue).

3.5 GC-MS analysis of other fermentation volatiles

To further support the grouping patterns observed in the PCA biplot of sensory data, GC-MS analysis was performed to quantify a range of other volatile compounds in the wines (Table 3.7). Sensorially-detectable concentrations were observed for 21 of the 29 volatile compounds analysed, and statistically significant differences were observed for 20 of these compounds (the exception being β-ionone).

Table 3.7 Concentrations (μg/L) of volatile compounds measured by GC-MS in Sauvignon Blanc wines made with different treatments

	Candida krusei	*Wickerhamomyces anomalus*	*Metschnikowia pulcherrima*	*Meyerozyma guillermondii*	*Kazachstania aerobia*	*Lachancea thermotolerans*	*Hanseniaspora uvarum*	*Torulaspora delbrueckii*	*Kazachstania servazzii*	EC1118	*Aureobasidium pullulans*	*Saccharomycodes ludwigii*
Ethyl esters												
Ethyl butanoate	455.8^{cd}	492.8^{bc}	604.3^{a}	463.5^{bcd}	452.9^{cd}	244.9^{f}	503.0^{b}	320.8^{e}	440.5^{d}	443.8^{d}	262.2^{f}	275.3^{f}
Ethyl decanoate	688.2^{a}	649.4^{b}	667.1^{ab}	635.9^{b}	514.0^{d}	371.9^{fg}	569.9^{c}	308.3^{h}	489.4^{d}	457.0^{e}	397.7^{f}	342.4^{g}
Ethyl hexanoate	1368.2^{a}	1204.6^{c}	1235.9^{b}	1102.8^{d}	861.7^{g}	722.3^{h}	967.9^{e}	442.9^{j}	856.3^{g}	941.9^{f}	302.7^{k}	472.1^{i}
Ethyl lactate*	6594.5^{l}	9539.9^{i}	9753.0^{h}	28262.9^{a}	11314.9^{e}	25858.2^{b}	14672.2^{d}	8333.8^{j}	10863.8^{f}	10055.5^{g}	21242.2^{c}	7041.4^{k}
Ethyl 2-phenylacetate*	1.9^{a}	1.3^{b}	0.9^{e}	1.0^{d}	0.9^{de}	1.0^{c}	0.8^{f}	0.6^{g}	1.0^{cd}	0.8^{f}	0.5^{h}	0.5^{gh}
Ethyl propanoate*	668.6^{d}	704.3^{c}	637.7^{e}	670.7^{d}	828.5^{b}	479.8^{g}	722.9^{c}	1117.5^{a}	852.7^{b}	555.2^{f}	416.4^{h}	1113.9^{a}
Ethyl 2-methylbutanoate	10.8^{a}	9.7^{bc}	9.1^{cd}	8.5^{de}	8.5^{de}	10.9^{a}	8.2^{e}	9.5^{c}	8.3^{de}	9.8^{bc}	9.1^{cd}	10.4^{ab}
Ethyl isobutyrate	376.0^{cd}	350.6^{de}	354.0^{de}	337.1^{e}	331.8^{e}	470.9^{a}	352.8^{de}	420.3^{b}	352.4^{de}	353.3^{de}	423.3^{b}	398.9^{bc}
Ethyl isovalerate	14.6^{a}	7.7^{b}	7.0^{cd}	6.1f^{g}	6.4^{ef}	6.7^{de}	5.9^{gh}	7.3^{c}	6.5^{e}	8.0^{b}	5.9^{gh}	5.6^{h}
Acetate esters												
Ethyl acetate	185218.1^{f}	644915.8^{a}	167432.4^{g}	189763.9^{e}	260989.8^{b}	54206.8^{l}	248147.7^{c}	106366.4^{h}	231145.0^{d}	74993.8^{j}	55765.8^{k}	81258.8^{i}
Isoamyl acetate	7453.2^{f}	11058.8^{a}	10132.2^{b}	7631.8^{f}	9797.4^{c}	1121.0^{i}	7922.1^{e}	2889.5^{h}	9523.5^{d}	4694.6^{g}	996.2^{i}	454.7^{j}

Hexyl acetate*	140.1^{f}	277.5^{cd}	229.8^{e}	338.2^{a}	308.6^{b}	19.3^{h}	359.9^{a}	52.5^{g}	293.1^{bc}	256.4^{d}	23.7^{h}	18.4^{h}
Alcohols												
1-Butanol	1166.3^{cd}	1229.2^{bc}	1088.6^{e}	1231.2^{bc}	1376.1^{a}	1301.8^{b}	1104.3^{de}	1230.9^{bc}	1270.1^{b}	1290.3^{b}	1384.6^{a}	884.0^{f}
1-Hexanol	841.5^{h}	1501.5^{f}	1080.4^{g}	1460.5^{f}	1846.7^{c}	2183.3^{b}	1692.2^{d}	1706.9^{d}	1706.8^{d}	1642.6^{e}	2283.6^{a}	1612.6^{e}
1-Propanol	56959.9^{a}	47812.5^{f}	54104.7^{b}	49766.8^{e}	52996.2^{c}	45607.5^{g}	49131.8^{e}	48167.9^{f}	49116.4^{e}	50812.2^{d}	49318.1^{e}	26875.6^{h}
2-Ethyl-1-hexanol*	15.6^{a}	14.7^{bc}	14.6^{bc}	13.0^{e}	15.2^{ab}	13.4^{de}	15.2^{ab}	12.9^{e}	11.6^{f}	13.5^{de}	14.0^{cd}	12.8^{e}
2-Phenylethanol	32201.7^{f}	37681.8^{d}	52428.6^{a}	34866.7^{e}	41423.8^{c}	32904.1^{f}	29774.7^{g}	42741.8^{b}	37251.4^{d}	31712.9^{f}	32921.7^{f}	13408.6^{h}
3-Methyl-1-butanol	276106.9^{a}	234186.8^{d}	251301.5^{b}	224669.4^{e}	251428.8^{b}	253766.0^{b}	209523.8^{f}	273692.9^{a}	235082.9^{d}	218217.3^{ef}	247630.6^{bc}	239248.6^{cd}
3-Octanol*	4.7^{c}	5.7^{ab}	1.3^{f}	6.0^{a}	2.4^{e}	3.4^{d}	5.1^{bc}	3.8^{d}	5.8^{ab}	1.6^{f}	1.1^{f}	3.4^{d}
4-Methyl-2-pentanol	135.0^{abc}	125.7^{bcd}	146.2^{ab}	130.2^{bc}	137.9^{abc}	50.5^{e}	111.6^{cd}	541^{e}	51.0^{e}	49.9^{e}	163.2^{a}	99.7^{d}
Benzyl alcohol*	81265.1^{a}	186.2^{b}	145.0^{b}	137.7^{b}	140.4^{b}	124.9^{b}	130.3^{b}	130.7^{b}	144.1^{b}	126.0^{b}	140.7^{b}	121.8^{b}
Isobutanol	33564.5^{c}	29631.1^{d}	54171.3^{a}	22617.3^{e}	11127.1^{f}	45359.6^{b}	10670.2^{f}	30535.8^{d}	10830.4^{f}	23521.0^{e}	44127.9^{b}	44940.4^{b}
Isoprenoids												
β-damascenone	15.4^{ab}	15.2^{abc}	15.8^{a}	15.8^{a}	13.1^{e}	14.6^{cd}	15.3^{ab}	15.5^{a}	14.7^{bc}	15.8^{a}	14.8^{bc}	14.0^{d}
1,8-Cineole	13.7^{b}	24.1^{a}	13.6^{b}	13.9^{b}	13.9^{b}	13.7^{b}	13.7^{b}	13.7^{b}	13.6^{b}	13.7^{b}	13.6^{b}	13.6^{b}
Acids												
3-methylbutanoic acid	1808.5^{a}	801.3^{b}	615.0^{c}	592.0^{cd}	546.7^{ef}	604.2^{c}	516.0^{fg}	614.2^{c}	557.0^{de}	779.7^{b}	610.3^{c}	503.3^{g}
Butanoic acid	43996.0^{a}	41386.9^{b}	40247.6^{b}	38666.5^{c}	26404.6^{e}	10012.4^{i}	31319.1^{d}	11405.8^{h}	23470.9^{f}	18068.9^{g}	12214.0^{h}	1928.2^{j}
Isobutyric acid	4051.7^{c}	2497.4^{e}	1895.4^{fgh}	2011.6^{f}	1681.6^{gh}	6453.4^{a}	1827.3^{fgh}	4468.1^{b}	1626.8^{h}	1964.2^{fg}	4541.1^{b}	3390.0^{d}
Others												
β-Ionone	92.7^{ab}	90.7^{cd}	91.7^{abcd}	91.8^{abcd}	90.2^{d}	92.4^{abc}	93.5^{a}	91.2^{bcd}	91.9^{abcd}	91.0^{bcd}	90.4^{d}	91.4^{bcd}

Data for each attribute are presented as mean values (n = 3); superscripted letters indicate significant differences amongst treatments ($p < 0.05$) based on one-way ANOVA with least significant difference (LSD) pairwise comparison.

* indicates that the concentrations obtained for these compounds were below the detection thresholds (detection thresholds listed in Table 2.3).

Based on PCA analysis performed on volatile compounds for yeast treatments, 55.67% of the variation was explained by the first two components, with similar clustering patterns to sensory analysis observed (Fig. 3.4). Specifically, yeasts producing wines evaluated with higher scores of fruity and floral notes in the sensory study were clustering, and more closely linked to volatiles with desirable characters, such as 2-phenylethanol recognised as floral and rosy (Flavornet). Further correlations and interpretations will be discussed in Section 4.3.

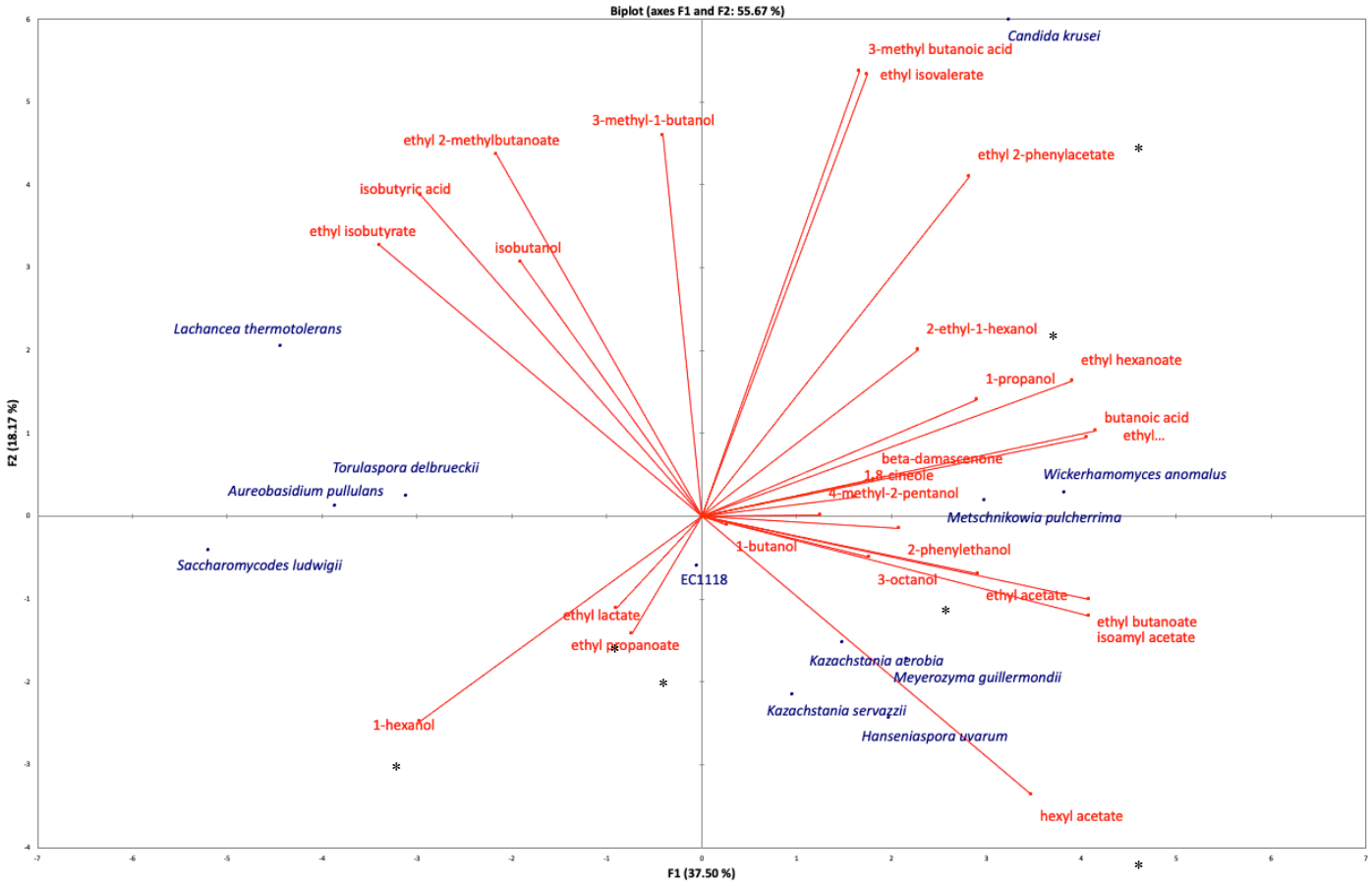

Figure 3.4 PCA biplot presenting scores and loadings of the standardised mean values for significant ($p < 0.05$) major volatile compounds (red) and different treatments (blue). *, concentrations of these compounds were below detection thresholds.

4 Discussion

4.1 Fermentation performance of different yeasts

More rapid fermenters were observed in a co-fermentation mode compared to the EC1118 monoculture. *S. ludwigii*, as an example, was reported to have similar fermentation ability in an 80 mL trial with *Vitis vinifera* L. *cv* Touriga Nacional, but the best results were obtained with the control *S. cerevisiae* QA23 monoculture (Esteves et al., 2019). *M. pulcherrima* also

exhibited comparable fermentation capacity with *S. cerevisiae* in a previous study (Sadoudi et al., 2017). Amongst the slow fermenters (*T. delbrueckii*, *L. thermotolerans* and *A. pullulans*) observed in this experiment, fermentation durations ranging from 9 to 25 days were reported for both *T. delbrueckii* and *L. thermotolerans*, depending on the strain, grape variety and fermentation volumes (Gobbi et al., 2013; van Breda et al., 2013; Belda et al., 2015; Mbuyane et al., 2018; Zhang et al., 2018), with slower fermentation rates reported for *L. thermotolerans* compared to other species (Benito, 2018).

High malic acid consumption extents were observed in several treatments (Fig. 4.1). Among them, 40.7% of malic acid was consumed by *M. guillermondii*, followed by *L. thermotolerans* at 27.4%, which is a known malic acid degrader and a high lactic acid producer (Benito et al., 2015; Hranilovic et al., 2018; Escribano et al., 2019). Substantial malic acid consumptions (~23.73%) was also observed for *A. pullulans* and *H. uvarum*, the latter of which was reported to exhibit similar malic acid-degrading capability in sequential inoculation with *S. cerevisiae* (Jood et al., 2017; Du Plessis et al., 2017). Further investigations for *M. guillermondii* and *A. pullulans* are encouraged due to the lack of available published data.

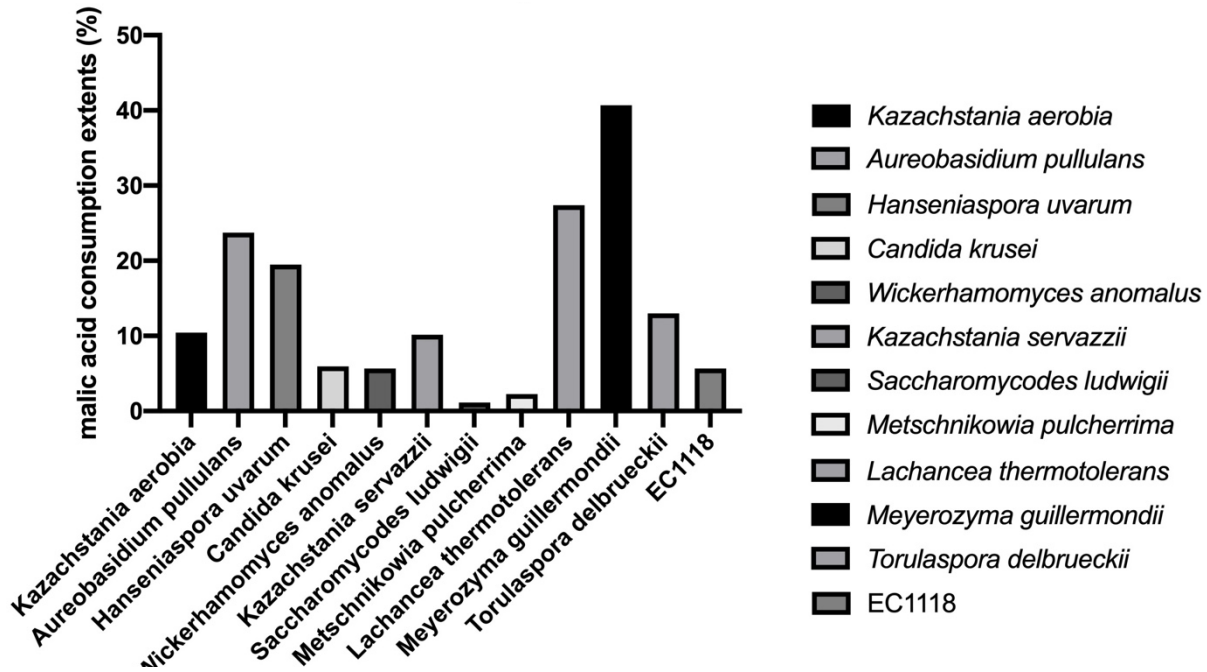

Figure 4.1 Malic acid consumption (Conc. $_{residual}$ / Conc. $_{original}$) for 12 treatments

Reduced alcohol production has become a research focus with the aim of catering for the increasing market demand for lower-alcohol beverages. *L. thermotolerans*, *T. delbrueckii*, *M. pulcherrima*, *S. ludwigii* and *H. uvarum* have all been reported to be capable of producing wines with markedly lower ethanol concentrations (i.e., ~1.6% decrease compared to monoculture of *S. cerevisiae*) from co-fermentations with *S. cerevisiae* compared with those from *S. cerevisiae* monocultures (Domizio et al., 2011; Belda et al., 2013; Gobbi et al., 2013; Contreras et al., 2014; Tristezza et al., 2016; Vejarano, 2018; Canonico et al., 2019). In contrast to these studies, results from the current study indicate statistically significant differences amongst treatments, although differences were small (i.e., at most 0.36% when comparing *W. anomalus* with EC1118). This suggests that net ethanol production might be dependent on multiple factors, the mechanisms being worthy of further investigation. On the other hand, the fact that the wines possessed similar ethanol levels implies that they present a similar matrix for sensory analysis, and that solvent properties should not significantly influence the headspace concentrations of the aroma compounds evaluated (Robinson et al., 2009; Villamor et al., 2013; King et al., 2013; Longo et al., 2017). Thus any sensory differences perceived can be considered genuine, with minimal influence from matrix effects.

4.2 Interpretation of IBMP concentrations

The IBMP concentrations obtained at two sampling points (i.e., at the start and finish of fermentation) were unexpected. Specifically, considerable variation was observed between IBMP concentrations measured at the first timepoint; concentrations ranged from 42.78-52.31 ng/L across treatments, despite each fermentation being spiked at 52 ng/L. Possible explanations for these differences include analytical errors during sample preparation and processing or rapid and differential adsorption of IBMP by the yeast inoculum. Based on the large standard deviations calculated for each treatment (~ 7.4 ng/L), it appears that analytical errors might be a significant contributor to concentration variations within and among treatments. On the other hand, adsorption might also explain decreased IBMP levels, particularly for treatments showing small differences (e.g., *M. pulcherrima*, 46.96-47.61 ng/L for replicates at the first sampling timepoint). Hence, both factors are proposed to be involved in the concentration variation observed at the first sampling timepoint.

Delta values (Conc. $_{Day0}$ − Conc. $_{finish}$) were used for pairwise comparisons, which were performed between treatments and the control, and between every two treatments to determine differences among yeast strains. No significant differences were observed between

treatments and the control, suggesting that the 11 non-*Saccharomyces* strains performed similarly to EC1118 with regards to influencing IBMP levels during fermentation. On the other hand, two groups of pairwise comparisons (*T. delbrueckii* and *K. aerobia*, *M. guillermondii* and *A. pullulans*) gave significantly different delta values (Table 4.1), indicating their putatively different impacts on IBMP concentrations.

Table 4.1 *p*-Values obtained from Student's *t*-test for pairwise comparison on delta values (Conc. $_{Day0}$ − Conc. $_{finish}$) between any two treatments

	K. a	*A. p*	*H. u*	*C. k*	*W. a*	*K. s*	*S. l*	*M. p*	*L. t*	*M. g*
K. a										
A. p	0.7434									
H. u	0.9904	0.3870								
C. k	0.9667	0.6909	0.9355							
W. a	0.1674	0.1618	0.1806	0.2576						
K. s	0.8938	0.4966	0.8074	0.8478	0.2962					
S. l	0.6151	0.8578	0.5578	0.3689	0.4546	0.6753				
M. p	0.3796	0.2887	0.1129	0.1213	0.5751	0.4035	0.4668			
L. t	0.6616	0.6127	0.4793	0.6009	0.9041	0.1250	0.8263	0.9694		
M. g	0.1085	**0.0232***	0.0652	0.1357	0.0880	0.0701	0.2307	0.1574	0.3851	
T. d	**0.0260***	0.1827	0.1660	0.1417	0.1987	0.2428	0.1067	0.1925	0.4990	0.6461

**p*-Values in bold indicate significant differences for IBMP delta concentrations between two treatments. Abbreviations: *K. a*, *Kazachstania aerobia; A. p, Aureobasidium pullulans; H. u, Hanseniaspora uvarum; C. k, Candida krusei; W. a, Wickerhamomyces anomalus; K. s, Kazachstania servazzii; S. l, Saccharomycodes ludwigii; M. p, Metschnikowia pulcherrima; L. t, Lachancea thermotolerans; M. g, Meyerozyma guillermondii; T. d, Torulaspora delbrueckii*.

Increased IBMP concentrations (statistically significant differences for *W. anomalus*, *S. ludwigii*, *M. pulcherrima*, *M. guillermondii*, *T. delbrueckii*) were observed in all finished wine samples (Table 3.3), with potential explanations investigated. Firstly, volume decrease due to evaporation during alcoholic fermentation could have led to such results, assuming that the absolute content of IBMP remained the same. Another hypothesis for increases in IBMP concentrations is production by yeasts. IBHP, the precursor of IBMP, was found in substantial quantities in harvested Cabernet Franc grapes (Ryona et al., 2010), suggesting the presence of IBHP in grape must. Additionally, putative methyltransferases, though not proven to be related to IBHP methylation, have been identified in *Saccharomyces cerevisiae* (Niewmierzycka and Clarke, 1999), which would also be required for this hypothesis to be

proven. Theoretically, however, the increase in IBMP content (~ 7.36 ng/L) observed in this experiment, accounted for only 3.13% of the IBHP pool reported for harvested Cabernet Franc grapes (Ryona et al., 2010). A similar investigation into a putative IBMP-producing ability of commercial wine yeasts during fermentation was conducted and no increase in IBMP concentration was observed (Harris, 2012), which further suggests that the increases in IBMP concentration seen in the experiments reported here were not due to yeast activity.

A follow-up trial was performed for further validation. Based on Student's *t*-test performed within each treatment on IBMP concentration changes during fermentation (Table 4.2), and the standard deviations for each treatment (Table 3.3), *W. anomalus* and *M. guillermondii* were selected. Grape juice was used with sterilisation for a targeted investigation, and the fermentation was performed at a 100 mL scale, with shaking and at the same fermentation temperature. Different fermentation kinetics were observed potentially due to the compositional changes of fermentation matrices. Nevertheless, no significant differences in IBMP concentrations (either increases or decreases) were observed compared to the control were observed. Decreased concentrations were noticed in all groups, potentially due to volatilisation by flask shaking during fermentation, which was supported by the similar extent of decline observed in the blank where no fermentation had occurred.

Table 4.2 *p*-Values obtained from Student's *t*-test on IBMP concentration variations within each treatment during first batch of fermentation

Treatment	*p*-value
Kazachstania aerobia	0.5751
Aureobasidium pullulans	0.1588
Hanseniaspora uvarum	0.3915
Candida krusei	0.3322
Wickerhamomyces anomalus	**0.0017***
Kazachstania servazzii	0.7993
Saccharomycodes ludwigii	**0.0146***
Metschnikowia pulcherrima	**0.0002***
Lachancea thermotolerans	0.2871
Meyerozyma guillermondii	**0.0050***
Torulaspora delbrueckii	**0.0230***
EC1118	0.5079

*p-Values in bold indicate significant differences for IBMP concentration variations within each treatment during fermentation.

This follow-up experiment indicated that IBMP production by yeasts during fermentation was unlikely to occur in significant amounts. Therefore, the reasons for the slight increase of IBMP concentrations in wines between inoculation and completion were concluded to be a result of volume loss during fermentation or analytical errors or both. Further work along these lines must therefore first secure a robust, accurate and reproducible analytical method for fermentation samples.

4.3 Sensory analysis

Despite the insignificant effects from yeast strains on IBMP content during fermentation, wine, as a complex matrix, comprises an array of flavour compounds that interact in a sophisticated manner to influence overall sensory quality. Therefore, an investigation of the impact of the different yeasts on wine sensory profiles was included to enable a more comprehensive evaluation of yeast performance. Diverse aroma profiles, including perception of green characters, were obtained via sensory analysis of wines from the different treatments were obtained from sensory study. The PCA plot (Fig. 3.3) and sensory data (Table 3.6) suggested that aroma attributes for these wines were clustered by yeast treatments, the majority of which were perceived by the RATA panel to be significantly different.

A range of green characters, typically associated with IBMP, were specifically included as descriptions that participants were asked to evaluate. Despite the non-significant differences in IBMP concentrations of these wines, statistically significant differences were observed for 5 out of 7 relevant attributes, amongst different treatments based on sensory analysis. The reason was proposed to be an aroma masking effect. Such an effect between fruity and vegetal attributes has been investigated in a relevant study in Cabernet Sauvignon wine (Hein et al., 2009). This work, focusing on the sensory perspective, revealed the interactive masking effect of both vegetal and fruity characters. Specifically, decreased perceptions of aroma intensities for either spectrum of attributes were observed due to the addition of flavouring compounds of the opposing characters. It was proposed that the overall aroma profile was driven by green characters in the presence of high levels of green capsicum aroma (mainly IBMP), and yet the intensity of this perception could have been diminished by elevated fruity characters. Similar sensory effects were observed in this experiment, though not in the same

wine matrices. These findings form a useful starting point for future and more in-depth research.

Treatments were noticeably discriminated, with three clusters identified in the PCA plot (Fig. 3.3), including: a group with fruit-forward aromas; one with prominent green characters; and *W. anomalus*, which was characterised by a strong solvent odour that dominated other attributes. Juice fermented using EC1118, the popular commercial *S. cerevisiae* strain, as the control, resulted in wine that was classified in the vegetative cluster, with higher scores for green characters rather than fruity aromas. Juices fermented with yeasts that resulted in wines with favourable fruity aroma attributes included *C. krusei*, *K. aerobia*, *H. uvarum*, *K. servazzii*, *M. guillermondii* and *M. pulcherrima*, with the rest exhibiting more pronounced green characters. According to the heatmap representing scores obtained for attributes of each yeast (Fig. 4.1), greenness was perceived as fairly evident for all treatments, but at significantly different levels. Based on the non-discrimination observed for wine IBMP concentrations, it was thereby reasoned that variation in the perception of green characters was largely due to different intensities of fruity aromas amongst the treatments, in agreement with the Hein's et al (2009) study.

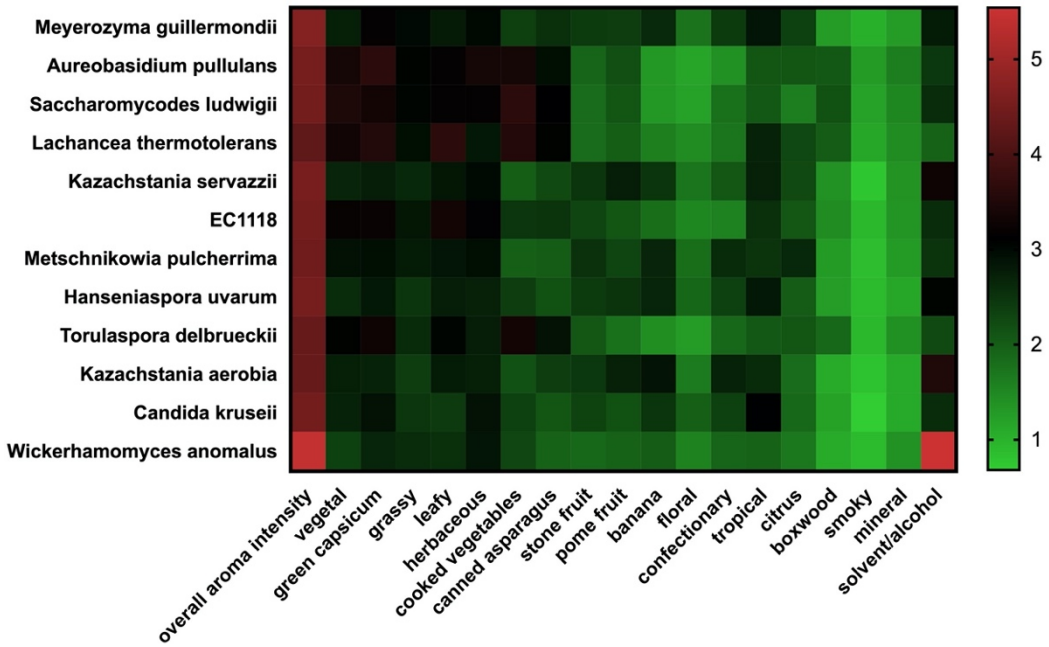

Figure 4.1 Heat map of sensory scores for each aroma character amongst treatments and the control.

Volatile profiles were obtained for the 12 wines to further validate the proposed aroma masking effect. Based on the partial least squares regression (PLS-R) analysis (Fig. 4.2), wine volatile compositional data, sensory data and yeast treatments were related to investigate the underlying relationships. Such a method has been applied to evaluate multiple variables in a wine matrix (Benkwitz et al., 2012; Wang et al., 2016; Liang et al., 2018). The first two components accounted for 27.9% of volatile compounds (*x*-variables), and 13.8% of sensory data (*y*-variables). Yeasts (*K. servazzii, M. pulcherrima, K. aerobia, H. uvarum, M. guillermondii*) clustered for fruity and floral attributes in PCA analysis for sensory data (Fig. 3.3), were observed with similar patterns in PLS-R analysis (Fig. 4.2), more linked to the relevant aroma attributes and volatile compounds, such as 2-phenylethanol, β-damascenone and ethyl propanoate. Similar trends were observed with the 'green-clustered' group (i.e., treatments evaluated with higher scores for green characters; *L. thermotolerans, T. delbrueckii, A. pullulans, S. ludwigii*) in both PLS-R plot (Fig. 4.2) and PCA analysis for volatile compounds (Fig. 3.5). Specifically, fewer fruity attributes (except citrus character) and desirable aroma compounds were linked with this cluster, indicating fewer masking effects from fruity characters. Interestingly, 1-hexanol, a C6 alcohol sensorially related to green characters in wine, was identified to be linked to the 'green-clustered' group though concentrations below the detection threshold were observed.

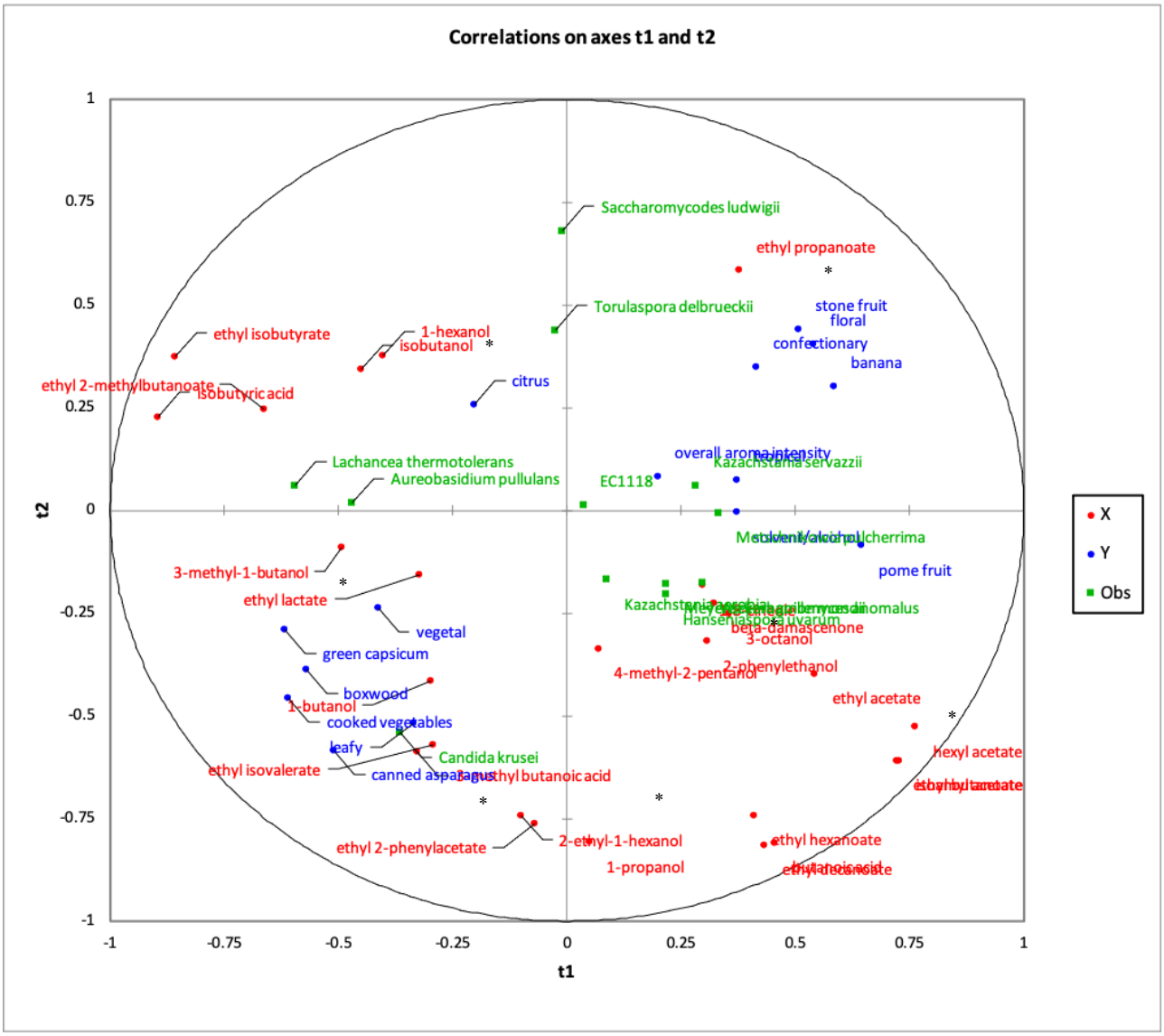

Figure 4.2 PLS regression plot of standardised mean values for significant ($p < 0.05$) wine volatile compounds (*x*-variables, red) and standardised mean values for significant ($p < 0.05$) sensory characters (*y*-variables, blue). Treatments are shown in green. *, concentrations of these compounds were below detection thresholds.

Analysis of other volatile compounds validated the masking effects. Specifically, the increased production of desirable aroma compounds by some yeasts explains the masking of green characters due to IBMP. For *L. thermotolerans, T. delbrueckii, A. pullulans, S. ludwigii*, for which pronounced green characters were perceived in the final wines, lower production of volatiles associated with fruity/floral attributes was observed, and therefore, less effective masking. Additionally, the putative contribution of 1-hexanol to the overall perception of green character is worth further investigation. It should also be acknowledged that correlations are proposed in this experiment, and that spiking studies would be needed to further support the hypothesis.

5 Conclusions

As a microbiological post-harvest approach to mitigating green characters in wine, this chapter explored the effects of 11 non-*Saccharomyces* yeasts on IBMP levels and the sensory profiles of wines, following fermentation. Despite non-significant differences in IBMP concentrations being observed amongst treatments, sensory analysis (using the RATA method) indicated that some wines, i.e., those produced by *K. servazzii, M. pulcherrima, K. aerobia, H. uvarum, M. guillermondii* and *C. krusei*, yielded more intense fruity and floral characters, which seemingly masked green, vegetal notes. In contrast, wines from *L. thermotolerans, T. delbrueckii, A. pullulans, S. ludwigii* and EC1118 were found to exhibit more pronounced greenness. A potential masking effect was therefore proposed whereby fruit/floral-forward characters decreased the perception of green notes. Various volatiles compounds were measured by GC-MS to validate this hypothesis. PCA of GC-MS data and PLS-R analysis of chemical and sensory data supported the sensory results. This suggested that treatments with more intense fruit notes were more closely associated with volatiles that impart pleasant aromas, rather than volatiles and sensory attributes ‘greenness’.

As a pilot fermentation trial, masking of IBMP-related sensory characters was achieved and may prove to be a feasible approach for Sauvignon Blanc winemaking to mitigate the perception of greenness. It should be acknowledged that this result is likely to be highlight variety-dependent, and diverse aroma precursors present in other varieties may lead to different aroma profiles obtained in wine, which may interact differently with green characters, thereby yielding different results. Further work needs to be undertaken to map the profile of yeast and variety interactions for the purpose of masking green characters.

Chapter 3 Screening for Microbial Degradation of IBMP

1 Introduction

1.1 Metabolism of 3-isobutyl-2-methoxypyrazine

Methoxypyrazines (MPs) are a group of naturally occurring compounds with aromas often reminiscent of vegetative or earthy notes. Buttery et al. (1969) first linked 3-isobutyl-2-methoxypyrazine (IBMP) with green bell pepper-like aromas and indicated their extremely low odour threshold. These compounds have been widely studied in the food industry due to their strong influence on the olfactory profile and much in-depth work has been performed, especially in the wine industry, because of their contributions to the green character of some grape varieties (Allen et al., 1991). It is therefore crucial to study the dynamics of MP accumulation and degradation in order to understand and manage MP concentrations in wine. The mechanisms of metabolism of these compounds have been studied widely, however, more work is needed to fully delineate these pathways. Among these compounds, a chemical synthesis pathway of IBMP proposed by Buttery et al. (1969), inspired by the work of Jones (1949) on hydroxypyrazine synthesis, is shown in Figure 1.1 and is proposed to be achieved from leucine as follows: a reaction between leucine, anhydrous HCl and methanol yields its methyl ester; reaction with anhydrous ammonia in methanol yields leucine amide; condensation with glyoxal transforms the amide to 3-isobutyl-2-hydroxypyrazine; methylation with diazomethane yields 3-isobutyl-2-methoxypyrazine. It was proposed that the biosynthesis of 3-isobutyl, *sec*-butyl and isopropyl-2-methoxypyrazines starts with leucine, isoleucine and valine (structures shown in Figure 1.2), respectively, due to the similarities in the alkyl groups of these compounds (Murry and Whitfield, 1975), but further validation is required. A biosynthesis scheme (Figure 1.3) was also proposed by Murray et al. (1970) and Gallois et al. (1988) suggesting the production of 3-alkyl-2-methoxypyrazine derives from the condensation of α-amino acids with α, β-dicarbonyl compounds. However, this putative pathway was challenged, as neither the amides of the common α-amino acids nor glyoxal were ever found naturally (Nursten and Sheen, 1974). Gallois et al. (1988) subsequently suggested the reaction of amides with dicarbonyl groups was chemically unlikely to occur. The hypothesis has since been disputed, whereas the precursor to IPMP was confirmed to be valine. Specifically, feeding *Pseudomonas taetrolens* and *Pseudomonas perolens* with ^{13}C labelled valine produced ^{13}C labelled IPMP, although the origin of C5 and

C6 remained ambiguous, but is less likely to be from glyoxal as previously proposed (Gallois et al., 1988; Leete et al., 1992).

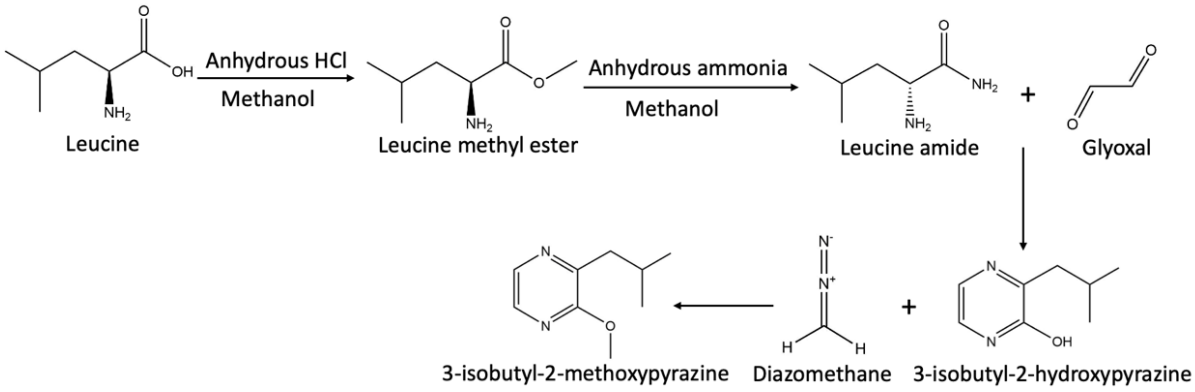

Figure 1.1 Proposed chemical synthesis pathway of IBMP. (Jones, 1949; Buttery et al., 1969)

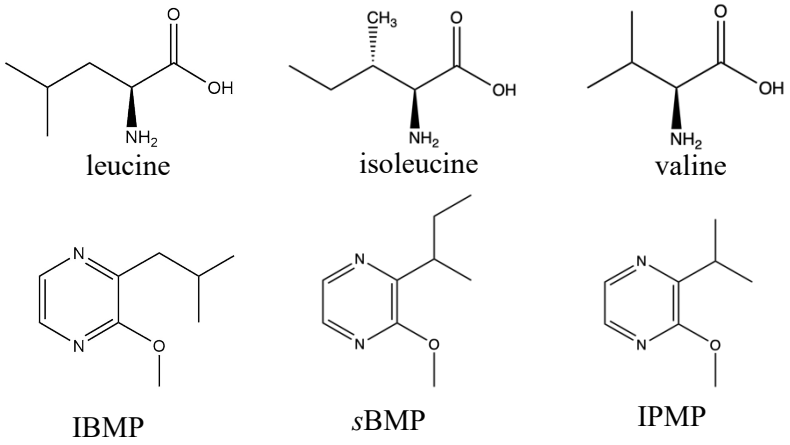

Figure 1.2 Structures of three major MPs and their hypothetical precursors.

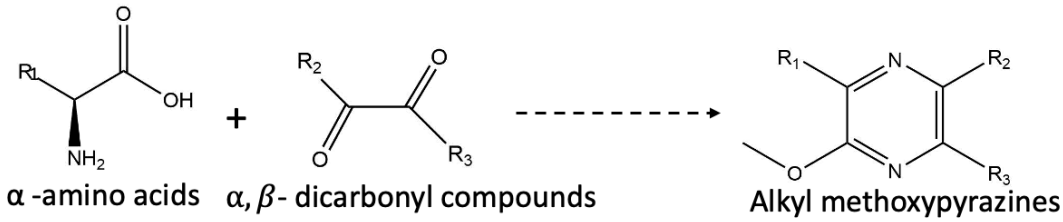

Figure 1.3 Proposed biosynthesis pathway for alkyl methoxypyrazines. (Murray et al., 1970; Gallois et al., 1988)

The final step of the biosynthesis, which involves the *O*-methylation of 3-alkyl-2-hydroxypyrazines to form 3-alkyl-2-methoxypyrazines has been confirmed and the responsible enzymes have been characterised. Hashizume et al. (2001) purified and characterised from *Vitis vinifera* L. *cv*. Cabernet Sauvignon an *S*-adenosyl-L-methionine-dependent *O*-methyltransferase capable of methylating 3-isopropyl/isobutyl-2-hydroxypyrazine to 3-isopropyl/isobutyl-2-methoxypyrazine. Genes encoding four *O*-methyltransferases (VvOMT1, VvOMT2, VvOMT3, VvOMT4) were later cloned from Cabernet Sauvignon following expression *in vitro*, their 3-alkyl-2-hydroxypyrazine methylation ability confirmed. Kinetic studies showed different substrate affinities for each enzyme, of which VvOMT1 and VvOMT2 showed greater methylating activity towards quercetin, resveratrol, caffeic acid, epicatechin and catechin than IBHP and IPHP. On the other hand, QTL analysis together with quantitative real-time PCR studies on *VvOMT3* and *VvOMT4* genes in the high IBMP producer, Cabernet Sauvignon, and low producer, Pinot Noir, indicated VvOMT 3 and, to a lesser extent, VvOMT4 are key enzymes in the last step of IBMP biosynthesis in grape berries (Dunlevy et al., 2010; Guillaumie et al., 2013).

By comparison, the degradation pathways of MPs remain unclear and some studies propose hypotheses that need more research for confirmation. Hawksworth et al. (1975) explored the metabolic fate of alkyl- and alkoxy-substituted pyrazines in rats by feeding the rats with these compounds and analysing urinary and biliary metabolites. Degradation patterns varied for different substrates, namely, ring hydroxylation and *O*-demethylation occurred for 2-methoxypyrazine, whereas no evidence for demethylation by intestinal bacteria was observed. For the bell pepper compound IBMP, IBHP was believed to be the major metabolite, though aliphatic side-chain oxidation also occurred to a minor degree. In grapes or other plants, no degradation metabolites of MPs have been reported, yet it is hypothesised that demethylation of IBMP to IBHP occurs during berry ripening, but the lack of an inverse correlation in concentrations of MPs and HPs during ripening argue against this hypothesis (Ryona et al., 2010; Harris et al., 2012).

1.2 Microbial degradation/transformation of pyrazines and methoxylated compounds

Since there are currently no reports on microbial MP degradation, it is worth reviewing the metabolism of other compounds with similar structures to shed light on the possible degradation pathways of IBMP.

Microbes have been widely studied for their abilities to degrade or transform alkyl pyrazines (Table 1) and some are utilised as cell factories to produce chemical compounds. A biotransformation study was conducted on resting cells of strain DMS 6920 of *Ralstonia*/*Burkholderia* sp. bacteria. Cells were first induced for 6-methylnicotinate-2-oxidoreductase activity before being incubated with different heterocyclic compounds, to reveal the strain's ability to hydroxylate pyrazine-2-carboxylic acid, 5-methylpyrazine-2-carboxylic acid and 5-chloropyrazine-2-carboxylic acid to produce 3-hydroxypyrazine-2-carboxylic acid, 3-hydroxy-5-methylpyrazine-2-carboxylic acid, and 3-hydroxy-5-chloropyrazine-2-carboxylic acid, respectively, with the production yields ranging from 50-74% (Tinschert et al., 2000). More hydroxylations of various pyrazine derivatives as either bioconversions or with an intermediate within a degradation pathway were discovered (Mattey and Harle, 1976; Kiener, 1993; Kiener et al., 1993A, 1993B; Kiener et al., 1994; Uchida et al., 2003; Rappert et al., 2006). Other types of biotransformation were identified as well, such as in the metabolically versatile *Pseudomonas putida* strain ATCC 33015 shown to oxidise methylated heterocyclic rings including 2,5-dimethylpyrazine, 2,3,6-trimethylpyrazine and 3-chloro-2,5-dimethylpyrazine to their corresponding monocarboxylic acids when grown on *p*-xylene (Kiener, 1992; Schmid et al., 2001). Hydroxypyrazine was metabolised aerobically by *Pseudomonas* PZ3 isolated from rat faeces, hypothesised to occur via the general pattern of aromatic ring oxidation by *Pseudomonas* species, namely, dihydroxylation, possibly to 2,6-dihydroxypyrazine, followed by ring cleavage by an oxygenase (Mattey and Harle, 1976).

Table 1.1 Bioconversion of pyrazines and derivatives

Substrates	Products	Organisms	Reference
Hydroxylation			
Pyrazine-2-carboxylic acid 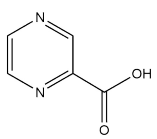	3-Hydroxypyrazine-2-carboxylic acid 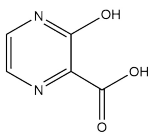	*Ralstonia*/*Burkholderia* sp. strain DSM 6920	Tinschert et al., (2000)
5-Methylpyrazine-2-carboxylic acid 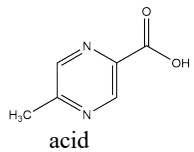	3-Hydroxy-5-methylpyrazine-2-carboxylic acid 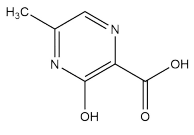		

5-Chloropyrazine-2-carboxylic acid 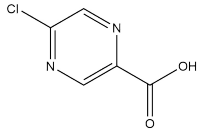	3-Hydroxy-5-chloropyrazine-2-carboxylic acid 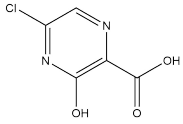		
2,5-Dimethylpyrazine 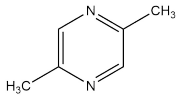	2,5-Dimethyl-3-hydroxypyrazine 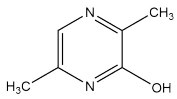	*Rhodococcus erythropolis* DSM 6138 *Arthrobacter* sp. DSM 6137	Kiener et al., (1993)
2-Methylpyrazine 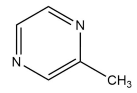	3-Hydroxy-2-methylpyrazine 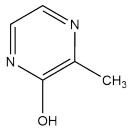		
2-Chloropyrazine 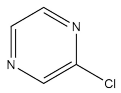	3-Hydroxy-2-chloropyrazine 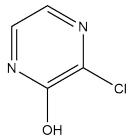		
2-Ethylpyrazine 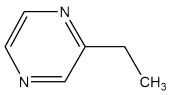	3-Hydroxy-2-ethylpyrazine 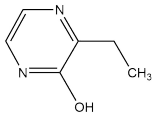		
2,6-Dimethylpyrazine 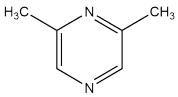	3-Hydroxy-2,6-dimethylpyrazine 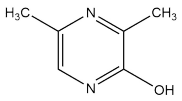		
2,5,6-Trimethylpyrazine 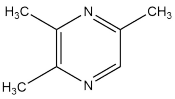	3-Hydroxy-2,5,6-dimethylpyrazine 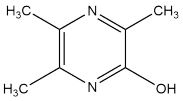		
6-Chloro-2,5-dimethylpyrazine 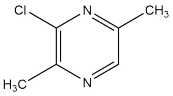	3-Hydroxy-6-chloro-2,5-dimethylpyrazine 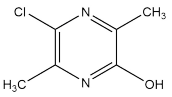		
2-Methyl-quinoxaline 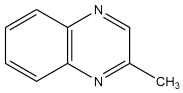	3-Hydroxy-2-methylquinoxaline 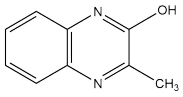		
Pyrazine-2,3-dicarboxylic acid 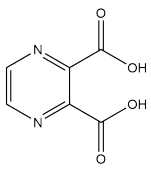	5-Hydroxypyrazine-2,3-dicarboxylic acid 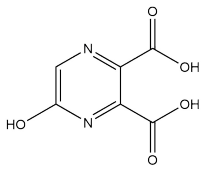	*Alcaligenes sp*. strain UK21	Uchida et al., (2003)

Pyrazine-2,3-dicarbonitrile 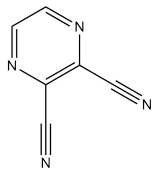	5-Hydroxypyrazine-2,3-dicarbonitrile 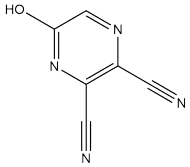		
Pyrazine-2-carboxylic acid 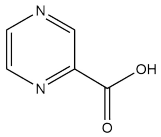	5-Hydroxypyrazine-2-carboxylic acid 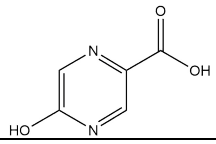	*Pseudomonas acidovorans* DSM 4746 and *Alcaligenes faecalis* DSM 6269	Kiener et al., (1994)
Hydroxypyrazine 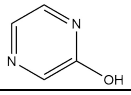	2,6-Dihydroxypyrazine 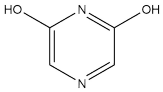	*Pseudomonas* PZ3	Mattey and Harle (1976)
3-Chloropyrazine 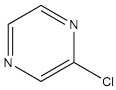	3-Chloro-2-hydroxypyrazine 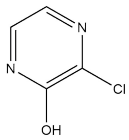	*Agrobacterium* sp. DSM 6136	Kiener et al., (1993)
2-Methylpyrazine 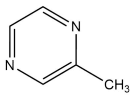	2-Hydroxy-6-methylpyrazine 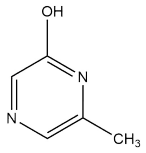		
2-Ethylpyrazine 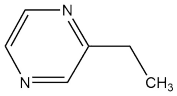	6-Ethyl-2-hydroxypyrazine 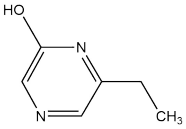		
2,3-Dimethylpyrazine 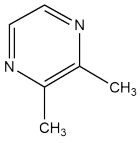	2-Hydroxy-5,6-dimethylpyrazine 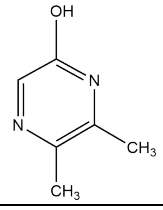		
Pyrazine carboxylic acid 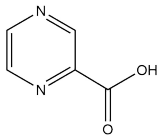	5-Hydroxypyrazinecarboxylic acid 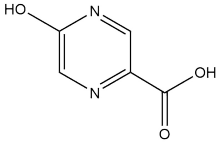	*Pseudomonas acidovorans* DSM 4746, *Pseudomonas putida* NCIB 10521, *Pseudomonas putida* NCIB 8176, *Achromobacter xylosoxydans* DSM 2402, *Achromobacter xylosoxydans* DSM 2783	Kiener (1993)

2,3-Diethyl-5-methylpyrazine 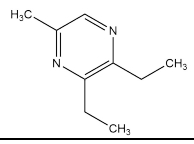	5,6-Diethyl-2-hydroxy-3-methylpyrazine 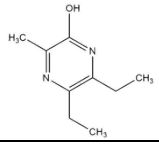	*Mycobacterium* sp. DM-11	Rappert et al., (2006)
Oxidation			
2,5-Dimethylpyrazine 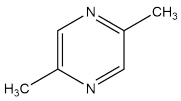	5-Methylpyrazine-2-carboxylic acid 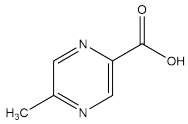	*Pseudomonas putida* ATCC 33015	Kiener et al., (1992); Schmid et al., (2001)
2,3,6-Trimethylpyrazine 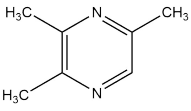	5,6-Dimethylpyrazine-2-carboxylic acid 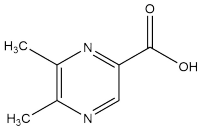		
3-Chloro-2,5-dimethylpyrazine 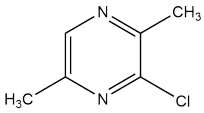	6-Chloro-5-methylpyrazine-2-carboxylic acid 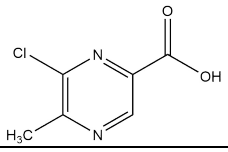		
Others			
2-Cyanopyrazine 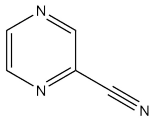	5-Hydroxypyrazine-2-carboxylic acid 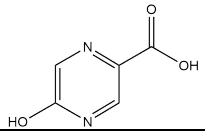	*Agrobacterium* sp. DSM 6336	Wieser et al., (1997)

Microbial bioconversion/degradation of methoxylated compounds and other compounds with a methyl moiety which present similar chemical structures, have therefore been investigated in various studies as extensively reviewed in the previous chapter. Despite the fact that there are currently no experimental findings concerning methoxypyrazine biodegradation/bioconversion, microbial transformation and degradation of IBMP analogues has therefore been reviewed due to the potential opportunities that may arise from these related studies, including around sampling and cultivation methods.

1.3 Aims

As has been mentioned in the previous chapter, IBMP is a naturally occurring aroma compound present in some cultivars of wine grapes, and their resultant wines, where it imparts an aroma reminiscent of bell pepper or green capsicum. High concentrations due to an early harvest or a cool climate during growth may be deleterious to wine quality, thus making it necessary to identify remediation methods, which are currently lacking, especially those applicable postharvest. Chapter 3 presented work on fermentation trials with wine-

related non-*Saccharomyces* yeasts in IBMP-spiked grape musts, and results revealed several promising strains apparently able to reduce the perception of IBMP. Given that no significant differences in IBMP concentrations were observed in any yeast-treated wines, the effect is proposed to be one of masking of IBMP, rather than degradation of IBMP.

Despite this promising result, the objective of identifying a strain that specifically diminishes IBMP concentrations remains to be accomplished. As such, the work described in this chapter sought to broaden the search for a microbial source of IBMP-modulating capability by exploring environmental samples as well as laboratory collections of further wine-related yeasts and bacteria. These microbes would ideally have been investigated for their abilities to degrade IBMP that was provided with at various, ideally nutritionally relevant, levels. But given the potent odourous nature of IBMP, as well as the absence of a quick analytical method, non-odourous analogues were selected based on their structural similarity, namely, possession of a methyl moiety, and used as substrates for higher-throughput screening. The principle followed was to use microbial growth or colour changes as indicators of the degradation of such analogues by potential demethylases, and to subsequently test these strains specifically for IBMP degradation.

2 Materials and methods

2.1 Chemicals, solutions and media

A list of the solutions and media used for this section of work, along with their formulations is listed in Table 2.1.

Table 2.1 Solutions and basic growth media used in this study

Solution/Medium	Components
1× Phosphate buffered saline (PBS)	137 mM NaCl, 2.7 mM KCl, 10 mM Na_2HPO_4, 1.8 mM KH_2PO_4, pH 7.4
Mineral salt medium	(per litre of deionised water) 2.5 g K_2HPO_4, 1.0 g KH_2PO_4, 2.0 g $(NH_4)_2SO_4$, 0.9 g glucose, 0.2 g $MgSO_4 \cdot 7H_2O$, pH 6.75
Nitrogen-free-mineral salt medium	(per litre of deionised water) 2.5 g K_2HPO_4, 1.0 g KH_2PO_4, 0.9 g glucose, 0.2 g $MgSO_4 \cdot 7H_2O$, pH 6.75
Carbon-free mineral salt medium	(per litre of deionised water) 2.5 g K_2HPO_4, 1.0 g KH_2PO_4, 2.0 g $(NH_4)_2SO_4$, 0.2 g $MgSO_4 \cdot 7H_2O$, pH 6.75

Nutrient-free mineral salt medium	(per litre of deionised water) 2.5 g K_2HPO_4, 1.0 g KH_2PO_4, 0.2 g $MgSO_4 \cdot 7H_2O$, pH 6.75
1000× Trace metals mix solution	50 mL 0.1 M $FeCl_3$ dissolved in 0.1 M HCl, 2 mL 1M $CaCl_2$, 1 mL 1 M $MnCl_2 \cdot 4H_2O$, 1 mL 1 M $ZnSO_4 \cdot 7H2O$, 1 mL 0.2 M $CoCl_2 \cdot 6H_2O$, 2 mL 0.1 M $CuCl_2 \cdot 2H_2O$, 1mL 0.2 M $NiCl_2 \cdot 6H_2O$, 2 mL 0.1 M $NaMoO_4 \cdot 5H_2O$, 2 mL 0.1 M $Na_2SeO_3 \cdot 5H_2O$, 2 mL 0.1 M H_3BO_3, add water to make up to 100 mL
Nutrient medium	(per litre of deionised water) 5 g peptone, 3 g yeast extract, 5 g NaCl, pH 6.8
IBMP-mineral salt agar	(per litre of deionised water) 2.5 g K_2HPO_4, 1.0 g KH_2PO_4, 0.2 g $MgSO_4 \cdot 7H_2O$, ~1 mM IBMP, pH 6.75
IBMP stock solution A (2 mM)	6.7 µL of 99.9% 3-isobutyl-2-methoxypyrazine solution, add water to make up to 20 mL
IBMP stock solution B (200 µM)	1.5 mL of stock solution A, add water to make up to 15 mL
Citrate/phosphate buffer for GC-MS analysis	100 mM $NaHPO_4$, 50 mM citric acid, pH 5.0
1× TAE buffer	40 mM Tris base, 20 mM acetic acid, 1 mM EDTA sodium salt dihydrate
5× loading buffer (for DNA electrophoresis)	50% (v/v) glycerol, 10% (w/v) SDS, 1.25 M Tris-HCl, 5% (v/v) β-mercaptoethanol, 0.025% (w/v) bromophenol blue, pH 6.8
YEPD medium	(per litre of deionised water) 10 g yeast extract, 20 g peptone, 20 g glucose
MRSAJ medium	(per litre of deionised water) 23 g MRS Broth powder, 20 mL MRS supplement, 100 mL apple juice (contains 0.8 g/L malic acid), 2.12 g malic acid, 21.6 mg natamycin

2.2 IBMP screening of environmental samples

2.2.1 Sample collection

Creek water (3 tubes) and creek sediment (3 tubes) were collected into sterile 50 mL tubes from Brown Hill Creek (SA 5062; 34.983816°S, 138.625437°E). Vineyard soil (5-10 cm of

top layer soil were removed before sampling), grape berries and unripe fig were collected into sterile 50 mL tubes from the vineyard and orchard located at the University of Adelaide, Waite Campus (SA 5064; 34.967341°S, 138.633784°E). Animal (mouse, koala, pigeon) faeces were collected from the ground at the University of Adelaide. For soil, grape berries, unripe fig and animal faeces, samples were washed with 1× PBS buffer before inoculation. Samples and washed buffer were stored at 4 °C until further use.

2.2.2 Screening with IBMP

Liquid samples (3 mL) or washed buffer were inoculated into 100 mL mineral salt medium/nitrogen-free mineral salt medium/carbon-free mineral salt medium/nutrient-free mineral salt medium, and substrate (3-isobutyl-2-methoxypyrazine) was provided at 1 μM as a supplement/nitrogen source/carbon source/sole nitrogen and carbon source, accordingly. Higher concentrations of IBMP compared to those used in Chapter 2 were applied in this experiment, since it was required as a nutrient in amounts that could result in observable differences in culture density. For negative controls, the same volumes of samples were autoclaved to denature. The cultures were incubated at room temperature (20 °C) with shaking (140 rpm) in specially customised Erlenmeyer flasks (Fig. 2.1) designed for easy sample collection without IBMP loss. Culture samples were taken at intervals during incubation for SPME-GC-MS analysis to monitor IBMP degradation during incubation.

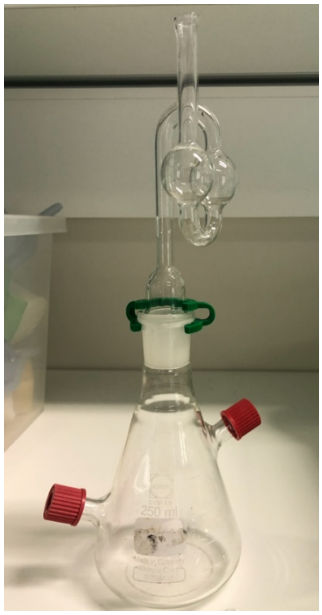

Figure 2.1 Customised Erlenmeyer flask

2.2.3 SPME-GC-MS quantification of IBMP

IBMP was quantified using the method adapted from Dunlevy et al. (2010) as described in Chapter 2. Cultures were diluted 100-fold with ultrapure water, 1 mL of which was added to 9 mL of citrate/phosphate buffer and dosed with 100 µL of 5 µg/L d_3-IBMP (CDN Isotopes, Quebec, Canada) as the internal standard. The solution was transferred to a 20 mL brown-glass headspace vial with 3 g of NaCl. Samples were analysed directly after sample preparation. For a detailed description of the rest of the analysis, including instrument operating parameters, please see Section 2.4 in Chapter 2.

2.2.4 Isolation and characterisation of microbes

According to the GC-MS results, the two most promising samples cultivated in nutrient-free mineral salt medium were derived from vineyard soil and creek sediment; these were subsequently used as inoculum for enrichment in nutrient medium with incubation at room temperature for 7 days. Enrichment cultures were then plated onto IBMP-mineral salt agar (IBMP as sole carbon and nitrogen sources in experimental groups, whereas neither IBMP nor other nutrients were added to control groups) with two different plating methods (spread plating and pour plating) to assess the oxygen requirement of the microbes.

Colonies growing in IBMP-mineral salt plates were dug out and plated onto nutrient agar and incubated at room temperature for 5 days. Isolated colonies were re-plated onto IBMP-mineral salt plates before further steps to confirm that they matched those in the original IBMP-mineral salt plates. Colonies were picked and their morphology checked microscopically.

2.2.5 Liquid cultivation

Microbes were cultivated in nutrient medium at 28 °C and genomic DNA was extracted for 16s rRNA PCR and sequencing. Cultures were re-inoculated into IBMP-mineral salt liquid media and samples were collected at the beginning and end of incubation for GC-MS analysis.

2.3 Alternative substrate screening with the laboratory collection of fungi and bacteria

2.3.1 Fungal isolate screening

Methyl leucine, vanillin, 2-methoxypyrazine and methyl violet, which share a structural similarity to IBMP by containing a methyl moiety, were selected as substrates with less

potent aroma for screening experiments with a collection of (mostly wine-related) fungi. These compounds were used for different nutritional purposes. Specifically, vanillin and 2-methoxypyrazine were used as carbon sources, methyl leucine as a nitrogen source and methyl violet as a supplement. Growth assays were conducted on a microplate scale (200 µL).

Mineral salt medium was modified as follows (Table 2.2, 2.3) for optimal growth to study the potential nutrient consumption by fungi.

Table 2.2 Modified mineral salt media for screening with methyl leucine

Medium	Ingredients (in deionized water; % w/v)	Notes
Methyl leucine mineral salt medium	**1% methyl leucine, 2% glucose**, 0.25% K_2HPO_4, 0.1% KH_2PO_4, 0.02% $MgSO_4 \cdot 7H_2O$, pH 6.75	methyl leucine as the sole nitrogen source
Carbon-free mineral salt medium	**1% methyl leucine**, 0.25% K_2HPO_4, 0.1% KH_2PO_4, 0.02% $MgSO_4 \cdot 7H_2O$, pH 6.75	methyl leucine as sole nutrient source
Carbon-free mineral salt medium	**1% leucine**, 0.25% K_2HPO_4, 0.1% KH_2PO_4, 0.02% $MgSO_4 \cdot 7H_2O$, pH 6.75	leucine as sole nutrient source
Nitrogen-free mineral salt medium	**2% glucose**, 0.25% K_2HPO_4, 0.1% KH_2PO_4, 0.02% $MgSO_4 \cdot 7H_2O$, pH 6.75	glucose as sole nutrient source
Nutrient mineral salt medium	**1% leucine, 2% glucose**, 0.25% K_2HPO_4, 0.1% KH_2PO_4, 0.02% $MgSO_4 \cdot 7H_2O$, pH 6.75	positive control

Table 2.3 Modified media for screening with vanillin/2-methoxypyrazine

Medium	Ingredients (in deionized water)	Notes
Vanillin/2-methoxypyrazine mineral salt medium	**1% vanillin/2-methoxypyrazine, 0.6% ammonium sulfate**, 0.25% K_2HPO_4, 0.1% KH_2PO_4, 0.02% $MgSO_4 \cdot 7H_2O$, pH 6.75	vanillin/2-methoxypyrazine as sole carbon source
Carbon-free mineral salt medium	**0.6% ammonium sulfate**, 0.25% K_2HPO_4, 0.1% KH_2PO_4, 0.02% $MgSO_4 \cdot 7H_2O$, pH 6.75	ammonium sulfate as sole nutrient source
Nitrogen-free mineral salt medium	**1% vanillin/2-methoxypyrazine**, 0.25% K_2HPO_4, 0.1% KH_2PO_4, 0.02% $MgSO_4 \cdot 7H_2O$, pH 6.75	vanillin/2-methoxypyrazine as sole nutrient source

Nitrogen-free mineral salt medium	**1% glucose**, 0.25% K_2HPO_4, 0.1% KH_2PO_4, 0.02% $MgSO_4 \cdot 7H_2O$, pH 6.75	glucose as sole nutrient source
Nutrient mineral salt medium	**1% glucose**, 0.6% **ammonium sulfate,** 0.25% K_2HPO_4, 0.1% KH_2PO_4, 0.02% $MgSO_4 \cdot 7H_2O$, pH 6.75	positive control

Fungi were revived from glycerol stocks and pre-cultured in YEPD medium at 25 °C for 2 days. Cultures were washed in sterile 1× PBS buffer to eliminate nutrients from the original YEPD medium and then inoculated into different media at an inoculation rate of 5×10^6 cells/mL. Cultures were incubated at 25 °C and the OD_{600} measured immediately after inoculation and at intervals for the following 3 weeks to monitor microbial growth. Samples were taken weekly from cultures for microscopic confirmation of the absence of contamination.

2.3.2 Screening of lactic acid bacteria

MRSAJ medium, commonly used for cultivating lactic acid bacteria, was not suitable for growth for the screening tests due to its multiple ingredients. Minimal media consisting of chemically defined carbon / nitrogen sources were therefore necessary for this experiment. Two media (Cavin et al., 1989; Wegkamp et al., 2009) or their modified versions (Table 2.4) were compared for growth tests with candidate bacteria.

Lactic acid bacteria collections were firstly revived from glycerol stocks and pre-cultured in MRSAJ medium and incubated in a CO_2 incubator (20%, v/v) at 30 °C for 3-5 days (depending on growth). Cultures were measured for growth by OD_{600} and diluted to 0.6 if necessary, before washing in sterile 1× PBS buffer to remove residual nutrients before inoculating at rate of 3% (v/v). Plates were incubated at 30 °C both anaerobically and aerobically in a CO_2 incubator (20%, v/v) and a standard aerobic incubator.

Table 2.4 Media recipes

Medium	Components (w/v)
Fructose Tween 80	Fructose (3.5%), glucose (0.5%), L-malic acid (1%), Tween 80 (0.1%), KH_2PO_4 (0.06%), KCl (0.045%), $CaCl_2 \cdot 2H_2O$ (0.013%), $MgSO_4 \cdot 7H_2O$ (0.013%), $MnSO_4.H_2O$ (0.0003%), casamino acids (0.5%), yeast extract (0.4%), pH 5.2

Modified FT 80 (yeast extract depleted)	Fructose (3.5%), glucose (0.5%), L-malic acid (1%), Tween 80 (0.1%), KH_2PO_4 (0.06%), KCl (0.045%), $CaCl_2.2H_2O$ (0.013%), $MgSO_4.7H_2O$ (0.013%), $MnSO_4.H_2O$ (0.0003%), casamino acids (0.5%), pH 5.2
Modified FT 80 (nitrogen source simplified)	Fructose (3.5%), glucose (0.5%), L-malic acid (1%), Tween 80 (0.1%), KH_2PO_4 (0.06%), KCl (0.045%), $CaCl_2.2H_2O$ (0.013%), $MgSO_4.7H_2O$ (0.013%), $MnSO_4.H_2O$ (0.0003%), leucine/arginine/$(NH_4)_2SO_4$ (0.5%), pH 5.2
PMM5	Glucose 1%, fructose 1%, K_2HPO_4 0.1%, KH_2PO_4 0.25%, sodium acetate 0.4%, $MgCl_2$ 0.02%, $MnCl_2$ 0.0003%, ascorbic acid 0.0123%, arginine 0.0125%, glutamic acid 0.05%, isoleucine 0.021%, leucine 0.0475%, methionine 0.0125%, phenylalanine 0.0275%, threonine 0.0225%, tyrosine 0.025%, valine 0.0325%, tryptophan 0.005%, nicotinic acid 0.0001%, pantothenate 0.0001%, riboflavin 0.0001%, pH 5.2

A pilot trial revealed the superiority of PMM5 medium in that more bacteria from the collections grew compared to FT 80 medium, thus these bacteria were used for the following screening tests with various substrates. For the convenience of modifying the medium with different carbon/nitrogen requirements, the ingredients within the medium were categorised into 4 groups (Table 2.5) and 6 different modifications were created (Table 2.6).

Table 2.5 Sub-groups of components within PMM5 medium

Base salts	Carbon	Amino acids	Vitamins
KH_2PO_4 0.1%	Glucose 1%	Arginine 0.0125%	Nicotinic acid 0.0001%
K_2HPO_4 0.1%	Fructose 1%	Glutamic acid 0.05%	Pantothenate 0.0001%
$MnCl_2$ 0.0003%	Sodium acetate 0.4%	Isoleucine 0.021%	Riboflavin 0.0001%
$MgCl_2$ 0.02%		Leucine 0.0475%	Ascorbic acid 0.0123%
		Methionine 0.0125%	
		Phenylalanine 0.0275%	
		Threonine 0.0225%	
		Tyrosine 0.025%	
		Valine 0.0325%	
		Tryptophan 0.005%	

Table 2.6 Recipes for modified PMM5 medium

Name	Ingredients	Notes
Original medium	Base salts, vitamins, amino acids, carbon	Positive control
Methyl leucine medium	Base salts, vitamins, carbon, methyl leucine (0.6%)	Methyl leucine as the nitrogen source to replace amino acids
Nitrogen-free medium	Base salts, vitamins, carbon	Negative control for methyl leucine medium
2-MP medium	Base salts, vitamins, fructose, 2-methoxypyrazine (1%)	2-MP as the carbon source, fructose to act as redox substrate provider
Vanillin medium	Base salts, vitamins, fructose, vanillin (1%)	Vanillin as the carbon source, fructose to act as redox substrate provider
Carbon-free medium	Base salts, vitamins, fructose	Negative control for 2-MP/vanillin media

Use of vanillin as a nutrient in the trial was abandoned due to the colour reaction during incubation impacting the OD_{600} reading. Instead, vanillic acid was used as supplementary nutrient at 5 mM in YEPD or MRSAJ media. Unspiked media were used as positive control groups for growth comparison.

2.3.3 Methyl violet colour assay

Methyl violet is a group of organic compounds containing methyl moieties. It is commonly used as a purple dye and previous studies have revealed that decolourisation occurs during degradation with *N*-demethylation reactions involved. It was therefore selected as the colour indicator for a demethylation assay. Yeasts and lactic acid bacteria were revived from glycerol stocks and pre-cultured in YEPD / MRSAJ medium, respectively and incubated at 28 °C / 30 °C for 2-5 days (depending on growth). Dilutions with the original medium were performed if necessary, to standardise the microbial growth (OD_{600} = 0.6) of each culture. Spot plating was preliminarily trialled aiming for the occurrence of transparent halos around colonies indicating the degradative ability of promising strains. For each culture, 5 μL was used for spot plating onto YEPD / MRSAJ agar containing 0.1 μM of methyl violet and 1× trace metals mix solution. Agar plates were incubated at 30 °C either aerobically or anaerobically according to the growing requirements of the strains. However, this proved difficult as the colour difference between original medium and methyl violet-spiked medium wasn't obvious enough to observe the potential halo. Liquid cultivation was therefore used,

with colour differences measured spectrophotometrically to validate the efficiency of the assay. Liquid media (YEPD/MRSAJ) were filter sterilised rather than autoclaved to minimise discolouration and were subsequently spiked with 0.1 μM of methyl violet and 1× trace metals mix solution. Mixtures were distributed into 96-well plates with 250 μL per well. Cultures were standardised based on OD_{600} for microbial growth before inoculation (7 μL per well). Plates were incubated at 28 °C for yeasts in a standard aerobic incubator, and 30 °C for bacteria in a CO_2 incubator (20%, v/v) for 7 days. Promising strains (all from the yeast collection) were repeated with cultivation on larger scales (5 mL and 40 mL) for confirmation. Cell pellets from confirmed groups were streaked onto YEPD agar for colony isolation, and single colonies were picked and colony cracked (0.1 mL of 20 mM NaOH, 96°C, 10 min) before identification by ITS PCR. PCR products were checked by gel electrophoresis for quality and concentration and were purified via an enzymatic clean-up method using exonuclease I and shrimp alkaline phosphatase. DNA sequence data was obtained for each of the purified PCR products by Sanger sequencing; BLAST searches with sequencing results were conducted to enable the identification of each isolate.

2.3.3.1 Further characterisation and preliminary trials with isolated strains

Two strains showing the ability to decolourise methyl violet were evaluated for their ability to degrade IBMP. Cultivation with IBMP spiked at 0.1 μM occurred in 5 mL cultures. Single colonies of two strains were cultured in YEPD broth for enrichment for 3 days at 28 °C before OD_{600} was measured for microbial growth standardisation. Autoclaved cultures were used as negative controls for excluding absorption effects and all cultures were inoculated at 1 mL and was incubated at room temperature for 7 days. Samples were collected at two timepoints, i.e. immediately after inoculation and at the end of incubation, for GC analysis.

Preliminary studies on the possible enzyme system responsible for degrading methyl violet was also conducted according to Bumpus and Brock's (1988) protocol. Extracellular fluids were obtained by centrifugation at 10,000 × *g* for 20 min, and peroxidase activity was tested by incubating the extracellular fluids with 0.1% H_2O_2 and 0.1 μM of methyl violet at 28 °C for 7 days.

3 Results

3.1 Preliminary screening of environmental samples with IBMP

All the media used for screening were analysed for IBMP concentrations by HS-SPME-GC-MS/MS. Based on the data from the blank groups with no inoculation, ~70% IBMP loss was observed in mineral salt medium over ~25 days of incubation at room temperature (20 °C, 140 rpm), which occurred in a stable linear manner (Fig. 3.1, Table 3.1).

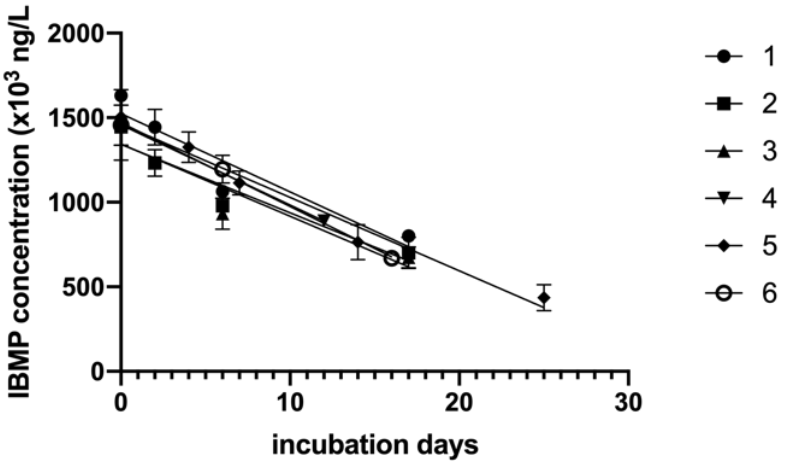

Figure 3.1 Nonlinear regression plot based on IBMP evolution in the blank group from 6 batches. Each data point is the mean of 3 samples with error bars showing standard deviation.

Table 3.1 Nonlinear regression analysis results for quantitative justification

	1	2	3	4	5	6
Best-fit values						
Y-intercept	1524	1343	1344	1458	1463	1471
slope	-46.26	-40.50	-42.71	-47.43	-43.40	-49.59
Goodness of Fit						
Degrees of Freedom	6	6	6	2	8	4
R squared	0.8695	0.8872	0.8549	0.8792	0.9579	0.9661
Sy.x*	136.0	109.6	133.5	149.2	89.42	75.10

*Sy.x=$\sqrt{\frac{\sum(residual^2)}{n-K}}$. The *residual* is the vertical distance (in Y units) of the point from the fit line. The value *n-K* is the number of degrees of freedom of the regression, where *K* is the number of parameters fit by regression.

Among the environmental samples collected, most did not show statistically significant differences between experimental groups and controls in any nutrient combinations where IBMP acted as a carbon source/ nitrogen source/ sole nutrient source/ supplementary nutritional source. For soil and sediment samples, significant differences were noted (Student's *t*-test, $p = 0.0312$ for soil groups, $p = 0.0406$ for sediment groups) with IBMP added as the sole nutrient source (Table 3.2). However, large error bars observed in many datasets indicated the difficulty in accurately quantitating IBMP concentrations, thereby reducing the reliability of results.

The same experiments were repeated on soil and sediment samples yielding slightly different results (Table 3.3), though no significant differences were recorded within each sample group. Nevertheless, considerable decreases were observed, especially compared with the negative control group, which offered some promise. Again, high standard deviations within replicates made validation more difficult. Considering the likelihood of result dispersion in quantifying IBMP in liquid cultures, an alternative confirmation method was applied, which involved plating cultures to IBMP-containing agar plates.

Table 3.2 Preliminary screening results for soil and sediment samples cultured with IBMP as the sole nutrient

Time (days)	0	2	6	17	*p*-value[a]
Soil	1446	753 ± 18	382 ± 107	207 ± 50	0.0312
Soil_control	1446	823 ± 61	681 ± 25	472 ± 45	
Sediment	1446	699 ± 33	483 ± 40	291 ± 37	0.0406
Sediment_control	1446	891 ± 7	725 ± 105	479 ± 41	
Blank	1446	1283 ± 149	1183 ± 169	755 ± 112	-

Data are summarised as means ± standard deviation (n = 3), representing IBMP concentrations measured in each culture.

[a] A comparison was conducted between the soil group *vs* the soil control group, and between the sediment group *vs* the sediment control group. *p*-values were calculated with the Student's *t*-test.

Table 3.3 Confirmation of results for soil and sediment samples cultured with IBMP as the sole nutrient

Time (days)	0	2	6	17	*p*-value[a]
Soil	1631.6	748 ± 84	306 ±40	323 ± 65	0.2279
Soil_control	1631.6	867 ± 33	804 ± 7	434 ± 63	
Sediment	1631.6	676 ± 56	504 ± 47	360 ± 62	0.0931
Sediment_control	1631.6	882 ± 77	799 ± 30	535 ± 52	
Creek water[b]	1631.6	1034 ± 65	833 ± 11	708 ± 26	0.3419
Creek water_control[b]	1631.6	978 ± 16	819 ± 51	683 ± 12	
Blank	1631.6	1443 ± 105	1063 ± 38	800 ± 3	-

Data are summarised as means ± standard deviation (n = 3).

[a]Comparison of the soil group *vs* soil control group, sediment group *vs* sediment control group. *p*-values were calculated with the Student's *t*-test.

[b]Creek water group set as negative control.

3.2 Further confirmation results

To confirm the findings described above, the isolates were plated onto solid media. For groups where the inocula were pre-washed in 1 × PBS buffer before plating, no colonies were seen to develop after incubation. The opposite was observed for groups that were not washed, however, such that colony growth was observed in both control and experimental groups that were not washed. Given the volume ratio between inoculum and medium per plate (1:3000), any residual nutrition introduced from the starter culture would likely only be a minor source of nutrition for both spread and pour plating groups. Within each experimental group, colonies grew within the agar, instead of on the surface, regardless of the plating method, but with slightly more colonies observed upon pour-plating. Colonies unique to experimental groups, in which IBMP was added as the sole nutrient, were compared to controls with no added nutrients (Fig. 3.2). Based on macroscopic and microscopic morphology, it was not clear whether colonies belonged to a single species.

Reasoning that the colonies growing within the agar may prefer a reduced oxygen atmosphere, colony samples were extracted from the agar and re-plated onto nutrient agar incubated aerobically or in 20% CO_2, v/v. Unfortunately, no growth was observed in the latter, while aerobic incubation produced colonies on the surface of the nutrient agar with diverse morphologies. Colonies isolated from the latter were identified both morphologically

as well as genetically via 16s rRNA identification methods, respectively (candidates are listed in Table 3.4).

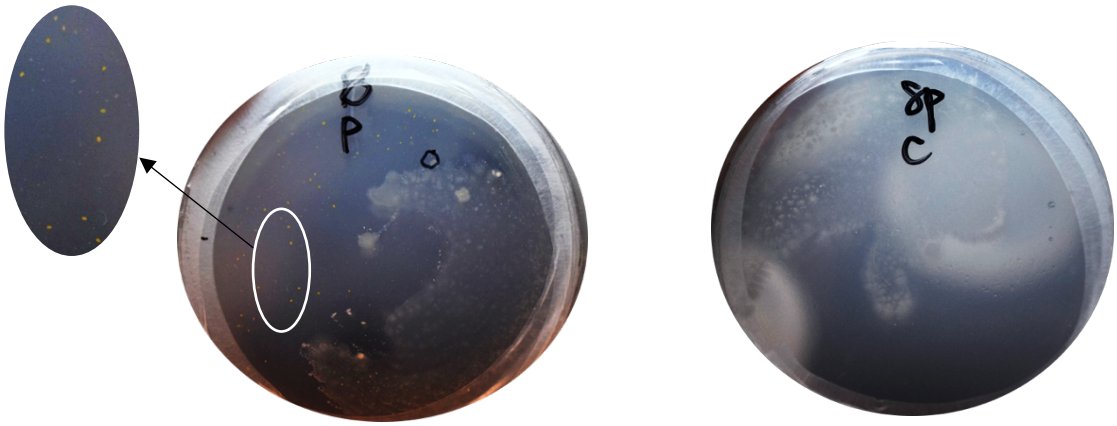

Figure 3.2 Colonies on IBMP-mineral salt plates (left: experimental plate with IBMP added; right: control plate without any nutrients)

Table 3.4 Putative isolate identity based on 16S rDNA sequencing and BLAST analysis

Isolate	Putative identity
1	*Rhizobium multihospitium*
2	*Rhizobium tropici*
3	*Sphingomonas sp.*
4	*Leclercia sp.*
5	*Enterobacter ludwigii*
6	*Pseudomonas fulva*
7	*Paenibacillus taichungensis*
8	*Stenotrophomonas sp.*

Monocultures of individual strains were re-inoculated into IBMP-containing medium in both solid and liquid form. In liquid culture, neither significant microbial growth nor decreases in IBMP concentration were observed in any monoculture groups (Fig. 3.3). Importantly, the degree of variation between individual treatments and their controls, showed significant variation, thus suggesting that this experimental design was not sufficiently robust to yield reliable results or warrant further investigation. This work was therefore abandoned.

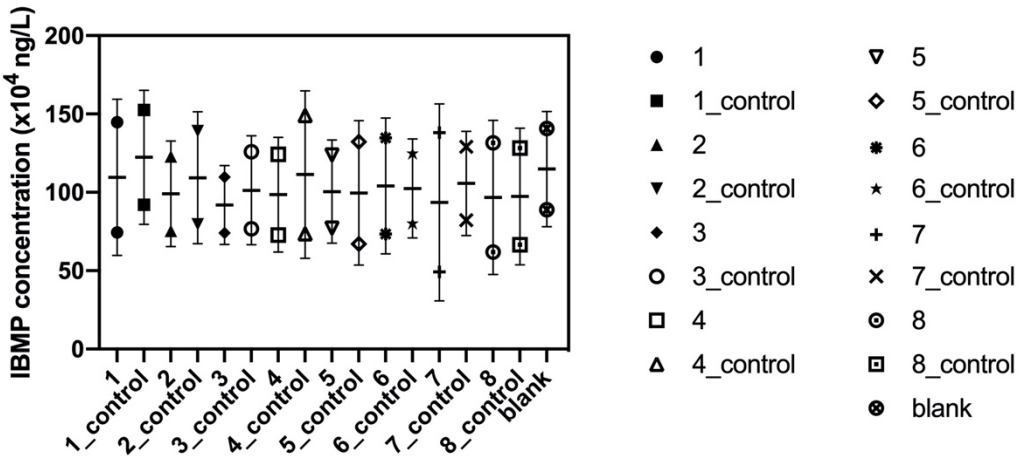

Figure 3.3 IBMP concentrations during incubation of 8 different monocultures. Symbols on the top: IBMP concentrations at the beginning of incubation. Symbols on the bottom: IBMP concentrations at the end of incubation.

3.3 Alternative screening substrates

Growth tests were conducted with various compounds whose structures resembled elements of IBMP in some way, for example, methyl leucine, 2-methoxypyrazine, vanillin, vanillic acid and methyl violet. Vanillin was ruled out of further use as trials revealed that it was prone to discolouration, presumably through reaction with carbonyl-bearing compounds released by the microbes and impacting OD_{600} measurements. Minimal media for yeasts and bacteria (Table 3.5) were trialled and the promising ones, i.e. those supporting growth within 3 days, were selected for screening of the microbial library.

Table 3.5 Recipes for optimal minimal medium suitable for yeast and bacterial growth

	Yeast medium	Bacteria medium
Carbon	1% glucose	1% glucose, 1% fructose, 0.4% sodium acetate
Nitrogen	0.6% ammonium sulfate	0.0125% arginine, 0.05% glutamic acid, 0.021% isoleucine, 0.0475% leucine, 0.0125% methionine, 0.0275% phenylalanine, 0.0225% threonine, 0.025% tyrosine, 0.0325% valine, 0.005% tryptophan
Others	0.25% K_2HPO_4, 0.1% KH_2PO_4, 0.02% $MgSO_4 \cdot 7H_2O$	0.1% KH_2PO_4, 0.1% K_2HPO_4, 0.0003% $MnCl_2$, 0.02% $MgCl_2$, 0.0001% nicotinic acid, 0.0001% pantothenate, 0.0001% riboflavin, 0.0123% ascorbic acid
pH	6.75	6.2

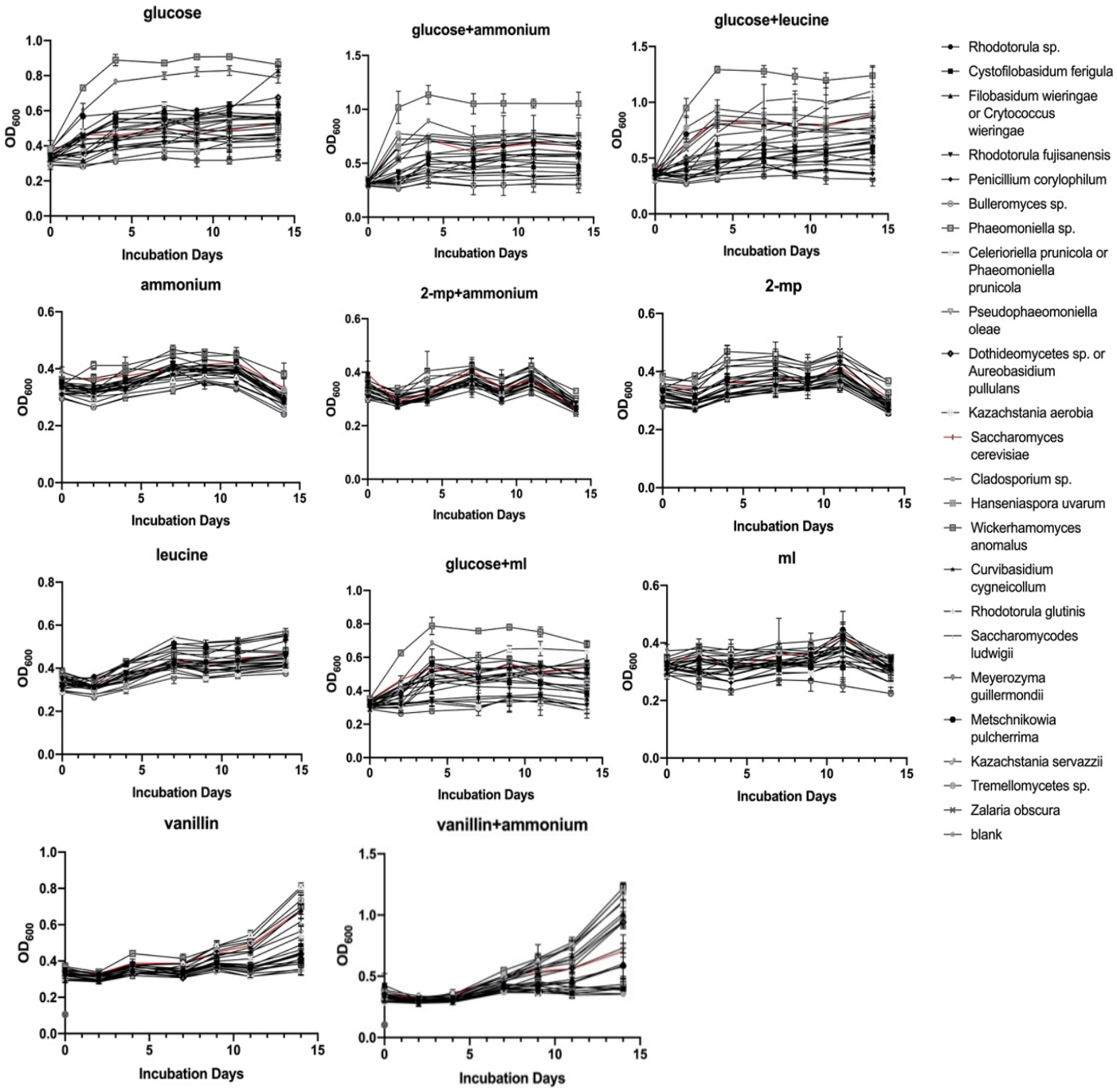

Figure 3.4 A selection of plots for 23 fungi showing growth with methyl leucine, 2-methoxypyrazine and vanillin provided as nutrients. The title of each plot represents the only nutrient provided to the respective group. Growth curves for *Saccharomyces cerevisiae* are highlighted in red. Abbreviation: 2-mp, 2-methoxypyrazine; ml, methyl leucine.

A total of 100 fungal and bacterial strains were trialled with these compounds as substrates. Microbial growth was monitored via optical density (OD_{600}) during incubations and growth curves of 23 fungal strains are plotted as examples (Fig. 3.4). Although superior growth was recorded for the *Wickerhamomyces anomalus* strain when glucose and methyl leucine were provided as carbon and nitrogen sources, growth was still not equivalent to that observed when glucose was provided as the sole nutrient source, indicating that methyl leucine did not play a positive role in supporting microbial growth.

As noted above, groups including vanillin and vanillin + ammonium increased during the incubation due to observation of colour intensification in cultures over time suggesting that the occurrence of colour reactions interfered with the absorbance results. As such, an alternative assay method was applied. Specifically, vanillic acid was used to supplement media for both fungal and bacterial collections.

Growth rates interpreted as slopes were calculated and analysed in the form of heat maps for ease of visualisation (Fig. 3.5). Positive controls contained ample nutrients and were included in each trial batch to benchmark the microbial growth under optimal conditions. Treatments then contained IBMP substitutes. It can be seen that the majority of strains that were tested failed to grow with IBMP substitutes as the sole source of nutrients. However, it was apparent that several strains exhibited growth comparable or potentially greater than that of positive controls, including: strains 3, 7, 8, 10, 13 and 16 in Fig. 3.5a with methyl leucine provided as the nutrient; strains 6, 10, 13, 22, 32, 34, 38, 41, 46 and 57 in Fig. 3.5c; strains 2, 8, 15, 16, 17, 18, 20, 23, 24, 27, 28, 34, 36, 38, 47, 56 and 61 in Fig. 3.5d; and strains 34 and 41 in Fig. 3.5e with 2-methoxypyrazine provided as the nutrient. These warranted further investigation to confirm the reproducibility of the results. One or more confirmation trials were performed on these strains with target compounds provided in a similar manner, but unfortunately similar results were not observed in these repeat trials (data not shown). Taken as a whole, these findings indicated that the microbes tested were not capable of utilising these three compounds of interest as nutrient sources, under the experimental conditions provided, at least not consistently.

1 *Rhodotorula sp.*
2 *Cystofilobasidum ferigula*
3 *Filobasidum wieringae* or *Crytococcus wieringae*
4 *Rhodotorula fujisanensis*
5 *Penicillium corylophilum*
6 *Bulleromyces sp.*
7 *Phaeomoniella sp.*
8 *Celerioriella prunicola* or *Phaeomoniella prunicola*
9 *Pseudophaeomoniella oleae*
10 *Dothideomycetes sp.* or *Aureobasidium pullulans*
11 *Cladosporium sp.*
12 *Curvibasidium cygneicollum*
13 *Rhodotorula glutinis*
14 *Zalaria obscura*
15 *Tremellomycetes sp.*
16 *Wickerhamomyces anomalus*
17 *Kazachstania aerobia*
18 *Hanseniaspora uvarum*
19 *Metschnikowia pulcherrima*
20 *Kazachstania servazzii*
21 *Meyerozyma guillermondii*
22 *Saccharomycodes ludwigii*
23 *Saccharomyces cerevisiae*
24 blank

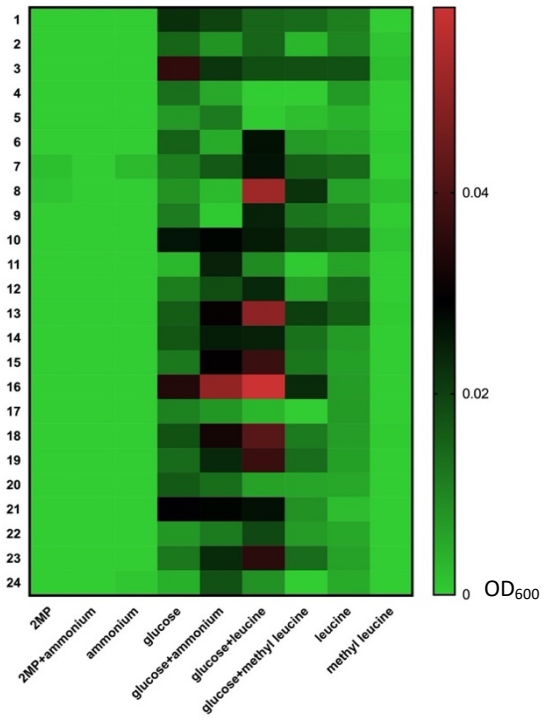

a

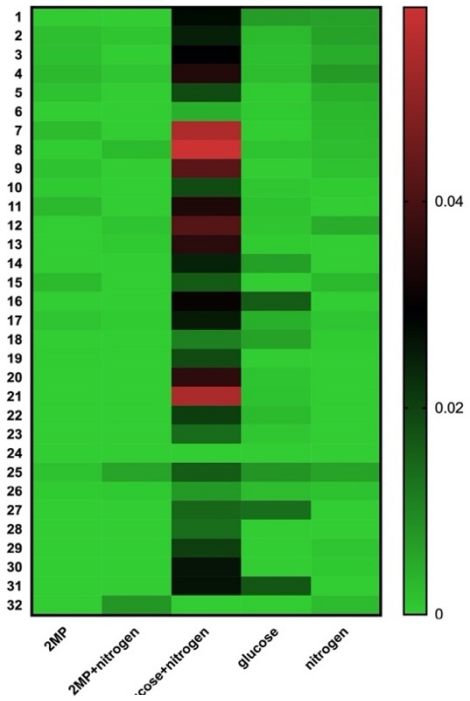

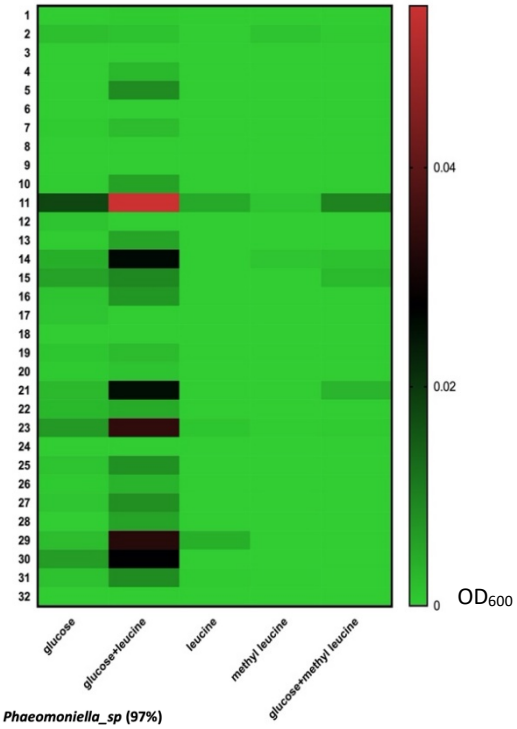

1 *Aureobasidium namibiae*
2 *Candida germanica* (96%)
3 *Penicillium multicolor*
4 *Hanseniaspora uvarum*
5 *Candida albicans*
6 *Candida stellimalicola*
7 *Penicillium citrinum*
8 *Kodamaea ohmeri*
9 *Candida intermedia*
10 *Pichia mandshurica*
11 *Hanseniaspora osmophila*
12 *Candida tallmaniae*
13 *Meyerozyma caribbica*
14 *Candida tallmaniae*
15 *Hanseniaspora valbyensis*
16 *Hanseniaspora osmophila*
17 *Lachancea cidri*
18 *Rhodotorula mucilaginosa*
19 *Phoma multirostrata*
20 *Candida kruisei*
21 *Debaryomyces coudertii*
22 *Candida railenensis*
23 *Phaeomoniella_sp* (97%)
24 *Debaryomyces hansenii*
25 *Zygosaccharomyces lentus* (90%)
26 *Kregervanrija delftensis*
27 *Torulaspora delbrueckii*
28 *Aureobasidium pullulans*
29 *Candida stellata*
30 *Lachancea thermotolerans*
31 *Saccharomyces cerevisiae*
32 blank

b

1 *Lactobacillus kunkeei* (99.9%)
2 *Lactobacillus mellis* (99.8%)
3 *Lactobacillus ixorae* (98.5%)
4 *Lactobacillus kunkeei* (99.7%)
5 *Enterococcus canintestini* (94.9%)
6 *Lactobacillus kosoi* (96.8%)
7 *Lactobacillus ixorae* (99.8%)
8 *Lactobacillus kimbladii* (99.1%)
9 *Lactobacillus ixorae* (98.4%)
10 *Lactobacillus kunkeei* (99.7%)
11 *Fructobacillus fructosus* (98.7%)
12 *Fructobacillus fructosus* (99.8%)
13 *Lactobacillus kunkeei* (99.7%)
14 *Lactobacillus ixorae* (98.4%)
15 *Fructobacillus fructosus* (99.7%)
16 *Fructobacillus fructosus* (100%)
17 *Bacillus megaterium* (100%)
18 *Lactobacillus kosoi* (96.7%)
19 *Lactobacillus ixorae* (98.2%)
20 *Lactobacillus kimbladii* (99.3%)
21 *Lactococcus lactis* (100%)
22 *Fructobacillus tropaeola* (99.8%)
23 *Lactobacillus bombi* (94.9%),
24 *Lactobacillus kosoi* (96.7%)
25 *Lactobacillus helsingborgensis* (99.9%)
26 *Lactobacillus kullabergensis* (100%)
27 *Lactobacillus kunkeei* (100%)
28 *Fructobacillus tropaeola* (99.9%)
29 *Lactobacillus bombi* (95%)
30 *Lactobacillus hilgardii* (93.6%)
31 *Lactobacillus melliventris* (99.9%)
32 *Lactobacillus ixorae* (99.5%)
33 *Lactobacillus ixorae* (98.7%)
34 *Lactobacillus bombi* (94.8%)
35 *Lactobacillus bombi* (94.7%)
36 *Fructobacillus fructosus* (99.7%)
37 *Lactobacillus mellifer* (99.8%)
38 *Lactobacillus melliventris* (99.7%)
39 *Lactobacillus plantarum* (100%)
40 *Lactobacillus bombi* (94.7%)
41 *Lactobacillus bombi* (94.7%)
42 *Lactobacillus brevis*
43 *Bacillus safensis* (100%)
44 *Fructobacillus tropaeola* (99.6%)
45 *Lactobacillus apinorum* (99.9%)
46 *Lactobacillus hilgardii* (93.6%)
47 *Lactobacillus kosoi* (96.7%)
48 blank
49 SD1_*Lactobacillus sanfranciscensis*
50 SD4_*Lactobacillus sanfranciscensis*
51 LOR_CHA_LAB7
52 PF_9_W15_*Lactobacillus brevis*
53 VP41
54 LOR_CHA_LAB1
55 LOR_CHA_LAB5
56 LOR_CHA_LAB6
57 G6_*O. oeni*
58 G5_*O.oeni*
59 G2_*O.oeni*
60 LOR_CHA_LAB2
61 LOR_CHA_LAB4
62 G9_*O.oeni*
63 LOR_CHA_LAB3
64 G1_*O.oeni*
65 G8_*O.oeni*
66 LOR_CHA_LAB8
67 G10_*O.oeni*
68 G11_*O.oeni*
69 SD2_*Lactobacillus sanfranciscensis* or Uncultured *Bacillus sp.*
70 SD3_*Lactobacillus sanfraciscensis*

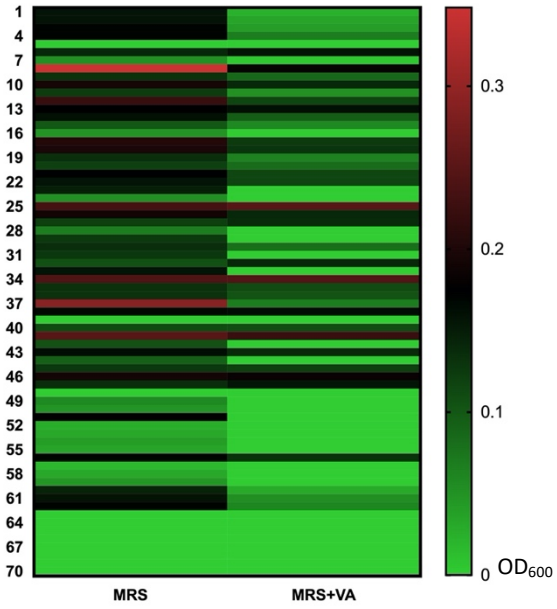

c

1 *Phaeomoniella sp* (97%)
2 *Candida intermedia*
3 EC1118
4 *Candida stellata*
5 *Torulaspora delbrueckii*
6 *Kregervanrija delftensis*
7 *Penicillium multicolor*
8 *Aureobasidium pullulans*
9 *Lachancea cidri*
10 *Penicillium citrinum*
11 *Hanseniaspora valbyensis*
12 *Candida krusei*
13 *Candida germanica* (96%)
14 *Lachancea thermotolerans*
15 *Candida tallmaniae*
16 *Hanseniaspora osmophila*
17 *Meyerozyma caribbica*
18 *Hanseniaspora osmophila*
19 *Phoma multirostrata*
20 *Candida stellimalicola*
21 *Hanseniaspora uvarum*
22 *Zygosaccharomyces lentus* (90%)
23 *Debaryomyces coudertii*
24 *Candida krusei*
25 *Pichia mandshurica*
26 *Candida albicans*
27 *Candida tallmaniae*
28 *Debaryomyces hansenii*
29 *Aureobasidium namibiae*
30 *Rhodotorula mucilaginosa*
31 *Candida railenensis*
32 blank
33 environ_20
34 environ_6
35 environ_9
36 environ_1
37 environ_7
38 environ_8
39 environ_10
40 environ_16
41 environ_5
42 environ_3
43 environ_2
44 environ_17
45 environ_18
46 environ_21
47 environ_11
48 environ_13
49 *Rhodotorula sp.*
50 *Cystofilobasidium ferigula*
51 *Filobasidium wieringae* or *Cryptococcus wieringae*
52 *Rhodotorula fujisanensis*
53 *Penicillium corylophilum*
54 *Bulleromyces sp.*
55 *Phaeomoniella sp.*
56 *Celerioriella prunicola* or *Phaeomoniella prunicola*
57 *Pseudophaeomoniella oleae*
58 *Dothideomycetes sp.* or *Aureobasidium pullulans*
59 *Cladosporium sp.*
60 *Curvibasidium cygneicollum* or *Uncultured Basidiomycota* or *Rhodotorula*
61 *Rhodotorula sp* or *R. glutinis*
62 *Zalaria obscura* or *Aureobasidium sp.*
63 *Tremellomycetes sp.*
64 *Wickerhamomyces anomalus*
65 *Kazachstania aerobia*
66 blank

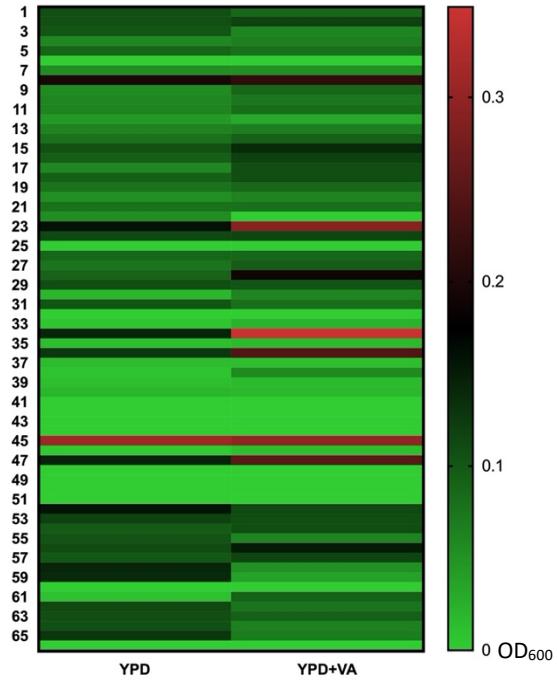

d

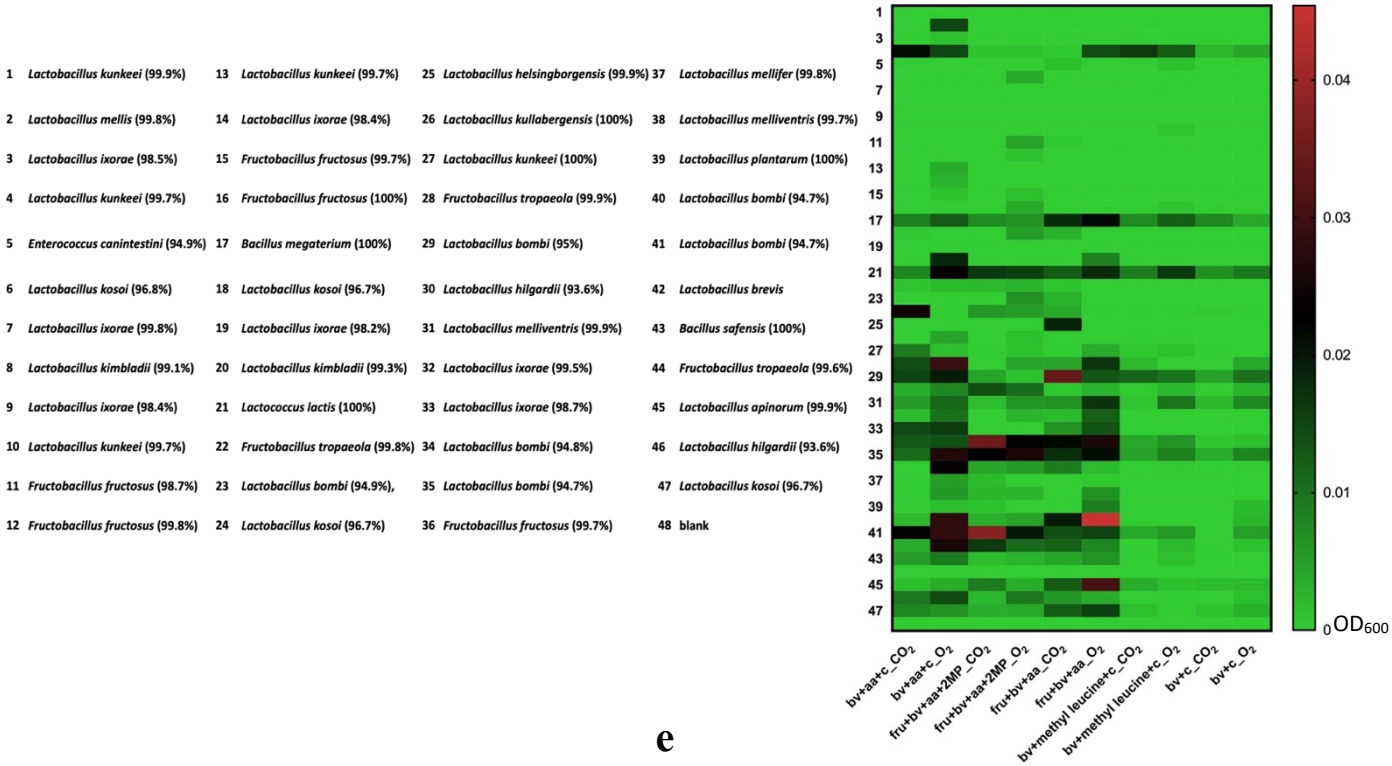

Figure 3.5 Heat map of growth rates calculated as slopes for each screening experiment. Panels a-f represent results obtained from various screens with either different microbial collections or different screening substrates. Key nutrient components are specified in column labels. Abbreviations: 2MP, 2-methoxypyrazine; bv, basic mineral salts + vitamins; aa, amino acids; c, carbon source; fru, fructose; VA, vanillic acid.

3.4 Methyl violet degradation trial

Given the structural similarity of methyl violet to parts of the IBMP molecule as well as the fact that it is free of odour and exhibits a pigment that is lost upon degradation, methyl violet was used in further screening trials. YEPD and MRSAJ media (both filter sterilised) were spiked with 0.1 µM of methyl violet. Both spiked and unspiked media were scanned across part of the UV-vis spectrum (350 nm- 900 nm) to determine the optimal wavelengths for each medium at which to conduct the screening assay. Absorbance maxima, based on the largest delta values of absorbance obtained in a preliminary test (Fig. 3.6), were 594 nm for YEPD and 590 nm for MRSAJ.

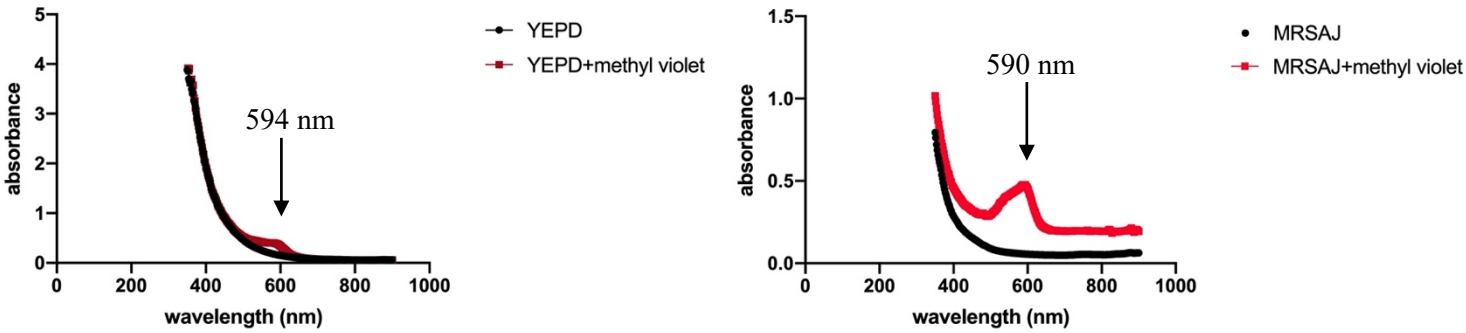

Figure 3.6 Spectral scan for YEPD / YEPD + methyl violet and MRSAJ / MRSAJ + methyl violet to determine optimal absorption wavelength.

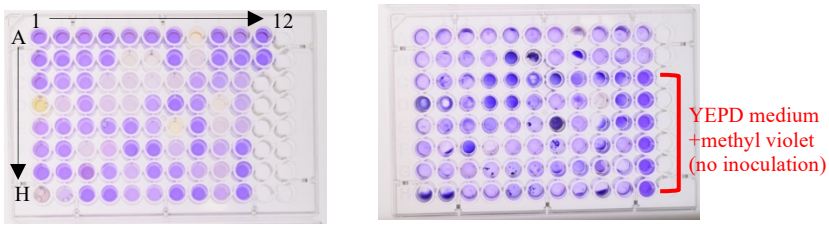

Figure 3.7 Culture appearances after 5 days of microbial incubation in YEPD medium spiked with 0.1 μM methyl violet. a, supernatants of yeast cultures; b, sediments of yeast cultures. The same locations in the two plates indicate the same microbial cultures.

With absorption maxima defined, assays were then established whereby biomass from YEPD and MRSAJ cultures was re-inoculated into YEPD/MRSAJ media spiked with 0.1 μM of methyl violet and were incubated for 5 days at 28 °C for yeasts and 30 °C for bacteria in 96-well plates. Cultures were centrifuged (5 min, 10, 000 × *g*) yielding supernatants to quantify decolourisation levels. There was no significant difference in colour degradation for the bacterial collection (data not shown). However, decolourisation was observed for several yeasts (Fig. 3.7), which in a few cases might have been due to the dye binding to the cells (such as D1, H1, B5, B6, C7, E7 in Fig. 3.7). Purple-coloured biomass was evident in most cell pellets indicating a potential basis for decolouration of the supernatant. Nevertheless, two strains (A8, D9 in Fig. 3.7) gave pale colours in cell pellets as well as decolouration of supernatants and were selected for further confirmation. Strains whose supernatants were decolourised were also included for confirmatory trials, which were conducted at scales ranging from 200 μL to 40 mL. Two strains were identified with the desired ability after several rounds of confirmation (Fig. 3.10). A mere change of medium pH as the basis for decolouration was excluded by checking the pH of both the selected cultures. Values

recorded were 6.05 and 6.13, well above the 0.15-3.2 pH range at which methyl violet is yellow. Replating and microscopic analysis indicated the isolates were pigmented yeast cells, potentially of distinctly different species (Fig. 3.8). ITS PCR was performed in order to identify the highlighted strains. Fragments were sequenced and BLAST results indicated that the isolates were *Rhodotorula glutinis* and *Rhodotorula mucilaginosa* with a 100% identity and query cover. Supernatants of methyl violet-spiked cultures were analysed via UV-vis scan and compared with non-spiked cultures and uninoculated media. Shifts in spectrum peaks in both cultures were observed, especially for the *R. mucilaginosa* strain, suggesting that methyl violet had been degraded to other compounds with different absorption wavelengths (Fig. 3.9), namely, 552 nm for the *R. mucilaginosa* culture and 588 nm for the *R. glutinis* culture.

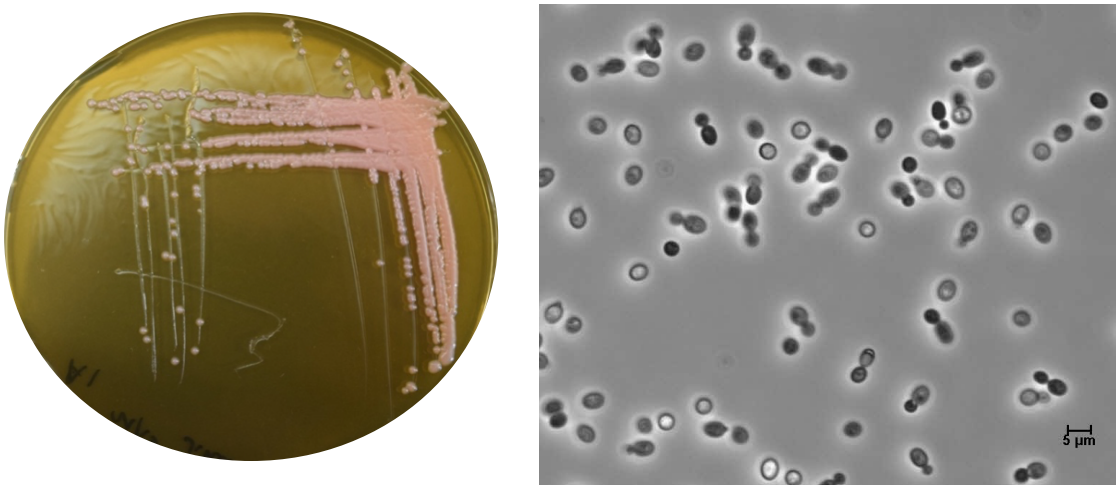

a

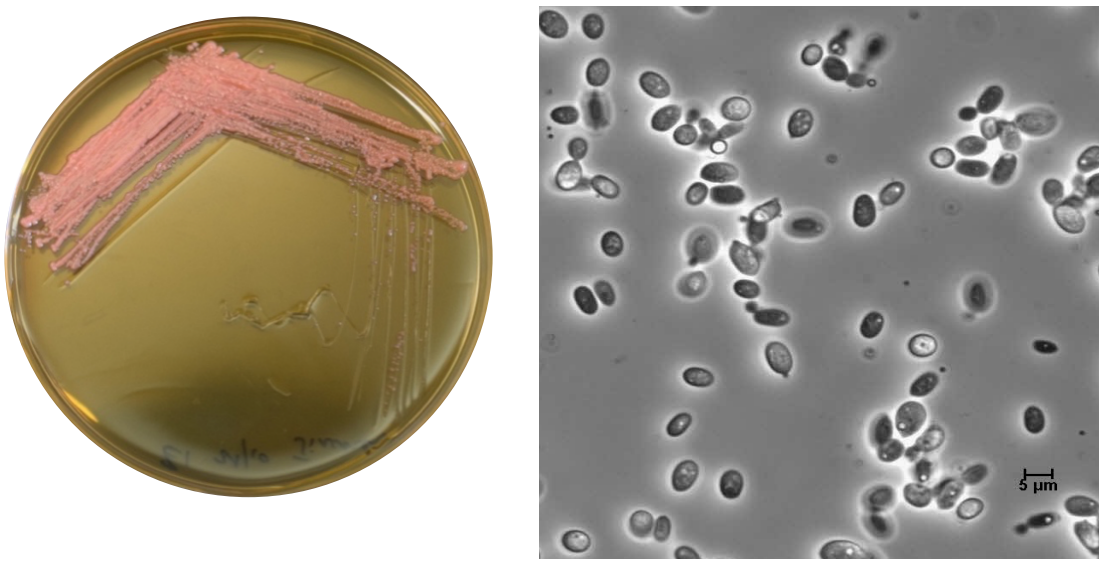

b

Figure 3.8 Colony morphology and microscopic pictures of two fungal strains, subsequently shown by ITS PCR, sequencing and BLAST analysis to be *Rhodotorula glutinis* (panel a) *and Rhodotorula mucilaginosa* (panel b).

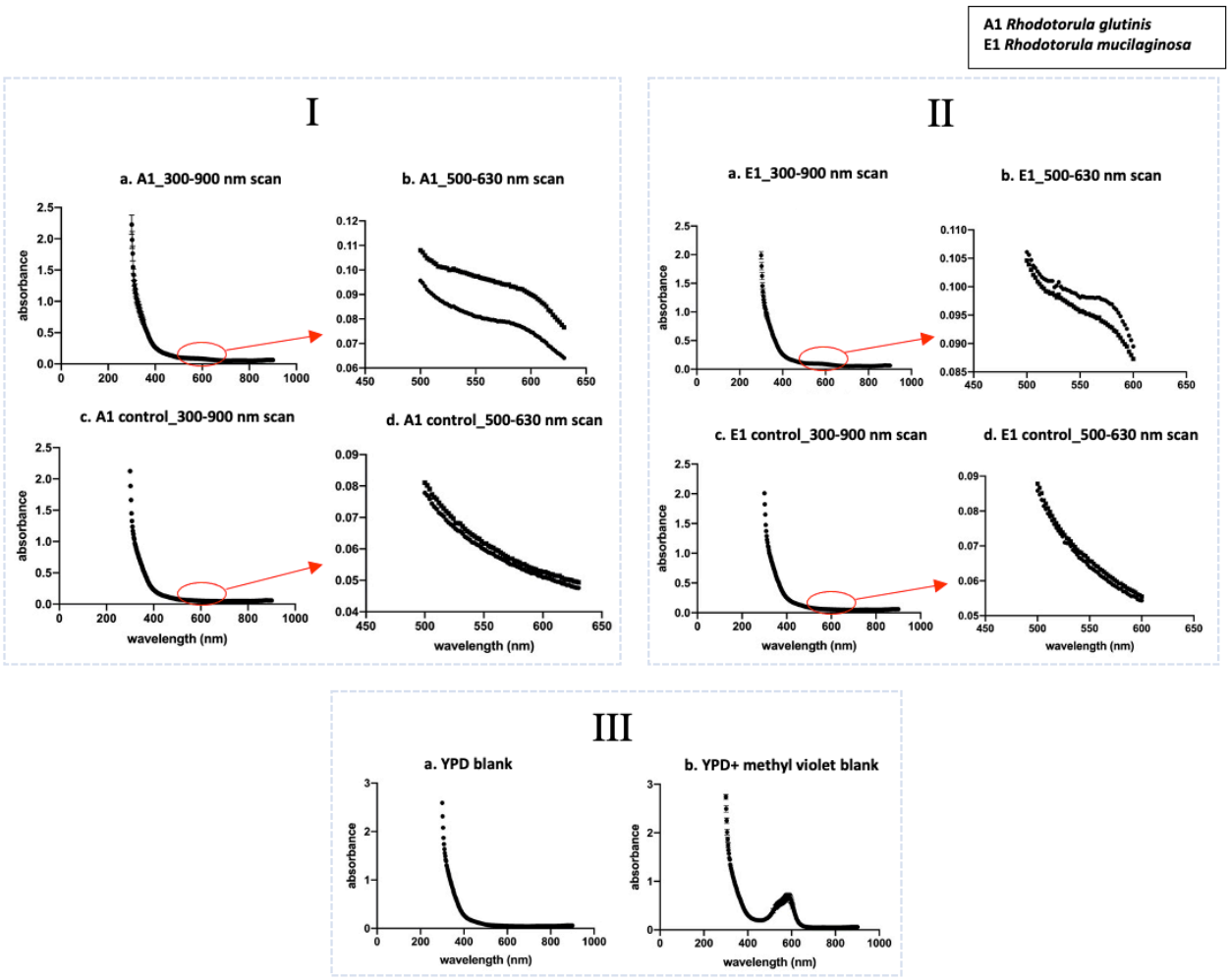

Figure 3.9 Absorbance scans (300-900 nm and 500-630 nm) of culture supernatants for potential methyl violet metabolite identification of *R. glutinis* and *R. mucilaginosa* in YEPD media. Panel I/II a, spectrum scan (300-900 nm) on supernatants of *R. glutinis* (I)/ *R. mucilaginosa* (II) cultures in YEPD media spiked with 0.1 μM methyl violet; panel I/II b, enlarged plots of spectrum scan (500-630 nm) for the same cultures with I/II a; panel I/II c, spectrum scan (300-900 nm) on supernatants of *R. glutinis* (I)/ *R. mucilaginosa* (II) cultures in YEPD media; panel I/II d, enlarged plots of spectrum scan (500-630 nm) for the same cultures with I/II c; panel III a, spectrum scan (300-900 nm) on supernatant of uninoculated YEPD medium spiked with 0.1 μM methyl violet; panel III b, spectrum scan (300-900 nm) on supernatant of uninoculated YEPD medium.

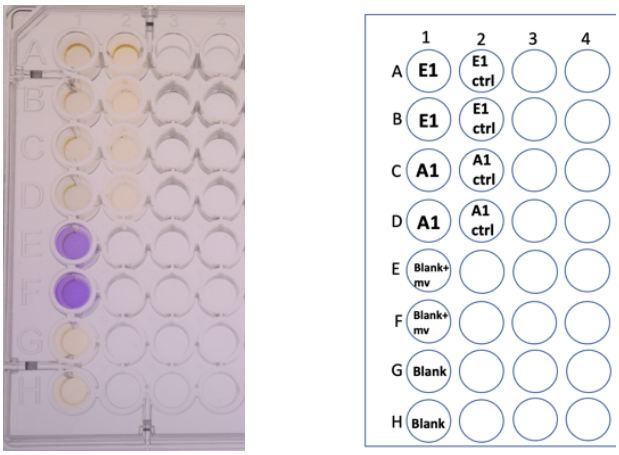

a b

Figure 3.10 Confirmation results for *R. mucilaginosa* and *R. glutinis* for methyl violet-degrading ability. a, Supernatants of different cultures and media, which were obtained after centrifugation of all media/cultures for 5 min (10, 000 × *g*); b. plate layout for confirmation tests. Abbreviations: E1, *R. mucilaginosa* culture in YEPD medium spiked with methyl violet; A1, *R. glutinis* culture in YEPD medium spiked with methyl violet; blank + mv, uninoculated YEPD medium spiked with methyl violet; blank, uninoculated YEPD medium; E1 ctrl, *R. mucilaginosa* culture in YEPD medium; A1 ctrl, *R. glutinis* culture in YEPD medium.

3.5 IBMP degradation test

Two strains capable of decolourising methyl violet were further characterised in an IBMP-containing medium to determine their ability to degrade the compound. IBMP was provided as a supplement in YEPD broth in a manner similar to the nutrient conditions applied in the methyl violet screening (Section 2.3.3). Each isolate along with a denatured control and uninoculated blank group was incubated in the medium for 7 days, with a GC-MS analysis carried out to determine the initial and final IBMP content. In all cases, the final IBMP concentrations was equal to or less than half the initial values, however no significant differences were seen between either strain and the control condition (Table 3.7).

Table 3.7 Initial and final IBMP concentrations in cultures of *Rhodotorula* isolates grown for 7 days. Concentrations are the mean of 3 determinations ± SD. Delta concentrations were used for pairwise Student's *t*-test within each strain for checks of significance.

	Day 0	Day 7	delta	*p*-value
R. glutinis	97 ± 3	41 ± 3	60 ± 5	0.39
*R. glutinis*_control	89 ± 16	42 ± 2	54 ± 14	
R. mucilaginosa	127 ± 28	45 ± 1	84 ± 28	0.25
*R. mucilaginosa*_control	101 ± 4	45 ± 0.5	62 ± 4	
Blank	138 ± 6	52 ± 4	85 ± 3	

4 Discussion

4.1 Nutrient conditions for xenobiotic metabolism

One of the key factors in designing microbial screens for the metabolism of xenobiotics (compounds that are not normally found in an organism or that are found at higher than usual concentrations) is the determination of the nutritional role that the target compound plays. Microbes could possess completely different mechanisms for xenobiotic biodegradation or biotransformation, which directly correlate with the nutrient level in the screening medium. Microbes may utilise the compound as a sole nutrient source, as a supplementary source or they may show a preference amongst nutrients. It is therefore important to include multiple combinations of the components to allow for the possibility of these different utilisation patterns.

The majority of studies seeking microbes for xenobiotic metabolism present the compound as a sole nutrient source to a range of often unknown isolates. For instance, two bacterial strains capable of degrading alkyl pyrazines, specifically, 2,3-diethyl-5-methylpyrazine and 2,5-dimethylpyrazine, were identified by providing the target pyrazines as the sole carbon and nitrogen sources in the isolation medium (Rappert 2006; 2007). This approach is reliable, quick in identifying desirable microbes through their growth (simply measured by OD_{600}) and taken as a proxy for substrate degradation. On the other hand, even growth in a nutrient-rich medium supplemented with 2,4,6-trichloroanisole (2,4,6-TCA) succeeded in isolating TCA-degrading fungal strains, such as *Phlebia radiata*, *Pleurotus pulmonarius* and *Postia placenta* (Campoy et al., 2009). Interestingly, TCA was proposed to be dehalogenated and degraded almost completely by one of the strains even in the presence of other carbon and nitrogen

sources such as glucose and peptone. The same degradation was also observed in a defined minimal medium with a low nitrogen concentration. The precise nutrient utilisation pattern has yet to be determined for this strain.

In another study using nutrient-rich media, screening revealed methoxychlor-transforming bacterial strains (Satsuma et al., 2012). Partial degradation including demethylation and dechlorination of this compound suggested that methoxychlor wasn't sufficient to support microbial growth. Therefore, other compounds in the nutrient-rich medium were thought to fulfill strain nutritional requirements. The authors suggest additional work is needed to define the mode of degradation.

In the current study, which aimed to eliminate IBMP, microbes exhibiting any degree of IBMP degradation were of interest. Accordingly, organisms arising under either scenario, i.e., utilising IBMP as a sole nutrient or as part of a complex nutrient mix, were considered valuable here. Both minimal and complex media were used in this study.

4.2 Possible reasons for microbial colony growth in IBMP agar

In the first part of the screening experiment, microbial colonies were seen to grow in IBMP-containing agar (Fig. 3.2), yet cultivation in liquid medium proved unsuccessful. Moreover, subsequent growth in IBMP-containing agar could not be reliably reproduced. Possible reasons for this phenomenon are worth considering as they may shed light on future microbial research with similar objectives.

Firstly, it was proposed that the observed colonies growing in the agar relied on nutrients other than IBMP, potentially agar in this case. Since the only difference between the control and the experimental groups was the addition of IBMP, and the IBMP stock solution was not sterile prior to spiking, it is possible that contaminants from the IBMP stock included microbes able to degrade agar, which comprises agarose, agaropectin and low levels of mineral ions (Amyl Media product brochure). Agar-degrading microorganisms include *Streptomyces coelicolor* (Stanier, 1942; Chi et al., 2012) and *Saccharophagus degradans* 2-40 (Andrykovitch and Marx, 1988; Gonzalez and Weiner, 2000; Ekborg et al., 2005; Chi et al., 2012). It may be that such microbes were responsible for the colony growth within the agar. Preliminary experiments designed to test this notion included use of different agar concentrations (0.1%-1%) to make mineral salt agar (using the same components as the

control group), with IBMP solution added as an ‘inoculum’ to check if similar growth occurred in embedded colonies. No colony growth was observed under any of these conditions, thereby making it impossible to define any potential influence of the concentration of agar, a proposed nutrient, on the growth of the hypothesised contaminant microbes.

As a further check of the possibility of microbial contamination of the IBMP stock, samples were examined microscopically. Particles resembling bacterial cells were observed at 1000× magnification (Fig. 4.1), although in minute amounts. Attempts to isolate these contaminants by growth on IBMP-containing mineral salt agar plates gave inconsistent results. These organisms were therefore proposed to be unculturable on the laboratory media used and/or viable but non-culturable (VBNC; Puspita et al., 2012). Cases encountered in this experiment, are likely to be VBNC, since colonies could be intermittently recovered, but could not be consistently regrown (Oliver, 2000).

Environmental stress such as a lack of nutrients, can enter bacteria into a resting state, which helps them cope with any adverse conditions, but able to recover under favourable conditions (Dworkin and Shah, 2010). It is proposed that the IBMP-containing medium used here represented an adverse environment in which microbes were dormant, thereby making it difficult to assess their potential to utilise IBMP. Future work should utilise a broader range of microbes and media to support the resuscitation of functional cells. The principle for cell resuscitation is to ensure relevant signals are emitted, such as bacterial communication compounds, or that stress factors are removed. Examples of this include the restoration of nutrients for starved cells and the addition of pyruvate or catalase to cells under oxidative stress (Dworkin and Shah, 2010; Kong et al., 2004; Mizunoe et al., 1999; O’Neill et al., 1992).

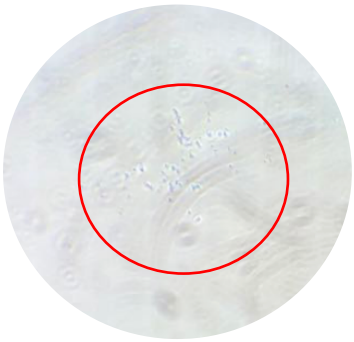

Figure 4.1 Micrograph (1000×) picture of IBMP stock solution; suspected microbial cells are highlighted in red circle.

4.3 Hypothetical degradation pathways for IBMP

As previously mentioned, the degradation and/or transformation patterns of IBMP remain a mystery, and although this experiment did not successfully isolate microbes with any reliable IBMP-degrading capability (despite exhaustive efforts), a possible degradative pathway for IBMP can be proposed based on other reports for compounds with similar structures. Again, this may help to guide future work on this significant problem.

Pyrazines, which are structurally related to IBMP, represent a group of reference compounds for studying the metabolic fate of IBMP. Alkyl pyrazines, namely, 2,5-dimethylpyrazine and 2,3-diethyl-5-methylpyrazine are degraded by the *Rhodococcus erythropolis* strain DP-45 and *Mycobacterium* sp. strain DM-11. In both cases, hydroxylation was proven to occur on the pyrazine ring at the carbon adjacent to one of the methyl groups as well as the nitrogen atom, followed by oxidative ring cleavage (Rappert et al., 2006; 2007). It was also theorised that in nitrogen-containing heterocycles such as pyridine, ring hydroxylation at the *ortho* position of the heteroatom is the first degradation step, with ring cleavage typically following to expose an otherwise stable ring to the more reactive state for ammonia liberation (Fig. 4.2; Fetzner, 1998; Rappert et al., 2007). The two most common patterns of pyrazine transformations are oxidation of the alkyl side chain and hydroxylation at the carbon atom adjacent to the nitrogen atom (Rajini et al., 2011).

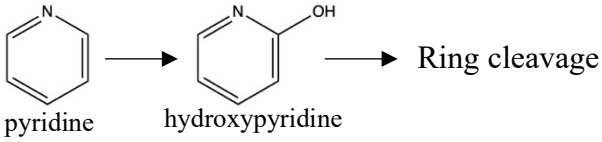

Figure 4.2 Proposed degradation pathway of pyridine (Fetzner, 1998; Rappert et al., 2007). Ring hydroxylation occurs at the *ortho* position of the nitrogen atom, after which ring cleavage takes place.

Therefore, ring hydroxylation and oxidation of the isobutyl side chain are the two most likely initial reactions for IBMP degradation or transformation. However, based on the experimental results from Rappert et al., (2006; 2007) with more pyrazine derivatives tested against the two strains for growth and degradation assays, only those with alkyl side chains and at least one vacant carbon atom were degradable, yet other substituents such as alkoxy groups and halogens seemed to block the pathway. IBMP, even with two carbon atoms unoccupied, may undergo a different degradation pathway due to the addition of the methoxy moiety. Metabolic patterns for methoxy group-containing compounds are therefore needed.

4.3.1 Demethylation of methoxylated aromatic compounds

Aromatic compounds are among the most extensively studied groups containing methoxy substituents as well as a ring structure. As such they are suited to being the reference group for the study of metabolism of the methoxy moiety. *O*-Demethylation is commonly recorded as a reaction among such compounds. Taking lignin degradation as an example, major metabolites of lignin depolymerisation, such as guaiacol and vanillin, contain a methoxy moiety in the ring structure, whose metabolic fate starts with demethylation. As an electron donating group, the electrons of the oxygen atom within the methoxy group are delocalised yielding an increased electron density in the ring conjugated system thus stabilising the overall structure. It is thereby reasonable for *O*-demethylation to occur as the first step in destabilising the general system and rendering a more reactive structure for follow-up reactions. However, it has to be taken into account that this is a structure-dependent case and the difference between a benzene ring and a pyrazine ring could potentially lead to completely different outcomes. In a pyrazine ring, a diazine, which replaces C1 and C4 carbon atoms with two nitrogen atoms, can be attacked at the C2, C3, C5 and C6 positions by nucleophilic reagents due to electron deficiencies if at least one electron-donating group is attached to the ring (Ram et al., 2019). On the other hand, the occurrence of electrophilic

reactions is applicable in that both isobutyl side chains and methoxy groups belong to electron-donating groups, which facilitate electrophilic substitution reactions such as ring hydroxylation. Hence, both ring hydroxylation and demethylation are reactions (Fig. 4.3) likely to occur with IBMP.

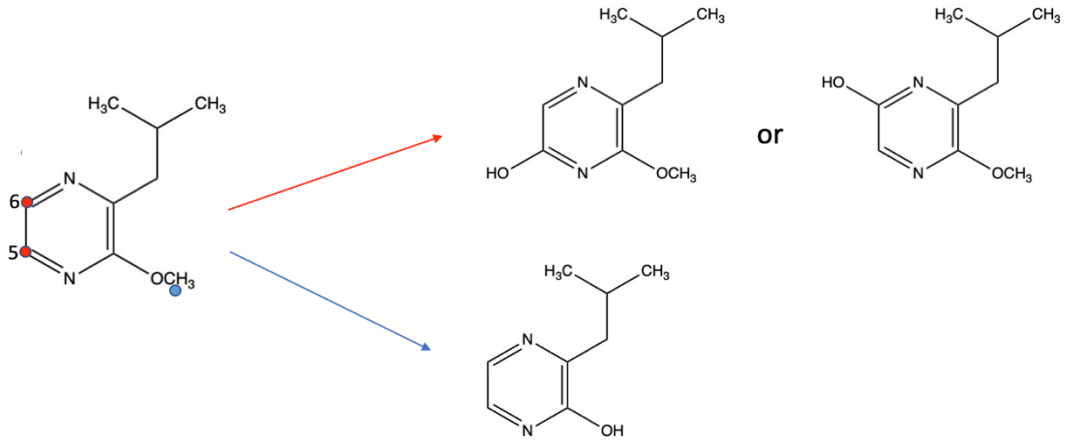

Figure 4.3 Proposed initial reaction for IBMP degradation/transformation. Two pathways are postulated. The red line and highlights indicate ring hydroxylation at the C5 and C6 position. The blue line and highlight indicate demethylation of the methoxy group.

4.4 Promising demethylase system and its potential application for the wine industry

Two strains were successfully discovered with the ability to degrade methyl violet (Section 3.3) suggesting a possible demethylase system therein, although this has not yet been identified. Speculation about the mechanism potentially responsible and its possible application in winemaking will be discussed.

Little is known about the enzyme system(s) involved in methyl violet degradation. Only one report has investigated the responsible demethylase. Specifically, a ligninolytic fungus, *Phanerochaete chrysosporium*, possessed the ability to *N*-demethylate methyl violet (Bumpus and Brock, 1988). The same degradation results were obtained for both extracellular fluids from ligninolytic cultures as well as a heterologous ligninolytic peroxidase system. Such findings indicated that a lignin-degrading system was involved in the demethylation of methyl violet. Substantial degradation of methyl violet in non-ligninolytic cultures was also recorded, suggesting that another degradation mechanism might be involved. Lignin peroxidases are able to catalyse a wide range of *N*-dealkylation reactions (Bumpus and Aust, 1987), and therefore similar peroxidase exploration trials were performed in this study. However, within the two strains identified, no positive results indicating the involvement of a

peroxidase were obtained. And no such responsible enzyme systems (demethylase) have so far been identified in published genomes. Nevertheless, future work seeks to further characterise the responsible enzyme system.

Microbial demethylases have been studied extensively and found to have the ability to degrade many xenobiotics. Such enzyme systems could be helpful in elimination of wine faults other than those due to IBMP, thereby highlighting a potential future research direction. As an example, the 'cork taint' compound, 2,4,6-trichloroanisole (2,4,6-TCA) produced by fungus in the cork used to produce wine closures (Campoy et al., 2009), remains a quality issue for the wine industry leading to significant economic losses (Pereira et al., 2000). As one of the remediation strategies, several white rot fungal strains have been shown to degrade this compound in a process initiated by cytochrome P450-catalysed demethylation. However, the demethylation product of TCA, 2,4,6-trichlorophenol, is toxic to humans (Yuan et al., 1993) and further degradation yielding harmless derivatives is required in a biological remediation approach.

Another undesirable character, 'smoke taint', is derived from grapevines and vineyards being exposed to smoke, and the taint is characterised by unpleasant smoky, burnt, ashy and medicinal aromas and flavours in wine (Kennison et al., 2007; Krstic et al., 2015). Increased concentrations of volatile phenols, such as guaiacols, have been identified in smoke-affected wines and are believed to be the major contributors of such unpalatable characters (Kennison et al., 2007). These pyrolysis products of lignin and their degradation pathways have been studied extensively in many microorganisms, with the responsible enzymes being elucidated (Janusz et al., 2017); demethylases have been shown to initiate degradation. For instance, a two-component guaiacol demethylase system identified in *Rhodococcus rhodochrous* and successfully expressed in a streamlined strain with better metabolic robustness, *Pseudomonas putida* EM42, could potentially be useful for providing exogenous metabolic pathways by which to degrade volatile phenols (García-Hidalgo et al., 2019). However, when developing such methods for the wine industry, consideration must be given to the nature of the downstream metabolites to ensure that they are non-toxic and impose little influence on overall wine quality. For example, the direct metabolite of guaiacol, which is catechol, is not an ideal compound to accumulate in wine due to its toxicity to humans (Schweigert et al., 2001). Luckily, microorganisms exist that have the ability to further oxidise catechol, albeit the downstream metabolites are yet to be identified (Dardas et al., 1985; Mallinson et al.,

2018); these microorganisms could therefore be used as references for tailoring metabolic pathways to yield more acceptable metabolites.

5 Conclusions

This chapter focused on exploring microbes with potential IBMP-degrading capability. Micro-organisms from diverse sources were included in the screening trials to expand the scope of microbial species and increase the possibility of discovering desired strain(s). Since IBMP has a low detection threshold (i.e., low ng/L) and is aromatically potent, work was restricted to a fume hood and quantitation required off-line, GC-MS analysis. These factors greatly limited the flexibility, scale and reliability of this screening approach. Whilst promising leads were nevertheless pursued through IBMP-based screening activities, most proved inconsistent or unreproducible. Alternative approaches were needed and included using IBMP and related compounds as growth nutrients. The most promising result arose from studies of microbial growth on methyl leucine, vanillic acid and 2-methoxypyrazine and/or decolourisation of methyl violet. Surprisingly, two fungal strains with the ability to decolourise methyl violet were identified, potentially via an *N*-demethylation process proposed previously. While these positive outcomes warrant further investigation, such work falls outside this candidature. Certainly, these possibilities will be taken up by the research group, whilst the accumulated screening expertise will help inform any future research efforts.

Chapter 4 Modification of VvOMT3, an *O*-Methyltransferase Responsible for IBMP Biosynthesis: An Attempt to Reverse Catalytic Activity

1 Introduction

The previous two chapters have described attempts to seek methods for IBMP remediation from a microbial perspective. In this chapter, trials on an enzymatic degradation strategy, are discussed in this chapter. As has been mentioned earlier (Chapter 1), no such enzyme has yet been discovered, potentially presenting a research gap/opportunity. Attempts to identify an enzyme capable of degrading IBMP were described in the previous chapter by exploring the degradation properties of environmental microbes. This chapter will focus on a different approach to achieving the same goal. VvOMT3, the key enzyme responsible for synthesising IBMP in grapes (Dunlevy et al., 2013), was selected as the target for enzyme engineering aimed at reversing the catalytic activity. Random mutagenesis was adopted for mutant library generation ahead of downstream screening. Whilst cloning, expression and enzyme production succeeded, no variants with a reverse capability were found. Possible reasons for this are discussed here as are insights that could support on future work using similar approaches.

1.1 VvOMT3, the key enzyme responsible for IBMP biosynthesis in grape berries

In another attempt to achieve IBMP remediation, an enzyme engineering-based trial was performed and is described in this chapter. The *O*-methyltransferase, VvOMT3, the key enzyme responsible for the final step in the biosynthesis of IBMP in certain *Vitis vinifera* cultivars (Dunlevy et al., 2013), was chosen as the template for enzyme modification due to close interactions with IBMP, as well as its hypothetical substrate, IBHP. This enzyme, together with three other highly homologous methyltransferases (VvOMT1, VvOMT2, VvOMT4) identified in certain *Vitis vinifera* varieties, can catalyse the methylation of 3-isobutyl-2-hydroxypyrazine (IBHP) to form 3-isobutyl-2-methoxypyrazine (IBMP). VvOMTs are members of a larger family of plant *O*-methyltransferases, that have been studied widely. Plant *O*-methyltransferases [OMTs, EC 2.1.1.6.x], catalyse the transfer of a methyl group from the donor S-adenosyl-L-methionine to a hydroxyl group of the acceptor. The role of these enzymes in the biosynthesis of plant-related phenolic compounds (including flavonoids and alkaloids) have been studied broadly (Ibrahim et al., 1998; Joshi and Chiang, 1998). Biochemical and molecular analysis of these plant OMTs suggest that despite their

different substrate specificities, they share highly similar amino acid sequences (Ibrahim et al., 1998). Furthermore, phylogenetic analysis categorised plant OMTs into two families, in which the OMT I family methylates caffeoyl and 5-hydroxyferuloyl CoA esters, whereas the OMT II family can catalyse the methylation of various substrates such as caffeic acid, 5-hydroxyferulic acid, caffeoyl-CoA ester and 5-hydroxyferuloyl ester (Joshi and Chiang, 1998).

A VvOMT was first identified and characterised in *Vitis vinifera* L. cv. Cabernet Sauvignon (Hashizume et al., 2001a, 2001b), and substrate specificity assays for the purified enzyme showed little difference in substrate discrimination among IBHP, 3-isopropyl-2-hydroxypyrazine (IPHP) and 3-*sec*-butylpyrazine (*s*BHP). However, like some other multifunctional plant OMTs (Li et al., 1997; Chiron et al., 2000), this enzyme showed activity, though very weak, towards a broad range of substrates, and amongst a group of methyl-acceptors commonly observed in plants, caffeic acid was the most favourable substrate. The N-terminal amino acid sequencing result for this enzyme indicated similarity with the OMTs from *Prunus armeniaca*, *Pinus taeda*, *Pinus radiata*, *Prunus dulcis* and *Pyris pyrifolia* (Hashizume et al., 2001b). Two cDNAs (*VvOMT1* and *VvOMT2*) encoding the *O*-methyltransferases involved in the methylation of IBHP and IPHP to form IBMP and IPMP, were subsequently identified by Dunlevy and colleagues (2010). Phylogenetically, these two enzymes belong to the plant OMT II family and are most homologous to a *Rosa chinensis* OMT. Enzymatic kinetic assays of the recombinant proteins revealed that VvOMT1 showed similar substrate affinity towards IBHP and IPHP, yet a higher turnover number, thus catalytic efficiency, for IBHP than IPHP. VvOMT2 presented higher substrate affinity towards IBHP, whereas a lower turnover number was observed for IBHP, hence catalytic efficiencies were comparable for both substrates. Taking IBHP as the substrate, VvOMT1 catalysed the reaction more efficiently than VvOMT2. However, many other substrates have been methylated by both enzymes, with greater catalytic activity demonstrated against flavonol quercetin, compared to other substrates including HPs (Dunlevy et al., 2010). Results from real-time PCR analysis indicated that the expression level of *VvOMT1* in the skin and flesh of Cabernet Sauvignon grapes during berry development coincided with the accumulation period of MPs in these tissues, whereas the greatest expression level for *VvOMT2* was found in roots, in which high concentrations of MPs were identified (Dunlevy et al., 2010).

Two other genes (*VvOMT3*, *VvOMT4*) encoding *O*-methyltransferases were identified by locus mapping in grapevine (Dunlevy et al., 2013). These two enzymes share 39%-45% amino acid identity with VvOMT1 and VvOMT2, and like VvOMT1/2, they belong to the plant OMT II family. Functional characterisation showed that both enzymes are capable of methylating IBHP and IPHP and k_{cat}/K_m values for VvOMT3 are far greater than those of VvOMT1/2/4 (Dunlevy et al., 2013). Unlike VvOMT1/2, which exhibited the greatest activity against other compounds, VvOMT3 had the highest specific activity towards HPs, while VvOMT4 did not show much difference in activity amongst the compounds tested, including HPs (Dunlevy et al., 2013). Analysis of gene expression within Cabernet Sauvignon and Pinot Noir berries during fruit development revealed a high expression level of *VvOMT3* pre-veraison, which correlated with the major accumulation period for IBMP (Dunlevy et al., 2013). In contrast, low expression was observed in Pinot Noir berries, which are known to lack significant quantities of IBMP. Results from their study indicated that the transcription of *VvOMT3* is the major controller for IBMP biosynthesis in grapes. Further research proposed VvOMT3 as the key gene responsible for IBMP biosynthesis in grapes, based on its different expression levels in Cabernet Sauvignon and Petit Verdot, which are high- and low-IBMP producers, respectively (Guillaumie et al., 2013). A separate study investigated the influence of different abiotic stressors, including restriction to sunlight exposure, and a combination of lateral shoot removal and water deficit, that were thought to affect both IBMP levels and expressions of *VvOMT1-4* genes, in seeded and parthenocarpic berries of Carmenere and Cabernet Sauvignon grapes (Vallarino et al., 2014). Introductions of these stressors yielded an increase in IBMP in seeded grapes compared with the control, but did not yield significant differences in IBMP in the resultant wine. This might be explained by the extractability of MPs during vinification process (Roujou de Boubee et al., 2002; Vallarino et al., 2014). Decreased IBMP levels were generally observed in parthenocarpic berries, but similar trends were observed as with seeded fruits. Results from analysis of *VvOMT1-4* gene expressions correlated with abiotic stressors revealed that *VvOMT3* was the only gene for which the expression level was consistent with IBMP concentrations, regardless of environmental stress. This confirmed *VvOMT3* plays a key role in IBMP biosynthesis in grapes. The regulation of this gene in grapevines was also studied by analysing histone modification patterns, and results suggested that histone tail methylation patterns are spatially and developmentally regulated at the *VvOMT3* locus (Battilana et al., 2017).

Details of the structure-function relationship for VvOMT3 (and three other VvOMTs) are essential for potential protein engineering. However, this information is only obtained only via homology modelling (Vallarino et al., 2011; Guillaumie et al., 2013); supportive experimental data is absent. Computer-based modelling and calculations have been performed for VvOMT1 and VvOMT2 to propose structural features responsible for different catalytic activities (Vallarino et al., 2011). Since the crystal structure for VvOMTs has not yet been determined, homology modelling instead referenced *Medicago sativa* isoflavone *O*-methyltransferase (IOMT, AF023481) (ID code: 1FP2; resolution: 1.4Å; R-value: 0.217). Computational analysis demonstrated that the active sites for both enzymes coincided with those of other OMTs. They also reasoned that steric hindrance for both substrate and SAM, due to two amino acid (M182 and H272 for VvOMT1) differences between VvOMT1 and VvOMT2 led to diverse catalytic efficiency (Vallarino et al., 2011). VvOMT3 has been subjected to similar computational modelling analysis, in comparison with VvOMT1 to elucidate the higher efficiency observed for VvOMT3 (Guillaumie et al., 2013). Replacement of Phe 178 and Phe 319 in VvOMT1 by Ile 162 and Leu 307 in VvOMT3, potentially leads to a larger and more flexible substrate-binding pocket, and is one of the reasons hypothesised for the improved catalytic efficiency of VvOMT3. Research on VvOMT3 and other VvOMTs is still preliminary, with the majority of studies focusing on gene identification, expression and interactions with environmental factors. More in-depth studies that aim to provide detailed information on enzyme structures are needed for further enzyme modification.

Apart from determination of the target enzyme for modification, another key consideration was the feasibility of the reversibility of this reaction, which is the methylation of IBHP yielding IBMP. However, thermodynamic data for the final step of methylation reaction are absent from all relevant studies, as the research focus has instead been on enzyme kinetics. As such, limited characterisation of the enzyme, or the reaction itself, have been performed. Evidence therefore has to be sourced from elsewhere to support the possibility that the reverse reaction can occur. The behaviour of IBHP has been investigated in wine grapes (Cabernet Franc) over a range of maturity levels to reveal the potential relationship between IBHP and IBMP during berry growth (Ryona et al., 2010; Harris et al., 2012). Observations that the concentration of IBHP peaked two weeks after IBMP levels were reached and then declined, led to the hypothesis that IBMP was demethylated to IBHP, prior to further degradation (Fig 1.2.1). This was supported by a subsequent study that reported IBHP and its glycoside were identified in rat urine after feeding with IBMP (Hawksworth and Scheline,

1975). It has therefore been suggested that the reverse reaction of IBHP methylation, i.e. IBMP demethylation, is quite likely achievable. This evidence provides the basis for the experiments described in this chapter.

1.2 Enzyme engineering

For millions of years, numerous natural biocatalysts or enzymes have evolved to support life on earth. However, in the ever-developing human society, attempts to develop enzymes for industrial applications have highlighted some disadvantage of enzymes. For example, the high specificity, and thus narrow substrate range of some enzymes, and instability of others, can make enzymes unsuitable for the needs of the biotechnology industry. Early attempts to evaluate natural microorganisms for desirable enzyme activity have largely involved labour-intensive screening of microbial cultures, whereas nowadays, this can be facilitated by technologies such as high-throughput screening (Rondon et al., 1999) and heterologous expression of enzymes. New possibilities have emerged with the advent of recombinant DNA technology, which allows genes to be manipulated in a more specific fashion, enabling the redesign or modification of enzymes at the molecular level. Amongst these ever-evolving technologies, directed evolution is one of the more mature and effective methods of enzyme manipulation that can be performed without requiring knowledge of structure-function relationships. This approach refers to a set of techniques that aim to modify existing enzymes by creating a diversity of mutants, which are then screened according to the desired phenotype. There are currently a range of methods that have been developed to construct enzyme mutants with great diversity, which will be described in detail below.

1.2.1 Site-directed mutagenesis

Site-directed mutagenesis is a PCR-based method to mutate specific nucleotides at will. It has been widely used to study the relationship between an individual amino acid or a residue and the structure and function of a certain protein, and as a rational approach to generate mutant pools for phenotype screening. (Robin et al., 2019; Wu et al., 2018; Xu et al., 2019ab) Saturation mutagenesis, which is derived from original site-directed mutagenesis, has been used widely in order to increase the probability of positive mutations. The principle of this method is to use degenerate primers to introduce the full diversity of 20 amino acids at a certain position. Successful cases have been reported for modification of enzymes with traits such as improved enzymatic activity (Wu et al., 2018; Xu et al., 2019a), and enhanced enzyme stability (Xu et al., 2019b). This technique has also been employed to construct novel

enzymes. Sadat and colleagues (2010) applied protein engineering to generate a novel NADPH-dependent xylose reductase from *Pichia stipites*, aiming for a more efficient cycle of NADPH between xylose reductase and xylitol dehydrogenase that used to be an obstacle for xylose fermentation in *Saccharomyces cerevisiae*.

Site-directed mutagenesis is considered a more rational approach for generating mutation libraries, due to its high specificity. However, the required knowledge of enzyme structure can be a barrier in cases where little information is available.

1.2.2 Random mutagenesis

Researchers tend to choose random mutagenesis when aiming to create larger sizes of mutation libraries, especially with limited knowledge of the functionally important regions of the wildtype enzyme, and this approach can create novel catalytic activity where drastic irrational changes occur (Sylvestre et al., 2006). Various random mutation methods are available, including ultraviolet and chemical mutagens (Chu et al., 1979), as well as incorporation of nucleotide analogues (Müller et al., 1978). However, the most convenient and frequently used approach is error-prone PCR (Cirino et al., 2003), which is a modification of standard PCR methods designed for increasing the natural error rate of the polymerase (Cadwell and Joyce, 1992). The rationale is to take advantage of the relatively low fidelity of *Taq* polymerase compared to other enzymes, such as modified T7 polymerase (Sequenase), Vent DNA polymerase (Ling et al., 1991) and T4 DNA polymerase (Sinha and Haimes, 1981). The reported error rate of *Taq* is 0.001-0.02% per nucleotide per pass of the enzyme (Eckert and Kunkel, 1991), which is far less efficient for creating mutations, and measures to modify the reaction conditions or enzyme itself are thus required to achieve the significant reduction in enzyme fidelity. The common methods developed (and subsequently improved by many researchers) include the addition of $MnCl_2$, increasing $MgCl_2$ and *Taq* polymerase concentrations, unbalancing the ratio of deoxyribonucleotides, increasing the extension time and cycle numbers (Cadwell and Joyce, 1992; Sylvestre et al., 2006), and the addition of dimethyl sulfoxide (DMSO) (Hardjasa et al., 2010). The resulting error rate has been claimed to be ~2% per position per PCR, and different proportions of transitions and transversions have been reported (Sylvestre et al., 2006).

It should be acknowledged that random mutagenesis is not completely random and that some mutation biases have been observed. While some studies report that transitions occur more

favourably against transversion for base substitution, the most vital part comes from the extremely low occurrence of two or three consecutive base substitutions in a codon. For instance, for a single codon AGT, this technique could produce only 9 different codons with higher chances encoding on average 5 amino acids at most, leaving about three quarters of the amino acids inaccessible. Despite this, many successful mutations have been achieved using this technique to modify enzymes with enhanced characters such as thermostability (Chen and Arnold, 1993; Moore and Arnold, 1996; Zhao and Arnold, 1999; Kim et al., 2001). On the other hand, altered catalytic activity has been achieved via random mutagenesis (Chen and Arnold, 1993). Specifically, this method has been used to generate mutants from *Bacillus subtilis* subtilisin E, which were subsequently screened by directed evolution to produce a novel enzyme with equivalent function to thermophilic thermitase from *Thermoactinomyces vulgaris*.

As mentioned earlier in this section, rational protein engineering strategies can be challenging when little is known about protein structure, which is the case for VvOMT3. Detailed structural information is not available for this enzyme, only limited knowledge of some active sites is available from software modelling (Vallarino et al., 2010; Guillaumie et al., 2013). Random mutagenesis may therefore be a better method for this case.

1.2.3 Other technologies

Apart from the common mutation methods mentioned above, some other techniques such as *de novo* gene synthesis and gene shuffling have also been developed and utilised widely to create mutation libraries.

The approach of synthesising diverse genes *de novo* is most suitable for cases where structure-function information is well understood, allowing the custom-tailored synthesis to occur. This method for generating diversity of mutations is performed via the assembly of designed oligonucleotides (ADO), prepared with guidance of the sequence information and could be applied to genes with low homology. It could minimise the chances of self-hybridisation of parental genes and high recombination frequency can be achieved by controlled overlapping of oligos (Zha et al., 2003). Such a method has been developed to increase the enantioselectivity of the lipases from *Bacillus subtilis* (Zha et al., 2003).

Gene shuffling is a method developed based on the idea of assembling DNA from oligos *in vitro*. The principle is that the progeny of parental genes, which have been pre-screened by natural selection as functional have a good chance of yielding genes with improved functional capability. There are many different gene shuffling methods, most of which are based on the fragmentation step of parental genes and are followed by PCR random reassembly of the segments. An example is the staggered extension process (StEP) which functions by extremely rapid melting, annealing and extension so that in each cycle, growing fragments anneal to different templates and extend further until a full-length sequence is formed (Zhao et al., 1998). However, these methods are all restricted to homologous recombination of genes, thereby limiting the range within a gene family. Nevertheless, some techniques to generate non-homologous recombination have been proposed and developed. An example, termed as incremental truncation for the creation of hybrid enzymes (ITCHY), works on direct ligation of segments generated by the fragmentation of two sequences with each being truncated from the opposite end. Whereas the way of ligation is hard to control, leading to possible generation of nonsense products (Lutz et al., 2001). An improvement (Thio-ITCHY) has thus been developed, targeting a simplification of the procedure of timed exonuclease digestion that is hard to control and optimise, to incorporate phosphorothioate linkages at random along the gene while generating templates and then followed by exonuclease digestion to generate fragments with desired lengths achieved by the insertion of nuclease-resistant phosphorothiate linkages (Lutz et al., 2001).

There are other techniques derived from the similar rationale of assembling genes or from improvements or modification being made to the techniques mentioned above. However, given the advantages and drawbacks of each method, it's important to choose a fit-for-purpose approach.

1.3 Aims of the project

Continuing the aim of previous chapters, but taking a novel approach, this chapter aimed to explore a possible biological method by which to degrade IBMP, using an enzyme developed through protein engineering. In this research, *VvOMT3*, which has been identified and characterised, was used as the template for enzyme mutagenesis. Given the limited knowledge that has so far been obtained on the structure-function relationship of this enzyme, random mutagenesis was chosen as the method to structurally modify the enzyme, so as to favour the reverse catalytic reaction. However, there was little information available on

enzyme engineering to enhance reverse enzymatic activity, so error-prone PCR was applied in order to create drastic changes amongst the sequence, which ideally would result in novel catalytic activity. The information gained from this chapter will shed some light on further research of this enzyme from a structural-functional perspective, which could potentially support applications for manipulating IBMP accumulation.

2 Materials and methods

2.1 Chemicals, solutions and media

All chemicals, solutions and media used in this experiment are listed in Table 2.1.

Table 2.1 Chemicals, solutions and media

Name	Ingredients
LB media	1% (w/v) tryptone, 0.5% (w/v) yeast extract, 1% (w/v) NaCl, pH 7.0. For solid media, 2% (w/v) agar
Kanamycin stock solution	25 mg/L
Chloramphenicol stock solution	25 mg/L
Plasmid extraction kit	Promega Wizard® Plus SV Minipreps DNA purification system
1× TAE buffer for DNA gel electrophoresis	40 mM Tris base, 20 mM acetic acid, 1 mM EDTA sodium salt dihydrate
5× Loading buffer for DNA gel electrophoresis	50% (v/v) glycerol, 10% (w/v) SDS, 1.25M Tris-HCl, 5% (v/v) β-mercaptoethanol, 0.025% (w/v) bromophenol blue, pH 6.8
Gel purification kit	Promega Wizard® SV Gel and PCR Clean-up system
Protein resuspension buffer	10 mM Na_2HPO_4, 10 mM NaH_2PO_4, 500 mM NaCl, 20 mM imidazole, pH 7.4
Protein storage buffer	50 mM Tris-HCl pH 7.4, 30 % glycerol and 500 mM NaCl
2× SDS-PAGE loading buffer	Bio-Rad Laemmli sample buffer
SDS-PAGE running buffer	40 mL ethanol, 10 mL acetic acid, 50 mL water
SDS-PAGE gel	Bio-Rad mini-protean TGX, Any KD
SDS-PAGE stain	Bio-Rad QC colloidal Coomassie
Citrate/phosphate buffer for GC-MS analysis	100 mM Na_2HPO_4, 50 mM citric acid, pH 5.0

2.2 Mutant library construction

VvOMT3 was used as the parent gene for mutant library construction. Error-prone PCR (EP-PCR) was performed, as the most common approach to (i) randomly create a single-gene-based combinatorial library and (ii) the method with the greatest potential to create drastic changes. The error-prone PCR protocol was modified from the original PCR protocol (i.e., the reaction system shown in Table 2.2.1, and reaction program shown in Table 2.2.2) in order to reduce the fidelity of *Taq* DNA polymerase, while maintaining optimal yield. Several pilot trials were conducted to optimise the reaction conditions. Error-prone PCR products were then used as templates (30%) for subsequent rounds to increase the overall mutation rates; in total, 20 rounds of EP-PCR were performed.

Table 2.2.1 Error-prone PCR reaction system

Component	Concentration for normal PCR	Concentration for EP-PCR
H_2O	-	-
Taq polymerase	40 U/mL	40 U/mL
Forward primer	0.6 μM	0.6 μM
Reverse primer	0.6 μM	0.6 μM
DMSO*	-	3%
$MgCl_2$ (50 mM) **	1.5 mM	4.5 mM
dGTP (100 mM) ***	0.2 mM	1.2 mM
dNTP (except dGTP)	0.2 mM	0.2 mM
Template DNA	10 ng	10 ng

*DMSO was used to increase PCR yield and mutation rate.

**The final concentration of Mg^{2+} (including master mix and additional $MgCl_2$) increased from 1.5 mM to 4.5 mM to reduce the fidelity of *Taq* DNA polymerase thus increasing mutation rate.

***The final concentration of dGTP (including master mix and additional dGTP) increased from 200 μM to 1 mM to create an unbalanced ratio of nucleotides aiming at increasing the error rate as well as minimising mutational bias.

Table 2.2.2 Error-prone PCR reaction program

Cycle step	Temperature (°C)	Time (sec)	Cycles
Initial denaturation	98	120	1
Denaturation	98	5	
Annealing	58	5	20**

Extension*	72	18	
Final extension	72	60	1

*increased polymerase extension time to increase mutation rate.

**cycle numbers are trialled first to ensure optimal mutation rate yet maintaining low yield of incomplete products.

2.3 Construction of recombinant expression vector and purification of mutant proteins

Mutated genes were cloned into the expression vector pET30a by adding restriction endonuclease site BamHI to the forward primers and site XhoI to the reverse. Double digested PCR products were then ligated into an equally treated pET30a vector. Constructs were transformed into *E. coli* BL21 (DE3), and transformants were plated onto LB plates containing 25 μg/mL of kanamycin and 25 μg/mL of chloramphenicol for selection and plates were incubated overnight at 37°C. Colonies were selected from LB plates and colony PCR was performed to check for positive transformants, before sequencing of the positive PCR products was conducted for the results of random mutation and also to confirm the desired insertion of sequences within the recombinant vector were in frame with the pET30a start codon.

Positive candidates were selected and cultured at 37°C until OD_{600} reached 0.6-0.8, when IPTG was added at the final concentration of 0.5 mM. Cultures were then incubated at 18°C for 96 h and centrifuged (× 5000 *g*) at 4 °C yielding cell pellets. Cells were resuspended in the buffer containing 0.2 mg/mL lysozyme and complete EDTA-free protease inhibitor and were then treated with ultrasonication for cell lysis. Crude protein extracts were obtained from the supernatant after centrifugation at 4 °C for 40 min and were kept in protein storage buffer at -80 °C for further assays.

SDS-PAGE was performed for the determination of recombinant protein in crude extracts before proceeding to library screening. Protein extracts were pre-mixed with loading buffer and incubated at 100 °C for 5 min before loading onto sample wells of Mini-PROTEAN TGX polyacrylamide gels (Bio-Rad) for gel electrophoresis which was performed at 80 V for 50 min. Finished gels were soaked in QC Colloidal Coomassie staining solution (Bio-Rad) overnight, followed by 3 h of de-staining in water to reveal the bands.

2.4 Mutant library screening

Mutant library screening was performed by enzymatic reactions followed by GC-MS/MS analysis. Apart from IBMP, IBHP was also used as a substrate to study the possible effects of mutations on the wildtype catalytic activity. Reaction mixtures (Table 2.4.1) were incubated for 6 h at 30 °C, and for control groups, crude extracts were heat denatured (100 °C for 5 min). Methanol was added to stop the reaction and solutions were kept at -20 °C until needed for IBMP analysis.

Table 2.4.1 Enzymatic reaction mixtures

IBMP biosynthesis	IBMP degradation
50 mM Tris-HCl, pH 7.5	50 mM Tris-HCl, pH 7.5
1 mM MgCl2	1 mM MgCl2
1 mM DTT	1 mM DTT
0.1 mM SAM	0.1 mM SAH
2 μM IBHP	0.5 μM IBMP

3 Results

3.1 Mutant library construction and protein expression

E. coli colonies with expression vectors successfully transformed were picked from agar plates for colony PCR, and products were sent for sequencing after excluding false positive candidates based on PCR results (Fig. 3.1.1). Of the 95 candidates sequenced, 89 passed the quality check with reliable sequence data generated. Based on the pairwise alignments of each candidate with the wildtype gene, 78 candidates gave complete sequences, and of these, 52 candidates showed various degrees of mutation. However, silent mutation sequences and sequences with the same mutations were observed, yielding 22 mutants with distinctive missense mutations (see sequence details for these 22 mutants in Appendix Fig. 1).

As the candidate pool comprised of products from 20 rounds of error-prone PCR, of which 30% were used as templates for subsequent rounds, different levels of mutations were noted among 22 mutants ranging from only 1 nucleotide change to as many as 12 nucleotide changes per sequence.

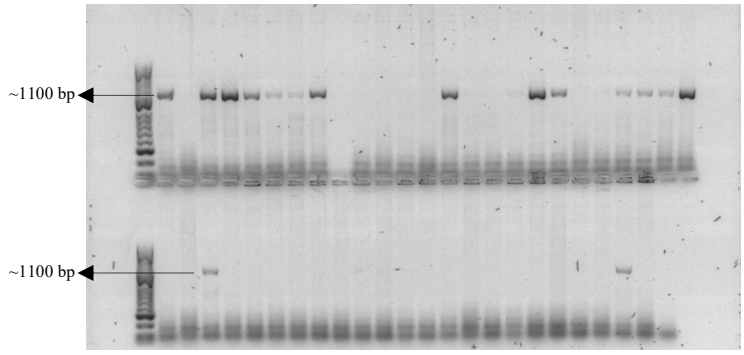

Figure 3.1.1 Colony PCR for selecting positive transformants. Lanes with bands indicate positive transformants, while those without bands suggest negative ones.

Each mutant was then induced for protein expression, and SDS-PAGE performed for assessment. Bands spotted at desired region (~50 kDa) for the wildtype gene, in accordance with previous reports, indicated the effectiveness of the induction, and 7 out of the 22 mutants were observed with similar-sized bands to the wildtype gene; the rest did not show the same trends in this region (Fig. 3.1.2), instead resembling a negative control (empty vector) suggesting that the desired proteins may not have been produced in these 15 other candidates.

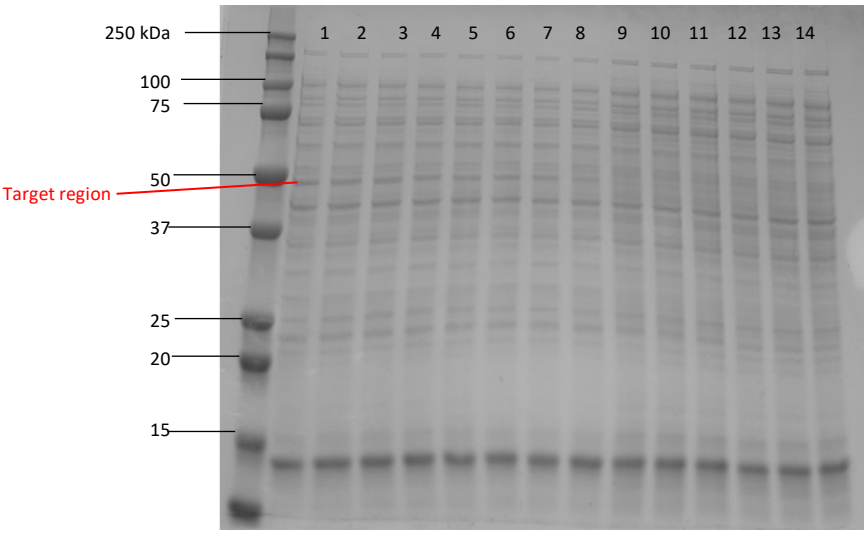

Figure 3.1.2 SDS-PAGE of protein crude extracts purportedly containing recombinant protein expressed from *E. coli* (DE3). Lane 1, positive control; lane 2 to 13, mutants 1, 34, 175, 212, 228, 249, 298, 2_17, 92, 102, 112, 208; lane 14, negative control

3.2 Mutation analysis

Mutation rates among the 22 missense mutants were analysed. Overall, 133 nucleotide changes including insertions and deletions occurred over a range of locations within the sequence, of which 92.94% of the changes were single nucleotide substitutions; 4.71% being single base deletions and the rest being insertions. Given that 30% of the templates for rounds 2-20 were products from previous rounds, and repeated mutations were observed in many sequences, the actual number of changes might have been less than 133. Considering the two most extreme cases, in which all of the repeated mutations were 'inherited' from the templates (yielding 85 changes), and all changes including recurring ones in different sequences were new mutations generated from each cycle (yielding 133 changes), the average mutation rate of each error-prone PCR treatment was 0.99%-1.52% nucleotide change per cycle.

More detailed analysis was performed accounting for repetition, and one of the most crucial parameters was mutational bias evaluation (Table 3.2.1). Other than that, mutation rates were also concluded (Fig. 3.2.2).

Table 3.2.1 Mutational analysis based on both potentially repetitive (133) and non-repetitive (85) mutations

Type(s) of mutations	133 mutations	85 mutations
Bias Indications		
Transition/Transversion	1.24%	1.47%
AT-> GC/GC->AT	0.7%	0.8%
A->N, T->N	37.59%	42.35%
G->N, C->N	54.89%	50.59%
Transitions		
A->G, T->C	22.76%	20.58%
G->A, C->T	32.52%	32.91%
Transversion		
A->T, T->A	8.13%	10.13%
A->C, T->G	9.76%	8.86%
G->C, C->G	13.01%	10.13%
G->T, C->A	13.82%	11.39%

Slight mutation bias was recorded for single base substitution, specifically, a higher ratio was observed for transition than transversion (Fig. 3.2.3). This seemed reasonable given a transition mutation is more likely to occur naturally than transversion due to the higher chance of substitution compared to changing for unequal number of rings in the structure. However, the higher chances of transitions might be one of the causes for the large

proportions of silent mutations. On the other hand, guanine (G) and thymine (T) are the most preferred nucleotide changes, regardless of possible repetition of mutations, while cytosine (C) is the least favoured nucleotide change, which correlates with C being the most reactive base for mutation to another nucleotide (Fig. 3.2.2a). It is therefore obvious that the number of C bases present in the gene decreased the most after mutation, while the number of T bases increased due to the higher rate nucleotide change into T, than from T. Amongst these changes in the numbers of bases, G and A bases remained relatively consistent during mutation.

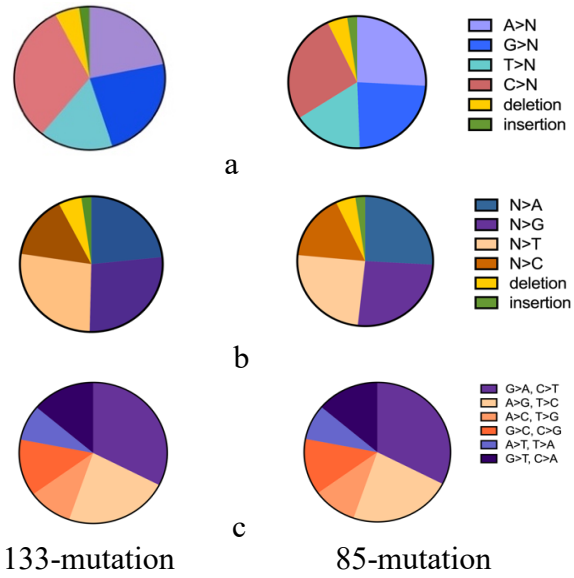

Figure 3.2.2 Detailed mutational analysis for two types of possible mutation occurrences. a, respective proportions for bases A, G, T, C change into; b, respective proportions for other bases change into bases A, G, T, C; c, respective proportions of transitions (A←→G, T←→C) and transversions (A←→C, G←→T, A←→T, G←→C). Pie charts on left panel were calculated based on 133 mutations; pie charts on right panel were calculated based on 85 mutations.

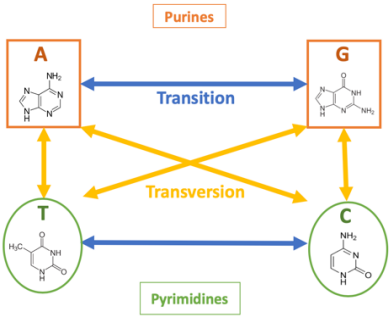

Figure 3.2.3 Transition and transversion patterns (Carr, 2014).

3.3 Enzyme activity screening

E. coli containing recombinant vectors were lysed after expression induction and cell crude extracts confirmed by SDS-PAGE were incubated with both IBHP and IBMP to screen for biosynthesis and degradation abilities.

Of the enzymes tested, the 7 (of 22) that showed bands in SDS-PAGE succeeded in producing IBMP, in agreement with the positive control (i.e., the wildtype VvOMT3 enzyme) with no significant difference in yield observed. While this validated the effectiveness of the method, none of the enzymes showed any ability to significantly decrease IBMP levels (Fig. 3.3.1b). Nevertheless, the chances were high that the mutations in the other 15 candidates may have disabled their biosynthesis ability, given IBMP was not detected after reaction with these enzymes. Sequence analysis showed that nucleotide changes within these 15 mutants contained nonsense mutations that resulted in truncated translation products, which most likely altered their structure and led to loss of function (see the example shown in Fig. 3.3.2); this might also explain the absence of bands in the SDS-PAGE results (Fig. 3.1.2).

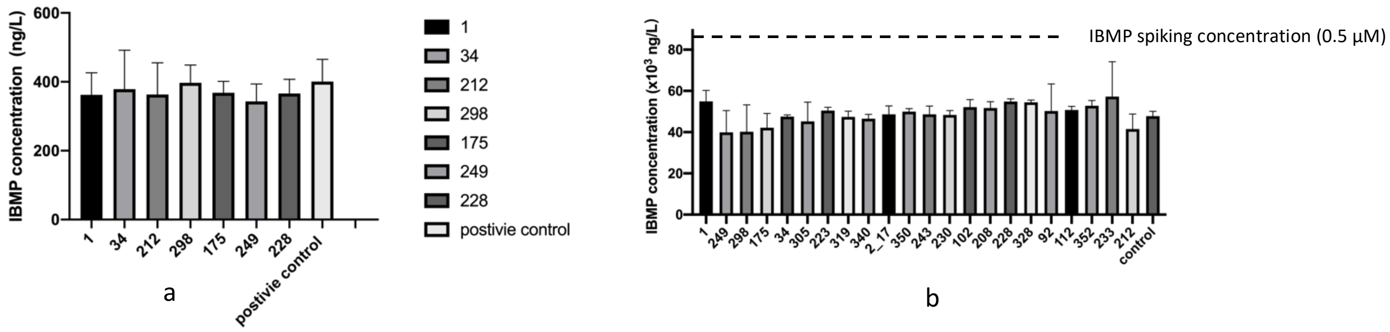

Figure 3.3.1 IBMP concentrations (ng/L) determined by GC-MS/MS analysis in biosynthesis tests and biodegradation tests with mutants. a. IBMP biosynthesis test with 7 mutants and the wildtype VvOMT3 as the positive control; b. IBMP degradation test with 22 mutants and denatured wildtype VvOMT3 as the control.

Figure 3.3.2a Pairwise alignment of mutant 2_17 with wildtype gene (*VvOMT3*); three point mutations (highlighted) including 1 deletion are observed.

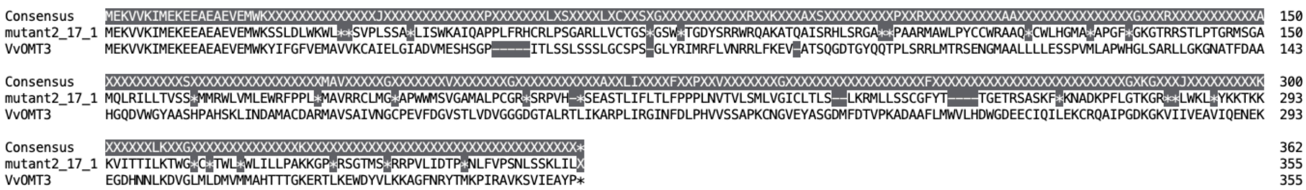

Figure 3.3.2b Pairwise alignment of predicted amino acid sequences between mutant 2_17 with wild type (VvOMT3); large changes including stop codons (highlighted) within mutant sequence are observed.

4 Discussion

According to the result of the functional tests, the mutants obtained from EP-PCR were not capable of degrading IBMP, and only 7 out of 22 retained their biosynthetic activity; the rest apparently lost functionality due to nonsense mutations. Overall the mutations amongst these 22 mutants likely weren't drastic enough in their effects to achieve the desired change in functionality. This would in part have been due to relatively small size of the mutant library generated. Other studies have screened ~10, 000 transformants to achieve improved enantioselectivity of a bacterial lipase (Reetz et al., 2010). Besides the lack of a complete profile of the mutant pool due to the limited library size, the drawback of the EP-PCR method used, as well as the difficulty in library screening, and potential improvements to address these issues, will be discussed below.

4.1 EP-PCR condition optimisation

Some of the issues experienced with EP-PCR were addressed during the experiment; one of which was deciding on the thermal cycle numbers to be used in EP-PCR. It has been reported that the determining factor for mutation rates is the number of doublings, rather than the number of cycles (Fig. 4.1.1) and that error rates will no longer increase once a plateau for DNA concentration is reached (Wilson and Keefe, 2000). Additionally, increased thermal cycles are not advisable as the shorter DNA fragments produced by mis-priming could have a stronger selective advantage for amplification especially with increased cycles (Wilson and Keefe, 2001). A preliminary trial containing 3 groups with different thermal cycle numbers (15, 20 and 40 cycles) was therefore performed, and results showed no difference for sequence integrity (Fig. 4.1.2) between 20 and 15 cycles, whereas a higher ratio of incomplete sequences was observed for the 40-cycle group. Thus, 20 cycles were selected as the number for each EP-PCR reaction in order to achieve a higher mutation rate. A larger proportion (70%) of the wildtype gene was also used in the template pool to minimise the effect of mis-priming with shorter amplification products. Nevertheless, it should be noted that the design of this pilot experiment was not statistically valid, as no replicates were set. The pilot experiment was only intended to inform the choice of cycle number for the formal experiments.

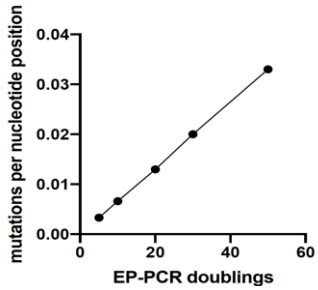

Figure 4.1.1 Average number of mutations per number of EP-PCR doublings (data adapted from Wilson and Keefe, 2000)

An additional improvement that was made during the pilot trial was to investigate the efficiency of DNA amplification per cycle, in order to further determine the optimal cycle number, as well as the template concentration. In each cycle of EP-PCR, the amount of DNA generally increases by a factor of 1.7-1.9, until it stops (Wilson and Keefe, 2001). Extra cycles are therefore not useful for accumulating desirable products, rather they increase risks of mis-priming. Thus, it is important to determine the amplification efficiency under the desired EP-PCR reaction conditions and to make adjustments to the reaction system accordingly, if needed. To achieve this, the concentrations of products obtained after different cycles were quantified by gel electrophoresis, with known amounts of templates (Fig. 4.1.3). The reaction conditions were chosen if DNA was amplified by a minimum of 1.7-fold per cycle.

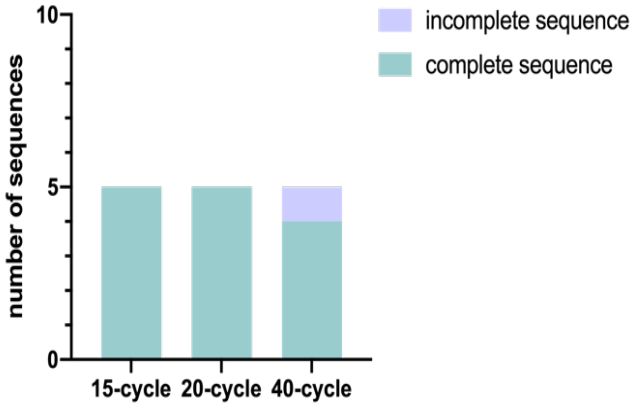

Figure 4.1.2 Pilot trial for determining optimal cycle numbers to minimise incomplete sequence numbers.

It was observed during the pilot trial that mutation rates within these 14 complete sequences were below expectation. Mutations were recorded in 66.7% of the candidates but with only an average of 1.5 nucleotide changes per sequence, which is far less enough for drastic mutations aiming for a novel catalytic activity. A slight modification was therefore adapted by mutagenizing a library with EP-PCR and iterative saturation mutation (Wilson and Keefe, 2001; Reetz and Carballeira, 2007). The details and outcomes of which are discussed below in 4.2.

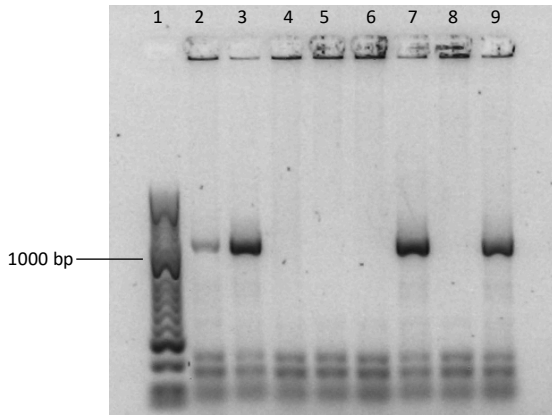

Figure 4.1.3 PCR reaction condition check. Lane 1, DNA ladder; lane 2, template DNA, lane 3-6, PCR products after 20 cycles in different conditions (lane 3 was determined as optimal condition); lane 7-9, PCR products after 40 cycles in different conditions.

4.2 Mutation method (Iterative Error-Prone PCR), and its possible consequences for mutation products

As mentioned, the enzyme screening method was a major hindrance for high throughput screening in this experiment, and limited the size of the mutant library, making it necessary to accumulate many mutations within an individual mutant sequence for efficiency improvement. On the other hand, multiple mutations within a sequence are especially desirable, to cater for the aim of this experiment, which was to generate novel catalytic activity (Wilson and Keefe, 2001).

In this section, method of Iterative Error-Prone PCR is discussed, along with its outcomes on mutation patterns. Mutation bias regarding mutation distribution in the sequence was proposed that clustered mutations were observed. However, further analysis on a larger

library disproved such hypothesis and suggested no mutation bias as reported in other studies. Nevertheless, the mutation clustering observed amongst candidate mutants possibly led to higher chances of occurrences of stop codon insertion as well as missense mutations, of which explanations are discussed in this section. One of the major drawbacks identified for the IEP-PCR method used in this experiment was the repetitive nucleotide changes observed amongst the mutant library which reduced mutation efficiency. Detailed analysis and explanations are discussed below.

A modified EP-PCR method that aimed to increase the proportion of mutants in the final pool was used, during which small portions of EP-PCR products were added to the templates used in the subsequent round, compared with normal EP-PCR which only used wildtype sequences as templates. A 'dilution and pooling of EP-PCR products' approach (Fig. 4.2.1a) whereby serial dilution of products from each round occurs every 4 cycles and a total of 64 cycles performed, has been described (Wilson and Keefe, 2001; McCullum et al., 2010). In this experiment, a similar procedure, iterative error-prone PCR (IEP-PCR) was adapted after each complete PCR program (comprising 20 cycles, as determined in the pilot trial), and this step re-occurred 20 times, to give final cycle numbers of 400 (Fig. 4.2.1b), after which products from each round of mutation are mixed together in the final pool.

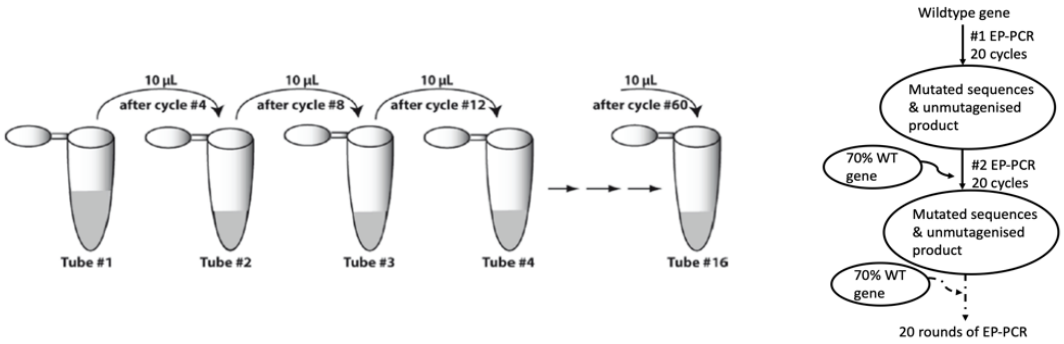

a b

Figure 4.2.1 Demonstrations for IEP-PCR workflow. a, Dilution and pooling technique used in EP-PCR (adapted from McCullum et al., 2010); b, IEP-PCR technique used in this experiment.

The mutation rates obtained using this method were greatly increased compared to those of the pilot trial. Nevertheless, it should be acknowledged that due to the restriction on mutant library screening, the library size was chosen at a small scale, so the data may not be

completely representative. Of the 89 mutants that were successfully sequenced, 52 were complete sequences comprising 152 mutations overall. Amongst them, 22 mutants with distinctive missense mutations containing a total of 133 changes were actually recorded after excluding repetitive and silent sequences. Therefore, the final error rate was 3.65% per nucleotide per PCR reaction (based on 4 cycles per reaction, standardised by McCullum et al., 2010), similar with the reported ~3.5% per nucleotide per PCR reaction (McCullum et al., 2010). However, high incidences of repetitive sequences (21 out of 52, 40.38%) and base mutations (54 out of 152, 35.53%) were encountered, which was one of the downsides of this method that lowered mutation efficiency. Overall, the average number of mutations for each mutant sequence was 6.05 for the final 22 mutants.

A similar approach, namely iterative saturation mutagenesis (ISM), has been proposed for and widely applied to enzyme modification. As a rational mutagenesis method, of which the structure-function relationship is clearer compared to cases for EP-PCR, the fundamental concept of ISM is the Cartesian view of the 3D protein structure (Reetz and Carballeira, 2007), which gives an overall idea on the regions or positions that may be crucial for modification. Similar to normal saturation mutagenesis, a mutant library is firstly created and screened until a best hit arises. This is then used as the template for another round of saturation mutagenesis. Unlike simple combinations of mutants with a hit, the advantage with ISM is that the chances of obtaining additive and/or cooperative effects of new mutations in desired regions are increased (Reetz and Carballeira, 2007). As an example, this method has been used to enhance the thermostability of a *Bacillus subtilis* lipase A (Lip A) (Reetz et al., 2006). Based on the X-ray data of the protein, and the fact that hyperthermophilic enzymes appear more rigid than mesophilic proteins (Matthews, 1993; Jaenicke and Böhm, 1998; Reetz and Carballeira, 2007), B factor reflecting thermal motions were used as the selection criterion (Reetz et al., 2006). The target regions within this protein displaying the highest B factor were chosen for iterative saturation mutagenesis. The mutant with the best hit from the first round of screening is used as the template for the next round, from which a second-best hit is generated, and the process continues in a hierarchical manner until all sites within this region have been mutated. This is a more rational approach compared to the EP-PCR method where the whole sequence is considered anew in each cycle, even though the crucial regions may only be a few positions. However, it has to be acknowledged that the rationale behind EP-PCR is to ‘mess up the sequence’ by nucleotide substitutions, insertions and deletions, with the latter two being more desirable in that frameshift, could occur leading to drastic

changes. The implication is that choosing the best mutation method from amongst those available is likely to be quite case-dependent.

When looking at the mutation pattern for these mutants, a conjecture might be made from the first glance, that mutation bias correlated with locations within a single sequence might exist. Specifically, for these 22 mutants, the chances of mutations occurring at different sites were not equal, in that large numbers of mutations were observed at the beginning and end of the sequence (Fig. 4.2.2). However, no similar studies have been found thus far to support this hypothesis, while reports with opposing results have been published, where nucleotide substitutions (insertions and deletions were excluded) were distributed relatively evenly within the sequence, with no obvious location bias (Fig. 4.2.3; Jensen et al., 2006). One factor that should also be considered as well is the IEP-PCR method that was applied was different to most of those reported previously, and this might have influenced the results. Specifically, a significant candidate pool was obtained, but only a small number of mutants were selected, and they might not have been representative. Unfortunately, mutation distribution analysis was not reported by the authors describing the 'dilution and pooling' method, making it difficult to evaluate results from the current study with findings from previous studies.

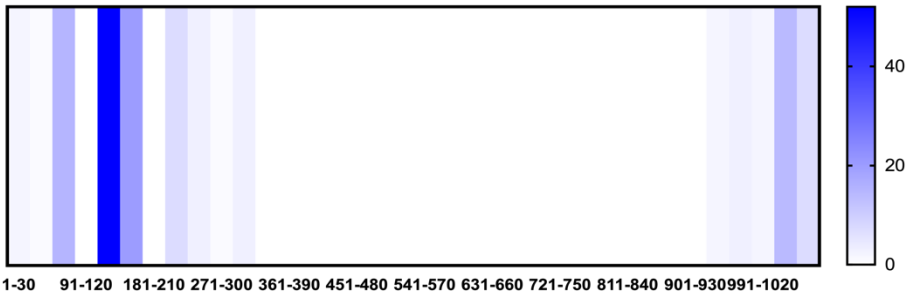

Figure 4.2.2 Mutation distribution within the sequence among 22 mutants

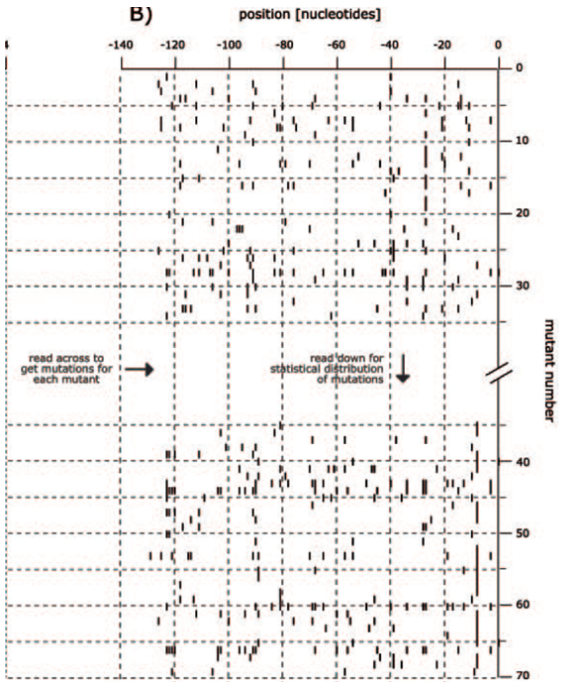

Figure 4.2.3 Mutation distribution plot adapted from Jensen et al. (2006)

A more detailed review of the mutant sequences, including the 14 silent mutants, provided a bigger perspective (Fig. 4.2.4) and the possibility that some mutations occurred at regions other than at the two clusters that were previously observed. This potentially validates the previous assumption that the 'clustering phenomenon' observed amongst 22 mutants was due to the small library size selected, and might therefore only represent the tip of an iceberg. Interestingly, fewer mutations were also observed within the 14 silent mutants (1.36 base changes per sequence), some of which were also observed in the final 22 candidates. This might suggest that these silent mutants were products yielded from earlier rounds of EP-PCR, where limited accumulative mutations were noted. This might mean that their 'descendants' or mutants with mutations at other regions might have been present, but unfortunately, these were not selected. This scenario can also explain the mutation clustering observed amongst the 22 mutants that were selected.

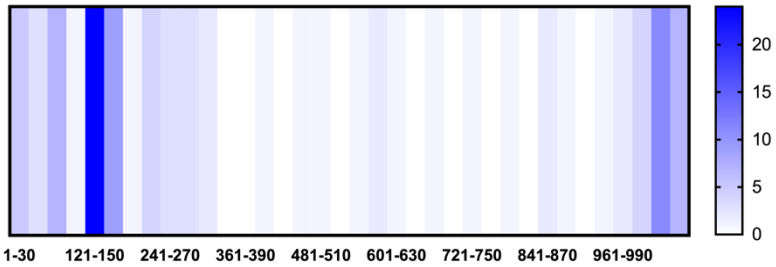

Figure 4.2.4 Mutation distribution within sequence among 52 mutants

The mutation distribution pattern with the larger library further validated the hypothesis that no mutation bias occurred under the IEP-PCR conditions. However, in order to draw a solid conclusion, and to gain a comprehensive view of the mutation pattern produced from this IEP-PCR method, more mutants must be collected to generate more representative data, which is acknowledged as a limitation of the experiment, due to the difficulty in high-throughput screening.

Similar issues were encountered when the functional assay was coupled with sequence analysis. Effects afforded by mutations seemed to sit at opposing ends of the spectrum, i.e. only non-functional or unaffected mutants were obtained according to the results from the biosynthesis tests. Potential explanations are discussed below.

IEP-PCR most likely introduced too many repetitive mutations, and some changes, nonsense mutations in particular, were observed in more than one sequence, elevating the occurrence of stop codons. Additionally, the majority of mutations that occurred were found within the first 160 bp of the sequence; the region where the likelihood of nonsense mutations occurring is higher, especially the region at 1-90 bp in the wildtype *VvOMT3* gene (Fig. 4.2.5, only single base substitution was considered in a codon within the wildtype open reading frame, based on the mutation bias nature of EP-PCR). This might further increase the possibility of stop codon occurrence, resulting in incomplete translation products. Of the 15 nonsense mutants, only 7 were found to contain the actual mutation patterns causing stop codon insertions; the rest most likely 'inherited' these from the templates. Two additional sequences (mutant 92 and mutant 102, see Appendix Fig. 1 for detailed sequences) showed largely the same mutations, which might explain the high proportion of repetitive sequences in the final IEP-PCR pool, as well as of the increased occurrence of nonsense mutations observed in the experiment. Based on detailed analysis of all 52 mutants obtained, the proportion of stop

codons amongst all mutations was 9.8% (Table 4.2.1), which was within the range previously reported, being 14.3% (Rasila et al., 2009). This was still a high level compared to the lowest proportion reported, i.e. 2.1% (Rasila et al., 2009). According to Rasila and colleagues, where different enzymes were trialled for EP-PCR, larger sample sizes yielded lower stop codon rates, in agreement with results from the current experiment. This suggests that a larger library may lead to more missense mutations, which would be more desirable. On the other hand, nonsense mutations may well be useful, if larger fragments of truncated products were obtained and helped to elucidate the key regions of the protein. Nevertheless, this was not achieved in the current experiment mainly due to the mutation clustering, possibly arising from IEP-PCR and/or the small library size that was selected.

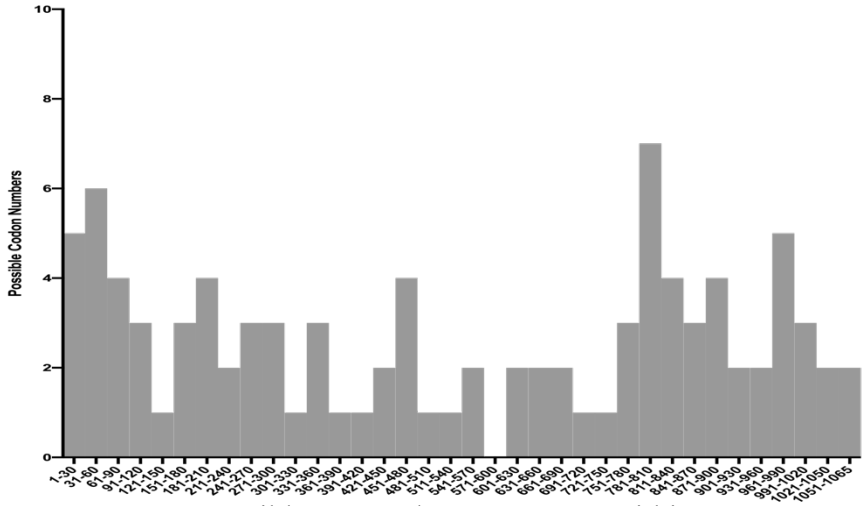

Figure 4.2.5 Possible stop codon occurrence within *VvOMT3* sequence

For the 7 missense mutants, no impacts on enzyme functions from amino acid changes seemed to occur, according to the biosynthesis assays; similar levels of IBMP were observed. However, since this experiment was designed as a preliminary trial for obtaining novel catalytic activity (IBMP-degradation), crude enzymatic assays were conducted to determine the presence of any desired character. It might still be too early to conclude that the sites being mutated were non-crucial regions and the mutations were non-effective given that no detailed enzyme kinetics studies on purified protein products with standardised enzyme concentrations were conducted. However, the results suggest that mutations at respective sites would not make the protein dysfunctional.

Based on previous analysis of homologous enzymes together with VvOMT1-4, (Vallarino et al., 2011; Guillaumie et al., 2013), some key sites within VvOMTs have been modelled coinciding with the homologous ones *Medicago sativa* isoflavone OMT and *Medicago sativa* caffeic acid OMT (Zubieta et al., 2001; 2002), making them reliable references for key residue determination of VvOMTs. Missense mutations obtained from this experiment occurred mainly at two regions of the sequence (30-160 bp, 1000-1065 bp), most of which were assumed to be out of the active sites of the enzyme, based on homology alignment with references (Fig. 4.2.6). On the other hand, amino acid substitutions were analysed (Table 4.2.1). For base substitutions, nonconservative amino acid changes (defined by BLOSUM62 matrix; Henikoff and Henikoff, 1992) took up 58.82%, and the proportion of non-conservative amino acid substitutions in this experiment agreed with the trend that non-conservative substitutions are more likely to happen (Henikoff and Henikoff, 1992). However, for the 7 mutants that successfully yielded IBMP, only conservative substitutions were observed, which might explain why the catalytic activity was maintained in these mutants. Nevertheless, it should be noted again that the library was too small to be representative, such that mutants with non-conservative amino acid changes without stop codon inserted might have been present in the pool but not picked for this experiment. This might be the reason for not seeing functionally-affected mutants in this experiment. On the other hand, it has been noted that several nonsense mutants, though yielding truncation products, also contained amino acid substitutions that have been predicted to affect protein structure (details discussed in 4.5), which might be a further indication that effective mutations were present in the pool but not selected.

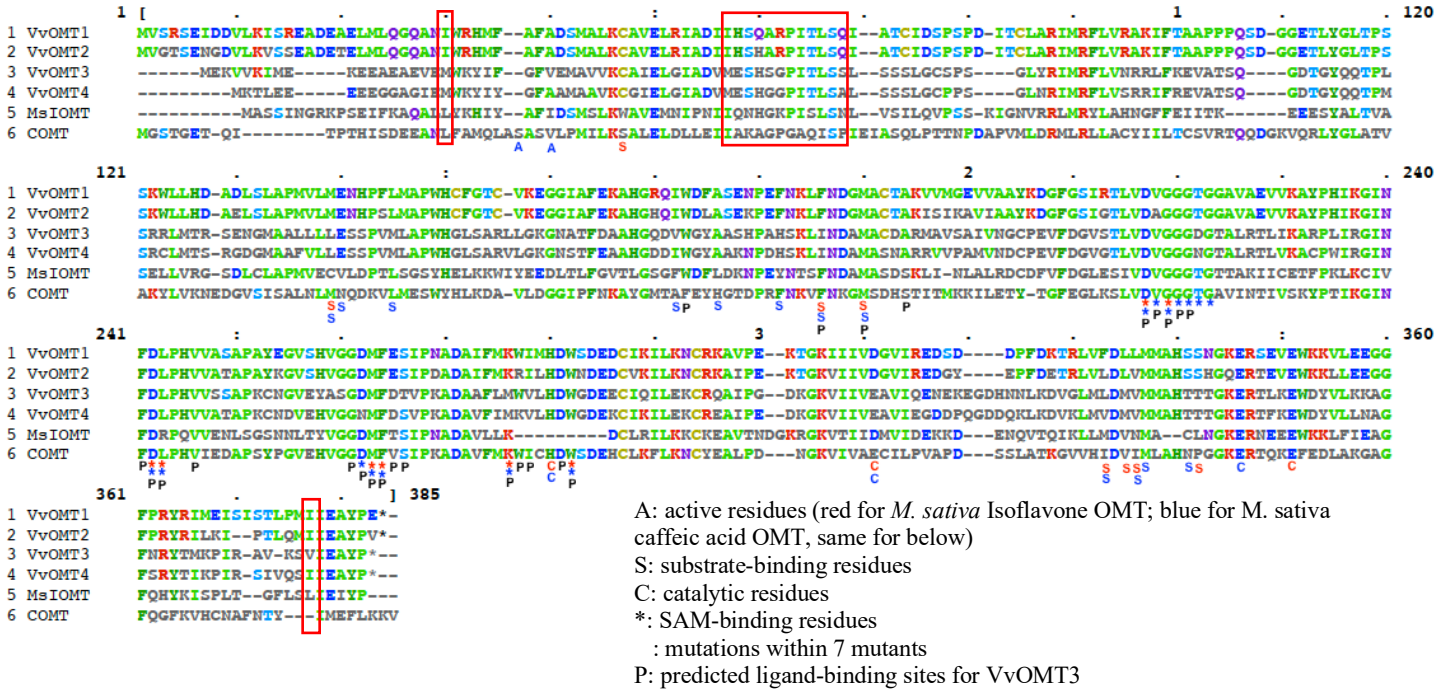

Figure 4.2.6 Multiple alignment of 7 missense mutants with VvOMTs, MsIOMT (*M. sativa* Isoflavone OMT, determined by Zubieta et al., 2001) and COMT (*M. sativa* caffeic acid OMT, determined by Zubieta et al., 2002). EMBL-EBI service (Madeira et al., 2019) was used to generate multiple alignment.

Another hypothesis for missing mutants in the library might be that certain mutation types are lethal to *E. coli* or suppressed its growth, thereby creating a selection bias. Such cases have been reported previously and are termed as synthetic dosage lethality when overexpression causes lethality in a mutant strain but not in the wildtype background (Kroll et al., 1996; Measday and Hieter, 2002; Prelich, 2012). This phenomenon has been devised for screening and normally two mutations are incorporated to cause lethality, and as has been noted, overexpression is required for suppression or lethality of the host cell. In this experiment, however, induction for overexpression did not take place during colony selection after transformation with the recombinant vector. Although functional studies coupled with site-specific mutations were absent in VvOMTs, similar methods were applied to study MsIOMT and COMT (Zubieta et al., 2001; 2002), and neither lethality nor suppression of *E. coli* growth was reported. As a result, the potential for certain mutation types to be lethal to host cells is very low, and a larger library of EP-PCR mutants containing comprehensive mutations along the whole sequence is desirable for validating the assumption. An easier

approach, such as site-directed mutagenesis at key residues, could also be used to provide a solid answer.

Table 4.2.1 Mutational analysis at protein level

	n	%
Total mutations	152	
Silent mutations	41	26.97
Missense mutations	96	63.16
Nonsense mutations	15	9.87
Impact of amino acid change	34	
Conservative	14	41.18
Nonconservative	20	58.82

Based on the sequence analysis and the subsequent function tests, it is clear that one of the downsides of IEP-PCR is the high proportion of repetitive nucleotide changes that were present in the mutant pool, which lowered the efficiency of downstream screening. An example of this was the majority of mutants (15 of 22) comprising nonsense mutations that resulted from only 7 mutation types, but that were potentially passed onto others in the 'dilution and pooling' method. Improvements could be made for future research using a similar method, by determining the optimal proportion of mutagenised products in the templates during the pilot trial.

Another major drawback of this experiment, which has already been acknowledged, is that all of the explanations and assumptions mentioned above are made based on results from a small mutant library, which statistically, might not be representative. The bottleneck for limiting the library size is the enzymatic screening method, which in the current experiment was GC-MS/MS analysis (which involves laborious and time-consuming sample preparation to measure IBMP at ng/L concentrations). It might therefore be beneficial to develop a quick screening method for IBMP, since detection of small changes in IBMP concentrations has long been a challenge for flavour chemists.

4.3 Improvements to the library screening method

Improvements to the library screening method, the step identified as the major impediment to this experiment, together with microbial screening for IBMP-degrading candidates, are

urgently required to increase the efficiency of further research. Traditionally, the most commonly used approaches for high-throughput library screening are agar plate- and microtiter plate-based, for which visual signals of enzymatic reactions or the growth of transformants, are desirable. pH changes, which are easily detected based on colour-changing indicators, were trialled in the current experiment, but pH changes did not occur under the enzymatic reaction conditions employed, or at the especially low levels at which substrates were added. Only two studies have considered the use of colour reagents with IBMP: Dragendorff's reagent and the Ziesel test, (Vasundhara and Parihar, 1980; Zeisel, 1885; Zeisel and Fanto, 1902; 1903; Chen, 1992), which were originally intended to react with alkaloids and methoxy groups, respectively. However, there are shortcomings with both of these methods, as they were used for quantitative determination less precisely prior to the development of nuclear magnetic resonance (NMR) spectroscopy and mass spectrometry. As such the detection thresholds of both methods are higher than the working range required in the current experiment. For the Ziesel test, the rationale is for the sample to react with acetic acid and hydrogen iodide to produce an alkyl iodide, which upon heating can react with silver nitrate to yield a red or yellow precipitate. However, the limit of detection for this method is 3 mg/L (Anderson and Duncan, 1960; Chen, 1992), compared to the ~83 µg/L IBMP concentrations used in this experiment, which make it a non-viable option. Sulfur-containing compounds have also been shown to interfere with the assay, resulting in the formation of hydrogen sulfide during acid treatment, which can then react with silver nitrate to produce a precipitation (Chen, 1992). As such, sulfur-containing compounds such as the methyl donor *S*-adenosyl-L-methionine, are not suitable for use in library screening in this experiment. Modified methods have been devised to circumvent this issue, namely, the use of bromine to convert the alkyl iodide to iodic acid by oxidation, which can simultaneously oxidise hydrogen sulfide into sulfuric acid (Vieböck and Brecher, 1930; Vieböck and Schwappach, 1930; Chen, 1992). The drawback of this modification is that the apparatus required for the series of reactions is too complicated to perform screening efficiently.

Dragendorff's reagent, on the other hand, is a quick method for detecting alkaloids which react to form an orange or orange-red precipitate as has been used for detecting pyrazines in roasted spices (Vasundhara and Parihar, 1980). The lowest detection limit reported was 2.5 µg/L, using thin layer chromatography (Vasundhara and Parihar, 1980). However, since this reagent reacts with all alkaloids, including pyrazines, it would not be able to differentiate

IBMP and IBHP in biosynthesis or degradation reaction mixtures, and therefore, changes in IBMP concentration during reaction.

The application of existing colour reagents suitable for the rapid detection of IBMP was not considered feasible, so other methods need to be considered. NMR spectroscopy methods can facilitate the screening of compound mixtures for components that bind with protein drug targets and have been used in drug discovery (Hajduk et al., 1999; Siriwardena et al., 2002). This approach could potentially be modified and evaluated as a method for preliminary library screening, excluding mutants that fail to bind with substrates or detecting those with higher binding potentials. Other strategies that detect compositional changes involved in the reaction, though not tested in this experiment due to time constraints, might be worthy of further investigation. For example, measuring changes in the concentration ratio of S-adenosyl-L-methionine/S-adenosyl-L-homocysteine, the methyl donor/receptor for IBMP and IBHP, might provide an indicator for screening. A similar assay has been applied to characterise a SAM-consuming deaminase using an isosteric fluorescent SAM-analogue and monitoring reaction progress through loss of fluorescence at a certain wavelength (Burgos et al., 2017). However, mechanisms within analogue binding with the enzyme need to be determined more clearly, so that mutants with mutations on SAM-binding sites don't miss the analogue, and a pilot experiment would be required to test the tolerance of VvOMT3 with the SAM-analogue so that the wildtype enzyme activity is sustained.

4.4 Structural analysis of mutants and prediction on structure-function relationship of VvOMT3

Mutations obtained from this experiment, coupled with functional tests, though preliminary, were still able to shed some light on the structure-function relationship of this enzyme. Detailed analysis will be discussed below.

Stop codon insertions occurred at different regions from residue No.10 to No.68 (Fig. 4.4.1), and mutant 328 yielding 45 residues with no other amino acid substitution within the truncated product indicated that protein fragment aa 1-45 was not sufficient to support the catalytic activity for IBMP biosynthesis.

Figure 4.4.1 Stop codon insertion mapping of VvOMT3. Symbol * above single amino acid indicates the respective substitution with stop codon.

For the 7 mutants with preserved catalytic activity, mutations were mapped onto the mutant sequences aligned with the reference enzymes of which key residues are demonstrated (Fig. 4.2.6). Most mutations occurred at the starting region of the protein, and no significant effects on function were observed according to enzymatic tests. This suggested that these amino acid substitutions did not impart significant structural influences. However, it should be acknowledged that the enzymatic test results were preliminary, and intended to support conclusions outlined above. Further computational analysis was therefore performed to model the resulting structural changes as a proof-of-principle support.

Protein modelling of the wildtype was performed using two software programs, I-TASSER (Roy et al., 2010; Yang et al., 2015; Yang and Zhang, 2015) and PHYRE2 (Kelley et al., 2015); the first of which performed quality check with built-in functionality. Both models were checked for quality using a third software program, SAVES (DOE-MBI services) which incorporates 5 different evaluation parameters (Fig. 4.4.2), resulting in the better quality model (model predicted by I-TASSER, Fig. 4.4.3) being selected as the template for subsequent analysis.

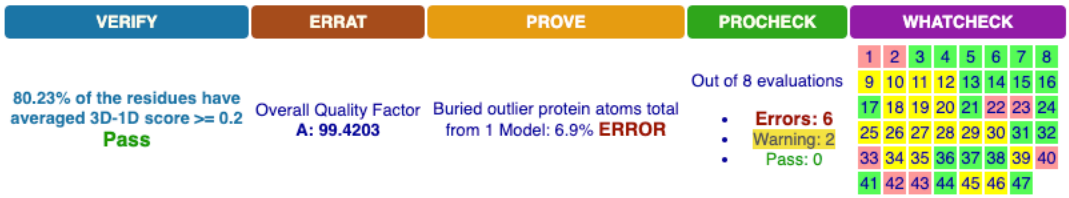

a

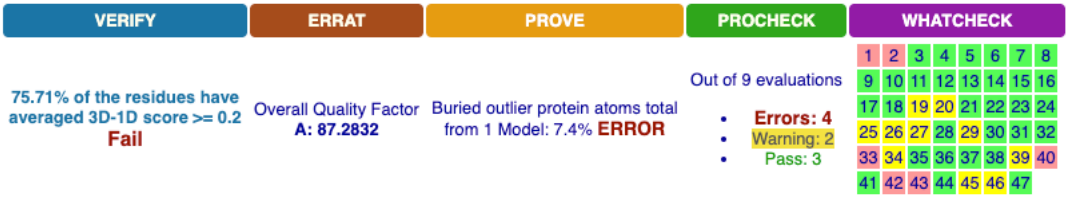

b

Figure 4.4.2 Quality check results by SAVES for predicted protein model quality. a. model predicted by I-TASSER; b. model predicted by PHYRE2. VERIFY 3D (Bowie et al., 1991; Lüthy et al., 1992); ERRAT (Colovos and Yeates, 1993); PROVE (Pontius et al., 1996); PROCHECK (Laskowski et al., 1993; 1996); WHATCHECK (Hooft et al., 1996)

Figure 4.4.3 Protein model of VvOMT3 predicted by I-TASSER, C-score*=0.37. Visualised by EzMol (Reynolds et al., 2018), rainbow colour applied from N- to C- terminal.
*C-score is a built-in quality evaluation parameter which shows confidence score for estimating the quality of the predicted model. It is calculated based on significance of threading template alignments and the convergence parameters of the structure assembly simulations. A higher value ranged between -5 and 2 signifies a model with a higher confidence.

Along with structural modelling, changes to amino acid categories were checked to explore other possible explanations. (Table 4.4.1).

Table 4.4.1 Amino acid substitutions among 7 mutants

Amino acid changes	Change of chemical groups*
I23M	Aliphatic-neutral
S48A	Neutral-aliphatic
V349I	Aliphatic
T52S	Neutral
L56I	Aliphatic
M44I	Neutral-aliphatic
S55Q	Neutral

*Amino acid groups, charged amino acid: D, E, H, K, R; neutral amino acids: C, M, P, S, T, N, Q; aromatic amino acids: F, Y, W; aliphatic amino acids: G, A, V, L, I

Potential structural changes introduced by amino acid substitutions were modelled using the UCSF Chimera software package (Pettersen et al., 2004) and Missense3D (Ittisoponpisan et al., 2019), and the protein model of the wildtype. Examples of mutants with changed chemical groups are shown in Fig. 4.4.4 (and Appendix Fig. 2), and changes to amino acids are shown within 5 Å of the mutation site. According to the results from the two software programs, no structural damage such as clash or significant cavity alteration was noted,

specifically, a list of criteria (Table 4.4.2) was included for analysis. It can be noted that the residues within 5Å of the mutated site made changes accordingly, but none of these were significant to alter the overall structure. This finding supports the earlier conclusions, from a theoretical perspective, that amino acid substitutions at these sites do not affect protein structure significantly.

Table 4.4.2 Criteria for predicting structural effects from missense variant

Analysis parameter
Disulphide breakage
Buried proline introduced
Clash
Buried hydrophilic introduced
Buried charge introduced
Secondary structure altered
Buried charges switch
Disallowed phi/psi
Buried charge replaced
Buried glycine replaced
Buried H-bond breakage
Buried salt bridge breakage
Cavity altered
Buried/ exposed switch
Cis proline replaced
Glycine in a bend

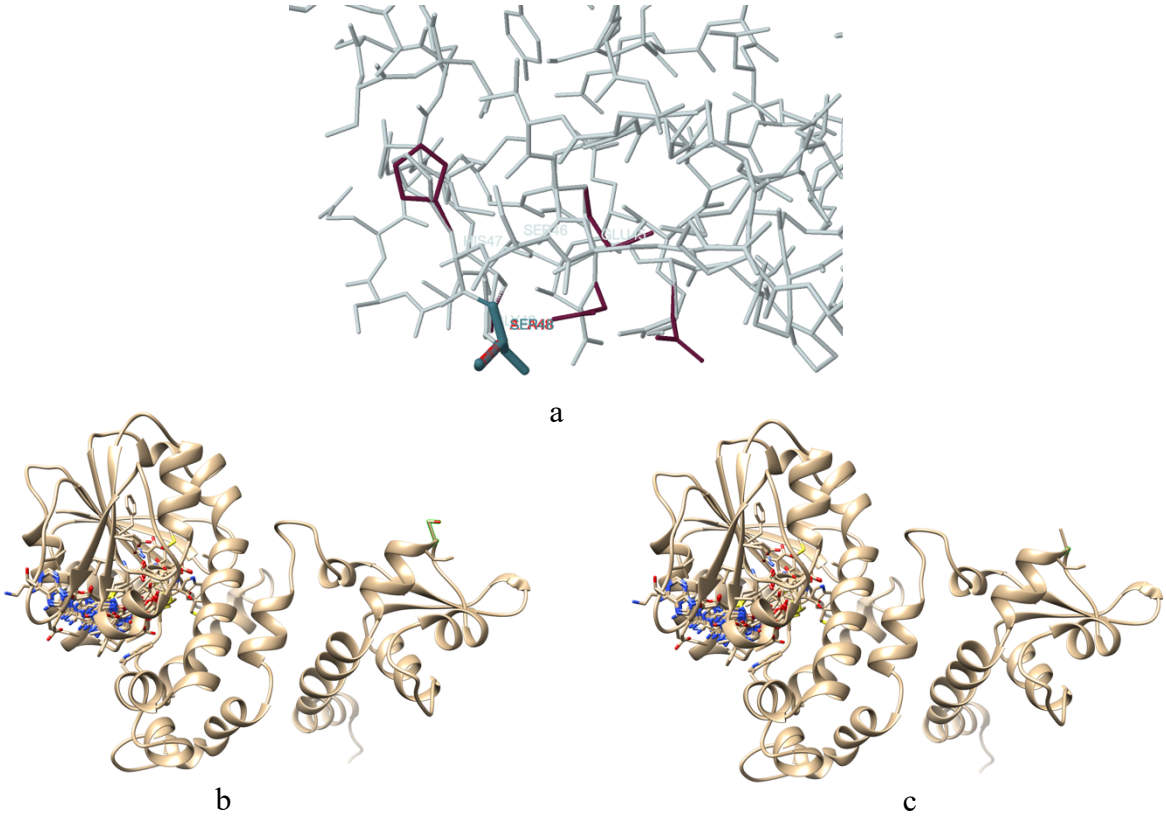

Figure 4.4.4 Structural modelling of amino acid substitution (S48A). a. combined structure within 5Å of residue 48S, residue in dark green/red indicates the wildtype/mutated residue Ser48/Ala48, neighbouring (within 5Å residues) sites in light grey/dark red indicate the wildtype/mutated neighbouring residues; b. predicted wildtype structure with ligand-binding site specified, 48S highlighted in green box; c. predicted structure with ligand-binding site specified after mutating 48S to 48A (mutation site highlighted in green box).

The structure-function relationship of VvOMT3 has not been thoroughly studied, although some knowledge has been reported, mainly based on modelling and phylogenetic analysis (Vallarino et al., 2011; Guillaumie et al., 2013). Similar predictions are made here and aim to provide a theoretical basis for future attempts to elucidate the structure of this enzyme. A template model of VvOMT3 was generated from I-TASSER and was used for protein function predictions.

Different prediction software has been used for modelling, including COFACTOR (Yang et al., 2013a; 2013b), COACH (Yang et al., 2013a; 2013b) and 3DLigandSite (Wass et al., 2010). COACH performs protein prediction at the ligand binding site via a meta-server approach. Specifically, two comparative methods were used to recognise ligand-binding

templates from the BioLiP protein function database (Yang et al., 2013b) by sequence and substructure comparison, and subsequently generate ligand binding site predictions. COFACTOR, on the other hand, applies a biological functional annotation method for proteins based on information of sequences, structures and protein-protein interactions. A similar prediction approach applies to 3DLigandSite. Prediction results from COACH and COFACTOR were compared and combined with other methods such as FINDSITE (Brylinski and Skolnick, 2008) and ConCavity (Capra et al., 2009) for final predictions.

In the current study, the predicted ligand binding sites and active site residues obtained were mapped onto multiple alignments with two known reference OMTs (Fig. 4.2.6), and binding models were also generated as well (Fig. 4.4.4b). It was interesting to observe that some residues coincided with those of references or fell within adjacent regions, which largely confirmed the reliability of referencing these homologous proteins for determining and studying crucial regions in VvOMTs. Otherwise, some predicted sites agreed with those proposed for substrate-binding by Guillaumie et al. (2013), based on model alignment with VvOMT1. Predictions yielded from this research, together with previously published findings, could potentially inform future work characterising and identifying the key residues of VvOMT3.

4.5 Application of protein truncation

A large number of mutation products obtained in this experiment were truncated proteins, whose sizes were predicted to be 1.1-7.3 kDa (Compute pl/Mw tool), and found to exhibit loss of function tested. A preliminary hypothesis was thus made that the first 45 residues from the N-terminus were not sufficient to support catalytic reaction, which agreed with the functional site prediction (Fig. 4.2.6), as well as the key sites identified in reference OMTs (Zubieta et al.,2001; 2002). Despite the fact that residue 35W in MsIOMT, 28S and 31V in COMT, corresponding to 34C, 24F and 27V in VvOMT3 have been identified as active sites for MsIOMT and COMT respectively, neither detectable IBMP in biosynthesis nor significant decrease in degradation was observed, which most likely indicates that these residues alone wouldn’t support the biosynthesis activity. However, another factor that should be taken into account is that amino acid substitutions occurred within some truncated products, which might potentially result in structural damage, and thus complicating the cause of dysfunction. Protein modelling, albeit with a low-quality score, was obtained by both software programs for the largest truncated product (mutant 305) to gain a clearer view

of its structure and potential function; a better quality model was obtained by PHYRE2. Based on ligand binding sites prediction (COFACTOR, COACH), the top prediction sites were 31, 34, 35, 38 and 40 with the ligand being chlorophyll A.

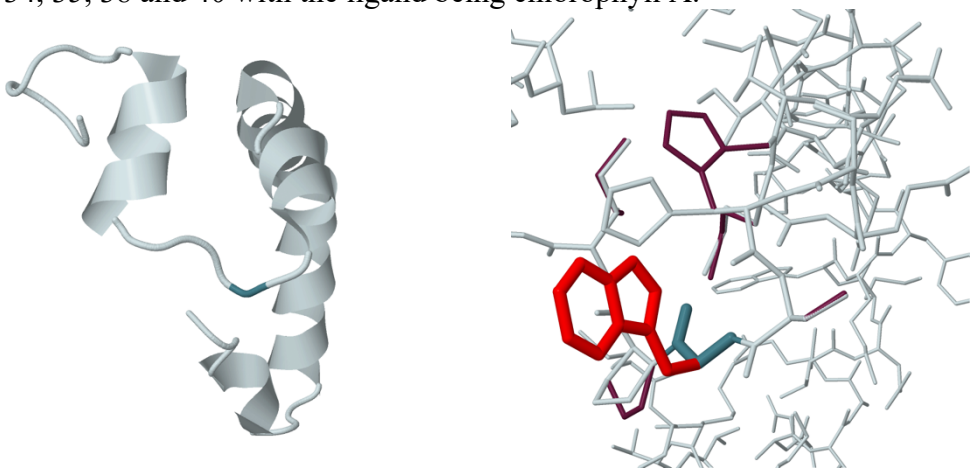

Figure 4.5.1 Structural modelling on amino acid substitution (G49W). a. mutation location within the predicted model. b. combined structure within 5Å of residue 49G pre- and post-mutation, residue in dark green/red indicates the wildtype/mutated residue Gly49/Trp49, neighbouring (within 5Å residues) sites in light grey/dark red indicate the wildtype/mutated neighbouring residues.

Same mutation prediction of structural changes of mutant 305 was performed by Missense3D (Fig. 4.5.1), revealing that an amino acid substitution occurred at residue 49 whereby glycine was replaced by tryptophan and might trigger a clash alert within the structure; the loss of glycine originally located in a bend curvature is not desirable either. It is possible, therefore, that amino acid substitution contributes further to protein dysfunction.

Although protein truncation did not work especially well in this experiment, it could be desirable in locating coding regions and identifying protein functions, the latter of which will be discussed in more detail due to its potential relevance to this experiment. Various methods have been used to deliberately create truncated proteins, such as site-directed mutagenesis and the DNA transposition method. An example of this is a study on the hepatitis B virus X protein, in which mutants targeted towards different conserved and non-conserved regions were constructed by site-directed mutagenesis. The truncated product showed the same activity as the wildtype, thereby revealing the crucial domain within the protein for desired function (Kumar et al., 1996). A similar approach could be adapted to define the border of the catalytic regions of the VvOMT3 protein. Key residues and conserved domains have been elucidated in its homologous enzymes, MsIOMT and COMT, which could be target areas for

designing truncation products, and different combinations of regions could be selected for creating truncations to map the key domain for this enzyme. More in-depth research could also be done to further study the structure-function relationship of the enzyme. An example of this was achieved by this method was for the S-layer protein SbsC of *Bacillus stearothermophilus* ATCC 12980. Jarosch et al. (2001) demonstrated that a certain region was responsible for anchoring the subunits of the protein to the rigid cell wall layer. This could determine the subunits responsible for different sub-functions within the crucial regions of the enzyme.

Therefore, in general terms, identifying the crucial regions within a protein via a truncation test could be a useful method if rational and detailed designs are made.

5 Conclusions

Random mutagenesis, specifically, error-prone PCR, was conducted on *VvOMT3*, the key gene responsible for biosynthesis of IBMP in *Vitis vinifera* with the intention of reversing catalytic activity. However, due to the impractically of library screening, only a small number of mutants were selected for screening and unfortunately none of these exhibited the desired degradation activity. Biosynthesis tests were performed and indicated several possible functionally non-affected mutation types, which were subsequently supported through mutational modelling. Additionally, more detailed enzymatic kinetic studies are needed to further confirm these results. Truncated products were also obtained with functional loss, suggesting that protein fragment aa 1-45 alone was not sufficient to support the catalytic activity. Despite the fact that a larger truncation product (68aa) was obtained, amino acid substitutions with the potential to significantly affect structure made it difficult to ascertain the cause of dysfunction. While protein truncation did not work in the current study, this test remains a powerful method for exploring the key domains of the enzymes, where rational design has been carefully made.

Iterative error-prone PCR, a modified EP-PCR method used in this experiment, originally aimed to enhance mutation rates, but ended up introducing too many repetitive mutations, which then decreased the efficiency. Comprehensive mutational patterns of this modified method could be investigated further by expanding the library size.

The major bottleneck in this experiment, which limited the size of the mutant library, was the lack of a high-throughput screening method. Potential approaches targeted at other relevant compositional changes during enzymatic reaction have been proposed, but requires further trials for confirmation.

In summary, the original aim of this experiment to reverse the catalytic activity of VvOMT3, was not achieved, but other potentially useful information was generated, which could inform future work. Given the little amount of knowledge available for reversing enzymatic activity, a more feasible and rational approach might be to firstly characterise the VvOMT3 enzyme in detail, and then perform modification accordingly. The development of a high-throughput enzymatic screening method for the presence of IBMP at low concentrations remains a crucial and high priority task.

Chapter 5 Paper manuscript

Microbial Demethylases: Their Catalytic Characteristics and Potential Applications

Jin-Chen Li, Christopher M. Ford, Kerry L. Wilkinson, Vladimir Jiranek*

School of Agriculture, Food and Wine, Waite Campus, The University of Adelaide, PMB 1, Glen Osmond, South Australia 5064, Australia
* Corresponding author. E-mail address: vladimir.jiranek@adelaide.edu.au.

Abstract

Demethylases catalyse a wide range of biochemical reactions including epigenetic modifications, and endogenous and xenobiotic metabolism. The latter topic is discussed in this review since compound metabolism plays a vital role in natural element cycles. Demethylases have been identified widely in nature, among which microbial demethylases have been studied extensively given their broad distribution and versatile functions. In this review, microbial demethylases are discussed based on their enzyme categories as well as catalytic mechanisms to shed light on further protein modifications. Additionally, such enzymes have been grouped and discussed based on their involvements in natural elemental cycles for potential industrialisation, for which studies on microbial demethylase applications are exemplified for demonstration and inspiration.

Key words

demethylase, CYP450, Rieske-type non-heme iron-dependent oxygenases, tetrahydrofolate-dependent demethylase, industrial biotechnology, environmental remediation, pharmaceutical application, natural elemental cycle

Statement of Authorship

Title of Paper	Microbial demethylases, their catalytic characteristics and potential applications
Publication Status	☐ Published ☐ Accepted for Publication ☐ Submitted for Publication ☒ Unpublished and Unsubmitted work written in manuscript style
Publication Details	

Principal Author

Name of Principal Author (Candidate)	Jin-Chen Li
Contribution to the Paper	Conception of ideas for the review, collection of references, literature and data interpretation, manuscript preparation and editing
Overall percentage (%)	80%
Certification:	This paper reports on original research I conducted during the period of my Higher Degree by Research candidature and is not subject to any obligations or contractual agreements with a third party that would constrain its inclusion in this thesis. I am the primary author of this paper.
Signature	Date 15/2/2021

Co-Author Contributions

By signing the Statement of Authorship, each author certifies that:

i. the candidate's stated contribution to the publication is accurate (as detailed above);

ii. permission is granted for the candidate in include the publication in the thesis; and

iii. the sum of all co-author contributions is equal to 100% less the candidate's stated contribution.

Name of Co-Author	Christopher M. Ford
Contribution to the Paper	Conception of ideas for the review and editing.
Signature	Date 15-FEB-21

Name of Co-Author	Kerry L. Wilkinson
Contribution to the Paper	Conception of ideas for the review and editing.
Signature	Date 15/2/2021

Name of Co-Author	Vladimir Jiranek		
Contribution to the Paper	Conception of ideas for the review and editing, and acted as corresponding author.		
Signature		Date	15.2.21

1 Introduction

In previous chapters, we have tried remediation approaches including non-*Saccharomyces* fermentation, microbial screens and VvOMT3 modification, among which moderate success was achieved. Now we propose to explore related enzymes, i.e. demethylases in a more specific way. Thus to contrast the non-targeted approaches used before, a detailed literature review was conducted to reveal possible microbes/enzymes to target as sources of related activities that might degrade IBMP.

Demethylases (EC 1.14, 1.18, 2.1) are a group of widespread enzymes, with functions ranging from epigenetic modification to metabolism of endogenous and xenobiotic compounds. They catalyse the removal of methyl groups ($-CH_3$) from proteins, nucleic acids and other molecules. The broad scope of substrates makes these enzymes a huge family, whose involvement with endogenous and xenobiotic metabolism will be discussed in this review.

Methyl groups have been observed attached to various atoms such as carbon, oxygen, nitrogen and sulfur, among which binding with the oxygen atom yields the widely distributed methoxy group. Furthermore, demethylations of methoxy groups, as well as other methyl-binding moieties, frequently occur as steps to initiate a chain of reactions, mostly in degradation pathways. Removal of methyl groups tends to produce metabolites that are less stable and more prone to further reactions. Demethylases are found in all domains of life, such as some cytochrome P450s present in humans responsible for xenobiotic metabolism (Brachtendorf et al., 2002) and demethylases in plants crucial to the synthesis of various endogenous compounds (Berim and Gang, 2013). Among these, microbial demethylases are of equal significance for investigation given their broad distribution in nature and the ready access to protein engineering for potential industrial applications in microbial systems. Furthermore, their versatile functions ranging from pollution remediation, drug metabolism, and endogenous biosynthesis, to involvement in carbon, nitrogen and halogen cycles, make these enzymes a feasible tool for many applications.

This review will discuss microbial demethylases, differentiated by their function-based categories with catalytic characterisations specified, and their current and potential industrial applications, to shed light on future exploration and applicable industrialisation.

2 Microbial demethylase categories based on structural and catalytic features

Several different types of enzymes with diverse catalytic features catalyse demethylation reactions, and these categories (Fig. 1), including cytochrome P450, Rieske-type non-heme iron-dependent oxygenases, tetrahydrofolate-dependent demethylases and others, will be discussed in detail in this section. Phylogenetic analysis (Fig. 2) was performed on the previously identified microbial demethylases to further review the enzymes via evolutionary development, which also adds to the current understanding of these enzyme families. Detailed information, including protein database IDs (UniProt entry numbers), encoding genes, organisms of origin, identified binding sites and regions, and amino acid sequences of some characterised demethylases are summarised, with crystal structures (where generated; Table 1 and Table 2), providing more direct messages for pairwise and clustering studies.

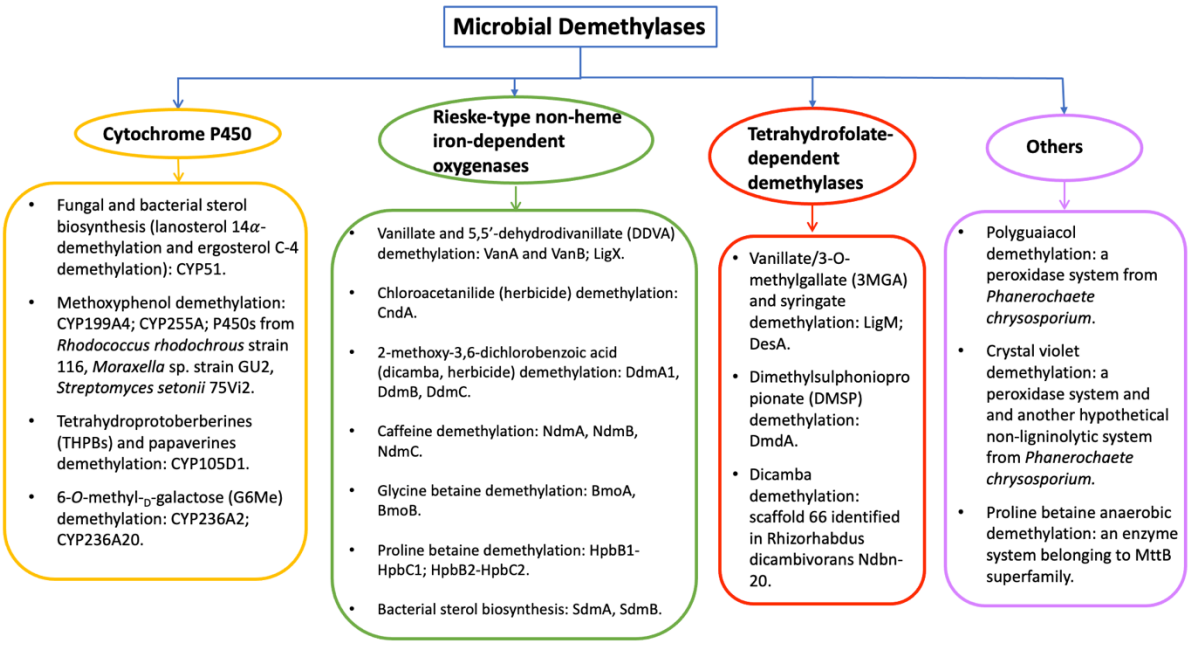

Figure 1 Microbial demethylase categorisation based on enzyme types

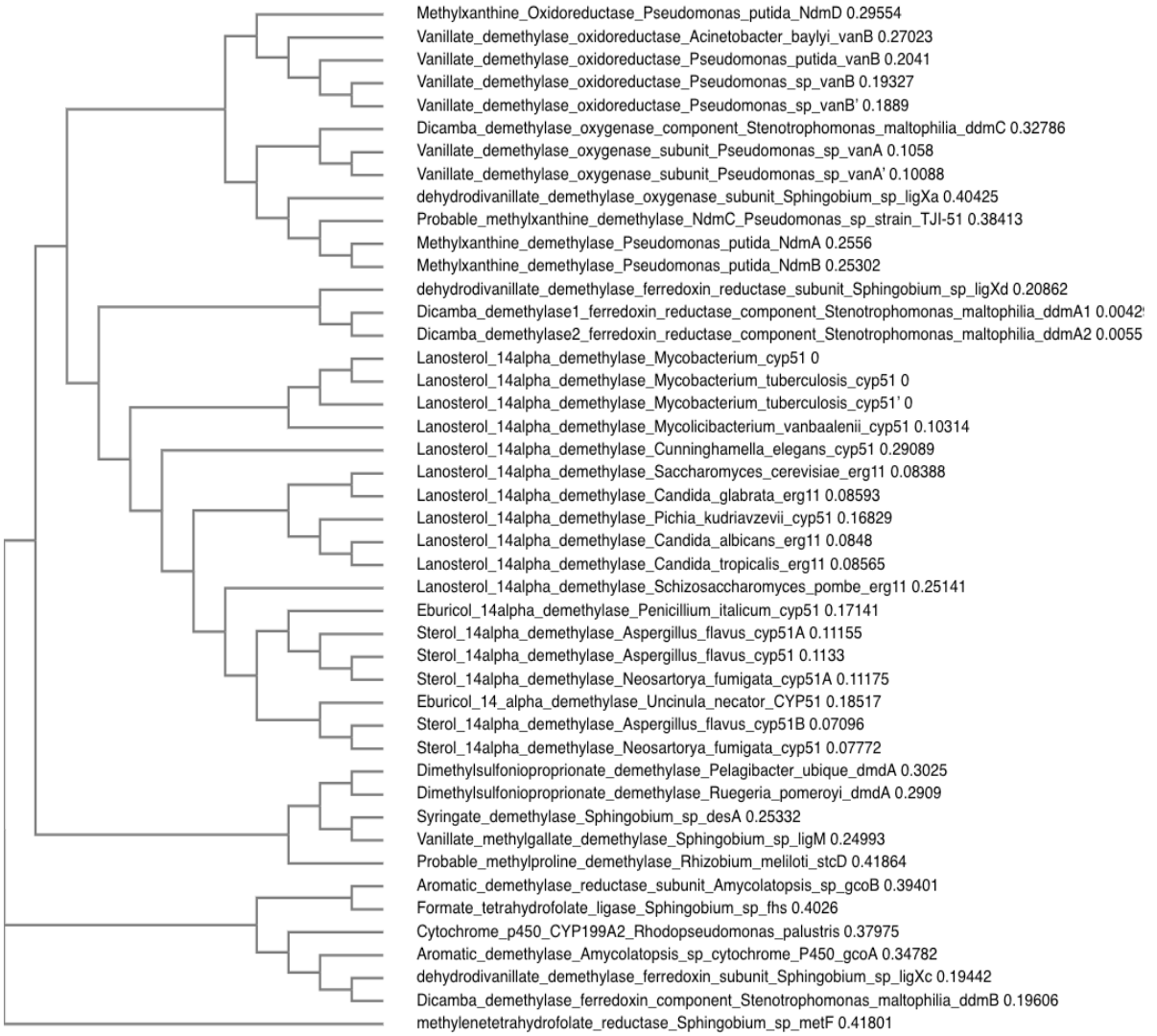

Figure 2 Phylogenetic tree of microbial demethylases, sequence data retrieved from UniProt, multiple alignment and phylogenetic analysis was performed by EMBL-EBI service (Madeira et al., 2019).

Table 1 Protein information of known microbial demethylases

Protein name	EC number	UniProt Entry number	Gene	Organism	Binding sites	Binding regions	References
vanillate *O*-demethylase oxidoreductase	1.14.13.-	O24840	vanB	*Acinetobacter baylyi* (strain ATCC 33305/BD413/ADP1)	266, 271, 274, 304 (iron-sulfur [2Fe-2S])	1-97, (FMN); 107-220, (NAD)	Segura et al., (1999); Barbe et al., (2004)
vanillate *O*-demethylase oxidoreductase	1.14.13.-	O54037	vanB	*Pseudomonas putida* (*Arthrobacter siderocapsulatus*)	263, 268, 271, 303 (iron-sulfur, [2Fe-2S])	1-94 (FMN); 104-217 (NAD)	Venturi et al., (1998)
vanillate *O*-demethylase oxygenase subunit	1.14.13.82	P12609	vanA	*Pseudomonas* sp. (strain ATCC 19151)	24, 43 (iron-sulfur, [2Fe-2S]); 26, 46 (iron-sulfur, [2Fe-2S], via pros nitrogen)		Brunel and Davison, (1988)
vanillate *O*-demethylase oxidoreductase	1.14.13.-	P12580	vanB	*Pseudomonas* sp. (strain ATCC 19151)	263, 268, 271, 302 (iron-sulfur, [2Fe-2S])	105-217 (NAD)	Brunel and Davison, (1988)
vanillate *O*-demethylase oxidoreductase	1.14.13.-	O05617	vanB	*Pseudomonas* sp. (strain HR199/DSM 7063)	266, 271, 274, 304 (iron-sulfur, [2Fe-2S])	105-220 (NAD)	Priefert et al., (1997)

vanillate *O*-demethylase oxygenase subunit	1.14.13.82	O05616	vanA	*Pseudomonas* sp. (strain HR199/DSM 7063)	47, 66 (iron-sulfur, [2Fe-2S]); 49, 69 (iron-sulfur, [2Fe-2S], via pros nitrogen)		Priefert et al., (1997)
cytochrome p450 cyp199A2	1.14.99.15	Q6N8N2	cyp199a2	*Rhodopseudomonas palustris* (strain ATCC BAA-98/CGA009)	247 (substrate); 361 (iron, heme axial ligand)		Larimer et al., (2004); Bell et al., (2006; 2008; 2012b)
cytochrome p450 cyp199A4	1.14.99.15	Q2IU02	Rpb_3613	*Rhodopseudomonas palustris* (strain HaA2)	359 (iron, heme axial ligand)		Bell et al., (2012b)
5,5'-dehydrodivanillate *O*-demethylase ferredoxin reductase subunit	1.14.13.-	G2ITT5	ligXd	*Sphingobium* sp. (strain NBRC 103272/SYK-6)	14, 298 (FAD, via amide nitrogen); 49, 130, 279 (FAD); 82 (FAD, via amide nitrogen and carbonyl oxygen)		Masai et al., (2012); Yoshikata et al., (2014)
5,10-methylenetetrahydrofolate reductase	1.5.1.20	G2IQS8	metF	*Sphingobium* sp. (strain NBRC 103272/SYK-6)	21 (proton donor/acceptor); 73, 140 (FAD); 107, 175, 215, 267 (substrate)	46-47 (NAD); 105-107, 114-115 (FAD)	Abe et al., (2005); Masai et al., (2012); Sonoki et al., (2002)
vanillate/3-*O*-methylgallate *O*-demethylase	2.1.1.341	G2IQS7	ligM	*Sphingobium* sp. (strain NBRC 103272/SYK-6)	31, 60, 122 (substrate); 57, 93, 165, 215, 256 (tetrahydrofolate); 120 (tetrahydrofolate, via carbonyl oxygen); 60, 247 (important for activity)		Abe et al., (2005); Masai et al., (2012); Kohler et al., (2017); Harada et al., (2017)
formate-tetrahydrofolate ligase	6.3.4.3	O66164	fhs	*Sphingobium* sp. (strain NBRC 103272/SYK-6)		67-74 (ATP)	Nishikawa et al., (1998); Abe et al., (2005); Masai et al., (2004; 2012)
5,5'-dehydrodivanillate *O*-demethylase oxygenase subunit	1.14.13.-	G2IN04	ligXa	*Sphingobium* sp. (strain NBRC 103272/SYK-6)	68, 87 (iron-sulfur [2Fe-2S]); 70, 90 (iron-sulfur [2Fe-2S], via pros nitrogen); 181, 186 (iron, via tele nitrogen); 306 (iron)		Sonoki et al., (2000); Masai et al., (2012); Yoshikata et al., (2014);
5,5'-dehydrodivanillate *O*-demethylase ferredoxin subunit	1.14.13.-	G2IN77	ligXc	*Sphingobium* sp. (strain NBRC 103272/SYK-6)	40, 46, 49, 86 (iron-sulfur [2Fe-2S])		Masai et al., (2012); Yoshikata et al., (2014)
syringate *O*-demethylase	2.1.1.-	G2IJ05	desA	*Sphingobium* sp. (strain NBRC 103272/SYK-6)			Masai et al., (2004; 2012)
lanosterol 14-alpha demethylase	1.14.14.154	P0A513	cyp51	*Mycobacterium bovis* (strain ATCC BAA-935/AF2122/97)	394 (iron, heme axial ligand)		Garnier et al., (2003); Malone et al., (2017)
lanosterol 14-alpha demethylase	1.14.14.154	P9WPP9	cyp51	*Mycobacterium tuberculosis* (strain ATCC 25618/H37Rv)	72, 76, 97, 326, 392 (heme); 259, 433 (substrate); 394 (iron, heme axial ligand)		Cole et al., (1998); Aoyama et al., (1998); Bellamine et al., (1999; 2001); Kelkar et al., (2011); Podust et al., (2001ab; 2004; 2007); Eddine et al., (2008); Chen et al., (2009)
lanosterol 14-alpha demethylase	1.14.14.154	P9WPP8	cyp51	*Mycobacterium tuberculosis* (strain CDC 1551/Oshkosh)	72, 76, 97, 326, 392 (heme); 259, 433 (substrate); 394 (iron, heme axial ligand)		Fleischmann et al., (2002)
lanosterol 14-alpha demethylase	1.14.14.154	Q5IZM4	cyp51	*Mycolicibacterium vanbaalenii* (strain DSM 7251/JCM13017/NRRL B-24157/PYR-1)	395 (heme, axial ligand)		Brezna et al., (2004); Copeland et al., (2006)
sterol 14-alpha demethylase	1.14.14.154	Q4WNT5	cyp51A	*Neosartorya fumigata* (strain ATCC MYA-4609/Af293/CBS 101355/FGSC A1100) (*Aspergillus fumigatus*)	107, 365(inhibitor); 219, 366 (inhibitor, via carbony oxygen); 454 (iron, heme axial ligand)		Nierman et al., (2005); Venkateswarlu and Kelly, (1997); Mellado et al., (2001); Mann et al., (2003); Diaz-Guerra et al., (2003)
sterol 14-alpha demethylase	1.14.14.154	E9QY26	cyp51B	*Neosartorya fumigata* (strain ATCC MYA-4609/Af293/CBS 101355/FGSC A1100) (*Aspergillus fumigatus*)	122, 374 (inhibitor); 234, 375 (inhibitor, via carbonyl oxygen); 463 (iron, heme axial ligand)		Nierman et al., (2005); Mellado et al., (2001); Mann et al., (2003); Alcazar-Fuoli et al., (2008);

							Buied et al., (2013)
eburicol 14-alpha-demethylase	1.14.14.154	O14442	cyp51	*Uncinula necator* (grape powdery mildew)	469 (iron, heme axial ligand)		Délye et al., (1997ab)
lanosterol 14-alpha demethylase	1.14.14.154	Q02315	cyp51	*Pichia kudriavzevii* (*Issatchenkia orientalis*)			Burgener-Kairuz et al., (1994)
Eburicol 14-alpha demethylase	1.14.14.154	Q12664	cyp51	*Penicillium italicum*	459 (iron, heme axial ligand)		Van Nistelrooy et al., (1996)
lanosterol 14-alpha demethylase	1.14.14.154	P10614	erg11	*Saccharomyces cerevisiae* (strain ATCC 204508/S288c)	470 (iron, heme axial ligand)		Kalb et al., (1987); Ishida et al., (1988); Johnston et al., (1994); Engel et al., (2014)
lanosterol 14-alpha demethylase	1.14.14.154	Q09736	erg11	*Schizosaccharomyces pombe* (strain 972/ATCC 24843) (Fission yeast)	442 (iron, heme axial ligand)		Wood et al., (2002); Todd et al., (2006); Matsuyama et al., (2006); Hughes et al., (2007)
methylxanthine *N*1-demethylase NdmA	1.14.13.178	H9N289	ndmA	*Pseudomonas putida* (*Arthrobacter siderocapsulatus*)	62, 81 (iron-sulfur, [2Fe-2S]); 64, 84 (iron-sulfur, [2Fe-2S], via pros nitrogen)		Summer et al., (2011; 2012); Kim et al., (2019)
methylxanthine *N*3-demethylase NdmB	1.14.13.179	H9N290	ndmB	*Pseudomonas putida* (*Arthrobacter siderocapsulatus*)	64, 87 (iron-sulfur, [2Fe-2S]); 66, 90 (iron-sulfur, [2Fe-2S], via pros nitrogen)		Summer et al., (2011; 2012); Kim et al., (2019)
oxidoreductase NdmD		H9N291	ndmD	*Pseudomonas putida* (*Arthrobacter siderocapsulatus*)	50, 69, 537, 542, 545, 575 (iron-sulfur, [2Fe-2S]); 52, 72 (iron-sulfur, [2Fe-2S], via pros nitrogen)		Summer et al., (2011; 2012); Kim et al., (2019)
probable methylxanthine *N*7-demethylase NdmC	1.14.13.128	F0E1K6	G1E_06898	*Pseudomonas* sp. (strain TJI-51)			Summers et al., (2012)
probable *N*-methylproline demethylase		O87278	stcD	*Rhizobium meliloti* (strain 1021). (*Ensifer meliloti*) (*Sinorhizobium meliloti*)	59, 299 (FMN, via amide nitrogen); 102, 220 (FMN); 396 (FAD, via amide nitrogen); 415, 423, 433 (FAD); 460 (FAD, via amide nitrogen and carbonyl oxygen)	321-322 (FMN)	Phillips et al. (1998); Finan et al. (2001); Galibert et al. (2001)
dimethylsulfoniopropionate demethylase DmdA	2.1.1.269	Q5LS57	dmdA	*Ruegeria pomeroyi* (strain ATCC 700808/DSM 15171/DSS-3) (*Silicibacter pomeroyi*)			Moran et al. (2004); Rivers et al. (2014); Howard et al. (2006); Reisch et al. (2008); (2011); Todd et al. (2012)
dicamba *O*-demethylase, oxygenase component	1.14.15.-	Q5S3I3	ddmC	*Stenotrophomonas maltophilia* (*Pseudomonas maltophilia*) (*Xanthomonas maltophilia*)	48, 67 (iron-sulfur [2Fe-2S]); 50, 70 (iron-sulfur [2Fe-2S], via pros nitrogen); 153, play a role in the stabilisation of the metal coordination; 159, 164 (iron, via tele nitrogen); 229, 284 (3,6-dichloro-2-methoxybenzoate); 250 (3,6-dichloro-2-methoxybenzoate, via tele nitrogen); 293 (iron)		Herman et al. (2005); Chakraborty et al. (2005); Wang et al. (1997); Robert et al. (2009); Dumitru et al. (2009)
dicamba *O*-demethylase 2, ferredoxin reductase component	1.18.1.3	Q5S3I1	ddmA2	*Stenotrophomonas maltophilia* (*Pseudomonas maltophilia*) (*Xanthomonas maltophilia*)	14, 298 (FAD, via amide nitrogen); 49, 130, 279 (FAD); 82(FAD, via amide nitrogen and carbonyl oxygen)		Herman et al. (2005)
dicamba *O*-demethylase, ferredoxin component		Q5S3I4	ddmB	*Stenotrophomonas maltophilia* (*Pseudomonas maltophilia*) (*Xanthomonas maltophilia*)	40, 46, 49, 86 (iron-sulfur [2Fe-2S])		Herman et al. (2005); Chakraborty et al. (2005); Wang et al. (1997)
dicamba *O*-demethylase 1, ferredoxin reductase component	1.18.1.3	Q5S3I2	ddmA1	*Stenotrophomonas maltophilia* (*Pseudomonas maltophilia*) (*Xanthomonas maltophilia*)	49, 130, 279 (FAD); 14, 298 (FAD, via amide nitrogen); 82 (FAD, via amide nitrogen and carbonyl oxygen)		Herman et al. (2005); Chakraborty et al. (2005); Wang et al. (1997)
dimethylsulfoniopropionate demethylase DmdA	2.1.1.269	Q4FP21	dmdA	*Pelagibacter ubique* (strain HTCC1062)	122, 204, 206 (tetrahydrofolate)		Giovannoni et al. (2005); Howard et al. (2006); Reisch et al. (2008);

								Schuller et al. (2012)

Table 2 Protein structure of crystallised demethylases

Protein name	UniProt entry number	PDB entry number	Method	Resolution	Chain	Position	Image	References
aromatic *O*-demethylase, reductase subunit	P0DPQ8	5OGX	X-Ray	1.72Å	A	1-334	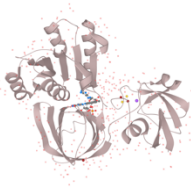	Mallinson et al. (2018)
aromatic *O*-demethylase, cytochrome P450 subunit	P0DPQ7	5NCB*	X-Ray	1.44Å	A	1-407	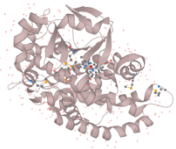	Mallinson et al. (2018)
lanosterol 14-alpha demethylase	P10613	5FSA*	X-Ray	2.86Å	A/B	49-528	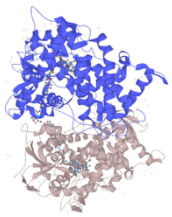	Hargrove et al. (2017)
lanosterol 14-alpha demethylase	P50859	5JLC	X-Ray	2.40Å	A	20-533	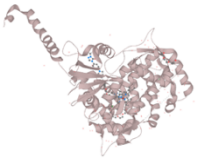	Keniya et al. (2018)
lanosterol 14-alpha demethylase	P9WPP9	1E9X*	X-Ray	2.10Å	A	1-451	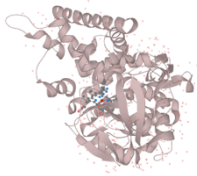	Podust et al. (2001)
sterol 14-alpha demethylase	E9QY26	4UYL*	X-Ray	2.81Å	A/B	50-518	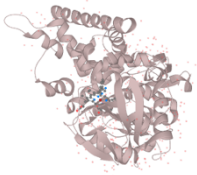	Hargrove et al. (2015)

dimethylsulfoniopropionate demethylase DmdA	Q4FP21	3TFH*	X-Ray	2.10Å	A/B	1-369	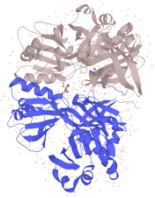	Schuller et al. (2012)
methylxanthine *N*1-demethylase NdmA	H9N289	6ICK*	X-Ray	1.95Å	A/B/C	1-351		Kim et al. (2019)
methylxanthine *N*3-demethylase NdmB	H9N290	6ICL	X-Ray	2.10Å	A	1-355		Kim et al. (2019)
oxidoreductase NdmD	H9N291	6ICM	X-Ray	2.96Å	D	502-588	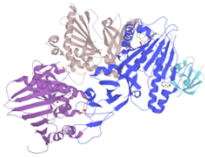	Kim et al. (2019)
cytochrome p450 cyp199A2	Q6N8N2	2FR7*	X-Ray	2.01Å	A	1-412	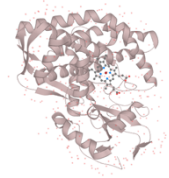	Bell et al. (2008)
cytochrome p450 cyp199A4	Q2IU02	4DNZ*	X-ray	2.60Å	A/B/C/D	1-410	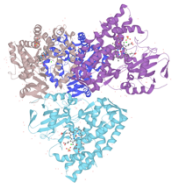	Bell et al. (2012b)
lanosterol 14-alpha demethylase	P10614	4LXJ*	X-Ray	1.90Å	A	1-530		Monk et al. (2014)
vanillate/3-*O*-methylgallate *O*-demethylase	G2IQS7	5TL4*	X-Ray	1.75Å	A/B/C/D	1-471	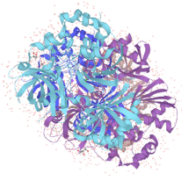	Kohler et al. (2017)

dicamba *O*-demethylase, oxygenase component	Q5S3I3	3GB4*	X-Ray	2.05Å	A/B/C	1-339	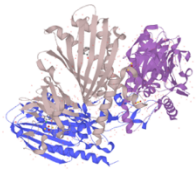	Robert et al. (2009)

*more than one crystal structures was obtained for this enzyme.

2.1 Cytochrome P450

Demethylation is one of the catalytic functions discovered within microbial P450s, facilitating both endogenous and xenobiotic metabolism. Cytochrome P450 (CYPs or P450s) are a superfamily of heme-containing enzymes functioning as monooxygenases which have been identified in all kingdoms of life and are known to have broad catalytic substrate ranges, including their involvement in drug and xenobiotic metabolism (McLean et al., 2015).

The catalysis of demethylation reactions associated with compound biosynthesis by microbial P450s has been widely explored, with a focus on sterol biosynthesis, and compounds such as ergosterol and lanosterol (Aoyama et al., 1984; Hitchcock et al., 1989; Bossche et al., 1993; Lamb et al., 1999; Sun et al., 2011b; Ke et al., 2017). Sterols are lipids with crucial roles in various physiological functions, such as cellular signalling in eukaryotic micro-organisms (Huang et al., 2016; Lee et al., 2018). Cytochrome P450s (CYP51) have been identified in many fungi, as well as a few bacteria, catalysing lanosterol 14α-demethylation and ergosterol C-4 demethylation during sterol biosynthesis (Aoyama et al., 1984; Hitchcock et al., 1989; Bossche et al., 1993; Lamb et al., 1999; Sun et al., 2011b; Ke et al., 2017). The occurrence of CYP51 reported in different fungi (Lamb et al., 1998; Aoyama et al., 1998; Bellamine et al., 1999; Jackson et al., 2002; Pietila et al., 2006; Ke et al., 2017) includes *Saccharomyces cerevisiae*, *Candida tropicalis*, *Candida albicans*, *Cryptococcus neoformans* var. *neoformans*, *Candida glabrata*, *Candida lusitaniae*, *Aspergillus fumigatus*, *Trichophyton mentagrophytes*, *Histoplasma capsulatum,* as well as bacteria such as *Rhodococcus triatomae*, *Mycobacterium tuberculosis*, *Mycobacterium smegmatis*, *Mycobacterium avium*, *Methylococcus capsulatus*. P450 demethylases are more widely studied with regards to their roles in biotransformation and biodegradation, given their versatile catalytic abilities on both endogenous and xenobiotic compounds. Since it has been suggested that the redox partner system is one of the efficiency-limiting factors for catalytic activity of P450 enzymes (Guengerich, 2002), it is crucial to explore and review the redox partners of different types of P450 demethylases, to shed light on further investigations and future applications.

Additionally, there is practical application derived from the broad substrate range and mechanisms of this family of enzymes.

Aryl-*O*-demethylases are one of the groups of microbial demethylases that have been investigated extensively, of which P450s make up a crucial part. CYP199A4 identified from *Rhodopseudomonas palustris* strain HaA2 has been subject to extensive mechanistic studies for catalysing *para*-substituted benzoic acids (Bell et al., 2012a). The key residues responsible for catalytic activity have been elucidated, and substrates other than substituted benzoic acids have been identified, such as veratric acid, to expand the substrate range. Additionally, catalysis of demethylation of methoxyphenols by P450 has been observed in many microbes such as *Rhodococcus rhodochrous* strain 116 (Eltis et al., 1993), *Moraxella* sp. strain GU2 (Dardas et al., 1985) and *Streptomyces setonii* 75Vi2 (Sutherland, 1986).

Broader ranges of substrates with methyl groups attached have been recognised to be demethylated by various P450s, either for degradation or biotransformation. CYP105D1 from *Streptomyces griseus* ATCC 13273 has been shown to perform regioselective *O*-demethylation on two drug-related metabolites, tetrahydroprotoberberines (THPBs) and papaverines (Shen et al., 2019ab), which are of potential pharmaceutical significance. Demethylation of methoxylated carbohydrates is also of research interest, due to the difficulty in dealkylation of carbohydrates brought by the high energy barrier for methyl group removal (Blanksby and Ellison, 2003). CYP236A2 and CYP236A20 identified from the marine bacteria *Zobellia galactanivorans* and *Formosa agariphila* respectively, were shown to demethylate 6-*O*-methyl-D-galactose (G6Me) (Reisky et al., 2018; Robb et al., 2018). Such findings have expanded the catalytic scope of carbohydrate-active enzymes to the cytochrome P450 superfamily, which is a second group of monooxygenases involved in the conversion of terrestrial carbohydrates apart from the recently characterised lytic polysaccharide monooxygenases (Hemsworth et al., 2013; Janusz et al., 2013).

There are many xenobiotic degradation/transformation reactions identified in microbes, with as yet unclear underlying enzymatic mechanisms. However, P450s have been proposed to be involved in many cases based on various experimental findings, of which the most commonly used are the use of cytochrome P450 enzyme inhibitors such as phenylimidazole (Correia et al., 2015). Such cases include the biotransformation procedure observed in the soil fungus, *Cunninghamella echinulate* NRRL 1384 for the production of buprenorphine by

regioselectively demethylating a thebaine derivative (Abel et al., 2003). Another similar finding applies to the biotransformation of acetamiprid, an insecticide, by the white-rot fungus *Phanerochaete sordida* YK-624, and to catalytic activity reduction by the addition of piperonyl butoxide which suggested that a P450 enzyme may play a crucial role in the *N*-demethylation reaction (Wang et al., 2012). The same inhibition studies revealed the possible contributions of three P450s to the biotransformation of chalcones to flavonoids in *Aspergillus alliaceus* UI 315, one of which catalysed the *O*-demethylation of chalcones (Sanchez-Gonzalez and Rosazza, 2004), but further validations are needed to identify the enzymes. Other proposed P450 demethylases have been reported, such as the enzymes responsible for the demethylation of methyl *tert*-butyl ether, a fuel oxygenate, by *Graphium* sp. strain ATCC 58400 (Hardison et al., 1997; Deeb et al., 2000), the demethylase system involved in the complete degradation of 2,4,6-trichloroanisole, a widely distributed chlorinated pollutant by the crust fungus, *Phlebia radiata* (Campoy et al., 2009), and the metabolism of methoxychlor, a chlorinated pesticide by *Cunninghamella elegans* ATCC36112 (Keum et al., 2009). Follow-up studies to validate and identify the catalytic mechanisms including the responsible enzymes for further potential applications are needed in each of these cases.

2.2 Rieske-type non-heme iron-dependent oxygenases

Rieske-type non-heme iron-dependent oxygenases (abbreviated as ROs), are similar to cytochrome P450 enzymes in that they both catalyse a wide range of reactions, including oxidation, desaturation, dealkylation and dichlorination (Perry et al., 2018). However, unlike CYPs, whose mechanisms have been studied extensively and widely, catalytic pathways among the ROs family of enzymes are much less explored (Resnick et al., 1996; Costas et al., 2004; Barry and Challis, 2013). ROs were first identified as oxygenases catalysing the degradation of various aromatic compounds by *Pseudomonas putida* (Gibson et al., 1968; Axcell and Geary, 1975; Barry and Challis, 2013). This group of enzymes has since attracted research interest due to their activity as catalysts of the initial attack on inert aromatic nuclei of compounds via *cis*-dihydroxylation, both regio- and stereo-specifically, producing chiral intermediate compounds of agrochemical and pharmaceutical significance (Ensley et al., 1983; Hudlicky et al., 1999; Boyd et al., 2005; Zezula and Hudlicky, 2005; Barry and Challis, 2013; Chakraborty et al., 2017). In contrast to other families of non-heme iron-dependent oxygenases, ROs have an iron-sulfur cluster, which further classifies enzymes into subgroups based on the numbers of iron and sulfide ions in the cluster: [2Fe-2S], [3Fe-4S], [4Fe-4S] and

other hybrid types (Cammack et al., 1999; Ferraro et al., 2005). A generic RO system consists of two or three components, which typically include electron transport protein cycles that facilitate shuttling of electrons to the oxygenase component. This is the non-heme iron centre in the active site from the reducing agent, catalysing the oxygenation of the substrates (Mason and Cammack, 1992; Ferraro et al., 2005; Chakraborty et al., 2017). Interestingly, the role of ROs has expanded far beyond aromatic degradation, to both biodegradative and biosynthetic activities of a greater scope of substrates (Chakraborty et al., 2017). Despite this family of enzymes having been identified widely in all organisms, bacteria seem to be more common hosts for this system compared to eukaryotes and archaea (Chakraborty et al., 2012), and all of the ROs identified with demethylation functions so far belong to the prokaryotic kingdom.

RO demethylases have been discovered in lignin degradation pathways, including vanillate and 5,5'-dehydrodivanillate (DDVA) demethylation (Priefert et al., 1997; Morawski et al., 2000; Thanbichler et al., 2007; Chen et al., 2012; Yoshikata et al., 2014). Apart from these activities, *N*-demethylation has also been uncovered among this enzyme group. Such cases include a three-component RO system in *Sphingomonads* DC-6 and DC-2 with the ability to *N*-dealkylate chloroacetanilide herbicides (Chen et al., 2014), a three-component RO system in bacterial strains such as *Pseudomonas maltophilia* strain DI-6 capable of *O*-demethylating the herbicide dicamba (2-methoxy-3,6-dichlorobenzoic acid) (Herman et al., 2005), and caffeine demethylation identified in *Pseudomonas putida* CBB5 and *Pseudomonas* sp. NCIM 5235 (Summers et al., 2012; 2013; Retnadhas and Gummadi, 2018). Additionally, RO systems have been discovered in the demethylation of glycine betaine and proline betaine, both of which are organic osmolytes, as well as carbon, nitrogen and energy sources for many bacteria (Kumar et al., 2014; Shao et al., 2018).

As previously mentioned, the catalytic scope of the RO family has extended beyond degradation to biosynthesis, an example of which has been reported in bacterial sterol biosynthesis (Lee et al., 2018). Unlike eukaryotic sterol synthesis, where cytochrome P450s play an essential role in demethylating processes, an RO system has been observed in aerobic methanotrophic γ-proteobacterium *Methylococcus capsulatus* responsible for the demethylation at C-4 position, namely, converting 4,4-dimethylsterols to 4α-methylsterols.

2.3 Tetrahydrofolate-dependent demethylase

Tetrahydrofolate (H_4folate) is a compound derived from folic acid which has been identified as a significant coenzyme component in many enzyme systems (Hitching., 1983), including the H_4folate-dependent demethylases. The whole enzyme system requires H_4folate, or a corrinoid protein to accept the methyl group removed from the substrate, by the methyltransferase yielding 5-methylH_4folate, 5,10-methyleneH_4folate, 5,10-methynylH_4folate and 10-formylH_4folate, in a stepwise manner, and finally H_4folate is regenerated with formic acid produced to recover the cofactor for future involvement in the demethylation process (Masai et al., 2007). H_4folate-dependent demethylases are not only essential for compound metabolism, but for the production of H_4folate derivatives, such as 5-methyl-H_4folate, which are crucial for the biosynthesis of methionine, thymidine and purine/fMet-tRNA (Maden, 2000).

Among the extensively studied lignin-related enzymes, vanillate/3-*O*-methylgallate (3MGA) *O*-demethylase LigM and syringate *O*-demethylase DesA, identified and explored in *Sphingomonas paucimobilis* SYK-6, both require a H_4folate component as the methyl group acceptor (Masai et al., 2004; Abe et al., 2005). Another metabolic pathway involving H_4folate-dependent demethylase is the degradation of dimethylsulphoniopropionate (DMSP) by *Ruegeria pomeroyl* DSS-3, a metabolite from marine phytoplankton (Howard et al., 2006; Reisch et al., 2011; 2013). Apart from natural compound metabolism, a H_4folate-dependent enzyme has been identified as being responsible for xenobiotic degradation, namely, the herbicide dicamba (Yao et al., 2019).

2.4 Others

There are many other demethylases identified in micro-organisms that are either unclassified or that do not belong to any of the enzyme types mentioned above, yet a comprehensive review on them could be helpful to identify future research directions.

For lignin-related degradation, a peroxidase system has been indicated in the demethylation of polyguaiacol by *Phanerochaete chrysosporium*, based on an *in vitro* assay with extracellular culture filtrates (Frick and Crawford, 1984). Interestingly, this same species has also been identified to demethylate the triphenylmethane dye, crystal violet (*N*, *N*, *N'*, *N'*, *N''*, *N''*-hexamethylpararosaniline) (Bumpus and Brock, 1988). A different enzyme system, one component of which belongs to the MttB superfamily of proteins, has been identified from

the human gut bacterium, *Eubacterium limosum* ATCC 8486, that is able to *N*-demethylate proline betaine anaerobically (Picking et al., 2019). The MttB superfamily consists of trimethylamine methyltransferases, catalysing the shuttle of a methyl group from trimethylamines to specific corrinoid proteins, in association with methanogenesis from trimethylamine (Paul et al., 2000).

3 Physiological, biochemical and ecological roles associated with microbial demethylases

The microbial demethylase categories introduced above are classed based on the different structural and catalytic features that underpin the mechanisms of these enzymes. However, the practical significance of demethylases should also be reviewed in terms of both their identified and potential applications, as well as their physiological, biochemical and ecological roles.

Microbial demethylases can be functionally categorised into 3 groups according to current findings (Fig. 3). Enzymes in each functional category are of great research interest given their close connections with xenobiotic metabolism and involvement in natural cycles. Among them, the degradative enzymes are further sub-grouped based on their contributions to different natural elemental cycles.

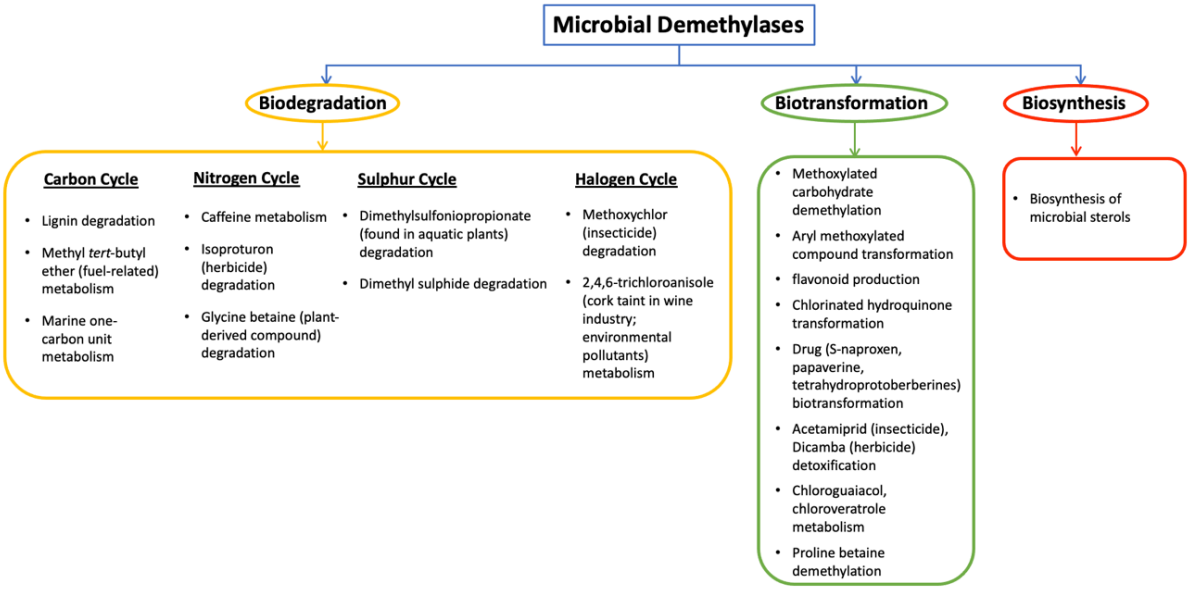

Figure 3 Function-based categories of microbial demethylases.

3.1 Biodegradation

3.1.1 Carbon cycle

Carbon cycles play fundamental roles in all of life, making it crucial to investigate natural cycles both for improved understanding and exploitation. Methyl group-containing compounds are usually stable in structure, while microbial demethylation facilitates carbon cycles by releasing the methyl group from the original substrate aiding the re-arrangement of carbon atoms and improving reactivity.

One of the most extensively studied elements of carbon cycle is lignin biodegradation (Fig. 4; Fig. 5). Lignin is the major building block of lignocellulose, comprising a generous reservoir of carbon sources that play an essential part in the terrestrial carbon cycle. As a group of highly methylated compounds, lignin is recalcitrant to biodegradation, due to the stable nature of the methoxy group, rendering it an under-utilised carbon source. However, both bacterial- and fungal-attacks on lignin have recently been identified in nature, including white-rot fungi and many bacterial strains belonging to *Brucella*, *Ochrobactrum*, *Sphingobium*, *Sphingomonas*, and *Streptomyces* genera (Tian et al., 2014; Janusz et al., 2017), making this group of compounds less mysterious and more practically applicable. The depolymerisation of lignin feedstock yields various low molecular weight lignins, including monomers and oligomers, suitable for further assimilation. *O*-Demethylases secreted by microbes perform the transformation of methylated substrates into phenolic metabolites amenable for bio-application as well as further carbon metabolism (Abdelaziz et al., 2016; Venkatesagowda, 2019).

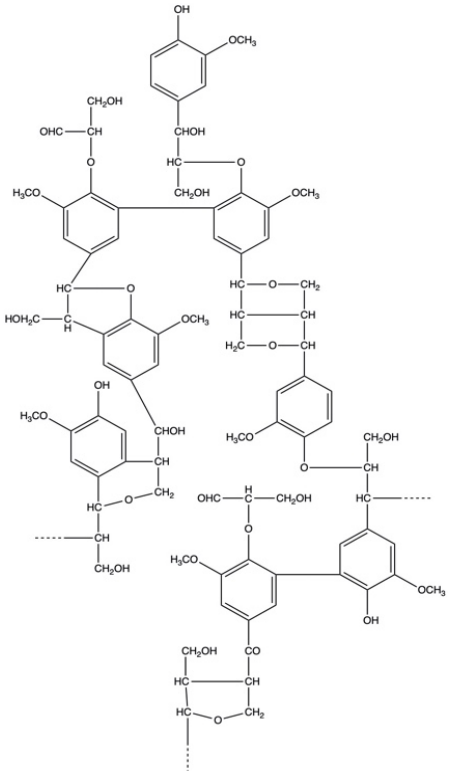

Figure 4 Partial structure of lignin.

O-Demethylases with different catalytic mechanisms against various methoxylated aromatic intermediates in lignin degradation have been identified (Fig. 4, Table 1). Vanillate demethylases, one of the most extensively studied demethylases, comprises two different systems in diverse microbes, LigM and VanA/VanB. LigM, a tetrahydrofolate-dependent system, identified in *Sphingobium* sp. SYK-6, is capable of catalysing the conversion of vanillate and 3-*O*-methylgallate to protocatechuate and gallate respectively, which are further degraded by other enzyme systems yielding metabolites that end up in the TCA (tricarboxylic acid) cycle (Masai et al., 2007). Based on crystal structure determinations (Harada et al., 2017; Kohler et al., 2017), LigM is similar to *E. coli* aminomethyltransferase (T-protein) GcvT, but some distinctive features are observed, especially in the active site. Based on this a hypothesis was proposed suggesting that LigM may have evolved from T-proteins while adaptively developing an active site for *O*-demethylation (Harada et al., 2017; Kamimura et al., 2017). Further studies revealed that *metF* and *ligH* genes located just downstream of *ligM* were proposed to be involved in the H_4folate-dependent cycle, specifically, *metF* was thought to encode for 5,10-methylene-H_4folate reductase and *ligH* for 10-formyl-H_4folate synthetase. Furthermore, the *O*-demethylation of vanillate by LigM has been indicated essential for

methionine production for supplying 5-methyl-H_4folate. On the other hand, another vanillate demethylase system (VanA/VanB) is a RO type enzyme, harbouring a Rieske-type cluster and a reductase accommodating a flavin and a [2Fe-2S] redox centre (Morawski et al., 2000). The electron flow within this enzyme for hydroxylation starts from NAD(P)H to flavin mononucleotide, and then to the [2Fe-2S] redox centre in reductase, and from Rieske-type centre to the iron site within the oxygenase, which is also the oxygen binding region (Tsang et al., 1989; Gassner et al., 1994; 1995; Pavel et al., 1994; Morawski et al., 2000). The two components are encoded by contiguous genes, *vanA* and *vanB* for the oxygenase and reductase respectively. This enzyme system has been identified in many bacterial species such as *Pseudomonas* sp. HR199, *Acinetobacter* sp. ADP1, *Caulobacter crescentus* CB15N and *Rhodococcus jostii* RHA1 (Priefert et al., 1997; Morawski et al., 2000; Thanbichler et al., 2007; Chen et al., 2012), and is responsible for vanillate demethylation except *Sphingomonas paucimobilis* SYK-6 (Kamimura et al., 2017).

VanA and VanB in *Pseudomonas* sp. HR199 were heterologously expressed and biochemical studies revealed the broad range of catalytic substrates. A carboxyl moiety appeared to be crucial for catalysis, which only occurred at the *meta* position of the aromatic ring in vanillate analogues (Morawski et al., 2000). On the other hand, the same heterologous expression of VanA and VanB from *Acinetobacter* strain ADP1 was performed and vanillate analogues were used for substrate range screening, and results indicated that although analogues with a methoxy or methyl group at the *meta* position relative to the carboxyl moiety can be transformed, those with a hydroxyl group or hydrogen atom at the same position, cannot (Morawski et al., 2000).

As described earlier, LigX, identified in *Sphingomonas paucimobilis* SYK-6, comprising three components LigXa (an oxygenase), LigXc (a ferredoxin) and LigXd (a ferredoxin reductase), is capable of catalysing the demethylation of 5,5'-dehydrodivanillate (DDVA) and has been proposed to belong to RO family (Yoshikata et al., 2014). Specifically, phylogenetic analysis on the deduced amino acid sequences showed similarities (26-27% identity) for LigXa with other ROs such as 3-chlorobenzoate-3,4-dioxygenase of the soil bacterium, *Comamonas testosterone* BR60 (Nakatsu et al., 1995). And LigXc and LigXd shared ~60% amino acid sequence identity with ferredoxin and ferredoxin reductase of dicamba *O*-demethylase of *Pseudomonas maltophilia* DI-6 (Herman et al., 2005), which is the electron transfer component of the three-component oxygeases belonging to RO family.

Last but not least, a syringate demethylase DesA has been discovered in *Sphingomonas paucimobilis* SYK-6 (Abe et al., 2005). DesA has been proven to demethylate syringate to give 3MGA only in the presence of H_4folate yielding 5-methyl-H_4folate, and it could also catalyse the demethylation of vanillate and 3MGA, but at relatively low activity. A gene disruption study of this specific gene yielded a growth reduction on syringate, but no effects were observed for vanillate, which further confirmed that *desA* is necessary for syringate demethylation.

The research concerning lignin metabolism by various microorganisms and enzymes has been extensively reviewed (Masai et al., 2007; Fuchs et al., 2011; Bugg et al., 2011; Kamimura et al., 2017; Venkatesagowda, 2019).

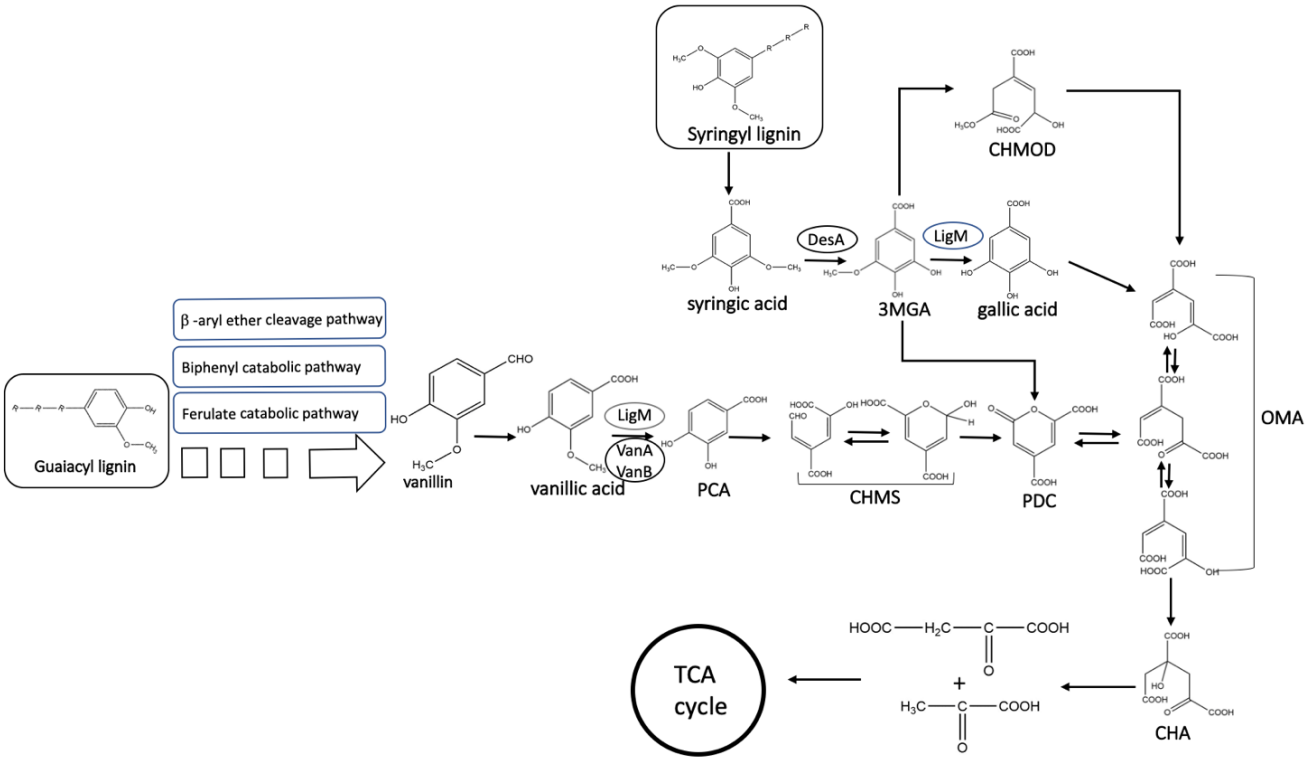

Figure 5 Lignin degradation, demethylases involved are highlighted in circle (Adapted from Masai et al., 2007). PCA, protocatechuate; CHMS, 4-carboxy-2-hydroxymuconate-6-semialdehyde; PDC, 2-pyrone-4,6-dicarboxylate; 3MGA, 3-*O*-methylgallate; CHMOD, 4-carboxy-2-hydroxy-6-methoxy-6-oxohexa-2,4-dienoate; OMA, 4-oxalomesaconate; CHA, 4-carboxy-4-hydroxy-2-oxoadipate; TCA, tricarboxylic acid.

Other methoxylated aromatic compounds, such as guaiacol (2-methoxyphenol), which is one of the major low molecular metabolites of lignin, have been studied widely as the subject for

the microbial attack catalysed by P450-*O*-dealkylases from various microbes. Cytochrome P450 enzymes identified from *Moraxella sp*. strain GU2 and *Streptomyces setonii* 75Vi2 have been shown to demethylate guaiacol and 2-ethoxyphenol, and guaiacol and veratrole respectively, with catechol being the demethylation product. One of these enzymes has been suggested as a non-specific *O*-dealkylase for compounds homologous with guaiacol with longer alkyl group in the side chain (Dardas et al., 1985; Sutherland, 1986). A detailed study on the P450 demethylase from *Rhodococcus rhodochrous* has been conducted for the identification of the two-component guaiacol demethylase system, specifically, the redox partner protein (García-Hidalgo et al., 2019). Four different polycistronic operons carrying both putative redox proteins and the cytochrome P450 were constructed and heterologously expressed in *Pseudomonas putida* EM42 with guaiacol consumption dynamics analysed for the efficacy of each recombinant system. Results indicated that a putative ferredoxin reductase from *R. rhodochrous* and putative ferredoxins from the same organism or *Amycolatopsis* ATCC 39116 can act as redox partner proteins (García-Hidalgo et al., 2019). A novel two-component P450 enzyme system consisting of a P450 protein from the family CYP255A (GcoA) and a reductase (GcoB) has been explored extensively from structural and biochemical perspectives (Mallinson et al., 2018). Originally identified as being capable of transforming guaiacol to catechol, this demethylase system showed promiscuous catalytic ability to bind with other monomers which was further investigated for structural causes. It was demonstrated that the active site within GcoA is sufficient for accommodating the turnover of many substrates including 3-methoxycatechol, anisole, guaethol, and 2-methylanisole, while vanillin, which substitutes the H at the C4 position of guaiacol with a formyl group has been reported to yield a partial substrate, which might reflect steric hindrance.

Demethylases have also been identified in other degradation pathways facilitating carbon cycles. Degradation of one of the fuel oxygenates, methyl tert-butyl ether (MTBE) has been discovered by both aerobic and anaerobic bacteria (Deeb et al., 2000; Stocking et al., 2000; Fayolle et al., 2001; Youngster et al., 2008). A demethylase, though not elucidated yet, has been suggested to be responsible for initiating the first step of degradation (Fig. 6a), followed by complete mineralisation releasing CO_2 back to natural cycles. An increased MTBE degradation rate was observed in a co-culture study with methoxylated aromatic compounds such as guaiacol and vanillate being co-substrates, and the hypothesis that acetogenic bacteria

may be responsible for the anaerobic degradation of MTBE was proposed (Youngster et al., 2008).

In addition to those discussed above, another cycle, accounting for a large proportion of C1 metabolism in aquifers is conducted by a group of marine bacteria and involves the delivery of C1 units from one compound to another via demethylation; such units include methyl, methylene, methenyl, formyl and formimino groups (Henderson, 1979; Sun et al., 2011a). The oceans harbour large amounts of dissolved organic carbon (DOC) and provide potential substrates for various one carbon unit metabolisms. The aerobic heterotrophic marine bacteria of the SAR11 clade are abundant in ocean surface waters and have been studied for their ability to demethylate a range of C1 compounds, such as trimethylamine N-oxide (TMAO). TMAO is degraded by *Candidatus Pelagibacter ubique* HTCC1062 via demethylation and oxidation, but some processes and enzymes remain unidentified (Sun et al., 2011a). Other compounds that have been found to undergo similar demethylation routes are dimethylsulfoniopropionate (DMSP) and glycine betaine (GBT), by the same axenic cultures (Sun et al., 2011a) (Fig. 6b).

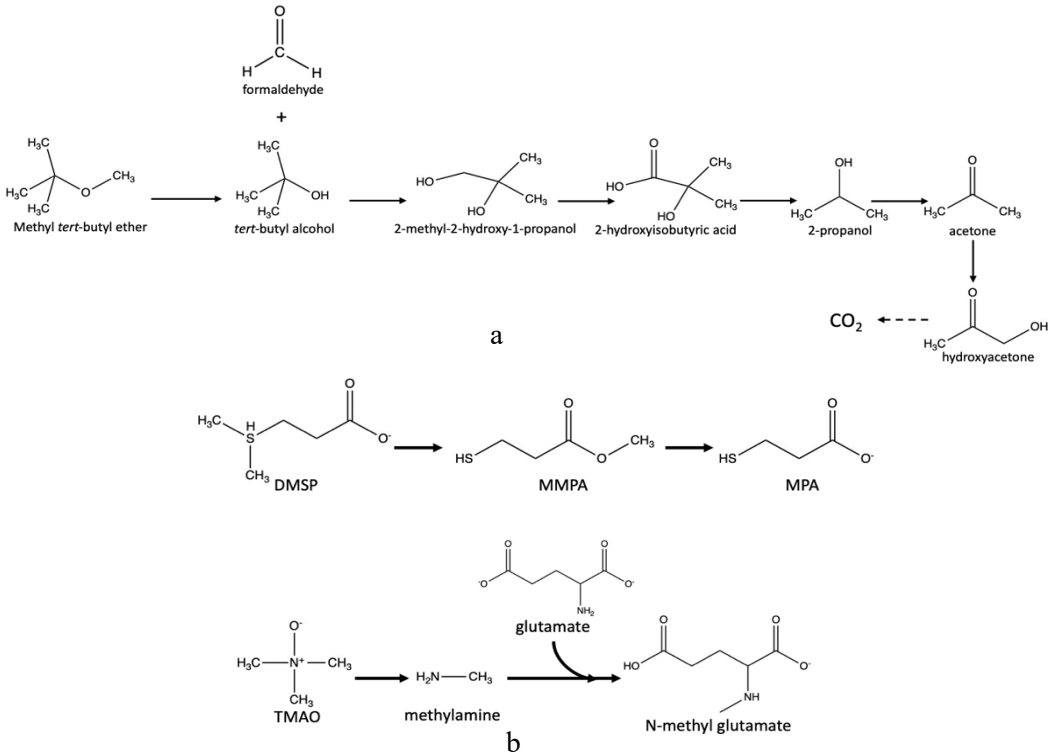

Figure 6 Demethylation involved in carbon cycle. a. methyl *tert*-butyl ether metabolism (Deeb et al., 2000); b. marine one carbon unit metabolism (Chen et al., 2011a). Abbreviations: DMSP, dimethylsulfoniopropionate; MMPA, methylmercaptopropionate; MPA, mercaptopropionate.

3.1.2 Nitrogen cycle

Like carbon, nitrogen occurs ubiquitously on earth, and is a crucial element for living organisms. As such, nitrogen cycles have long been of particular research interest due to the underlying environmental importance and potential industrial applications of N-containing compounds. Apart from natural nitrogen movement, anthropogenic activities in the pharmaceutical industry, fossil fuel exploitation and artificial fertiliser utilisation have imposed great impacts on the global nitrogen cycle. Microbes play a key role in facilitating the return of artificial nitrogen to natural elemental cycles, and the microbial nitrogen-cycling network has been studied extensively (Kuypers et al., 2018). Demethylation, as one of the essential steps of the N-cycle will be discussed in detail in this section.

Caffeine metabolism has been studied in both fungi and bacteria, with diverse pathways elucidated, among which demethylation is the initiating step (Fig. 7a). RO-type demethylase systems have been discovered in *Pseudomonas* sp. NCIM 5235 and *Pseudomonas putida* CBB5 (Summers et al., 2013; Retnadhas and Gummadi, 2018), with the latter characterised in further detail. Specifically, three demethylases NdmA, NdmB and NdmC, with position-specific catalytic activity were reported, sharing one reductase (NdmD). One interesting finding about reductase NdmD, was demonstrated that, an additional [2Fe-2S] Rieske domain exists in the N-terminal region, but its role might not be for the reductase nor demethylation activity when partnering with NdmA. Instead, it has been suggested that this domain fused with the reductase NdmD acted as the transition phase of an adaptation process for higher catalytic efficiency. Additionally, a structural protein NdmE has also been suggested to be required for the catalytic activity of NdmC (Summers et al., 2013).

Glycine betaine is an organic osmolyte, as well as a carbon, nitrogen and energy source for many bacteria, and has been linked with various metabolic pathways (Müller et al., 1981; Oren, 1990; Fig. 7b). One particular pathway involving demethylation catalysed by a novel RO system has been characterised in *Chromohalobacter salexigens* DSM 3043 (Shao et al., 2018). This two-component enzyme, BmoA and BmoB, acts as the terminal oxygenase and the flavin reductase. *In vitro* enzymatic analysis suggested that BmoB was NADH-dependent and accommodated a noncovalently bound FAD as the prosthetic group. BmoA, however, showed narrow catalytic specificity only towards glycine betaine aerobically. The breakdown of a similar compound, proline betaine, has been demonstrated in *Paracoccus denitrificans* and *Rhodobacter sphaeroides* (Kumar et al., 2014). Both Rieske-type proteins HpbB1-

HpbC1 and HpbB2-HpbC2 have been identified to be active with demethylating L-proline betaine to produce *N*-methyl-L-proline (Kumar et al., 2014). However, more detailed characterisations of these two enzyme systems, as well as the complete metabolic pathway, are required.

Apart from naturally occurring compounds, degradation of nitrogen-containing chemicals produced by human activities has also been investigated for remediation purposes, with *N*-demethylation being observed as the starting step of the majority of degradations. This is the case for the herbicide isoproturon, for which *N*-demethylation initiates degradation (Sun et al., 2009; Fig. 7c), although in the case of metabolism by *Sphingobium* sp. YBL1, YBL2 and YBL3 the *N*-demethylase has yet to be identified.

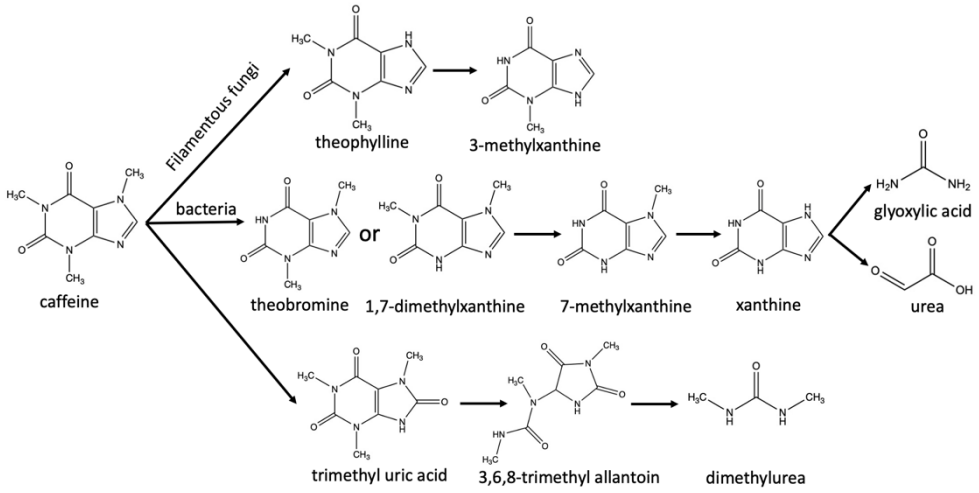

a

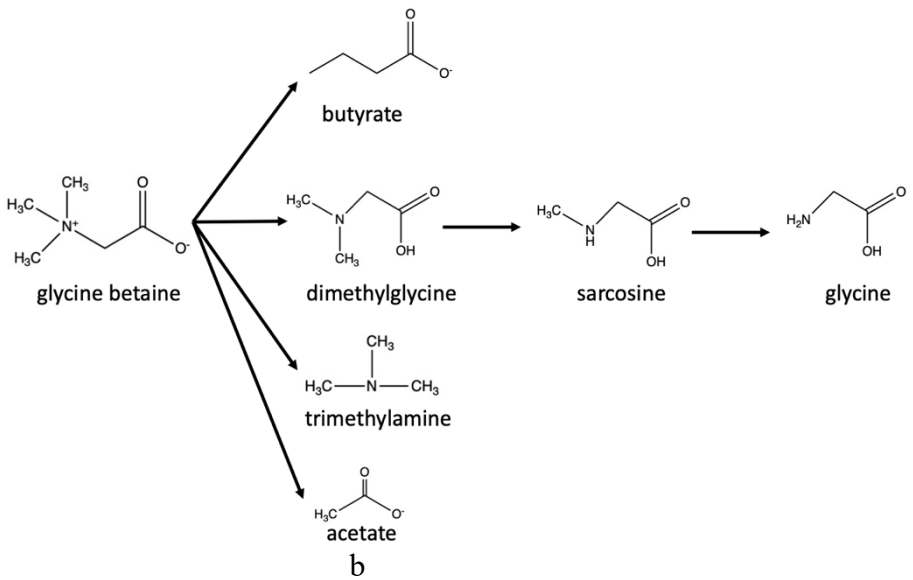

b

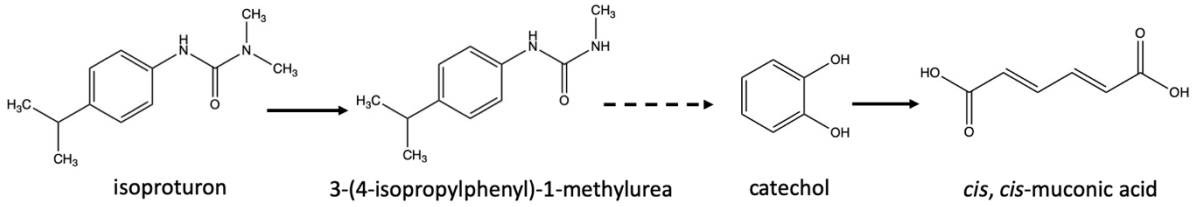

c

Figure 7 Demethylation involved in the nitrogen cycle. a. caffeine degradation (Summers et al., 2013; Retnadhas and Gummadi, 2018). b. glycine betaine degradation (Müller et al., 1981; Oren, 1990). c. isoproturon degradation (Sun et al., 2009).

3.1.3 Other cycles

Sulfur is another essential element and a constituent of proteins, enzyme cofactors and oxidants or reductants involved in microbial anaerobic respiration (Madigan et al., 1997). Steps in the global sulfur cycle include the mineralisation of organic sulfur, incorporation of inorganic sulfur into an organic form, oxidation and reduction, among which microbial demethylation plays a key role for selected compounds.

DMSP, which has been mentioned in previous one-carbon unit cycle, has been explored extensively. It is synthesised by phytoplankton, possibly as an osmoprotectant and an antioxidant (Malin and Erst, 1997; Stefels, 2000; Sunda et al., 2002), and makes up the majority of organic sulfur flow from primary producers in marine microbial systems (Vila-Costa et al., 2006). Two degradation mechanisms have been identified (Fig. 8a), with demethylation being found in one pathway releasing methanethiol, whereas cleavage produces dimethylsulphide (DMS) in the other. These metabolites also play crucial roles in global sulfur cycles, in addition to DMSP (Yoch, 2002; Reisch et al., 2013). The primary metabolites, DMS and methanethiol, are further metabolised by different microbes during

which demethylation takes place to transform the organic sulfur into an inorganic form (Lomans et al., 2002; Fig. 8b).

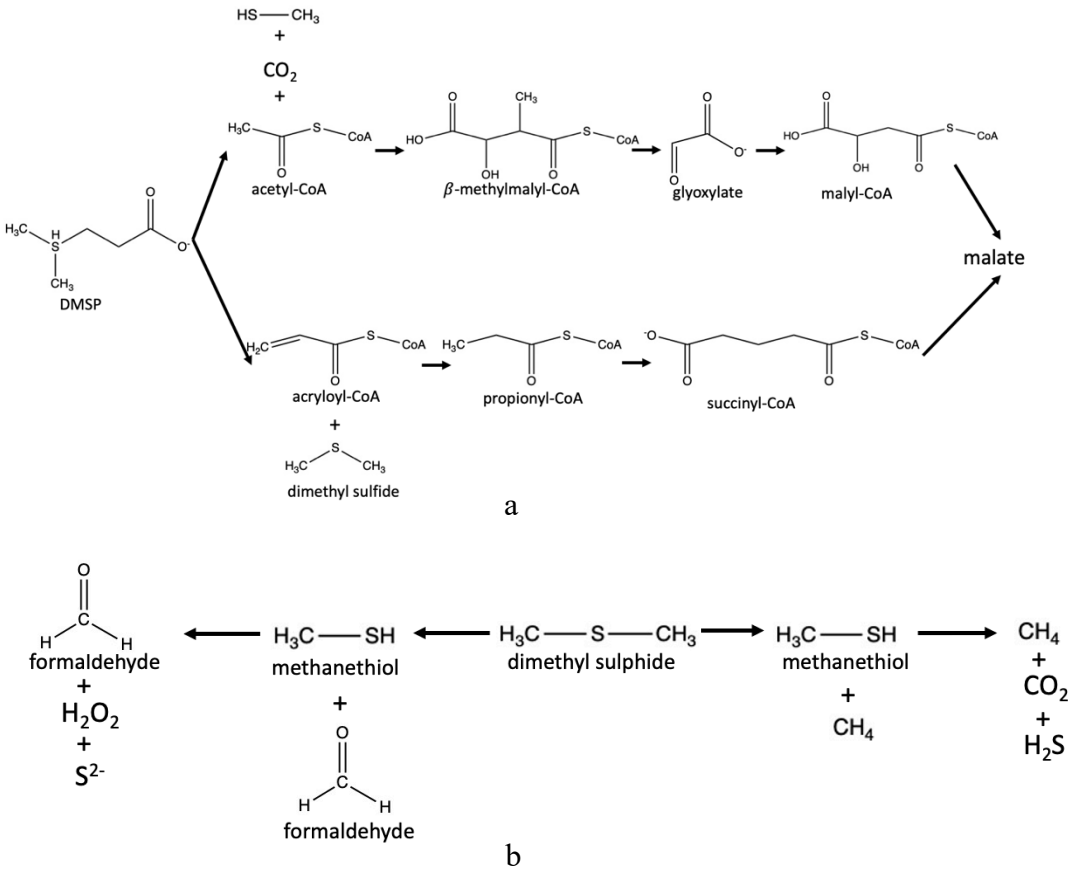

Figure 8 Demethylation involved in sulfur cycle. a. DMSP degradation (Reisch et al., 2013). b. DMS degradation (Lomans et al., 2002).

Last but not least, demethylation has been reported in halogen cycling, specifically, chlorine cycling. Chlorine is one of the most abundant trace elements (Winterton, 2000), and chlorinated compounds are distributed widely in nature, either naturally or from anthropogenic origins. Chlorine degradation mechanisms have been explored among microorganisms for various aims. Methoxychlor is commonly used as a chlorinated pesticide, and *O*-demethylation has been observed in both eukaryotic and prokaryotic microbes as metabolic fates (Castro and Yoshida, 1971; Fogel et al., 1982; Golovleva et al., 1984; Muir and Yarechewski, 1984; Keum et al., 2009; Masuda et al., 2012; Fig. 9a). A P450 demethylase has been proposed to be responsible for the demethylation in *Cunninghamella elegans* activating the degradation (Keum et al., 2009), yet further evidence is required for validation and enzyme characterisation. 2,4,6-Trichloroanisole (2,4,6-TCA) is a widely distributed pollutant, and the aroma compound responsible for 'cork taint' (Campoy et al., 2009), a wine fault, occurs naturally and as a consequence of human activity. Complete degradation has been investigated in several white-rot fungi, among which a *Phlebia radiata* strain was selected as the model organism for detailed exploration due to its high degradation ability (Campoy et al., 2009; Fig. 9b). A microsomal P450 demethylase has been revealed to be responsible for demethylating 2,4,6-TCA yielding 2,4,6-trichlorophenol (2,4,6-TCP), whereas further enzymatic characterisation was absent.

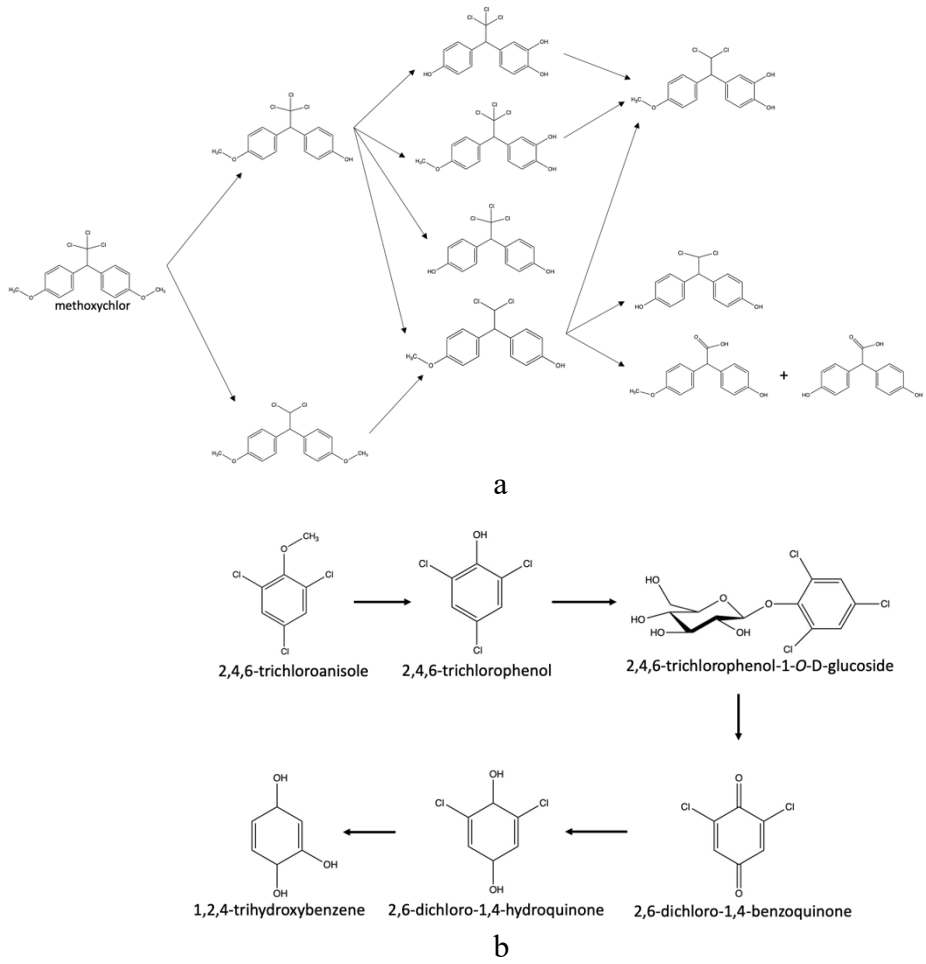

Figure 9 Demethylation involved in chlorine cycle. a. methoxy degradation (Castro and Yoshida, 1971; Fogel et al., 1982; Golovleva et al., 1984; Muir and Yarechewski, 1984; Keum et al., 2009; Masuda et al., 2012). b. 2,4,6-trichloroanisole degradation (Campoy et al., 2009).

3.2 Biotransformation

Microbial biotransformation has been extensively studied for various purposes from environmental remediation to industrial bio-production and pharmaceutical studies (Reisky et al., 2018; Shen et al., 2019a, b). Unlike biodegradation, microbial biotransformation applies to a broader scope of reactions ranging from simple structural alterations to complete mineralisation of organic compounds to CO_2, H_2O and NH_4^+. Diverse reactions are involved in biotransformation, among which demethylation is a vital step, rendering desirable intermediates or even final products.

Two microbial demethylases catalysing the biotransformation of *para*-substituted benzoates have been characterised in detail. The thorough understandings of catalytic mechanisms render a useful tool for rational design on biocatalysts of various *para*-substituted benzene derivatives. These cytochrome P450 enzymes, CYP199A4 and CYP199A2 identified from *Rhodopseudomonas palustris* strain HaA2 and strain CGA009 respectively, catalyse demethylation of methoxybenzoate. They have been investigated thoroughly for their ability to demethylate *para*-substituted benzoic acids (Bell, 2012a). These two demethylases show 86% sequence identity and similar substrate specificity (Bell et al., 2010). For CYP199A4, substrates with nitrogen and sulfur moieties at the *para* position were explored as well for the *N*-dealkylation and *S*-dealkylation potentials, and results suggested that sulfoxidation instead of *S*-dealkylation occurred, whereas *N*-dealkylation could be catalysed (Coleman, 2018). Crystal structures for both enzymes have been obtained with mechanisms involving substrate binding and catalytic reaction elucidated, offering solid bases for constructing a model system for structural study of P450 reactions.

On the other hand, more demethylases or microbes possessing demethylation capabilities have been identified, with some further characterised for the purpose of other applications. CYP236A2, a 6-*O*-methyl-D-galactose (G6Me)-demethylating P450 enzyme, identified in the marine bacterium *Zobellia galactanivorans*, has been studied in-depth for its catalytic mechanism, since dealkylation of carbohydrates is considered a difficult task due to the high energy barrier required for removal of methyl groups (Blanksby et al., 2003; Robb et al., 2018; Fig. 10a). Unlike other P450s which complete electron transfer by generic accessory proteins, this enzyme requires its cognate redox partner, a ferredoxin and a ferredoxin reductase. Enzymatic and kinetic analysis demonstrated that this enzyme is highly specialised for G6Me and the product couldn't be further oxidised, even when still located in the active centre (Reisky et al., 2018). A further P450 enzyme, CYP235A20 from *Formosa agariphila*, with the same catalytic ability as G6Me, has been studied in pairs with CYP236A2, and a redox system has been shown to be fully compatible between the two enzymes (Reisky et al., 2018). Phylogenetic analysis indicated that enzymes catalysing similar degradation pathways share highly conserved sequences among algal polysaccharide-degrading marine bacteria (Reisky et al., 2018).

Another demethylase, also belonging to the cytochrome P450 enzyme family, has been characterised in detail due to its versatile catalytic ability against different drug-related

substrates. CYP105D1, identified from *Streptomyces griseus* ATCC 13273, exhibited regioselective *O*-demethylation activity on tetrahydroprotoberberine (THPB)-related compounds, specifically, on the D-ring (Fig. 10b). Tetrahydropalmatine has been selected as the model substrate for demonstration of enantioselective demethylation demonstration, and results indicated that (*R*)-tetrahydropalmatine could be demethylated sequentially, whereas (*S*)-tetrahydropalmatine could only be demethylated at the C-10 position. However, a highly efficient whole-cell system for (*S*)-corydalmine production from (*S*)-tetrahydropalmatine, with pharmaceutical applications has been proposed. A homologous redox partner with Fdr1560/SoyB being the ferredoxin reductase/ferredoxin was identified as the electron transfer system for the whole-cell catalysis system, can be of practical significance (Shen et al., 2019a). Papaverine has also been elucidated to be regioselectively demethylated by this same enzyme (Shen et al., 2019b; Fig. 10c). A different electron transfer partner has been demonstrated comprising putidaredoxin/putidaredoxin reductase that aids electron transportation from NAD(P)H to the active centre. Similarly, a whole-cell bioconversion system has been developed for efficient production of 6-*O*-demethyl-papaverine, which is of pharmaceutical interest.

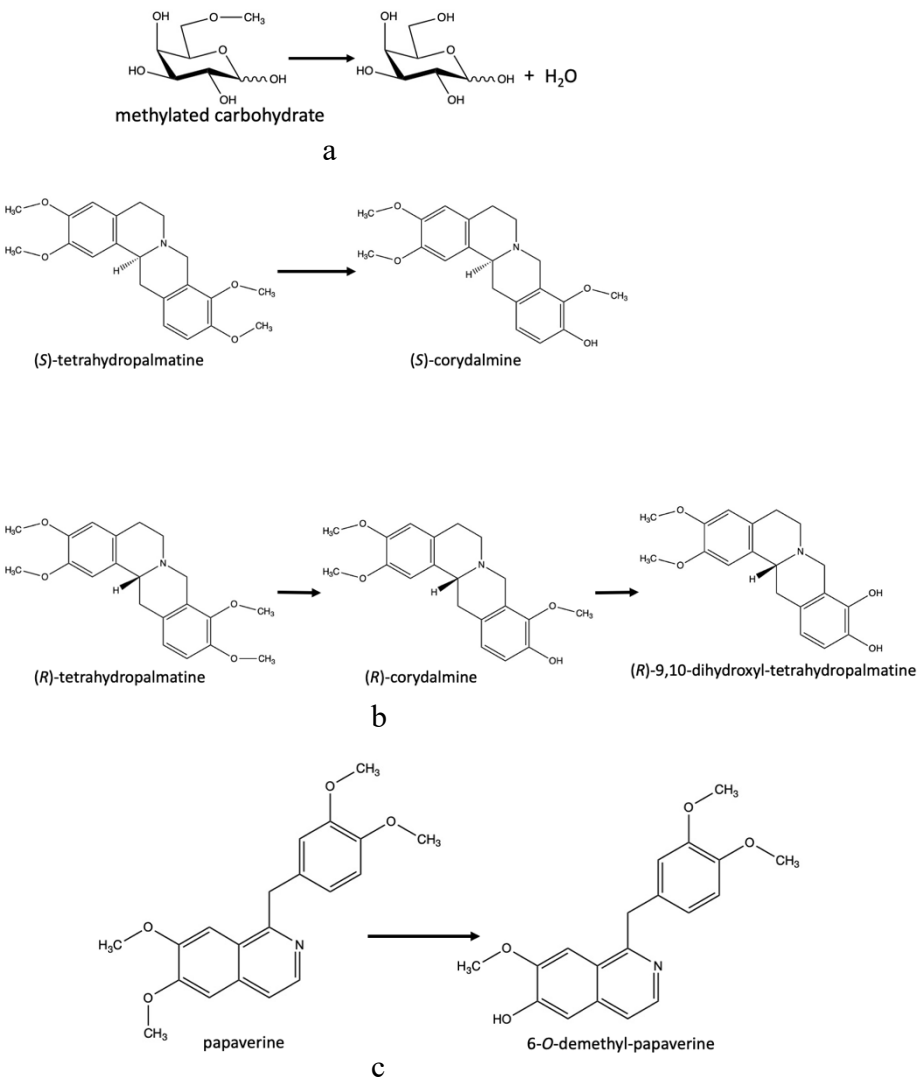

Figure 10 Demethylation reactions identified for 6-*O*-methyl-D-galactose (a), tetrahydropalmatine (b), and papaverine (c). (Robb et al., 2018; Shen et al., 2019ab)

Proline betaine, a compound similar to glycine betaine, has been found to be *N*-demethylated anaerobically by a three-component enzyme system identified from the human gut bacterium *Eubacterium limosum* ATCC 8486 (Picking et al., 2019; Fig. 11a). One component belongs to the MttB superfamily. Specifically, in this study, three proteins, MtpB (MttB family member, the proline betaine methyltransferase), MtqC (a corrinoid protein) and MtqA (a corrinoid-dependent tetrahydrofolate methyltransferase) were detected with greater abundance in cells cultured in proline betaine than lactate. A catalytic mechanism has been proposed, whereby MtpB initiated the methylation of H_4folate via MtqC and MtqA forming a multicomponent system which allowed the entry of a methyl moiety from proline betaine to

the acetogenic metabolism, producing *N*-methyl proline as the end product (Picking et al., 2019).

Biotransformation via demethylation of some herbicides has also been studied. For chloroacetanilide herbicides, a three-component RO system identified in *Sphingomonads* DC-6 and DC-2 with *N*-demethylation ability has been investigated (Chen et al., 2014). It consists of a homo-oligomer oxygenase CndA accommodating a Rieske [2Fe-2S] domain and a non-heme iron (II) domain, a [2Fe-2S] ferredoxin and a glutathione-reductase-type reductase (Chen et al., 2014). Interestingly, CndA, which is the oxygenase component, shares a low specificity for the electron transport system while accepting electrons only from NADH according to *in vitro* studies. Dicamba (2-methoxy-3,6-dichlorobenzoic acid), which is another herbicide, has also been tested in many bacterial strains for evidence of a demethylation reaction. *Pseudomonas maltophilia* strain DI-6 has been shown to be capable of *O*-demethylation, producing DCSA (3,6-dichlorosalicyclic acid) (Herman et al., 2005; Fig. 11b), with an enzyme system similar to that of chloroacetanilide demethylase mentioned above. However, a different enzyme system catalysing dicamba demethylation has been revealed in another bacterial strain, *Rhizorhabdus dicambivorans* Ndbn-20, with a hypothetical gene cluster elucidated (Yao et al., 2019). This cluster contains a dicamba demethylase gene, a 5,10-methylene-H_4folate reductase (*metF1*), a 5,10-methylene-H_4folate dehydrogenase-5,10-methylene-H_4folate cyclohydrolase (*folD1*) and a 10-formyl-H_4folate deformylase (*purU*). An *in vitro* biochemical assay revealed that *metF1* didn't exhibit the predicted activity, whereas 5-methyl-H_4folate dehydrogenase activity has been observed, suggesting that the activity of converting 5-methyl-H_4folate to 5,10-methylene-H_4folate was the physiological role of MetF1 in this strain (Yao et al., 2019). A gene disruption study indicated that *metF1* was crucial for dicamba demethylation, while *folD1* was dispensable for this demethylation system.

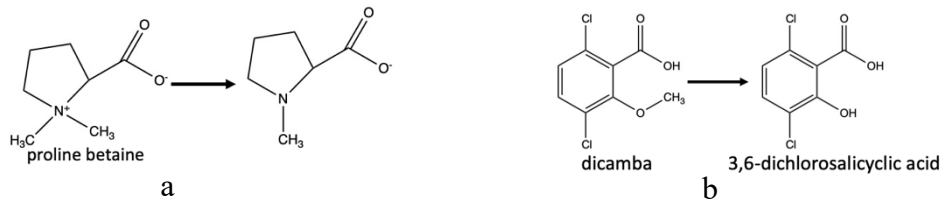

a b

Figure 11 Demethylation reactions identified for proline betaine (a) and dicamba (b). (Herman et al., 2005; Picking et al., 2019)

For many other xenobiotic biotransformation reactions, microbial P450s have been proposed to be involved. These reactions have been described in the above cytochrome P450 section and catalytic schemes are illustrated (Fig. 12). Further identification and characterisation of these enzymes are still needed for potential application. Additionally, several demethylation reactions have been observed in various microbes with the responsible enzymes yet to be determined. For example, demethylation of S-naproxen (Fig. 12), which will be discussed in the applications for pharmaceutics section.

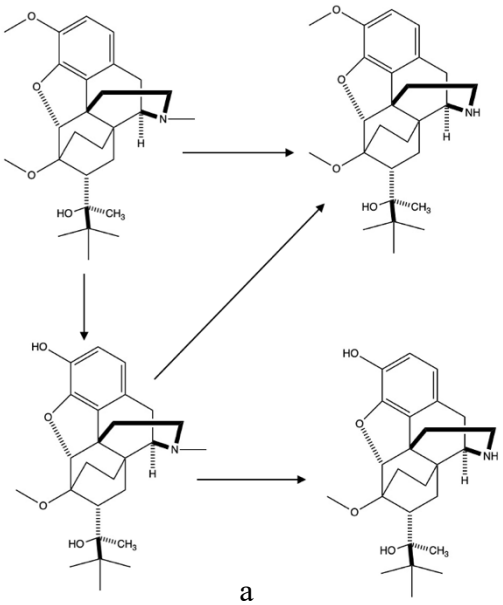

a

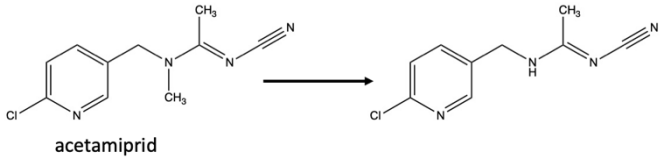

acetamiprid

b

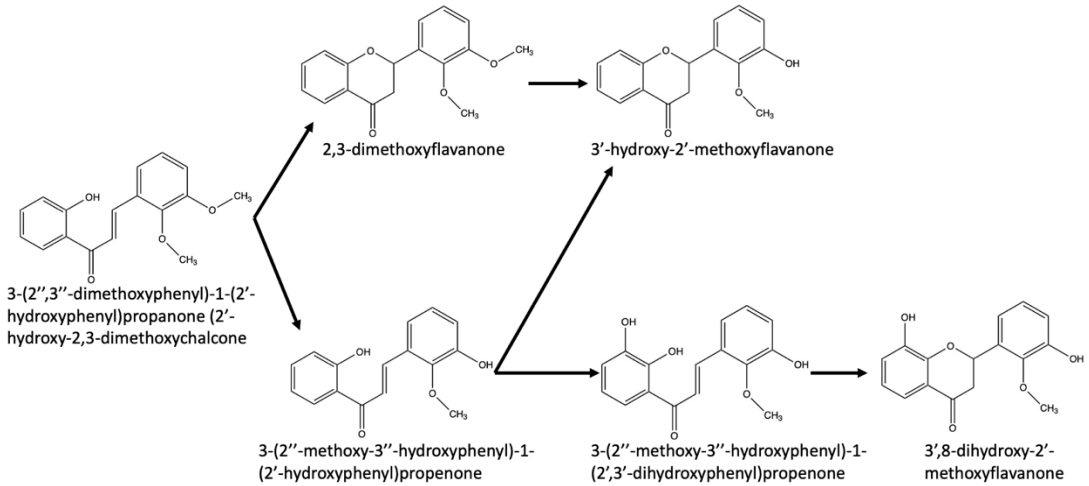

c

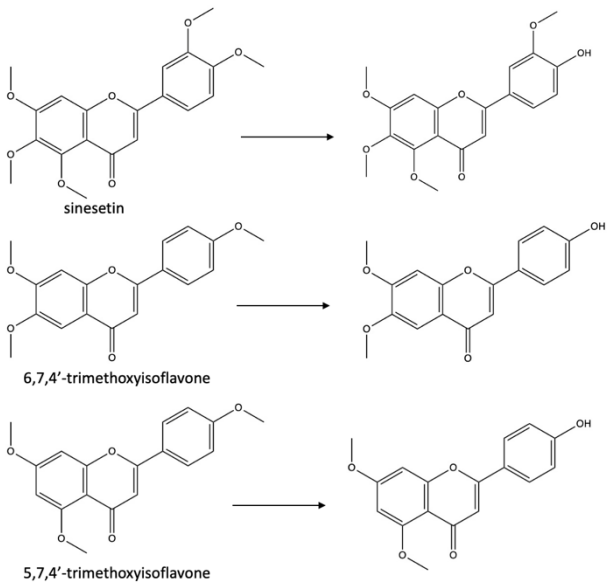

d

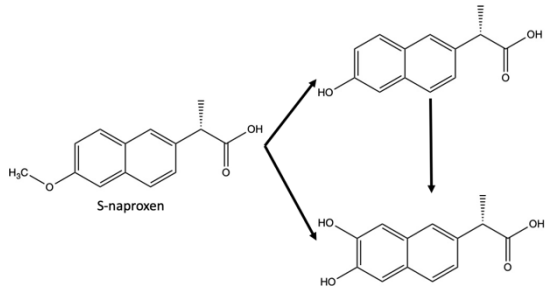

e

Figure 12 Demethylation reactions identified for thebaine derivative (a), acetamiprid (b), chalcone derivative (c), polymethoxyflavone (d), S-naproxen (e). (Abel et al., 2003; He and Rosazza, 2003; Miyazawa et al., 2006; Okuno and Miyazawa, 2006; Wang et al., 2012; Sanchez-Gonzalez and Rosazza, 2004)

3.3 Biosynthesis

Fewer reports of the involvement of demethylation reactions in biosynthesis exist. As has been discussed in the cytochrome P450 section, P450 demethylases have been widely discovered in fungal sterol synthesis, whereas only a few cases have been reported for bacteria. Fungal P450 enzymes are not self-sufficient, and NADPH-dependent cytochrome P450 reductases are required as electron transporters for P450 to receive two electrons to perform the catalytic activity (Lamb et al., 1999). An electron transfer system for CYP51 has been proposed in *Candida albicans* such that cytochrome b5/NADH cytochrome b5 reductase system can work efficiently and entirely as cytochrome P450 reductases to support the CYP51-mediated sterol 14α-demethylation catalysis, while for some other P450s, this system alone could only support reactions inefficiently (Lamb et al., 1999).

A bacterial CYP51 was characterised from *Rhodococcus triatomae* and was identified to share 25-68% amino acid sequence identity with other sterol 14α-demethylases. Study of the exogenous electron transfer system study indicated that *Acinetobacter* sp. OC4 ferredoxin and ferredoxin reductase (FdR-Fdx) system was the most efficient in supporting the catalysis of lanosterol demethylation by this enzyme *in vitro*, compared to two other systems which are *E. coli* flavodoxin and flavodoxin reductase, and *Nocardia farcinica* iron-sulfur containing NADPH-P450 reductase (Ke et al., 2017). A relatively high turnover number of 0.63 min $^{-1}$ (nmol lanosterol metabolised/ nmol P450/ min), the highest number ever reported being 0.72 min $^{-1}$ (Jackson et al., 2003), makes this enzyme a highly ranked bacterial CYP51 for catalytic activity against lanosterol. Nevertheless, a different demethylase system from

CYP51 responsible for bacterial sterol synthesis has been identified in the γ-roteobacterium *Methylococcus capsulatus* (Lee et al., 2018). The RO system consists of two components, an oxygenase (SdmA) and an NAD(P)H-dependent reductase (SdmB), and homologs of both genes have been identified in a wide range of bacteria, indicating that sterol C-4 demethylation may be widely distributed in the bacterial domain and different catalytic mechanisms compared with eukaryotes should therefore be present.

4 Biotechnological applications of microbial demethylases

Micro-organisms have long been considered as useful sources and tools for both biochemical and industrial applications due to their versatile metabolic abilities, as well as their potential as "cell factories" producing various enzymes. Microbial demethylases offer enzymatic functionality that can be of great use in many fields.

4.1 Pharmaceutics- drug design and development

CYP51, which represents the sterol 14α-demethylases responsible for eukaryotic sterol biosynthesis, has long been considered as a target for developing antifungal agents with high specificities. Recent decades have seen increasing emergence of invasive fungal infections (Bassetti et al., 2017) along with the occurrence of drug-resistant fungal strains (Zhang et al., 2017). It has been reported that the decrease in susceptibility as antifungal agents is related to the breakdown of CYP51-mediated resistance in many strains (Zhang et al., 2019). Further investigation of CYP51 is therefore needed to allow the rational design of durable and effective inhibitors. Moreover, fungal CYP51s could be helpful as models for the study of treatments for diseases by protozoan parasites, namely, Chagas disease, sleeping sickness and leishmaniasis, caused by the Trypanosomatidae family (Friggeri et al., 2018). Relevant exploration has focused on repurposing antifungal azoles as potential treatment agents, which have proven to be one of the most successful solutions (Urbina et al., 1996; 1998; Pinazo et al., 2010; Mondolfi et al., 2011; Leslie, 2011; Friggeri et al., 2018). The rationale behind this treatment was that azoles could inhibit CYP51 activity, hence sterol biosynthesis, and eventually fungal growth (Lepesheva and Waterman; 2007), and the resemblance of sterol synthesis mechanisms in both fungi and Trypanosomatidae further confirm the feasibility of trialling and improving azoles as a treatment strategy (Lepesheva and Waterman, 2011). Structure-directed modifications of the original inhibitor, catering for parasitic CYP51 binding sites were applied and potential structures were thereby selected for *in vivo* tests.

Utilising microbial demethylases directly for drug development has also been reported. CYP105D1, characterised from *Streptomyces griseus* ATCC 13273, has demonstrated regioselectivity for demethylation of both nonhydroxyl- and monohydroxyl-tetrahydroprotoberberines (THPB) on the D-ring (Shen et al., 2019a). The nonhydroxyl-THPB compound, (*S*)-tetrahydropalmatine, which has been used clinically as an analgesic in China, was used as a substrate for characterising CYP104D1. This enzyme exhibited different demethylation mechanisms towards (*S*)- and (*R*)-tetrahydropalmatine which are both nonhydroxyl-THPBs and the demethylation product of (*S*)-tetrahydropalmatine, (*S*)-corydalmine is of great pharmacological significance for the provision of pain relief in bone cancer (Shen et al., 2019a). Interestingly, this enzyme has also been found to be able to regioselectively demethylate papaverine, a promising anti-tumour agent, and the demethylation product, 6-*O*-demethyl-papaverine, has been reported to have less cytotoxicity than papaverine, rendering it a more promising drug candidate (Shen et al., 2019b). These demethylation reactions are highly regio- and enantioselective, and a CYP105D1-based whole-cell system has been demonstrated as an efficient production method for both compounds. This expands the enzymatic strategies available for selective demethylation as well as the potential applications for producing derivatives that may be useful in the pharmaceutical industry.

Apart from beneficial applications in drug development, microbial demethylases have also been involved in other studies. *Aspergillus niger* ATCC 9142 has been used as the model micro-organism to study the biotransformation of (*S*)-6-methoxy-α-methyl-2-naphthylacetic acid, a nonsteroidal anti-inflammatory drug, to facilitate the understanding of mammalian drug metabolism, and to enable large-scale production of drug metabolites for functional characterisation (He and Rosazza, 2003). Microorganisms have been proposed as models for studying mammalian drug metabolism due to their comprehensive metabolic systems (Smith and Rosazza, 1975). *O*-Desmethylnaproxen was identified as the major metabolite of (*S*)-6-methoxy-α-methyl-2-naphthylacetic acid, indicating that *O*-demethylation occurred as the main metabolic degradation, which resembles the metabolic transformation pathway in mammals (He and Rosazza, 2003).

4.2 Agriculture-related applications

Dicamba, a chlorinated herbicide, is used to control over 200 broadleaf weeds and is considered a suitable target herbicide for constructing genetically engineered herbicide-

resistant crops, due to its cost-effective character, easy-degradative ability and low mammalian toxicity (Stevens and Sumner, 1991; Behrens et al., 2007). It is therefore beneficial to investigate the genes involved in dicamba degradation or biotransformation as potential references for the construction of relevant GM (genetically modified) crops. Several microbial strains with the ability to degrade and utilise dicamba as their sole carbon and energy source have been identified, such as *Sphingomonas* sp. strain Ndbn-10, *Sphingomonas* sp. strain Ndbn-20, *Rhizorhabdus dicambivorans* Ndbn-20, and *Pseudomonas maltophilia* DI-6 (Herman et al., 2005; Yao et al., 2015; 2016; 2019). *O*-Demethylation has been observed in all of the strains mentioned above, catalysing different enzyme systems, rendering an array of potential applications.

4.3 Industrial productions

As a natural biopolymer and carbon reservoir, lignin offers considerable potential in applications such as biofuel production and epoxy resin production. Microbial demethylases play a crucial role in both activating lignin structures and facilitating transformation to the degradation product. The rigid and complex structure of lignin polymers are recalcitrant to many reactions, and various modification reactions have been trialled to improve activation (Laurichesse and Avérous, 2014). Among them, demethylation has shown great potential in converting methoxy moieties to hydroxyl groups, resulting in improved reactivity of lignin. The subsequent phenolic hydroxyls yielded are ideal substitutes for bisphenol A (BPA) to synthesise epoxy resin, since BPA has known toxicity and carcinogenic effects. Additionally, the aromatic ring adds to the overall stability, including thermal properties of the resultant resin (Asada et al., 2015). Therefore, the microbial demethylases identified in some bacteria and various fungi, such as brown-rot and white-rot fungi, have been shown to demethylate lignin yielding intermediates ready for biobased epoxy resin synthesis (Laurichesse and Avérous, 2014; Asada et al., 2015).

Flavonoids are a group of naturally occurring compounds that play various biochemical roles in plants, including supporting plant growth and development, and protecting against pests and microbes (Dixon and Steele, 1999). Dietary flavonoids also offer positive effects for human health, and biological and pharmaceutical benefits have gradually been revealed, such as antioxidant, antibacterial, antifungal, anti-diabetic, anti-inflammatory and anticancer activities (Escriche et al., 2014; Xi et al., 2014; Barreca et al., 2014; Liu et al., 2014; Xiao et al., 2015; Xiao and Högger, 2015; Li et al., 2014; Santos et al., 2013; Schnekenburger et al.,

2014). Apart from production by plants, there are many other strategies available for producing bioactive flavonoids, such as microbial biotransformation and enzyme engineering, in which microbial demethylases are involved (Xiao et al., 2014). Microorganisms have long been exploited for their abilities to biotransform chalcones to flavonoids to screen for potential candidates as bioactive flavonoid producers (Ibrahim et al., 2003; Sanchez-Gonzalez and Rosazza, 2004; Okuno and Miyazawa, 2004; 2006; Miyazawa et al., 2004; 2006; Buisson et al., 2007; Roh et al., 2009; Kostrzewa-Susłow et al., 2014). *Aspergillus alliaceus* UI315 has been selected for further study based on its ability to reproducibly transform chalcones to flavonoids in good yield (Sanchez-Gonzalez and Rosazza, 2004). Inhibition studies suggested that three cytochrome P450 monooxygenases may be involved in the biotransformation, with one of them being responsible for *O*-demethylation. Additionally, *Cunninghamella*, *Streptomyces*, and other *Aspergillus* strains have all been identified to be flavonoid producers with excellent yields (Ibrahim et al., 2003; Sanchez-Gonzalez and Rosazza, 2004; Okuno and Miyazawa, 2004; 2006; Miyazawa et al., 2004; 2006; Buisson et al., 2007; Roh et al., 2009; Kostrzewa-Susłow et al., 2014).

4.4 Environmental bioremediation

Human activity has produced many synthetic compounds and environmental pollutants that require removal and/or detoxification. Microbial remediation has long been considered a powerful tool for the treatment of environmental pollutants due to the versatile metabolic activities shown by microorganisms, as well as the feasibility for their large-scale cultivation (Bouwer, 1993). Among them, demethylases play a vital role in the removal of the methyl moiety from methylated substrates, which are usually stable, and demethylation facilitates reactivity, and thus further degradation or conversion.

Fuel, as one of the most commonly distributed synthetic organic mixtures, causes many environmental concerns, and various remediation solutions have been sought (Stupp, 2007). Methyl *tert*-butyl ether (MTBE), as one example, creates persistent and widespread contamination of aquifers around the world, and microbial degradation mechanisms by both aerobic and anaerobic bacteria has been studied extensively (Deeb et al., 2000; Stocking et al., 2000; Fayolle et al., 2001; Youngster et al., 2008). Demethylation occurred as the first step of degradation, rendering *tert*-butyl alcohol as the dominant detectable intermediate regardless of the completeness of the metabolism (Youngster et al., 2008). Another artificial chemical, *N*-methyl-pyrrolidone, is industrially produced as a solvent and widely used in

diverse industries including electronics, pharmaceuticals and agrochemicals (Solís-González et al., 2018). Though not posing a high risk to the environment due to its low acute toxicity, the biodegradation pattern of this compound has been studied and rapid biodegradation has been observed under aerobic condition (Solís-González et al., 2018). Several bacterial strains of *Acinetobacter*, *Cupriavidus*, *Pseudomonas* and *Paracoccus* are reported to degrade this compound at high levels (>99.5% disappearance), and two pathways have been identified, both of which involve *N*-demethylation (Lee et al., 2010).

Chemicals produced for agro-related purposes have resulted in various negative effects to the ecosystem. Isoproturon is one of the most widely used herbicides and is frequently detected in water ecosystems (Pérès et al., 1996); the negative impacts it brings to the environment have made it necessary to develop remediation solutions (Morvan et al., 2006; Mansour et al., 1999; Pérès et al., 1996). Bacteria with isoproturon-degrading ability have been identified and *N*-demethylation has been observed with 3-(4-isopropylphenyl)-1-methylurea as the preliminary metabolite detected; catechol was identified as a downstream intermediate, and is further oxidised to *cis*, *cis*-muconic acid (Sun et al., 2009). Acetamiprid (ACE), a systemic broad-spectrum insecticide applicable to both plants and animals for pest control, has received great research interest in biotransformation due to its potential toxicity to humans (Arther et al., 1997; Pramanik et al., 2006). Research has revealed that the lignin-degrading white-rot fungus, *Phanerochaete sordida* YK-624 was able to eliminate ACE (Wang et al., 2012). Specifically, the *N*-demethylation product (*E*)-N^1-[(6-chloro-3-pyridyl)-methyl]-N^2-cyano-acetamidine, with much lower toxicity than ACE was identified, and cytochrome P450 enzyme was proposed to be involved based on the inhibition tests.

Chlorinated organic compounds, both man-made and naturally occurring, make up a large proportion of pollutants. Crystal violet is widely used in human and veterinary medicine, and as a fabric dye, contributes to the pollution of aqueous ecosystems (Kingsland and Anderson, 1976; Michaels and Lewis, 1985; Bumpus and Brock, 1988). Several microbes have been identified as being capable of degradation or bioconversion, including white-rot fungus *Phanerochaete chrysosporium*, bacterial strains *Nocardia corallina* IAM 12121, and *Pseudomonas mendocina* MCM B-402 (Bumpus and Brock, 1988; Yatome et al., 1993; Sarnaik and Kanekar, 1999). A lignin-degrading system, namely, a lignin peroxidase has been identified in the fungal cultures and is proposed to be the responsible *N*-demethylase. Chloroanisoles, produced by *O*-methylation from the precursors, chlorophenolic pesticides,

are widely distributed in both terrestrial and aqueous environments (Barakat et al., 2002; Jiang et al., 2000; D'Angelo and Reddy, 2000). Though non-toxic, they have been shown to be transformed to toxic chlorophenols in mammals (Yuan et al., 1993). It has been reported that various microbes including bacteria and white-rot fungi exhibit degradative abilities on 2,4,6-trichloroanisole, a compound produced by filamentous fungi on cork seals, imparting negative effects to wine aroma profiles (Álvarez-Rodríguez et al., 2002; Campoy et al., 2009). Different levels of biodegradation rates have been reported, among which a *Phlebia radiata* strain, showed 94.5% TCA elimination during 10-day incubations with TCA spiked in the medium. *O*-Demethylation catalysed by a microsomal cytochrome P450 enzyme produced 2,4,6-trichlorophenol (2,4,6-TCP), and subsequent reactions proposed mineralisation of this substrate to release CO_2, H_2O and Cl^-. Methoxychlor, an organochlorine pesticide, is recognised as one of the most notorious environmental pollutants due to its recalcitrant properties and toxicological effects (Bulger et al., 1978; Cummings, 1997; Blizard et al., 2001). *O*-Demethylation of this compound by both eukaryotic and prokaryotic organisms has been reported (Castro and Yoshida, 1971; Fogel et al., 1982; Golovleva et al., 1984; Muir and Yarechewski, 1984; Keum et al., 2009; Masuda et al., 2012). *Cunninghamella elegans*, as a model organism involved in xenobiotic metabolism, has been tested for its ability to degrade this chemical (Keum et al., 2009). It was found that cytochrome P450-catalysed demethylation mediated the activation of reactions, and further hydroxylation, dechlorination and oxidation were involved transforming the substrates to sugar conjugates, therefore achieving detoxification.

Caffeine, as one of the plant-derived purine alkaloids, is of great commercial importance as it acts as an active psychostimulant (Smith, 2002; Lorist and Tops, 2003; Dash and Gummadi, 2006) and is distributed widely in human diets, as well as in pharmaceutical preparations (Ashihara and Crozier, 2001; Dash and Gummadi, 2006). However, caffeine-containing by-products generated from relevant factories make up a substantial proportion of agro-industrial waste. Specifically, the presence of caffeine in soil can negatively affect its fertility (Friedman and Waller, 1983) and chlorinated forms detected in aquifers can also impose adverse effects on local ecosystems (White and Rasmussen, 1998). Caffeine removal from by-products during industrial production is therefore needed and microbial remediation, as one of the most specific and efficient solutions has been studied extensively. Of these solutions, demethylation is a critical reaction to remove methyl groups, thereby activating nitrogen atoms for further degradation, and has been observed by various microbes. The

ability to degrade caffeine via different mechanisms has been reported by both fungi and bacteria (Woolfolk, 1975; Mazzafera, 2002; 2004; Gokulakrishnan et al., 2005; Dash and Gummadi, 2010). Specifically, a degradation pathway in filamentous fungi has been detected and the caffeine-theophylline-3-methylxanthine route was believed to be involved. Bacterial degradation has been studied and characterised in greater detail. Several mechanisms have been elucidated among different species, most of which undergo demethylation as the primary step, whereas in some species such as *Rhodococcus* and *Klebsiella*, oxidation of caffeine occurs directly, yielding methyluric acid (Dash and Gummadi, 2006; Retnadhas and Gummadi, 2018).

5 Conclusions

Current research emphasis is mainly focused on the exploration and investigation of the scope and capability of microbial demethylases, with some structure-function relationships elucidated that are potentially useful in future applications. Such work can be advocated, since the existence of versatile microbes and demethylases has been revealed. An example is the CYP105D1 identified from *Streptomyces griseus* ATCC 13273 which is capable of regio- and enantioselectively demethylating two drug-related compounds, producing metabolites of significant pharmaceutical potential (Shen et al., 2019a; 2019b). Demethylases with promiscuous substrate specificity are widely distributed, thereby attracting research interest. It is exciting that the microbial demethylases currently available proved an enormous resource pool for both biosynthesis and biodegradation functions, which could be of direct industrial use via either whole cell systems or enzyme preparations through large-scale production. It should be noted that, apart from direct industrialisation, some microbial demethylases with broad substrate ranges could offer models for enzyme engineering to investigate the mechanisms and structures more in-depth. Such knowledge could be applied for modifying homologous enzymes with desirable catalytic characteristics to aid enzyme engineering techniques.

Future directions on biological remediations of IBMP are proposed based on this review, since IBMP demethylation is one of the putative degradation pathways. Some microbes and their respective enzyme systems can be selected as the target sources for potential IBMP-degrading ability. Specifically, demethylases such as the extensively studied CYP199A4 can be trialled and used as a target for further enzyme modifications based on the illustrated

protein structure to ideally catalyse IBMP demethylation. Demethylases with crystal structures elucidated (Table 2) can be included in the candidate pool for catalytic ability screen and potential enzyme modifications. On the other hand, metabolically versatile microbes covered in this review can also be included for IBMP-degrading ability tests, such as *Sphingomonas*, *Sphingobium*, *Streptomyces* and *Pseudomonas* genera. Nevertheless, nutritional requirements and optimal growing conditions need to be explored given the potentially different roles IBMP plays in microbial metabolisms.

Chapter 6 Conclusions

IBMP, which is a naturally occurring aroma compound identified in many wine grape varieties such as Cabernet Sauvignon, Merlot and Sauvignon Blanc (Allen and Lacey, 1998), which imparts green capsicum-like character to wine and contributes to aroma and flavour complexity. However, elevated concentrations in grapes due to a cool growing season or early harvest for alcohol management can lead to wines with overly green characters and thus inferior perceived quality. After the relationship between IBMP and green characters in wine was discovered (Allen et al., 1991), strategies for IBMP remediation have been of great research interest, many of which focus on vineyard practices such as canopy management (Sala et al., 2002) aimed at minimising the levels of IBMP and associated compounds in harvested grapes. Nonetheless, residual IBMP levels in grapes at harvest can be high and practices that reduce these during winemaking are limited and mainly involve non-selective strategies such as adsorption or heat pre-treatment, which can negatively impact wine quality. Liang et al. (2018) reported the development of molecularly imprinted polymers (MIP) to remove excessive IBMP with high specificity and evaluated this in a small-scale fermentation trial. As one of the most promising postharvest remediation methods currently available, evaluation results based on GC-MS analysis unfortunately demonstrated the significant adsorption of other volatile compounds during MIP treatment, but with no effect on other aroma properties was observed by sensory analysis. Accordingly, demand for an effect and specific postharvest IBMP treatment remains.

The research undertaken in this project explored the possibility of remediating IBMP using biological methods, specifically by investigating a range of microbial options for the breakdown of IBMP into non-sensorially significant products. The outcomes of these strategies, though not completely positive, were nevertheless promising and could be used to either deliver proof-of-concept support for further research or provide the industry with practical advice.

The investigation started with an evaluation of how yeasts can influence IBMP levels in wine during fermentation. Earlier work to study the effects of several commercial *Saccharomyces cerevisiae* strains in IBMP concentration adjustment (Treloar and Howell, 2006), was unable to show any effect on this compound following yeast growth. As an alternate approach the

present study sought to take advantage of the wide ranges of enzymatic activities identified among various non-*Saccharomyces* yeasts (Chapter 2). These yeasts were assessed for their abilities to remediate excessive IBMP deliberately spiked into grape must during fermentation. From the standpoint of industry application, both sequential inoculation and static incubation were employed to resemble common winemaking techniques. No significant decrease in IBMP was observed among any of the yeast strains tested according to GC-MS analysis, indicating that IBMP was not markedly degraded by these microbes under conditions representative of most commercial winemaking.

Wine is a complex solution comprising an array of flavour compounds. The perception of green character is not solely dependent on IBMP, but is influenced by the presence of, and interactions with, other odorants. A sensory analysis of wines produced in this study with non-*Saccharomyces* yeasts validated the masking interaction between vegetal and fruity characters. Specifically, diverse levels of greenness were reported for differently treated wines even though comparable concentrations of IBMP were observed. Such dissimilar aroma profiles between wine were most evident through the use of different yeasts for the primary fermentation, such as *Metschnikowia pulcherrima*, *Kazachstania servazzii* and *Kazachstania aerobia*. Increased concentrations of volatiles with fruity characters were identified in these wines, which were beneficial to masking green characters. Given the readiness with which the industry uses non-*Saccharomyces* yeasts, primarily in sequential or co-inoculation with *Saccharomyces cerevisiae*, makes this approach very attractive for adoption in winery practices.

This study was the first of its kind to investigate the effects of a broader range of wine yeasts on IBMP levels and the resultant green characters in wine during alcoholic fermentation. But despite its promise, the fermentation trial was conducted on a scale (0.5 L) much smaller than conventional industry practices. As such, difference in fermentation volumes may influence final wine outcome and scale-up experiments are therefore required to confirm if results with similar trends are obtained at commercial scales. Additionally, only one grape variety (Sauvignon Blanc) was evaluated in this trial, so results might be variety-dependent, in that yeasts might bring out more diverse sensory properties in varieties that contain distinctive aroma precursors. Consequently, altered aroma profiles may interact dissimilarly with green characters leading to a different outcome. Hence, it is vital to investigate different varieties so

as to optimise the yeast strain(s) that best achieves reduced levels of green characters for each variety.

As described in Chapter 3, further work aimed at trying to identify microbes able to degrade IBMP was carried out. Almost 100 microbial strains including environmental isolates were tested for IBMP degradative activity. Strains were tested following growth in both rich and minimal media supplemented with IBMP. Due to difficulties with the rapid analysis of IBMP, alternative compounds with similar chemical features, specifically, methyl moiety(s), were used as substrates to enable screening with high efficiency by monitoring microbial growth or colour changes.

Unfortunately, under the screening conditions employed, no microbes were found to be capable of consuming IBMP. However, amongst all the screening substrates, two yeast strains, *Rhodotorula mucilaginosa* and *Rhodotorula glutinis*, were identified with the ability to decolourise, and therefore, to potentially degrade methyl violet in YEPD medium via an *N*-demethylation process proposed previously. Downstream metabolites are yet to be identified by HPLC-MS, whereas preliminary spectrophotometry analysis was performed and yielded wavelength shifts compared with the uninoculated control group, which further suggested the presence of degradation metabolites. Nevertheless, these two strains failed to show any ability to reduce IBMP concentrations in the same nutrient conditions used for the methyl violet screening.

Additional work is needed to characterise the two methyl violet degrading strains in order to characterise their demethylation system(s). These system(s) might be further characterised and tested with other similar-structured wine-related compounds including IBMP, under optimal catalytic conditions. Microbial screening could also be scaled up to include more microbial candidates, as well as alternative substrates with related chemical structures. Analogues such as methyl violet that show colour changes as an indicator of compositional changes are ideal for such high-throughput screening, since IBMP is difficult to quantify with precision when dealing with ng/L concentrations, as relevant to winemaking. However, IBMP reactions involving colour changes or chromogenic IBMP substrates are yet to be discovered.

Enzymatic remediation, as a straightforward strategy to remove IBMP from juice, must or wine was also investigated. Among the demethylases previously identified, none are closely related to methoxypyrazine in terms of substrate structure. The experiments described in Chapter 4 aimed to modify relevant enzymes known to be involved in IBMP metabolism and screen these for the desired catalytic activity, namely the demethylation of IBMP. VvOMT3, which is an *O*-methyltransferase responsible for synthesising IBMP from its precursor IBHP, has been identified and characterised in some wine grape cultivars such as Cabernet Sauvignon (Dunlevy et al., 2013). It was therefore chosen as the target enzyme to work with due to the close correlation of its catalytic structure with relevant substrates. The rationale was to modify this enzyme to favour the reverse catalytic reaction, using a protein engineering approach.

Based on the limited information available on the structure-function relationship of this enzyme, random mutagenesis was chosen as the modification method for achieving vast changes in the final structure. Enzymatic assays for IBMP degradation in crude extracts of heterologously expressed mutated genes revealed no positive mutants among the 95 candidates selected. IBMP biosynthesis tests were also conducted with crude extracts to explore the potential mutation effects in each candidate. Where protein truncation at the N-terminal was apparent, no synthesising abilities were observed, while in other, full-length mutants with no significant differences in the levels of IBMP produced were observed, suggesting no effects from these mutations. However, it has to be acknowledged that crude extracts were used for enzymatic assays with no specific kinetics studies performed, and this may have influenced the findings of the biosynthesis tests. Therefore, these results are somewhat preliminary and more detailed investigation, particularly with a greater number of the non-truncated mutants, is needed to determine if in fact catalytic activity is reversed.

This rather preliminary chapter on an exploration of potential enzymatic remediation methods leaves scope for more work to be done. As potential follow-up work, more detailed knowledge on VvOMT3, especially regarding the structure-function relationship, would be of great help in guiding further modifications. For the best results, protein crystallisation incorporated with key residue identifications are required, thereby providing in-depth references to modification of protein structures. On the other hand, one of the major bottlenecks of this experiment was the screening method used for both IBMP degradation and biosynthesis, i.e. quantitative GC-MS analysis, which tends to be laborious and time-

consuming. A rapid screening method is a high priority to enhance screening efficiency. As discussed in Chapter 4, it may be feasible to monitor compositional changes in the reaction mixture via a simple analysis such as spectrophotometry. A pilot study would be needed to identify the concentration correlation between the target compound and IBMP. However, such a method may only be restricted to this specific reaction, and therefore other broader approaches are still needed. Lastly, a broader scope of enzymes besides VvOMT3 could be included in the screening, for example aromatic compound demethylases. Specifically, those for which structural information exists would be preferable candidates for any structure-based modification for substrate binding. Moreover, incorporation of knowledge obtained for IBMP-binding enzymes may potentially shed light on enzyme engineering of existing demethylases.

As a commencement of a more targeted approach to the identification of a demethylase that either may degrade IBMP as is or may be a candidate for modification to enhance degradation, a literature review on the subject of demethylases was conducted. This detailed investigation (Chapter 5) highlights several potential candidates that could be pursued in further work. These include *O*-demethylases with crystal structures illustrated such as CYP199A2 for potential modification, and metabolically versatile microbes such as *Sphingomonas*.

There is currently no biological method available for postharvest remediation of IBMP. This work explored several possible approaches, contributing preliminary and/or promising results. Specifically, for overly green Sauvignon Blanc grapes, non-*Saccharomyces* strains including *Kazachstania servazzii*, *Hanseniaspora uvarum*, *Kazachstania aerobia*, *Candida krusei*, *Meyerozyma guillermondii*, and *Metschnikowia pulcherrima*, could be used in sequential inoculation with *Saccharomyces cerevisiae* EC1118 to produce wines with enhanced varietal fruit aromas that better mask undesirable green characters. Impacts for other batches of Sauvignon Blanc as well as other varieties are yet to be explored. No positive results for direct IBMP degradation were obtained through two other approaches used here (i.e., microbial screening and VvOMT3 modification), nevertheless findings that could potentially be useful in future research were obtained. As such this thesis describes endeavours towards the biological degradation of IBMP, and lays the foundation for future research.

Appendix

Table 1 Primers used for EP-PCR and sequencing

EP-PCR-BamHI	GCGGATCCATGGAGAAAGTGGTA
EP-PCR-XhoI	GCTCGAGCTAAGGATAAGCTTCG
T7 promoter	TAATACGACTCACTATAGG
T7 terminator	GCTAGTTATTGCTCAGCGG

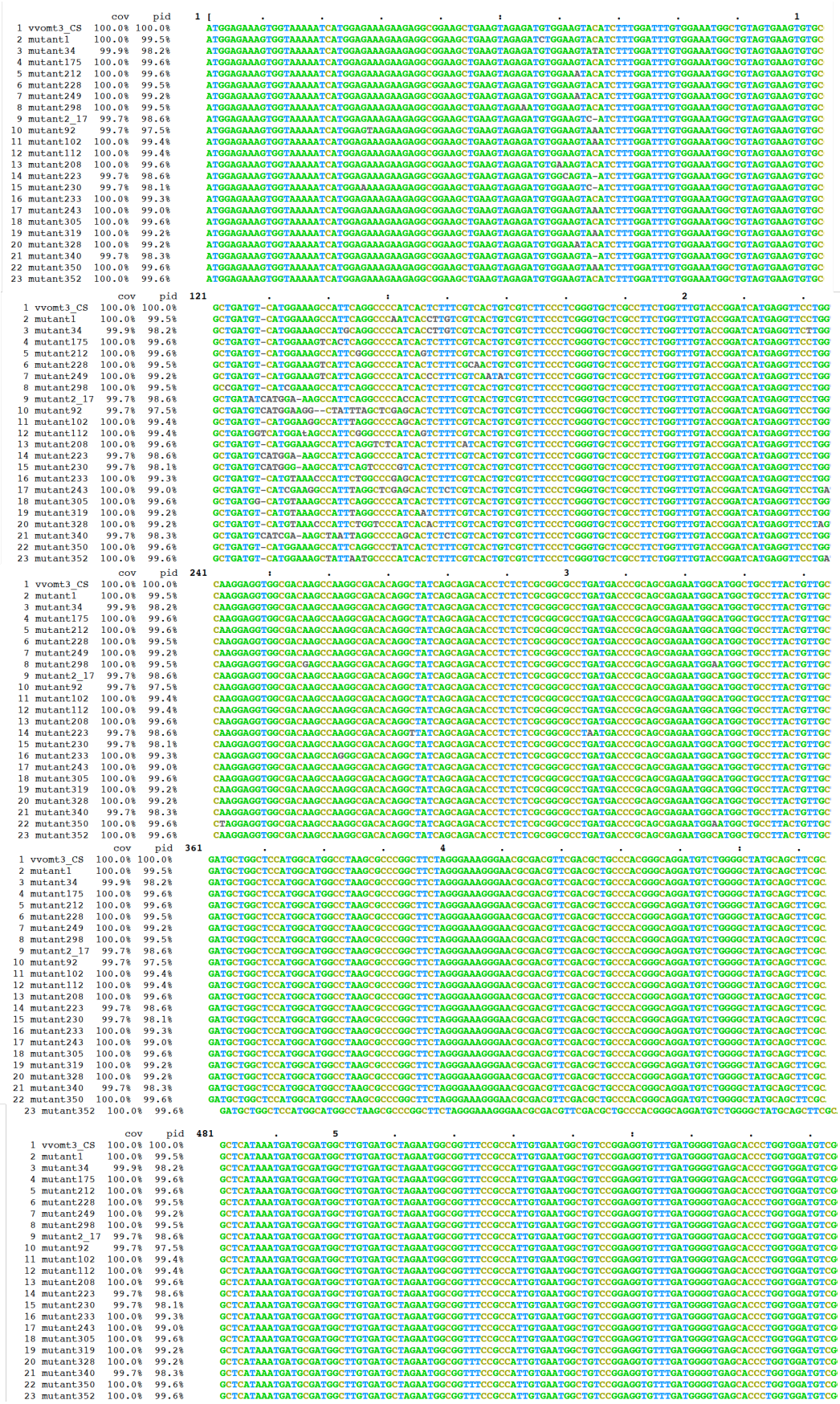

a

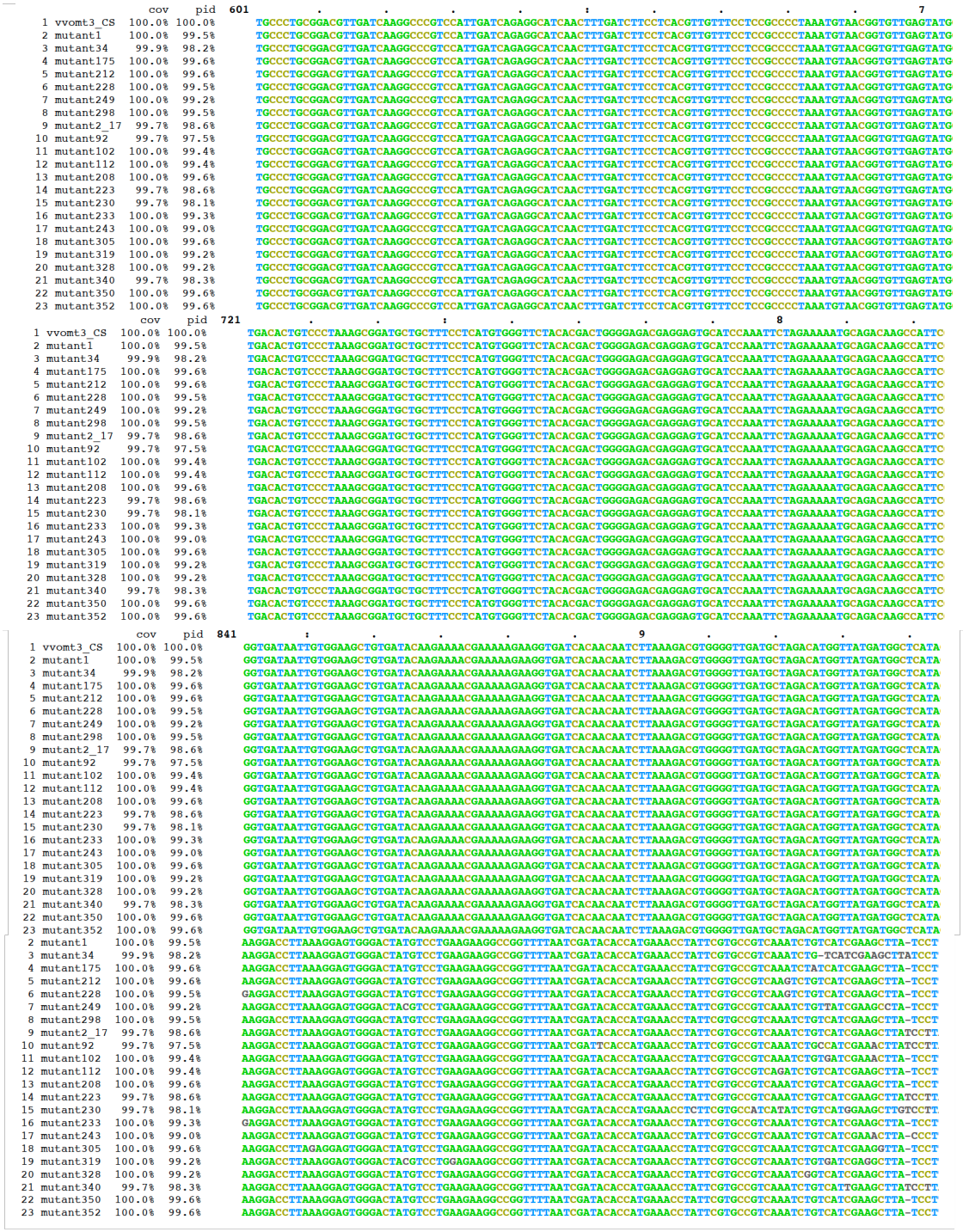

b

Figure 1 Multiple alignment of 22 mutant nucleotide sequences with *VvOMT3*. a, multiple alignment of No. 1-600 nucleotides; b, multiple alignment of No. 601- 1056 nucleotides.

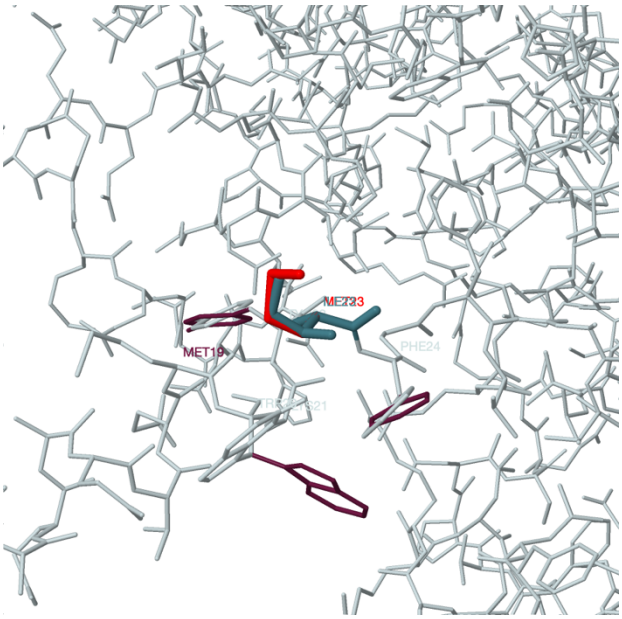

a. combined structure within 5Å of residue 23I pre- and post-mutation, residue in dark green/red indicates the original/mutated residue Ile23/Met23, neighbouring (within 5Å residues) sites in light grey/dark red indicate the original/mutated neighbouring residues

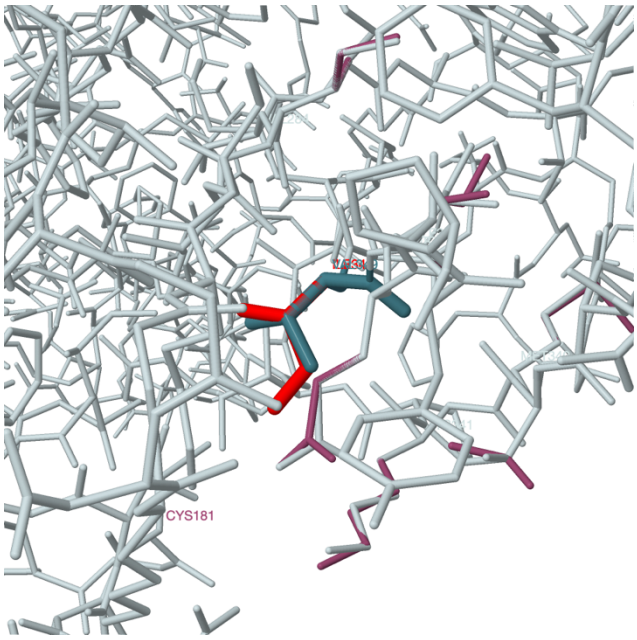

b. combined structure within 5Å of residue 349I pre- and post-mutation, residue in dark green/red indicates the original/mutated residue Ile349/Val349, neighbouring (within 5Å residues) sites in light grey/dark red indicate the original/mutated neighbouring residues

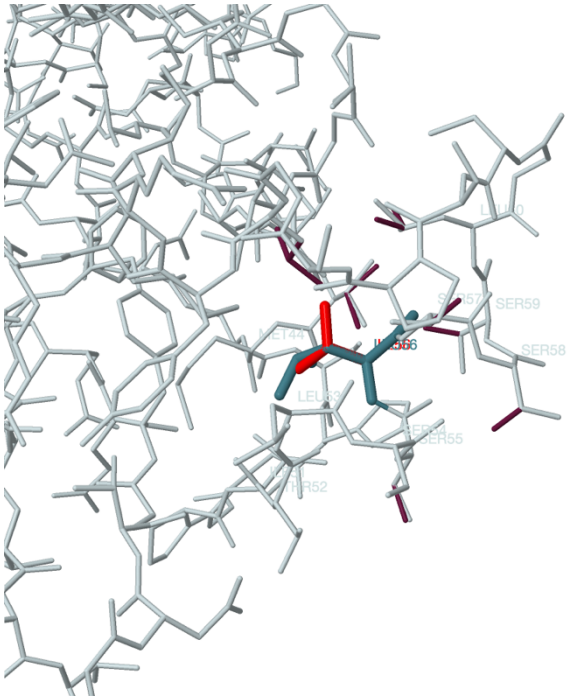

c. combined structure within 5Å of residue 56L pre- and post-mutation, residue in dark green/red indicates the original/mutated residue Leu56/Ile56, neighbouring (within 5Å residues) sites in light grey/dark red indicate the original/mutated neighbouring residues

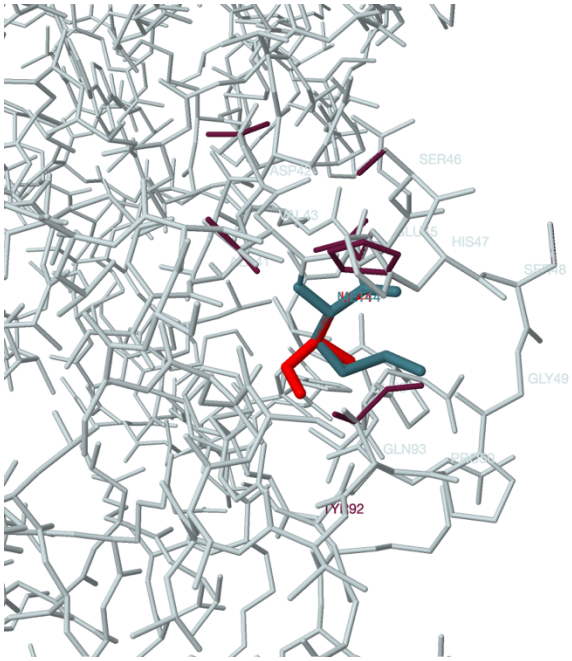

d. combined structure within 5Å of residue 44M pre- and post-mutation, residue in dark green/red indicates the original/mutated residue Met44/Ile44, neighbouring (within 5Å residues) sites in light grey/dark red indicate the original/mutated neighbouring residues

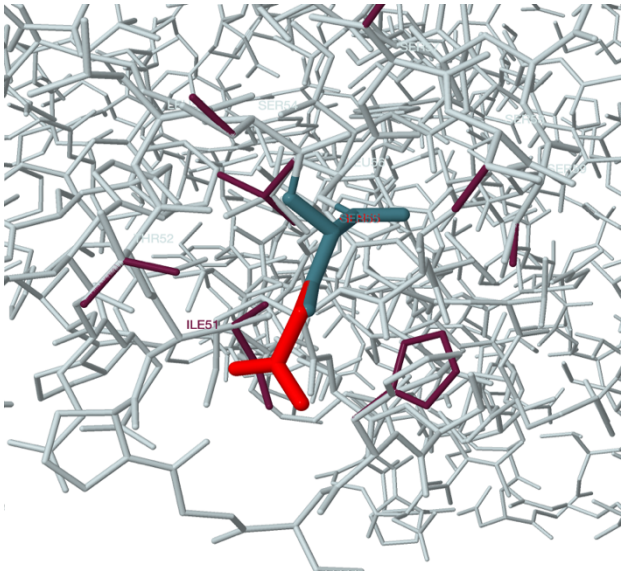

e. combined structure within 5Å of residue 55S pre- and post-mutation, residue in dark green/red indicates the original/mutated residue Ser55/Gln55, neighbouring (within 5Å residues) sites in light grey/dark red indicate the original/mutated neighbouring residues

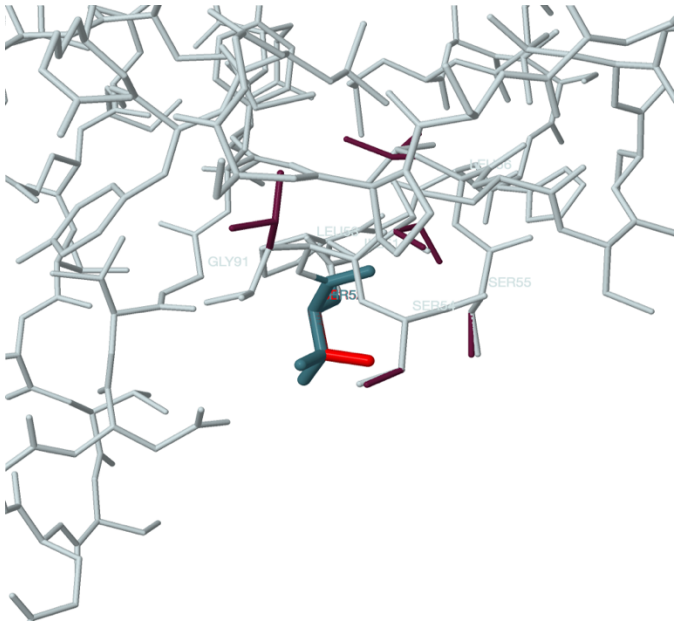

f. combined structure within 5Å of residue 52T pre- and post-mutation, residue in dark green/red indicates the original/mutated residue Thr52/Ser52, neighbouring (within 5Å residues) sites in light grey/dark red indicate the original/mutated neighbouring residues

Figure 2 Structural modelling on mutational changes

References

Abdelaziz, O. Y., Brink, D. P., Prothmann, J., Ravi, K., Sun, M., Garcia-Hidalgo, J., Sandahl, M., Hulteberg, C. P., Turner, C., Lidén, G., Gorwa-Grauslund, M. F. (2016). Biological valorization of low molecular weight lignin. *Biotechnology Advances*, *34*(8), 1318-1346.

Abe, T., Masai, E., Miyauchi, K., Katayama, Y., & Fukuda, M. (2005). A tetrahydrofolate-dependent *O*-demethylase, LigM, is crucial for catabolism of vanillate and syringate in *Sphingomonas paucimobilis* SYK-6. *Journal of Bacteriology*, *187*(6), 2030-2037.

Abel, A. M., Carnell, A. J., Davis, J. A., & Paylor, M. (2003). The synthesis of buprenorphine intermediates by regioselective microbial *N*-and *O*-demethylation reactions using *Cunninghamella echinulata* NRRL 1384. *Enzyme and Microbial Technology*, *33*(5), 743-748.

Adams, T. B., Doull, J., Feron, V. J., Goodman, J. I., Marnett, L. J., Munro, I. C., Newberne, P. M., Portoghese, P. S., Smith, R. L.,Waddell, W J., & Wagner, B. M. (2002). The FEMA GRAS assessment of pyrazine derivatives used as flavor ingredients. *Food and Chemical Toxicology*, *40*(4), 429-451.

Agar-bacteriological grade. Amyl media product brochure. https://amylmedia.com.au/orders/agar-agar-bacteriological-grade/

Ahmad, M., Taylor, C. R., Pink, D., Burton, K., Eastwood, D., Bending, G. D., & Bugg, T. D. (2010). Development of novel assays for lignin degradation: comparative analysis of bacterial and fungal lignin degraders. *Molecular Biosystems*, *6*(5), 815-821.

Akashi, T., Sawada, Y., Shimada, N., Sakurai, N., Aoki, T., & Ayabe, S. I. (2003). cDNA cloning and biochemical characterization of *S*-adenosyl-L-methionine: 2, 7, 4′-trihydroxyisoflavanone 4′-*O*-methyltransferase, a critical enzyme of the legume isoflavonoid phytoalexin pathway. *Plant and Cell Physiology*, *44*(2), 103-112.

Alcazar-Fuoli, L., Mellado, E., Garcia-Effron, G., Lopez, J. F., Grimalt, J. O., Cuenca-Estrella, J. M., & Rodriguez-Tudela, J. L. (2008). Ergosterol biosynthesis pathway in *Aspergillus fumigatus*. *Steroids*, *73*(3), 339-347.

Alimardani-Theuil, P., Gainvors-Claisse, A., & Duchiron, F. (2011). Yeasts: an attractive source of pectinases—from gene expression to potential applications: a review. *Process Biochemistry*, *46*(8), 1525-1537.

Allen, M. S., & Lacey, M. J. (1998). Methoxypyrazines of grapes and wines. In *Chemistry of Wine Flavor* (pp. 31-38). ACS publications, Washington, DC.

Allen, M. S., Lacey, M. J., Harris, R. L., & Brown, W. V. (1991). Contribution of methoxypyrazines to Sauvignon Blanc wine aroma. *American Journal of Enology and Viticulture*, *42*(2), 109-112.

Allen, M. S., & Lacey, M. J. (1993). Methoxypyrazine grape flavour: influence of climate, cultivar and viticulture. *Wein-Wissenschaft*, *48*(3-6), 211-213.

Allen, M. S., Lacey, M. J., & Boyd, S. (1994). Determination of methoxypyrazines in red wines by stable isotope dilution gas chromatography-mass spectrometry. *Journal of Agricultural and Food Chemistry*, *42*(8), 1734-1738.

Altschul, S. F., Madden, T. L., Schäffer, A. A., Zhang, J., Zhang, Z., Miller, W., & Lipman, D. J. (1997). Gapped BLAST and PSI-BLAST: a new generation of protein database search programs. *Nucleic Acids Research*, *25*(17), 3389-3402.

Álvarez-Rodríguez, M. L., López-Ocana, L., López-Coronado, J. M., Rodríguez, E., Martínez, M. J., Larriba, G., & Coque, J. J. R. (2002). Cork taint of wines: role of the filamentous fungi isolated from cork in the formation of 2, 4, 6-trichloroanisole by *O*-methylation of 2, 4, 6-trichlorophenol. *Applied and Environmental Microbiology*, *68*(12), 5860-5869.

Anderson, D. M. W., & Duncan, J. L. (1960). Applications of infrared spectroscopy—II: observations on some aspects of the Zeisel alkoxyl determination. *Talanta*, *7*(1-2), 70-79.

Andorrà, I., Berradre, M., Rozès, N., Mas, A., Guillamón, J. M., & Esteve-Zarzoso, B. (2010). Effect of pure and mixed cultures of the main wine yeast species on grape must fermentations. *European Food Research and Technology*, *231*(2), 215-224.

Andrykovitch, G., & Marx, I. (1988). Isolation of a new polysaccharide-digesting bacterium from a salt marsh. *Applied and Environmental Microbiology*, *54*(4), 1061-1062.

Aoyama, Y., Yoshida, Y., & Sato, R. (1984). Yeast cytochrome P-450 catalyzing lanosterol 14 alpha-demethylation. II. lanosterol metabolism by purified P-450 (14) DM and by intact microsomes. *Journal of Biological Chemistry*, *259*(3), 1661-1666.

Aoyama, Y., Horiuchi, T., Gotoh, O., Noshiro, M., & Yoshida, Y. (1998). CYP51-like gene of *Mycobacterium tuberculosis* actually encodes a P450 similar to eukaryotic CYP51. *The Journal of Biochemistry*, *124*(4), 694-696.

Ares, G., Bruzzone, F., Vidal, L., Cadena, R. S., Giménez, A., Pineau, B., Hunter, D. C., Paisley, A. G., Jaeger, S. R. (2014). Evaluation of a rating-based variant of check-all-that-apply questions: Rate-all-that-apply (RATA). *Food Quality and Preference*, *36*, 87-95.

Arther, R. G., Cunningham, J., Dorn, H., Everett, R., Herr, L. G., & Hopkins, T. (1997). Efficacy of imidacloprid for removal and control of fleas (*Ctenocephalides felis*) on dogs. *American Journal of Veterinary Research*, *58*(8), 848-850.

Asada, C., Basnet, S., Otsuka, M., Sasaki, C., & Nakamura, Y. (2015). Epoxy resin synthesis using low molecular weight lignin separated from various lignocellulosic materials. *International Journal of Biological Macromolecules*, *74*, 413-419.

Ashihara, H., & Crozier, A. (2001). Caffeine: a well known but little mentioned compound in plant science. *Trends in Plant Science*, *6*(9), 407-413.

Augustyn, O. P. H., & Rapp, A. (1982). Aroma components of *Vitis vinifera* L. *cv*. Chenin Blanc grapes and their changes during maturation. *South African Journal of Enology and Viticulture*, *3*(2), 47-51.

Augustyn, O. P. H., Rapp, A., & Van Wyk, C. J. (1982). Some volatile aroma components of *Vitis vinifera* L. *cv*. Sauvignon Blanc. *South African Journal of Enology and Viticulture*, *3*(53-60), 1-12.

Axcell, B. C., & Geary, P. J. (1975). Purification and some properties of a soluble benzene-oxidizing system from a strain of *Pseudomonas*. *Biochemical Journal*, *146*(1), 173-183.

Azzolini, M., Fedrizzi, B., Tosi, E., Finato, F., Vagnoli, P., Scrinzi, C., & Zapparoli, G. (2012). Effects of *Torulaspora delbrueckii* and *Saccharomyces cerevisiae* mixed cultures on fermentation and aroma of Amarone wine. *European Food Research and Technology*, *235*(2), 303-313.

Barakat, A. O., Kim, M., Qian, Y., & Wade, T. L. (2002). Organochlorine pesticides and PCB residues in sediments of Alexandria Harbour, Egypt. *Marine Pollution Bulletin*, *44*(12), 1426-1434.

Barbe, V., Vallenet, D., Fonknechten, N., Kreimeyer, A., Oztas, S., Labarre, L., Cruveiller, S., Robert, C., Duprat, S., Wincker, P., Ornston, L. N., Weissenbach, J., Marlière, P.,

Cohen, G., Médigue, C. (2004). Unique features revealed by the genome sequence of *Acinetobacter* sp. ADP1, a versatile and naturally transformation competent bacterium. *Nucleic Acids Research*, *32*(19), 5766-5779.

Barreca, D., Bellocco, E., Laganà, G., Ginestra, G., & Bisignano, C. (2014). Biochemical and antimicrobial activity of phloretin and its glycosilated derivatives present in apple and kumquat. *Food Chemistry*, *160*, 292-297.

Barry, S. M., & Challis, G. L. (2013). Mechanism and catalytic diversity of Rieske non-heme iron-dependent oxygenases. *ACS Catalysis*, *3*(10), 2362-2370.

Bassetti, M., Garnacho-Montero, J., Calandra, T., Kullberg, B., Dimopoulos, G., Azoulay, E., ... & Sanguinetti, M. (2017). Intensive care medicine research agenda on invasive fungal infection in critically ill patients. *Intensive Care Medicine*, *43*(9), 1225-1238.

Battilana, J., Dunlevy, J. D., & Boss, P. K. (2017). Histone modifications at the grapevine VvOMT3 locus, which encodes an enzyme responsible for methoxypyrazine production in the berry. *Functional Plant Biology*, *44*(7), 655-664.

Baumes, R. (2009). Wine aroma precursors. In *Wine chemistry and biochemistry* (pp. 251-274). Springer, New York, NY.

Beedham, C., (1988). Molybdenum Hydroxlyases. In *Metabolism of xenobiotics* (pp. 51-58). Taylor & Francis, London.

Behrens, M. R., Mutlu, N., Chakraborty, S., Dumitru, R., Jiang, W. Z., LaVallee, B. J., Herman, P. L., Clemente, T. E., Weeks, D. P. (2007). Dicamba resistance: enlarging and preserving biotechnology-based weed management strategies. *Science*, *316*(5828), 1185-1188.

Belancic, A., & Agosin, E. (2007). Methoxypyrazines in Grapes and Wines of *Vitis vinifera cv*. Carmenere. *American Journal of Enology and Viticulture*, *58*(4), 462-469.

Belda, I., Navascués, E., Marquina, D., Santos, A., Calderon, F., & Benito, S. (2015). Dynamic analysis of physiological properties of *Torulaspora delbrueckii* in wine fermentations and its incidence on wine quality. *Applied Microbiology and Biotechnology*, *99*(4), 1911-1922.

Belda, I., Ruiz, J., Alastruey-Izquierdo, A., Navascués, E., Marquina, D., & Santos, A. (2016). Unraveling the enzymatic basis of wine "flavorome": a phylo-functional study of wine related yeast species. *Frontiers in Microbiology*, *7*, 12.

Bell, S. G., Hoskins, N., Xu, F., Caprotti, D., Rao, Z., & Wong, L. L. (2006). Cytochrome P450 enzymes from the metabolically diverse bacterium *Rhodopseudomonas palustris*. *Biochemical and Biophysical Research Communications*, *342*(1), 191-196.

Bell, S. G., Xu, F., Forward, I., Bartlam, M., Rao, Z., & Wong, L. L. (2008). Crystal structure of CYP199A2, a *para*-substituted benzoic acid oxidizing cytochrome P450 from *Rhodopseudomonas palustris*. *Journal of Molecular Biology*, *383*(3), 561-574.

Bell, S., Tan, A. H., Johnson, E. D., & Wong, L. L. (2010). Selective oxidative demethylation of veratric acid to vanillic acid by CYP199A4 from *Rhodopseudomonas palustris* HaA2. *Molecular Biosystems-Electronic Edition*, *6*(1), 196-204.

Bell, S. G., Zhou, R., Yang, W., Tan, A. B., Gentleman, A. S., Wong, L. L., & Zhou, W. (2012a). Investigation of the substrate range of CYP199A4: modification of the partition between hydroxylation and desaturation activities by substrate and protein engineering. *Chemistry–A European Journal*, *18*(52), 16677-16688.

Bell, S. G., Yang, W., Tan, A. B., Zhou, R., Johnson, E. O., Zhang, A., Zhou, W., Rao, Z., Wong, L. L. (2012b). The crystal structures of 4-methoxybenzoate bound CYP199A2 and CYP199A4: structural changes on substrate binding and the identification of an anion binding site. *Dalton Transactions*, *41*(28), 8703-8714.

Bellamine, A., Mangla, A. T., Nes, W. D., & Waterman, M. R. (1999). Characterization and catalytic properties of the sterol 14α-demethylase from *Mycobacterium tuberculosis*. *Proceedings of the National Academy of Sciences*, *96*(16), 8937-8942.

Bellamine, A., Mangla, A. T., Dennis, A. L., Nes, W. D., & Waterman, M. R. (2001). Structural requirements for substrate recognition of *Mycobacterium tuberculosis* 14α-demethylase: implications for sterol biosynthesis. *Journal of Lipid Research*, *42*(1), 128-136.

Bely, M., Stoeckle, P., Masneuf-Pomarède, I., & Dubourdieu, D. (2008). Impact of mixed *Torulaspora delbrueckii–Saccharomyces cerevisiae* culture on high-sugar fermentation. *International Journal of Food Microbiology*, *122*(3), 312-320.

Berim, A., & Gang, D. R. (2013). The roles of a flavone-6-hydroxylase and 7-*O*-demethylation in the flavone biosynthetic network of sweet basil. *Journal of Biological Chemistry*, *288*(3), 1795-1805.

Bernhardt, F. H., Pachowsky, H., & Staudinger, H. (1975). A 4-methoxybenzoate *O*-demethylase from *Pseudomonas putida*: a new type of monooxygenase system. *European Journal of Biochemistry*, *57*(1), 241-256.

Benito, Á., Calderón, F., Palomero, F., & Benito, S. (2015). Combine use of selected *Schizosaccharomyces pombe* and *Lachancea thermotolerans* yeast strains as an alternative to the traditional malolactic fermentation in red wine production. *Molecules*, *20*(6), 9510-9523.

Benkwitz, F., Tominaga, T., Kilmartin, P. A., Lund, C., Wohlers, M., & Nicolau, L. (2012). Identifying the chemical composition related to the distinct aroma characteristics of New Zealand Sauvignon Blanc wines. *American Journal of Enology and Viticulture*, *63*(1), 62-72.

Blake, A., Kotseridis, Y., Brindle, I. D., Inglis, D., Sears, M., & Pickering, G. J. (2009). Effect of closure and packaging type on 3-alkyl-2-methoxypyrazines and other impact odorants of Riesling and Cabernet Franc wines. *Journal of Agricultural and Food Chemistry*, *57*(11), 4680-4690.

Blanco, P., Sieiro, C., & Villa, T. G. (1999). Production of pectic enzymes in yeasts. *FEMS Microbiology Letters*, *175*(1), 1-9.

Blanksby, S. J., & Ellison, G. B. (2003). Bond dissociation energies of organic molecules. *Accounts of Chemical Research*, *36*(4), 255-263.

Blizard, D., Sueyoshi, T., Negishi, M., Dehal, S. S., & Kupfer, D. (2001). Mechanism of induction of cytochrome P450 enzymes by the proestrogenic endocrine disruptor pesticide-methoxychlor: interactions of methoxychlor metabolites with the constitutive androstane receptor system. *Drug Metabolism and Disposition*, *29*(6), 781-785.

Boelens, M. H., & Van Gemert, L. J. (1995). Structure-activity relationships of natural volatile nitrogen compounds. *Perfumer & Flavorist*, *20*(5), 63-76.

Botezatu, A., Kemp, B. S., & Pickering, G. J. (2016). Chemical and sensory evaluation of silicone and polylactic acid-based remedial treatments for elevated methoxypyrazine levels in wine. *Molecules*, *21*(9), 1238.

Bossche, H. V., Marichal, P., Le Jeune, L., Coene, M. C., Gorrens, J., & Cools, W. (1993). Effects of itraconazole on cytochrome P450-dependent sterol 14 alpha-demethylation and

reduction of 3-ketosteroids in *Cryptococcus neoformans*. *Antimicrobial Agents and Chemotherapy*, *37*(10), 2101-2105.

Botezatu, A., Kemp, B. S., & Pickering, G. J. (2016). Chemical and sensory evaluation of silicone and polylactic acid-based remedial treatments for elevated methoxypyrazine levels in wine. *Molecules*, *21*(9), 1238.

Bouwer, E. J. (1993). Microbial Remediation: Strategies, Potentials, and Limitations. In *Integrated Soil and Sediment Research: A Basis for Proper Protection* (pp. 533-544). Springer, Dordrecht.

Bowie, J. U., Luthy, R., & Eisenberg, D. (1991). A method to identify protein sequences that fold into a known three-dimensional structure. *Science*, *253*(5016), 164-170.

Boyd, D. R., Sharma, N. D., O'Dowd, C. R., Carroll, J. G., Loke, P. L., & Allen, C. C. (2005). cis-Dihydrodiol, arene oxide and phenol metabolites of dictamnine: key intermediates in the biodegradation and biosynthesis of furoquinoline alkaloids. *Chemical Communications*, *31*, 3989-3991.

Brachtendorf, L., Jetter, A., Beckurts, K. T., Hölscher, A. H., & Fuhr, U. (2002). Cytochrome P450 enzymes contributing to demethylation of maprotiline in man. *Pharmacology & Toxicology*, *90*(3), 144-149.

Brunel, F., & Davison, J. (1988). Cloning and sequencing of *Pseudomonas* genes encoding vanillate demethylase. *Journal of Bacteriology*, *170*(10), 4924-4930.

Brylinski, M., & Skolnick, J. (2008). A threading-based method (FINDSITE) for ligand-binding site prediction and functional annotation. *Proceedings of the National Academy of Sciences*, *105*(1), 129-134.

Bugg, T. D., Ahmad, M., Hardiman, E. M., & Rahmanpour, R. (2011). Pathways for degradation of lignin in bacteria and fungi. *Natural Product Reports*, *28*(12), 1883-1896.

Buied, A., Moore, C. B., Denning, D. W., & Bowyer, P. (2013). High-level expression of *cyp51B* in azole-resistant clinical *Aspergillus fumigatus* isolates. *Journal of Antimicrobial Chemotherapy*, *68*(3), 512-514.

Buisson, D., Quintin, J., & Lewin, G. (2007). Biotransformation of polymethoxylated flavonoids: access to their 4-*O*-demethylated metabolites. *Journal of Natural Products*, *70*(6), 1035-1038.

Bulger, W. H., Muccitelli, R. M., & Kupfer, D. (1978). Studies on the *in vivo* and *in vitro* estrogenic activities of methoxychlor and its metabolites. Role of hepatic mono-oxygenase in methoxychlor activation. *Biochemical Pharmacology*, *27*(20), 2417-2423.

Bumpus, J. A., & Aust, S. D. (1987). Biodegradation of environmental pollutants by the white rot fungus *Phanerochaete chrysosporium*: involvement of the lignin degrading system. *BioEssays*, *6*(4), 166-170.

Bumpus, J. A., & Brock, B. J. (1988). Biodegradation of crystal violet by the white rot fungus *Phanerochaete chrysosporium*. *Applied and Environmental Microbiology*, *54*(5), 1143-1150.

Burapan, S., Kim, M., & Han, J. (2017). Demethylation of polymethoxyflavones by human gut bacterium, *Blautia* sp. MRG-PMF1. *Journal of Agricultural and Food Chemistry*, *65*(8), 1620-1629.

Burdock, G. A. (2009). Fenaroli's Handbook of Flavor Ingredients. CRC Press, Boca Raton.

Burgener-Kairuz, P., Zuber, J. P., Jaunin, P., Buchman, T. G., Bille, J., & Rossier, M. (1994). Rapid detection and identification of *Candida albicans* and *Torulopsis* (*Candida*) *glabrata* in clinical specimens by species-specific nested PCR amplification of a cytochrome P450 lanosterol-alpha-demethylase (L1A1) gene fragment. *Journal of Clinical Microbiology*, *32*(8), 1902-1907.

Burgos, E. S., Walters, R. O., Huffman, D. M., & Shechter, D. (2017). A simplified characterization of *S*-adenosyl-L-methionine-consuming enzymes with 1-Step EZ-MTase: a universal and straightforward coupled-assay for *in vitro* and *in vivo* setting. *Chemical Science*, *8*(9), 6601-6612.

Buttery, R. G., Seifert, R. M., Guadagni, D. G., & Ling, L. C. (1969). Characterization of some volatile constituents of bell peppers. *Journal of Agricultural and Food Chemistry*, *17*(6), 1322-1327.

Buttery, R. G., Turnbaugh, J. G., & Ling, L. C. (1988). Contribution of volatiles to rice aroma. *Journal of Agricultural and Food Chemistry*, *36*(5), 1006–1009.

Cadwell, R. C., & Joyce, G. F. (1992). Randomization of genes by PCR mutagenesis. *Genome Research*, *2*(1), 28-33.

Cammack, R., Gay, E., & Shergill, J. K. (1999). Studies of hyperfine interactions in [2Fe-2S] proteins by EPR and double resonance spectroscopy. *Coordination Chemistry Reviews*, *190*, 1003-1022.

Campo, E., Ferreira, V., Escudero, A., & Cacho, J. (2005). Prediction of the wine sensory properties related to grape variety from dynamic-headspace gas chromatography-olfactometry data. *Journal of Agricultural and Food Chemistry*, *53*(14), 5682-5690.

Campoy, S., Álvarez-Rodríguez, M. L., Recio, E., Rumbero, A., & Coque, J. J. R. (2009). Biodegradation of 2, 4, 6-TCA by the white-rot fungus *Phlebia radiata* is initiated by a phase I (*O*-demethylation)–phase II (*O*-conjugation) reactions system: implications for the chlorine cycle. *Environmental Microbiology*, *11*(1), 99-110.

Canonico, L., Comitini, F., & Ciani, M. (2019). *Metschnikowia pulcherrima* selected strain for ethanol reduction in wine: influence of cell immobilization and aeration condition. *Foods*, *8*(9), 378.

Capra, J. A., Laskowski, R. A., Thornton, J. M., Singh, M., & Funkhouser, T. A. (2009). Predicting protein ligand binding sites by combining evolutionary sequence conservation and 3D structure. *PLoS Computational Biology*, *5*(12), e1000585.

Carr, S. M., (2014). Transition versus transversion mutations. https://www.mun.ca/biology/scarr/Transitions_vs_Transversions.html

Castro, T. F., & Yoshida, T. (1971). Degradation of organochlorine insecticides in flooded soils in the Philippines. *Journal of Agricultural and Food Chemistry*, *19*(6), 1168-1170.

Cavin, J. F., Prevost, H., Lin, J., Schmitt, P., & Divies, C. (1989). Medium for screening *Leuconostoc oenos* strains defective in malolactic fermentation. *Applied and Environmental Microbiology*, *55*(3), 751-753.

Chakraborty, S., Behrens, M., Herman, P. L., Arendsen, A. F., Hagen, W. R., Carlson, D. L., Wang, X-Z., Weeks, D. P. (2005). A three-component dicamba *O*-demethylase from *Pseudomonas maltophilia*, strain DI-6: purification and characterization. *Archives of Biochemistry and Biophysics*, *437*(1), 20-28.

Chakraborty, J., Ghosal, D., Dutta, A., & Dutta, T. K. (2012). An insight into the origin and functional evolution of bacterial aromatic ring-hydroxylating oxygenases. *Journal of Biomolecular Structure and Dynamics*, *30*(4), 419-436.

Chakraborty, J., Suzuki-Minakuchi, C., Okada, K., & Nojiri, H. (2017). Thermophilic bacteria are potential sources of novel Rieske non-heme iron oxygenases. *AMB Express*, *7*(1), 17.

Chapman, D. M., Thorngate, J. H., Matthews, M. A., Guinard, J. X., & Ebeler, S. E. (2004). Yield effects on 2-methoxy-3-isobutylpyrazine concentration in Cabernet Sauvignon using a solid phase microextraction gas chromatography/mass spectrometry method. *Journal of Agricultural and Food Chemistry*, *52*(17), 5431-5435.

Chen, C. K., Doyle, P. S., Yermalitskaya, L. V., Mackey, Z. B., Ang, K. K., McKerrow, J. H., & Podust, L. M. (2009). *Trypanosoma cruzi* CYP51 inhibitor derived from a *Mycobacterium tuberculosis* screen hit. *PLoS Neglected Tropical Diseases*, *3*(2), e372.

Chen, C. L. (1992). Determination of methoxyl groups. In *Methods in Lignin Chemistry* (pp. 465-472). Springer, Berlin, Heidelberg.

Chen, H. P., Chow, M., Liu, C. C., Lau, A., Liu, J., & Eltis, L. D. (2012). Vanillin catabolism in *Rhodococcus jostii* RHA1. *Applied and Environmental Microbiology*, *78*(2), 586-588.

Chen, K., & Arnold, F. H. (1993). Tuning the activity of an enzyme for unusual environments: sequential random mutagenesis of subtilisin E for catalysis in dimethylformamide. *Proceedings of the National Academy of Sciences*, *90*(12), 5618-5622.

Chen, Q., Wang, C. H., Deng, S. K., Wu, Y. D., Li, Y., Yao, L., Jiang, J-D, Yan, X., He, J., Li, S. P. (2014). Novel three-component Rieske non-heme iron oxygenase system catalyzing the *N*-dealkylation of chloroacetanilide herbicides in *Sphingomonads* DC-6 and DC-2. *Applied and Environmental Microbiology*, *80*(16), 5078-5085.

Cheng, T. B., Reineccius, G. A., Bjorklund, J. A., & Leete, E. (1991). Biosynthesis of 2-methoxy-3-isopropylpyrazine in *Pseudomonas perolens*. *Journal of Agricultural and Food Chemistry*, *39*(5), 1009-1012.

Chi, W. J., Chang, Y. K., & Hong, S. K. (2012). Agar degradation by microorganisms and agar-degrading enzymes. *Applied Microbiology and Biotechnology*, *94*(4), 917-930.

Chomsri, N. O. (2008). Impact of protease activity of yeasts on wine fermentation and formation of volatile and non-volatile metabolites (Doctoral dissertation). *Germany: Justus Liebig-University.*

Chiron, H., Drouet, A., Claudot, A. C., Eckerskorn, C., Trost, M., Heller, W., Ernst, D., & Sandermann Jr, H. (2000). Molecular cloning and functional expression of a stress-induced multifunctional *O*-methyltransferase with pinosylvin methyltransferase activity from Scots pine (*Pinus sylvestris* L.). *Plant Molecular Biology*, *44*(6), 733-745.

Christensen, A. B., Gregersen, P. L., Olsen, C. E., & Collinge, D. B. (1998). A flavonoid 7-*O*-methyltransferase is expressed in barley leaves in response to pathogen attack. *Plant Molecular Biology*, *36*(2), 219-227.

Chu, C. T., Parris, D. S., Dixon, R. A., Farber, F. E., & Schaffer, P. A. (1979). Hydroxylamine mutagenesis of HSV DNA and DNA fragments: introduction of mutations into selected regions of the viral genome. *Virology*, *98*(1), 168-181.

Ciani, M., & Ferraro, L. (1998). Combined use of immobilized *Candida stellata* cells and *Saccharomyces cerevisiae* to improve the quality of wines. *Journal of Applied Microbiology*, *85*(2), 247-254.

Ciani, M., Morales, P., Comitini, F., Tronchoni, J., Canonico, L., Curiel, J. A., Oro, L., Rodrigues, A., Gonzalez, R. (2016). Non-conventional yeast species for lowering ethanol content of wines. *Frontiers in Microbiology*, *7*, 642.

Cirino, P. C., Mayer, K. M., & Umeno, D. (2003). Generating mutant libraries using error-prone PCR. In *Directed Evolution Library Creation* (pp. 3-9). Humana Press, New York.

Clemente-Jimenez, J. M., Mingorance-Cazorla, L., Martínez-Rodríguez, S., Las Heras-Vázquez, F. J., & Rodríguez-Vico, F. (2005). Influence of sequential yeast mixtures on wine fermentation. *International Journal of Food Microbiology*, *98*(3), 301-308.

Cole, S., Brosch, R., Parkhill, J., Garnier, T., Churcher, C., Harris, D., Gordon, S.V., Eiglmeier, K., Gas, S., Barry III, C. E., Tekaia, F., Badcock, K., Basham, D., Brown, D., Chillingworth, T., Connor, R., Davies, R., Devlin, K., Feltwell, T., Gentles, S., Hamlin, N., Holroyd, S., Hornsby, T., Jagels, K., Krogh, A., McLean, J., Moule, S., Murphy, L., Oliver, K., Osborne, J., Quail, M. A., Rajandream, M. -A., Rogers, J., Rutter, S., Seeger, K., Skelton, J., Squares, R., Squares, S., Sulston, J. E., Taylor, K., Whitehead, S., Barrell, B. G. (1998). Deciphering the biology of *Mycobacterium tuberculosis* from the complete genome sequence. *Nature*, *393*(6685), 537-544.

Coleman, T. (2018). Utilising CYP199A4 from *Rhodopseudomonas palustris* HaA2 for investigation of the mechanism of cytochrome P450-catalysed oxidations (Doctoral dissertation). *Australia: University of Adelaide*.

Colovos, C., & Yeates, T. O. (1993). Verification of protein structures: patterns of nonbonded atomic interactions. *Protein Science*, *2*(9), 1511-1519.

Comitini, F., Capece, A., Ciani, M., & Romano, P. (2017). New insights on the use of wine yeasts. *Current Opinion in Food Science*, *13*, 44-49.

Comitini, F., Gobbi, M., Domizio, P., Romani, C., Lencioni, L., Mannazzu, I., & Ciani, M. (2011). Selected non-*Saccharomyces* wine yeasts in controlled multistarter fermentations with *Saccharomyces cerevisiae*. *Food Microbiology*, *28*(5), 873-882.

Contreras, A., Hidalgo, C., Henschke, P. A., Chambers, P. J., Curtin, C., & Varela, C. (2014). Evaluation of non-*Saccharomyces* yeasts for the reduction of alcohol content in wine. *Applied and Environmental Microbiology*, *80*(5), 1670-1678.

Correia, M. A., & Hollenberg, P. F. (2015). Inhibition of cytochrome P450 enzymes. In *Cytochrome P450: Structure, Mechanism, and Biochemistry* (pp. 177-259). Springer, Boston.

Costas, M., Mehn, M. P., Jensen, M. P., & Que, L. (2004). Dioxygen activation at mononuclear nonheme iron active sites: enzymes, models, and intermediates. *Chemical Reviews*, *104*(2), 939-986.

Cummings, A. M. (1997). Methoxychlor as a model for environmental estrogens. *Critical Reviews in Toxicology*, *27*(4), 367-379.

D'Angelo, E. M., & Reddy, K. (2000). Aerobic and anaerobic transformations of pentachlorophenol in wetland soils. *Soil Science Society of America Journal*, *64*(3), 933-943.

Dardas, A., Gal, D., Barrelle, M., Sauret-Ignazi, G., Sterjiades, R., & Pelmont, J. (1985). The demethylation of guaiacol by a new bacterial cytochrome P-450. *Archives of Biochemistry and Biophysics*, *236*(2), 585-592.

Dash, S. S., & Gummadi, S. N. (2006). Catabolic pathways and biotechnological applications of microbial caffeine degradation. *Biotechnology Letters*, *28*(24), 1993-2002.

Dash, S. S., & Gummadi, S. N. (2010). Biodegradation of caffeine by *Pseudomonas* sp. NCIM 5235. *Research Journal of Microbiology*, *5*(8), 745-753.

Deeb, R. A., Scow, K. M., & Alvarez-Cohen, L. (2000). Aerobic MTBE biodegradation: an examination of past studies, current challenges and future research directions. *Biodegradation*, *11*(2-3), 171-185.

Delcroix, A., Günata, Z., Sapis, J. C., Salmon, J. M., & Bayonove, C. (1994). Glycosidase activities of three enological yeast strains during winemaking: effect on the terpenol content of Muscat wine. *American Journal of Enology and Viticulture*, *45*(3), 291-296.

Délye, C., Laigret, F., & Corio-Costet, M. F. (1997a). Cloning and sequence analysis of the eburicol 14α-demethylase gene of the obligate biotrophic grape powdery mildew fungus. *Gene*, *195*(1), 29-33.

Délye, C., Laigret, F., & Corio-Costet, M. F. (1997b). A mutation in the 14 alpha-demethylase gene of *Uncinula necator* that correlates with resistance to a sterol biosynthesis inhibitor. *Applied and Environmental Microbiology*, *63*(8), 2966-2970.

Diaz-Guerra, T. M., Mellado, E., Cuenca-Estrella, M., & Rodriguez-Tudela, J. L. (2003). A point mutation in the 14α-sterol demethylase gene *cyp51A* contributes to itraconazole resistance in *Aspergillus fumigatus*. *Antimicrobial Agents and Chemotherapy*, *47*(3), 1120-1124.

Di Menna, M. E. (1959). Some physiological characters of yeasts from soils and allied habitats. *Microbiology*, *20*(1), 13-23.

Dixon, R. A., & Steele, C. L. (1999). Flavonoids and isoflavonoids–a gold mine for metabolic engineering. *Trends in Plant Science*, *4*(10), 394-400.

Domizio, P., Romani, C., Lencioni, L., Comitini, F., Gobbi, M., Mannazzu, I., & Ciani, M. (2011). Outlining a future for non-*Saccharomyces* yeasts: selection of putative spoilage wine strains to be used in association with *Saccharomyces cerevisiae* for grape juice fermentation. *International Journal of Food Microbiology*, *147*(3), 170-180.

Du Plessis, H., Du Toit, M., Nieuwoudt, H., Van der Rijst, M., Kidd, M., & Jolly, N. (2017). Effect of *Saccharomyces*, non-*Saccharomyces* yeasts and malolactic fermentation strategies on fermentation kinetics and flavor of Shiraz wines. *Fermentation*, *3*(4), 64.

Dunlevy, J. D., Soole, K. L., Perkins, M. V., Dennis, E. G., Keyzers, R. A., Kalua, C. M., & Boss, P. K. (2010). Two *O*-methyltransferases involved in the biosynthesis of

methoxypyrazines: grape-derived aroma compounds important to wine flavour. *Plant Molecular Biology*, *74*(1-2), 77-89.

Dunlevy, J., Dennis, E., Soole, K., Perkins, M., Davies, C., & Boss, P. (2013a). A methyltransferase essential for the methoxypyrazine-derived flavour of wine. *Plant Journal, 75*(4), 606-617.

Dunlevy, J. D., Nicholson, E. L., Maffei, S. M., Boss, P. K., Soole, K. V., & Perkins, M. (2013b). Determining the methoxypyrazine biosynthesis variables affected by light exposure and crop level in Cabernet Sauvignon. *American Journal of Enology and Viticulture, 64*(4), 450-458.

Dumitru, R., Jiang, W. Z., Weeks, D. P., & Wilson, M. A. (2009). Crystal structure of dicamba monooxygenase: a Rieske nonheme oxygenase that catalyzes oxidative demethylation. *Journal of Molecular Biology*, *392*(2), 498-510.

Dworkin, J., & Shah, I. M. (2010). Exit from dormancy in microbial organisms. *Nature Reviews Microbiology*, *8*(12), 890-896.

Eckert, K. A., & Kunkel, T. A. (1991). DNA polymerase fidelity and the polymerase chain reaction. *Genome Research*, *1*(1), 17-24.

Eddine, A. N., von Kries, J. P., Podust, M. V., Warrier, T., Kaufmann, S. H., & Podust, L. M. (2008). X-ray structure of 4, 4′-dihydroxybenzophenone mimicking sterol substrate in the active site of sterol 14α-demethylase (CYP51). *Journal of Biological Chemistry*, *283*(22), 15152-15159.

Ekborg, N. A., Gonzalez, J. M., Howard, M. B., Taylor, L. E., Hutcheson, S. W., & Weiner, R. M. (2005). *Saccharophagus degradans* gen. nov., sp. nov., a versatile marine degrader of complex polysaccharides. *International Journal of Systematic and Evolutionary Microbiology*, *55*(4), 1545-1549.

Eltis, L. D., Karlson, U., & Timmis, K. N. (1993). Purification and characterization of cytochrome P450RR1 from *Rhodococcus rhodochrous*. *European Journal of Biochemistry*, *213*(1), 211-216.

Engel, S. R., Dietrich, F. S., Fisk, D. G., Binkley, G., Balakrishnan, R., Costanzo, M. C., Dwight, S. S., Hitz, B. C., Karra, K., Nash, R. S., Weng, S., Wong, E. D., Lloyd, P., Skrzypek, M. S., Miyasato, S. R., Simison, M., Cherry, J. M (2014). The reference

genome sequence of *Saccharomyces cerevisiae*: then and now. *G3: Genes, Genomes, Genetics*, *4*(3), 389-398.

Ensley, B. D., Ratzkin, B. J., Osslund, T. D., Simon, M. J., Wackett, L. P., & Gibson, D. T. (1983). Expression of naphthalene oxidation genes in *Escherichia coli* results in the biosynthesis of indigo. *Science*, *222*(4620), 167-169.

Escriche, I., Kadar, M., Juan-Borrás, M., & Domenech, E. (2014). Suitability of antioxidant capacity, flavonoids and phenolic acids for floral authentication of honey. Impact of industrial thermal treatment. *Food Chemistry*, *142*, 135-143.

Escribano, R., González-Arenzana, L., Portu, J., Garijo, P., López-Alfaro, I., López, R., Santamaría, P., Gutiérrez, A. R. (2018). Wine aromatic compound production and fermentative behaviour within different non-*Saccharomyces* species and clones. *Journal of Applied Microbiology*, *124*(6), 1521-1531.

Escudero, A., Campo, E., Fariña, L., Cacho, J., & Ferreira, V. (2007). Analytical characterization of the aroma of five premium red wines. Insights into the role of odor families and the concept of fruitiness of wines. *Journal of Agricultural and Food Chemistry*, *55*(11), 4501-4510.

Esteves, M., Barbosa, C., Vasconcelos, I., Tavares, M. J., Mendes-Faia, A., Pereira Mira, N., & Mendes-Ferreira, A. (2019). Characterizing the potential of the non-conventional yeast *Saccharomycodes ludwigii* UTAD17 in winemaking. *Microorganisms*, *7*(11), 478.

Fayolle, F., Vandecasteele, J. P., & Monot, F. (2001). Microbial degradation and fate in the environment of methyl *tert*-butyl ether and related fuel oxygenates. *Applied Microbiology and Biotechnology*, *56*(3-4), 339-349.

Fernández, M., Ubeda, J. F., & Briones, A. I. (2000). Typing of non-*Saccharomyces* yeasts with enzymatic activities of interest in wine-making. *International Journal of Food Microbiology*, *59*(1-2), 29-36.

Fernández-González, M., Ubeda, J. F., Vasudevan, T. G., Otero, R. C., & Briones, A. I. (2004). Evaluation of polygalacturonase activity in *Saccharomyces cerevisiae* wine strains. *FEMS Microbiology Letters*, *237*(2), 261-266.

Ferraro, D. J., Gakhar, L., & Ramaswamy, S. (2005). Rieske business: structure–function of Rieske non-heme oxygenases. *Biochemical and Biophysical Research Communications*, *338*(1), 175-190.

Ferraro, L., Fatichenti, F., & Ciani, M. (2000). Pilot scale vinification process using immobilized *Candida stellata* cells and *Saccharomyces cerevisiae*. *Process Biochemistry*, *35*(10), 1125-1129.

Ferreira, V., López, R., & Cacho, J. F. (2000). Quantitative determination of the odorants of young red wines from different grape varieties. *Journal of the Science of Food and Agriculture*, *80*(11), 1659–1667.

Ferreira, V., San Juan, F., Escudero, A., Cullere, L., Fernandez-Zurbano, P., Saenz-Navajas, M. P., & Cacho, J. (2009). Modeling quality of premium Spanish red wines from gas chromatography-olfactometry data. *Journal of Agricultural and Food Chemistry*, *57*(16), 7490–7498.

Fetzner, S. (1998). Bacterial degradation of pyridine, indole, quinoline, and their derivatives under different redox conditions. *Applied Microbiology and Biotechnology*, *49*(3), 237-250.

Finan, T. M., Weidner, S., Wong, K., Buhrmester, J., Chain, P., Vorhölter, F. J., Hernandez-Lucas, I., Becker, A., Cowie, A., Gouzy, J., Golding, B., Pühler, A (2001). The complete sequence of the 1,683-kb pSymB megaplasmid from the N2-fixing endosymbiont *Sinorhizobium meliloti*. *Proceedings of the National Academy of Sciences*, *98*(17), 9889-9894.

Fleet, G. H. (2003). Yeast interactions and wine flavour. *International Journal of Food Microbiology*, *86*(1-2), 11-22.

Fleet, G. H. (2008). Wine yeasts for the future. *FEMS Yeast Research*, *8*(7), 979-995.

Fleischmann, R. D., Alland, D., Eisen, J. A., Carpenter, L., White, O., Peterson, J., DeBoy, R., Dodson, R., Gwinn, M., Haft, D., Hickey, E., Kolonay, J. F., Nelson, W. C., Umayam, L. A., Ermolaeva, M., Salzberg, S. L., Delcher, A., Utterback, T., Weidman, J., Khouri, H., Gill, J., Mikula, A., Bishai, W., Jacobs Jr, W. R., Venter, J. C., Fraser, C. M. (2002). Whole-genome comparison of *Mycobacterium tuberculosis* clinical and laboratory strains. *Journal of Bacteriology*, *184*(19), 5479-5490.

Fogel, S., Lancione, R. L., & Sewall, A. E. (1982). Enhanced biodegradation of methoxychlor in soil under sequential environmental conditions. *Applied and Environmental Microbiology*, *44*(1), 113-120.

Fors, S. M., & Olofsson, B. K. (1986). Alkylpyrazines, volatiles formed in the maillard reaction. II. sensory properties of five alkylpyrazines. *Chemical Senses*, *11*(1), 65-77.

Francis, L. (2012). Fermentation-derived aroma compounds and grape-derived monoterpenes. *Applied Microbiology and Biotechnology*, *96*, 601-618.

Frick, T. D., & Crawford, R. L. (1984). Enzymic demethylation of lignin model polymers. *Applied Biochemistry and Biotechnology*, *9*(4), 319-320.

Friedman, J., & Waller, G. R. (1983). Caffeine hazards and their prevention in germinating seeds of coffee (*Coffea arabica* L.). *Journal of Chemical Ecology*, *9*(8), 1099-1106.

Friggeri, L., Hargrove, T. Y., Rachakonda, G., Blobaum, A. L., Fisher, P., de Oliveira, G. M., da Silva, C. F., Soeiro, M. N. Z., Nes, W. D., Lindsley, C. W., Villalta, F., Guengerich, F. P., Lepesheva, G. I. (2018). Sterol 14α-demethylase structure-based optimization of drug candidates for human infections with the protozoan *Trypanosomatidae*. *Journal of Medicinal Chemistry*, *61*(23), 10910-10921.

Fuchs, G., Boll, M., & Heider, J. (2011). Microbial degradation of aromatic compounds—from one strategy to four. *Nature Reviews Microbiology*, *9*(11), 803-816.

Galibert, F., Finan, T. M., Long, S. R., Pühler, A., Abola, P., Ampe, F., Barloy-Hubler, F., Barnett, M. J., Becker, A., Boistard, P., Bothe, G., Boutry, M., Bowser, L., Buhrmester, J., Cadieu, E., Capela, D., Chain, P., Cowie, A., Davis, R. W., Dreano, S., Federspiel, N. A., Fisher, R. F., Gloux, S., Godrie, T., Goffeau, A., Golding, B., Gouzy, J., Gurjal, M., Hernandez-Lucas, I., Hong, A., Huizar, L., Hyman, R. W., Jones, T., Kahn, D., Kahn, M. L., Kalman, S., Keating, D. H., Kiss, E., Komp, C., Lelaure, V., Masuy, D., Palm, C., Peck, M. C., Pohl, T. M., Portetelle, D., Purnelle, B., Ramsperger, U., Surzycki, R., Thebault, P., Vandenbol, M., Vorholter, F. J., Weidner, S., Wells, D. H., Wong, K., Yeh, K. C., Batut, J. (2001). The composite genome of the legume symbiont *Sinorhizobium meliloti*. *Science*, *293*(5530), 668-672.

Gallois, A., Kergomard, A., & Adda, J. (1988). Study of the biosynthesis of 3-isopropyl-2-methoxypyrazine produced by *Pseudomonas taetrolens*. *Food Chemistry*, *28*(4), 299-309.

Gallois, A., & Grimont, P. A. (1985). Pyrazines responsible for the potato-like odor produced by some *Serratia* and *Cedecea* strains. *Applied and Environmental Microbiology*, *50*(4), 1048-1051.

Gallois A., Kergomard A. and Adda J. (1988) Study of the biosynthesis of 3-isopropyl-2-methoxypyrazine produced by *Pseudomonas taetrolens*. *Food Chemistry*, *28*, 299-309.

Gang, D. R., Lavid, N., Zubieta, C., Chen, F., Beuerle, T., Lewinsohn, E., Noel, J. P., & Pichersky, E. (2002). Characterization of phenylpropene *O*-methyltransferases from sweet basil facile change of substrate specificity and convergent evolution within a plant *O*-methyltransferase family. *The Plant Cell*, *14*(2), 505-519.

García-Hidalgo, J., Ravi, K., Kuré, L. L., Lidén, G., & Gorwa-Grauslund, M. (2019). Identification of the two-component guaiacol demethylase system from *Rhodococcus rhodochrous* and expression in *Pseudomonas putida* EM42 for guaiacol assimilation. *AMB Express*, *9*(1), 34.

Gardner, J. M., McBryde, C., Vystavelova, A., Lopes, M. D. B., & Jiranek, V. (2005). Identification of genes affecting glucose catabolism in nitrogen-limited fermentation. *FEMS Yeast Research*, *5*(9), 791-800.

Garnier, T., Eiglmeier, K., Camus, J. C., Medina, N., Mansoor, H., Pryor, M., Duthoy, S., Grondin, Sp., Lacroix, C., Monsempe, C., Simon, S., Harris, B., Atkin, R., Doggett, J., Mayes, R., Keating, L., Wheeler, P. R., Parkhill, J., Barrell, B. G., Cole, S. T., Gordon, S. V., Hewinson, R. G. (2003). The complete genome sequence of *Mycobacterium bovis*. *Proceedings of the National Academy of Sciences*, *100*(13), 7877-7882.

Gassner, G., Wang, L., Batie, C., & Ballou, D. P. (1994). Reaction of phthalate dioxygenase reductase with NADH and NAD: kinetic and spectral characterization of intermediates. *Biochemistry*, *33*(40), 12184-12193.

Gassner, G. T., Ludwig, M. L., Gatti, D. L., Correll, C. C., & Ballou, D. P. (1995). Structure and mechanism of the iron-sulfur flavoprotein phthalate dioxygenase reductase. *The FASEB Journal*, *9*(14), 1411-1418.

Gibson, D. T., Koch, J. R., & Kallio, R. E. (1968). Oxidative degradation of aromatic hydrocarbons by microorganisms. I. enzymic formation of catechol from benzene. *Biochemistry*, *7*(7), 2653-2662.

Gil, J. V., Mateo, J. J., Jiménez, M., Pastor, A., & Huerta, T. (1996). Aroma compounds in wine as influenced by apiculate yeasts. *Journal of Food Science*, *61*(6), 1247-1250.

Giovannoni, S. J., Tripp, H. J., Givan, S., Podar, M., Vergin, K. L., Baptista, D., Bibbs, L., Eads, J., Richardson, T. H., Noordewier, M., Rappé, M. S., Short, J. M., Carrington, J. C.,

Mathur, E. J. (2005). Genome streamlining in a cosmopolitan oceanic bacterium. *Science*, *309*(5738), 1242-1245.

Gobbi, M., Comitini, F., Domizio, P., Romani, C., Lencioni, L., Mannazzu, I., & Ciani, M. (2013). *Lachancea thermotolerans* and *Saccharomyces cerevisiae* in simultaneous and sequential co-fermentation: a strategy to enhance acidity and improve the overall quality of wine. *Food Microbiology*, *33*(2), 271-281.

Gokulakrishnan, S., Chandraraj, K., & Gummadi, S. N. (2005). Microbial and enzymatic methods for the removal of caffeine. *Enzyme and Microbial Technology*, *37*(2), 225-232.

Golovleva, L. A., Polyakova, A. B., Pertsova, R. N., & Finkelshtein, Z. I. (1984). The fate of methoxychlor in soils and transformation by soil microorganisms. *Journal of Environmental Science & Health Part B*, *19*(6), 523-538.

Gonzalez, J. M., & Weiner, R. M. (2000). Phylogenetic characterization of marine bacterium strain 2-40, a degrader of complex polysaccharides. *International Journal of Systematic and Evolutionary Microbiology*, *50*(2), 831-834.

Guengerich FP. (2002). Rate-limiting steps in cytochrome P450 catalysis. *Biological Chemistry*. *383*(10), 1553-1564.

Guillaumie S., Ilg, A., Réty, S., Brette, M., Trossat-Magnin, C., Decroocq, S., Leon, C., Keime, C., Ye, T., Baltenweck-Guyot, B., Claudel, P., Bordenave, L., Vanbrabant, S., Duchene, E., Delrot, S., Darriet, P., Hugueney, P., Gomès, E. (2013). Genetic analysis of the biosynthesis of 2-methoxy-3-isobutylpyrazine, a major grape-derived aroma compound impacting wine quality. *Plant Physiology, 162*(2), 604-615.

Guth, H. (1997). Quantitation and sensory studies of character impact odorants of different white wine varieties. *Journal of Agricultural and Food Chemistry*, *45*(8), 3027–3032.

Hajduk, P. J., Meadows, R. P., & Fesik, S. W. (1999). NMR-based screening in drug discovery. *Quarterly Reviews of Biophysics*, *32*(3), 211-240.

Harada, A., Kamimura, N., Takeuchi, K., Yu, H. Y., Masai, E., & Senda, T. (2017). The crystal structure of a new *O*-demethylase from *Sphingobium* sp. strain SYK-6. *The FEBS Journal*, *284*(12), 1855-1867.

Hardjasa, A., Ling, M., Ma, K., & Yu, H. (2010). Investigating the effects of DMSO on PCR fidelity using a restriction digest-based method. *Journal of Experimental Microbiology and Immunology*, *14*, 161-164.

Hardison, L. K., Curry, S. S., Ciuffetti, L. M., & Hyman, M. R. (1997). Metabolism of diethyl ether and cometabolism of methyl *tert*-butyl ether by a filamentous fungus, a *Graphium* sp. *Applied and Environmental Microbiology*, *63*(8), 3059-3067.

Hargrove, T. Y., Wawrzak, Z., Lamb, D. C., Guengerich, F. P., & Lepesheva, G. I. (2015). Structure-functional characterization of cytochrome P450 sterol 14α-demethylase (CYP51B) from *Aspergillus fumigatus* and molecular basis for the development of antifungal drugs. *Journal of Biological Chemistry*, *290*(39), 23916-23934.

Hargrove, T. Y., Friggeri, L., Wawrzak, Z., Qi, A., Hoekstra, W. J., Schotzinger, R. J., York, J. D., Guengerich, F. P, Lepesheva, G. I. (2017). Structural analyses of *Candida albicans* sterol 14α-demethylase complexed with azole drugs address the molecular basis of azole-mediated inhibition of fungal sterol biosynthesis. *Journal of Biological Chemistry*, *292*(16), 6728-6743.

Harris, R. L. N., Lacey, M. J., Brown, W. V., & Allen, M. S. (1987). Determination of 2-methoxy-3-alkylpyrazines in wine by gas chromatography/mass spectrometry. *VITIS-Journal of Grapevine Research*, *26*(4), 201.

Harris, S. (2012). Quantification of 3-isobutyl-2-hydroxyprazine, a key intermediate in IBMP Metabolism (Master dissertation). *US: Cornell University*.

Harris, S. A., Ryona, I., & Sacks, G. L. (2012). Behavior of 3-isobutyl-2-hydroxypyrazine (IBHP), a key intermediate in 3-isobutyl-2-methoxypyrazine (IBMP) metabolism, in ripening wine grapes. *Journal of Agricultural and Food Chemistry*, *60*(48), 11901-11908.

Hashizume, K., & Samuta, T. (1997). Green odorants of grape cluster stem and their ability to cause a wine stemmy flavor. *Journal of Agricultural and Food Chemistry, 45*(4), 1333-1337.

Hashizume, K., & Samuta, T. (1999). Grape maturity and light exposure affect berry methoxypyrazine concentration. *American Journal of Enology and Viticulture*, *50*(2), 194-198.

Hashizume, K., Tozawa, K., Endo, M., & Aramaki, I. (2001a). *S*-Adenosyl-L-methionine-dependent *O*-methylation of 2-hydroxy-3-alkylpyrazine in wine grapes: a putative final

step of methoxypyrazine biosynthesis. *Bioscience, Biotechnology, and Biochemistry*, *65*(4), 795-801.

Hashizume, K., Tozawa, K., Hiraga, Y., & Aramaki, I. (2001). Purification and characterization of a *O*-methyltransferase capable of methylating 2-hydroxy-3-alkylpyrazine from *Vitis vinifera* L. (*cv*. Cabernet Sauvignon). *Bioscience, Biotechnology, and Biochemistry*, *65*(10), 2213-2219.

Hawksworth, G., & Scheline, R. R. (1975). Metabolism in the rat of some pyrazine derivatives having flavour importance in foods. *Xenobiotica*, *5*(7), 389-399.

He, A., & Rosazza, J. P. N. (2003). Microbial transformations of *S*-naproxen by *Aspergillus niger* ATCC 9142. Die Pharmazie-*An International Journal of Pharmaceutical Sciences*, 58(6), 420-422.

Heard, G. M., & Fleet, G. H. (1985). Growth of natural yeast flora during the fermentation of inoculated wines. *Applied Environmental Microbiology*, *50*(3), 727-728.

Hein, K., Ebeler, S. E., & Heymann, H. (2009). Perception of fruity and vegetative aromas in red wine. *Journal of Sensory Studies*, *24*(3), 441-455.

Helwi, P., Habran, A., Guillaumie, S., Thibon, C., Hilbert, G., Gomes, E., Delrot, S., Darriet, P., van Leeuwen, C. (2015). Vine nitrogen status does not have a direct impact on 2-methoxy-3-isobutylpyrazine in grape berries and wines. *Journal of Agricultural and Food Chemistry*, *63*(44), 9789-9802.

Hemsworth, G. R., Taylor, E. J., Kim, R. Q., Gregory, R. C., Lewis, S. J., Turkenburg, J. P., Parkin, A., Davies, G. J., Walton, P. H. (2013). The copper active site of CBM33 polysaccharide oxygenases. *Journal of the American Chemical Society*, *135*(16), 6069-6077.

Henderson, J. F. (1979). Teaching one-carbon metabolism. *Biochemistry Education*, *7*(3), 51-52.

Henderson, M. E. (1961). Isolation, identification and growth of some soil hyphomycetes and yeast-like fungi which utilize aromatic compounds related to lignin. *Microbiology*, *26*(1), 149-154.

Henniger, G., & Mascaro Jr, L. (1985). Enzymatic-ultraviolet determination of glucose and fructose in wine: collaborative study. *Journal of the Association of Official Analytical Chemists*, *68*(5), 1021-1024.

Henikoff, S., & Henikoff, J. G. (1992). Amino acid substitution matrices from protein blocks. *Proceedings of the National Academy of Sciences*, *89*(22), 10915-10919.

Henschke, P.A.; Jiranek, V. (1993) Yeasts-metabolism of nitrogen compounds. In Wine microbiology and biotechnology (pp 77-164). Harwood Academic Publishers, Chur, Switzerland.

Herman, P. L., Behrens, M., Chakraborty, S., Chrastil, B. M., Barycki, J., & Weeks, D. P. (2005). A three-component dicamba *O*-demethylase from *Pseudomonas maltophilia*, strain DI-6 gene isolation, characterization, and heterologous expression. *Journal of Biological Chemistry*, *280*(26), 24759-24767.

Heymann, H., & Noble, A. C. (1987). Descriptive analysis of commercial Cabernet Sauvignon wines from California. *American Journal of Enology and Viticulture*, *38*(1), 41-44.

Hitchcock, C. A., Brown, S. B., Evans, E. G. V., & Adams, D. J. (1989). Cytochrome P450-dependent 14α-demethylation of lanosterol in *Candida albicans*. *Biochemical Journal*, *260*(2), 549-556.

Hitchings, G. H. (1983). Functions of tetrahydrofolate and the role of dihydrofolate reductase in cellular metabolism. In *Inhibition of Folate Metabolism in Chemotherapy* (pp. 11-23). Springer, Berlin, Heidelberg.

Hooft, R. W., Vriend, G., Sander, C., & Abola, E. E. (1996). Errors in protein structures. *Nature*, *381*(6580), 272-272.

Howard, E. C., Henriksen, J. R., Buchan, A., Reisch, C. R., Bürgmann, H., Welsh, R., Ye, W., González, J. M., Mace, K., Joye, S. B., Kiene, R. P., Whitman, W. B., Moran, M. A. (2006). Bacterial taxa that limit sulfur flux from the ocean. *Science*, *314*(5799), 649-652.

Hranilovic, A., Albertin, W., Capone, D. L., Gallo, A., Grbin, P. R., Danner, L., Bastian, S. E. P., Masneuf-Pomarede, I., Coulon, J., Bely, M., Jiranek, V. (2021). Impact of *Lachancea thermotolerans* on chemical composition and sensory profiles of Merlot wines. *Food Chemistry*, 129015.

Hranilovic, A., Li, S., Boss, P. K., Bindon, K., Ristic, R., Grbin, P. R., Van der Westhuizen, Jiranek, V. (2018). Chemical and sensory profiling of Shiraz wines co-fermented with commercial non-*Saccharomyces* inocula. *Australian Journal of Grape and Wine Research*, *24*(2), 166-180.

Hudlicky, T., Gonzalez, D., Gibson, D. T. (1999). Enzymatic dihydroxylation of aromatics in enantioselective synthesis: expanding asymmetric methodology. *Aldrichimica Acta*, *32*, 35-62.

Huang, P., Nedelcu, D., Watanabe, M., Jao, C., Kim, Y., Liu, J., & Salic, A. (2016). Cellular cholesterol directly activates smoothened in hedgehog signaling. *Cell*, *166*(5), 1176-1187.

Hughes, A. L., Powell, D. W., Bard, M., Eckstein, J., Barbuch, R., Link, A. J., & Espenshade, P. J. (2007). Dap1/PGRMC1 binds and regulates cytochrome P450 enzymes. *Cell Metabolism*, *5*(2), 143-149.

Huynh, V. B., & Crawford, R. L. (1985). Novel extracellular enzymes (ligninases) of *Phanerochaete chrysosporium*. *FEMS Microbiology Letters*, *28*(1), 119-123.

Ibrahim, A. R. S., Galal, A. M., Ahmed, M. S., & Mossa, G. S. (2003). *O*-demethylation and sulfation of 7-methoxylated flavanones by *Cunninghamella elegans*. *Chemical and Pharmaceutical Bulletin*, *51*(2), 203-206.

Ibrahim, R. K., Bruneau, A., & Bantignies, B. (1998). Plant *O*-methyltransferases: molecular analysis, common signature and classification. *Plant Molecular Biology*, *36*(1), 1-10.

Ishida, N., Aoyama, Y., Hatanaka, R., Oyama, Y., Imajo, S., Ishiguro, M., Oshima, T., Nakazato, H., Noguchi, T., Maitra, U. S., Mohan, V. P., Sprinson, D. B., Yoshida, Y. (1988). A single amino acid substitution converts cytochrome P45014DM to an inactive form, cytochrome P450SG1: complete primary structures deduced from cloned DNAs. *Biochemical and Biophysical Research Communications*, *155*(1), 317-323.

Isobutyric acid, chemical book website. https://www.chemicalbook.com/ChemicalProductProperty_EN_CB3367722.htm

Ittisoponpisan, S., Islam, S. A., Khanna, T., Alhuzimi, E., David, A., & Sternberg, M. J. (2019). Can predicted protein 3D structures provide reliable insights into whether missense variants are disease associated? *Journal of Molecular Biology*, *431*(11), 2197-2212.

Izquierdo Canas, Palacios García, A. T., P. M., García Romero, E. (2011). Enhancement of flavour properties in wines using sequential inoculations of non-*Saccharomyces* (*Hanseniapora* and *Torulaspora*) and *Saccharomyces* yeast starter. *VITIS-Journal of Grapevine Research*, *50*(4), 177-182.

Jackson, C. J., Lamb, D. C., Marczylo, T. H., Warrilow, A. G., Manning, N. J., Lowe, D. J., Kelly, D. E., Kelly, S. L. (2002). A novel sterol 14α-demethylase/ferredoxin fusion protein (MCCYP51FX) from *Methylococcus capsulatus* represents a new class of the cytochrome P450 superfamily. *Journal of Biological Chemistry*, *277*(49), 46959-46965.

Jackson, C. J., Lamb, D. C., Marczylo, T. H., Parker, J. E., Manning, N. L., Kelly, D. E., & Kelly, S. L. (2003). Conservation and cloning of CYP51: a sterol 14α-demethylase from *Mycobacterium smegmatis*. *Biochemical and Biophysical Research Communications*, *301*(2), 558-563.

Jaenicke, R., & Böhm, G. (1998). The stability of proteins in extreme environments. *Current Opinion in Structural Biology*, *8*(6), 738-748.

Janusz, G., Kucharzyk, K. H., Pawlik, A., Staszczak, M., & Paszczynski, A. J. (2013). Fungal laccase, manganese peroxidase and lignin peroxidase: gene expression and regulation. *Enzyme and Microbial Technology*, *52*(1), 1-12.

Janusz, G., Pawlik, A., Sulej, J., Świderska-Burek, U., Jarosz-Wilkołazka, A., & Paszczyński, A. (2017). Lignin degradation: microorganisms, enzymes involved, genomes analysis and evolution. *FEMS Microbiology Reviews*, *41*(6), 941-962.

Jarosch, M., Egelseer, E. M., Huber, C., Moll, D., Mattanovich, D., Sleytr, U. B., & Sára, M. (2001). Analysis of the structure–function relationship of the S-layer protein SbsC of Bacillus stearothermophilus ATCC 12980 by producing truncated forms. *Microbiology*, *147*(5), 1353-1363.

Jensen, K., Alper, H., Fischer, C., & Stephanopoulos, G. (2006). Identifying functionally important mutations from phenotypically diverse sequence data. *Applied and Environmental Microbiology*, *72*(5), 3696-3701.

Jiang, X., Martens, D., Schramm, K. W., Kettrup, A., Xu, S. F., & Wang, L. S. (2000). Polychlorinated organic compounds (PCOCs) in waters, suspended solids and sediments of the Yangtse River. *Chemosphere*, *41*(6), 901-905.

Johnston, M., Andrews, S., Brinkman, R., Cooper, J., Ding, H., Dover, J., Du, Z., Favello, A., Fulton, L., Gattung, S. (1994). Complete nucleotide sequence of *Saccharomyces cerevisiae* chromosome VIII. *Science*, *265*(5181), 2077-2082.

Jolly, N. P., Augustyn, O. P. R., & Pretorius, I. S. (2003). The effect of non-*Saccharomyces* yeasts on fermentation and wine quality. *South African Journal of Enology and Viticulture*, *24*(2), 55-62.

Jolly, N. P., Varela, C., & Pretorius, I. S. (2014). Not your ordinary yeast: non-*Saccharomyces* yeasts in wine production uncovered. *FEMS Yeast Research*, *14*(2), 215-237.

Jones, R. G. (1949). Studies on imidazole compounds. I. a synthesis of imidazoles with functional groups in the 2-position. *Journal of the American Chemical Society*, *71*(2), 383-386.

Jood, I., Hoff, J. W., & Setati, M. E. (2017). Evaluating fermentation characteristics of *Kazachstania spp.* and their potential influence on wine quality. *World Journal of Microbiology and Biotechnology*, *33*(7), 129.

Joshi, C. P., & Chiang, V. L. (1998). Conserved sequence motifs in plant *S*-adenosyl-L-methionine-dependent methyltransferases. *Plant Molecular Biology*, *37*(4), 663-674.

Kalb, V. F., Woods, C. W., Turi, T. G., Dey, C. R., Sutter, T. R., & Loper, J. C. (1987). Primary structure of the P450 lanosterol demethylase gene from *Saccharomyces cerevisiae*. *DNA*, *6*(6), 529-537.

Kamimura, N., Takahashi, K., Mori, K., Araki, T., Fujita, M., Higuchi, Y., & Masai, E. (2017). Bacterial catabolism of lignin-derived aromatics: New findings in a recent decade: Update on bacterial lignin catabolism. *Environmental Microbiology Reports*, *9*(6), 679-705.

Kaminński, E., Libbey, L. M., Stawicki, S., & Wasowicz, E. (1972). Identification of the predominant volatile compounds produced by *Aspergillus flavus*. *Applied Microbiology*, *24*(5), 721-726.

Kapsopoulou, K., Mourtzini, A., Anthoulas, M., & Nerantzis, E. (2007). Biological acidification during grape must fermentation using mixed cultures of *Kluyveromyces thermotolerans* and *Saccharomyces cerevisiae*. *World Journal of Microbiology and Biotechnology*, *23*(5), 735-739.

Ke, X., Ding, G. J., Ma, B. X., Liu, Z. Q., Zhang, J. F., & Zheng, Y. G. (2017). Characterization of a novel CYP51 from *Rhodococcus triatomae* and its NADH-

ferredoxin reductase-coupled application in lanosterol 14α-demethylation. *Process Biochemistry*, *62*, 59-68.

Kelkar, D. S., Kumar, D., Kumar, P., Balakrishnan, L., Muthusamy, B., Yadav, A. K., Shrivastava, P., Marimuthu, A., Anand, S., Sundaram, H., Kingsbury, R., Harsha, H. C., Nair, B., Prasad, T. S. K., Chauhan, D. S., Katoch, K., Katoch, V. M., Kumar, P., Chaerkady, R., Ramachandran, S., Dash, D., Pandey, A. (2011). Proteogenomic analysis of *Mycobacterium tuberculosis* by high resolution mass spectrometry. *Molecular & Cellular Proteomics*, *10*(12).

Kelley, L. A., Mezulis, S., Yates, C. M., Wass, M. N., & Sternberg, M. J. (2015). The Phyre2 web portal for protein modeling, prediction and analysis. *Nature Protocols*, *10*(6), 845-858.

Kennison, K. R., Wilkinson, K. L., Williams, H. G., Smith, J. H., & Gibberd, M. R. (2007). Smoke-derived taint in wine: Effect of postharvest smoke exposure of grapes on the chemical composition and sensory characteristics of wine. *Journal of Agricultural and Food Chemistry*, *55*(26), 10897-10901.

Keniya, M. V., Sabherwal, M., Wilson, R. K., Woods, M. A., Sagatova, A. A., Tyndall, J. D., & Monk, B. C. (2018). Crystal structures of full-length lanosterol 14α-demethylases of prominent fungal pathogens *Candida albicans* and *Candida glabrata* provide tools for antifungal discovery. *Antimicrobial Agents and Chemotherapy*, *62*(11).

Keum, Y. S., Lee, Y. H., & Kim, J. H. (2009). Metabolism of methoxychlor by *Cunninghamella elegans* ATCC36112. *Journal of Agricultural and Food Chemistry*, *57*(17), 7931-7937.

Kiener, A. (1993). *U.S. Patent No. 5,273,893*. Washington, DC: U.S. Patent and Trademark Office.

Kiener, A. (1994). Microbiological process for the production of 5-hydroxy-2-pyrazine carboxylic acid. *European Patent 0578137A1*. European Patent Office.

Kiener, A., Gameren, Y. V., & Bokel, M. (1993). *U.S. Patent No. 5,229,278*. Washington, DC: U.S. Patent and Trademark Office.

Kiener, A., Heinzmann, K., & Bokel, M. (1993). *U.S. Patent No. 5,266,482*. Washington, DC: U.S. Patent and Trademark Office.

Kiener, A., Roduit, J. P., Tschech, A., Tinschert, A., Heinzmann, K. (1994). Regiospecific enzymatic hydroxylations of pyrazinecarboxylic acid and a practical synthesis of 5-chloropyrazine-2-carboxylic acid. *Synlett, 10*, 814-816.

Kiener, A., Van Gameren, Y., & Bokel, M. (1994). *U.S. Patent No. 5,284,767*. Washington, DC: U.S. Patent and Trademark Office.

Kim, J. H., Kim, B. H., Brooks, S., Kang, S. Y., Summers, R. M., & Song, H. K. (2019). Structural and mechanistic insights into caffeine degradation by the bacterial *N*-demethylase complex. *Journal of Molecular Biology*, *431*(19), 3647-3661.

Kim, P., Yoon, S. H., Seo, M. J., Oh, D. K., & Choi, J. H. (2001). Improvement of tagatose conversion rate by genetic evolution of thermostable galactose isomerase. *Biotechnology and Applied Biochemistry*, *34*(Pt 2), 99-102.

King, E. S., Dunn, R. L., & Heymann, H. (2013). The influence of alcohol on the sensory perception of red wines. *Food Quality and Preference*, *28*(1), 235-243.

King, A., & Richard Dickinson, J. (2000). Biotransformation of monoterpene alcohols by *Saccharomyces cerevisiae, Torulaspora delbrueckii* and *Kluyveromyces lactis*. *Yeast*, *16*(6), 499-506.

Kingsland, G. C., & Anderson, J. (1976). A study of the feasibility of the use of gentian violet as a fungistat for poultry feed. *Poultry Science*, *55*(3), 852-857.

Kirsch, F., & Buettner, A. (2013). Odor qualities and thresholds of physiological metabolites of 1,8-cineole as an example for structure-activity relationships considering chirality aspects. *Chemistry & Biodiversity*, *10*(9), 1683-1695.

Knize, M. G., Övervik, E., Midtvedt, T., Turteltaub, K. W., Happe, J. A., Gustafsson, J. Å., & Felton, J. S. (1989). The metabolism of 4, 8-DiMeIQx in conventional and germ-free rats. *Carcinogenesis*, *10*(8), 1479-1484.

Koch, A. L. (2009). Quantification of the effects of genotype and the environment on 2-methoxy-3-isobutylpyrazine in the fruit of *Vitis vinifera* L. *cv.* Cabernet Sauvignon (Doctoral dissertation). *US: University of California, Davis*.

Koch, A., Doyle, C. L., Matthews, M. A., Williams, L. E., & Ebeler, S. E. (2010). 2-Methoxy-3-isobutylpyrazine in grape berries and its dependence on genotype. *Phytochemistry*, *71*(17-18), 2190-2198.

Koch, A., Ebeler, S. E., Williams, L. E., & Matthews, M. A. (2012). Fruit ripening in *Vitis vinifera*: light intensity before and not during ripening determines the concentration of 2-methoxy-3-isobutylpyrazine in Cabernet Sauvignon berries. *Physiologia plantarum*, *145*(2), 275-285.

Kögel, S., Botezatu, A., Hoffmann, C., & Pickering, G. (2015). Methoxypyrazine composition of *Coccinellidae*-tainted Riesling and Pinot Noir wine from Germany. *Journal of the Science of Food and Agriculture*, *95*(3), 509-514.

Kögel, S., Gross, J., Hoffmann, C., & Ulrich, D. (2012). Diversity and frequencies of methoxypyrazines in hemolymph of *Harmonia axyridis* and *Coccinella septempunctata* and their influence on the taste of wine. *European Food Research and Technology*, *234*(3), 399-404.

Kohler, A. C., Mills, M. J., Adams, P. D., Simmons, B. A., & Sale, K. L. (2017). Structure of aryl *O*-demethylase offers molecular insight into a catalytic tyrosine-dependent mechanism. *Proceedings of the National Academy of Sciences*, *114*(16), E3205-E3214.

Kong, I. S., Bates, T. C., Hülsmann, A., Hassan, H., Smith, B. E., & Oliver, J. D. (2004). Role of catalase and oxyR in the viable but nonculturable state of Vibrio vulnificus. *FEMS Microbiology Ecology*, *50*(3), 133-142.

Kostrzewa-Susłow, E. D. Y. T. A., Dymarska, M., & Janeczko, T. (2014). Microbial transformations of 3-methoxyflavone by strains of *Aspergillus niger*. *Polish Journal of Microbiology*, *63*(1), 111-114.

Kotseridis, Y., Beloqui, A. A., Bertrand, A., & Doazan, J. P. (1998). An analytical method for studying the volatile compounds of Merlot Noir clone wines. *American Journal of Enology and Viticulture*, *49*(1), 44-48.

Kotseridis, Y. S., Spink, M., Brindle, I. D., Blake, A. J., Sears, M., Chen, X., Soleas, G., Inglis, D., & Pickering, G. J. (2008). Quantitative analysis of 3-alkyl-2-methoxypyrazines in juice and wine using stable isotope labelled internal standard assay. *Journal of Chromatography A*, *1190*(1), 294-301.

Kroll, E. S., Hyland, K. M., Hieter, P., & Li, J. J. (1996). Establishing genetic interactions by a synthetic dosage lethality phenotype. *Genetics*, *143*(1), 95-102.

Krstic, M. P., Johnson, D. L., & Herderich, M. J. (2015). Review of smoke taint in wine: smoke-derived volatile phenols and their glycosidic metabolites in grapes and vines as

biomarkers for smoke exposure and their role in the sensory perception of smoke taint. *Australian Journal of Grape and Wine Research*, *21*, 537-553.

Kumar, R., Zhao, S., Vetting, M. W., Wood, B. M., Sakai, A., Cho, K., Solbiati, J., Almo, S. C., Sweedler, J. V., Jacobson, M. P., Gerit, J. A., Cronan, J. E. (2014). Prediction and biochemical demonstration of a catabolic pathway for the osmoprotectant proline betaine. *MBio*, *5*(1).

Kumar, V., Jayasuryan, N., & Kumar, R. (1996). A truncated mutant (residues 58-140) of the hepatitis B virus X protein retains transactivation function. *Proceedings of the National Academy of Sciences*, *93*(11), 5647-5652.

Kurtzman, C. P. (2003). Phylogenetic circumscription of *Saccharomyces, Kluyveromyces* and other members of the *Saccharomycetaceae*, and the proposal of the new genera *Lachancea, Nakaseomyces, Naumovia, Vanderwaltozyma* and *Zygotorulaspora*. *FEMS Yeast Research*, *4*(3), 233-245.

Kuypers, M. M., Marchant, H. K., & Kartal, B. (2018). The microbial nitrogen-cycling network. *Nature Reviews Microbiology*, *16*(5), 263.

Lacey, M. J., Allen, M. S., Harris, R. L., & Brown, W. V. (1991). Methoxypyrazines in Sauvignon Blanc grapes and wines. *American Journal of Enology and Viticulture*, *42*(2), 103-108.

Lallemand (2014). Level2-solutions. https://www.lallemandwine.com/wp-content/uploads/2014/04/Level2-Solutions-brochure.pdf

Lamb, D. C., Kelly, D. E., Manning, N. J., & Kelly, S. L. (1998). A sterol biosynthetic pathway in *Mycobacterium*. *FEBS Letters*, *437*(1-2), 142-144.

Lamb, D. C., Kelly, D. E., Manning, N. J., Kaderbhai, M. A., & Kelly, S. L. (1999). Biodiversity of the P450 catalytic cycle: yeast cytochrome b5/NADH cytochrome b5 reductase complex efficiently drives the entire sterol 14-demethylation (CYP51) reaction. *FEBS Letters*, *462*(3), 283-288.

Lambrechts, M. G., & Pretorius, I. S. (2000). Yeast and its importance to wine aroma-a review. *South African Journal of Enology and Viticulture*, *21*(1), 97-129.

Larimer, F. W., Chain, P., Hauser, L., Lamerdin, J., Malfatti, S., Do, L., Land, M. L., Pelletier, D. A., Beatty, J. T., Lang, A. S., Tabita, F. R., Gibson, J. L., Hanson, T. E., Bobst, c., Torres y Torres, J. L., Peres, C., Harrison, F. H., Gibson, J., Harwood, C. S.

(2004). Complete genome sequence of the metabolically versatile photosynthetic bacterium *Rhodopseudomonas palustris*. *Nature Biotechnology*, *22*(1), 55-61.

Laskowski, R. A., MacArthur, M. W., Moss, D. S., & Thornton, J. M. (1993). PROCHECK: a program to check the stereochemical quality of protein structures. *Journal of Applied Crystallography*, *26*(2), 283-291.

Laskowski, R. A., Rullmann, J. A. C., MacArthur, M. W., Kaptein, R., & Thornton, J. M. (1996). AQUA and PROCHECK-NMR: programs for checking the quality of protein structures solved by NMR. *Journal of Biomolecular NMR*, *8*(4), 477-486.

Laurichesse, S., & Avérous, L. (2014). Chemical modification of lignins: towards biobased polymers. *Progress in Polymer Science*, *39*(7), 1266-1290.

Lavid, N., Wang, J., Shalit, M., Guterman, I., Bar, E., Beuerle, T., Menda, N., Shafir, S., Zamir, D., Adam, Z., Vainstein, A., Weiss, D., Pichersky, E & Lewinsohn, E. (2002). *O*-methyltransferases involved in the biosynthesis of volatile phenolic derivatives in rose petals. *Plant Physiology*, *129*(4), 1899-1907.

Lee, A. K., Banta, A. B., Wei, J. H., Kiemle, D. J., Feng, J., Giner, J. L., & Welander, P. V. (2018). C-4 sterol demethylation enzymes distinguish bacterial and eukaryotic sterol synthesis. *Proceedings of the National Academy of Sciences*, *115*(23), 5884-5889.

Lee, W. J., Lee, J. K., Chung, J., Cho, Y. J., & Park, D. H. (2010). Effects of electrochemical reduction reactions on the biodegradation of recalcitrant organic compounds (ROCs) and bacterial community diversity. *Journal of Microbiology and Biotechnology*, *20*(8), 1230-1239.

Leete, E., Bjorklund, J. A., Reineccius, G. A., & Cheng, T. B. (1992). Biosynthesis of 3-isopropyl-2-methoxypyrazine and other alkylpyrazines: widely distributed flavour compounds. *Bioformation of Flavours. The Royal Society of Chemistry, Cambridge*, *75*.

Lei, Y., Xie, S., Chen, H., Guan, X., & Zhang, Z. (2019). Behavior of 3-isobutyl-2-methoxypyrazine biosynthesis related to proposed precursor and intermediate in wine grape. *Food Chemistry*, *277*, 609-616.

Lema, C., Garcia-Jares, C., Orriols, I., & Angulo, L. (1996). Contribution of *Saccharomyces* and non-*Saccharomyces* populations to the production of some components of Albarino wine aroma. *American Journal of Enology and Viticulture*, *47*(2), 206-216.

Lepesheva, G. I., & Waterman, M. R. (2004). CYP51-the omnipotent P450. *Molecular and Cellular Endocrinology*, *215*(1-2), 165-170.

Lepesheva, G. I., & Waterman, M. R. (2007). Sterol 14α-demethylase cytochrome P450 (CYP51), a P450 in all biological kingdoms. *Biochimica et Biophysica Acta (BBA)-General Subjects*, *1770*(3), 467-477.

Lepesheva, G., & R Waterman, M. (2011). Sterol 14alpha-demethylase (CYP51) as a therapeutic target for human trypanosomiasis and leishmaniasis. *Current Topics in Medicinal Chemistry*, *11*(16), 2060-2071.

Leslie, M. (2011). Drug developers finally take aim at a neglected disease. *Science*, 333(6045), 933-935.

Li, H., Deng, Z., Liu, R., Loewen, S., & Tsao, R. (2014). Bioaccessibility, *in vitro* antioxidant activities and *in vivo* anti-inflammatory activities of a purple tomato (*Solanum lycopersicum* L.). *Food Chemistry*, *159*, 353-360.

Li, L., Popko, J. L., Zhang, X. H., Osakabe, K., Tsai, C. J., Joshi, C. P., & Chiang, V. L. (1997). A novel multifunctional *O*-methyltransferase implicated in a dual methylation pathway associated with lignin biosynthesis in loblolly pine. *Proceedings of the National Academy of Sciences*, *94*(10), 5461-5466.

Liang, C., Ristic, R., Jiranek, V., & Jeffery, D. W. (2018). Chemical and sensory evaluation of magnetic polymers as a remedial treatment for elevated concentrations of 3-isobutyl-2-methoxypyrazine in Cabernet Sauvignon grape must and wine. *Journal of Agricultural and Food Chemistry*, *66*(27), 7121-7130.

Ling, L. L., Keohavong, P., Dias, C., & Thilly, W. G. (1991). Optimization of the polymerase chain reaction with regard to fidelity: modified T7, Taq, and vent DNA polymerases. *Genome Research*, *1*(1), 63-69.

Liu, Y. J., Zhan, J., Liu, X. L., Wang, Y., Ji, J., & He, Q. Q. (2014). Dietary flavonoids intake and risk of type 2 diabetes: a meta-analysis of prospective cohort studies. *Clinical Nutrition*, *33*(1), 59-63.

Lomans, B. P., Van der Drift, C., Pol, A., & Den Camp, H. O. (2002). Microbial cycling of volatile organic sulfur compounds. *Cellular and Molecular Life Sciences CMLS*, *59*(4), 575-588.

Longo, R., Blackman, J. W., Torley, P. J., Rogiers, S. Y., & Schmidtke, L. M. (2017). Changes in volatile composition and sensory attributes of wines during alcohol content reduction. *Journal of the Science of Food and Agriculture*, *97*(1), 8-16.

Lopez, R., Ferreira, V., Hernandez, P., & Cacho, J. F. (1999). Identification of impact odorants of young red wines made with Merlot, Cabernet Sauvignon and Grenache grape varieties: a comparative study. *Journal of the Science of Food and Agriculture*, *79*(11), 1461-1467.

Lorist, M. M., & Tops, M. (2003). Caffeine, fatigue, and cognition. *Brain and Cognition*, *53*(1), 82-94.

Lüthy, R., Bowie, J. U., & Eisenberg, D. (1992). Assessment of protein models with three-dimensional profiles. *Nature*, *356*(6364), 83-85.

Lutz, S., Ostermeier, M., & Benkovic, S. J. (2001). Rapid generation of incremental truncation libraries for protein engineering using α-phosphothioate nucleotides. *Nucleic Acids Research*, *29*(4), e16-e16.

Madeira, F., Park, Y. M., Lee, J., Buso, N., Gur, T., Madhusoodanan, N., Basutkar, P., Tivey, A. R. N., Potter, S. C., Finn, R. D., Lopez, R. (2019). The EMBL-EBI search and sequence analysis tools APIs in 2019. *Nucleic Acids Research*, *47*(W1), W636-W641.

Maden, B. E. H. (2000). Tetrahydrofolate and tetrahydromethanopterin compared: functionally distinct carriers in C1 metabolism. *Biochemical Journal*, *350*(3), 609-629.

Madigan, M. T., Martinko, J. M., & Parker, J. (1997). Chapter 4 Nutrition, culture and metabolism of microorganisms. In *Brock Biology of Microorganisms* (Vol. 13). Pearson, Upper Saddle River, NJ.

Maga, J. A. (1990). Sensory and stability properties of added methoxypyrazines to model and authentic wines. In *Flavors and Off-flavors;* Proceedings of the 6th international flavor conference; Charalambous, G., Ed. (pp 61-70). Elsevier Science Publishers, Amsterdam, The Netherlands.

Maga, J. A., & Sizer, C. E. (1973). Pyrazines in foods. Review. *Journal of Agricultural and Food Chemistry*, *21*(1), 22-30.

Magyar, I., & Tóth, T. (2011). Comparative evaluation of some oenological properties in wine strains of *Candida stellata*, *Candida zemplinina*, *Saccharomyces uvarum* and *Saccharomyces cerevisiae*. *Food Microbiology*, *28*(1), 94-100.

Malin, G., & Erst, G. O. (1997). Algal production of dimethyl sulfide and its atmospheric role 1. *Journal of Phycology*, *33*(6), 889-896.

Mallinson, S. J., Machovina, M. M., Silveira, R. L., Garcia-Borràs, M., Gallup, N., Johnson, C. W., Allen, M. D., Skaf, M. S., Crowley, M. F., Neidle, E. L., Houk, K. N., Beckham, G. T., DuBois, J. L., McGeehan, J. E. (2018). A promiscuous cytochrome P450 aromatic *O*-demethylase for lignin bioconversion. *Nature Communications*, *9*(1), 1-12.

Malone, K. M., Farrell, D., Stuber, T. P., Schubert, O. T., Aebersold, R., Robbe-Austerman, S., & Gordon, S. V. (2017). Updated reference genome sequence and annotation of *Mycobacterium bovis* AF2122/97. *Genome Announcements*, *5*(14).

Mann, P. A., Parmegiani, R. M., Wei, S. Q., Mendrick, C. A., Li, X., Loebenberg, D., DiDomenico, B., Hare, R. S., Walker, S. S., McNicholas, P. M. (2003). Mutations in *Aspergillus fumigatus* resulting in reduced susceptibility to posaconazole appear to be restricted to a single amino acid in the cytochrome P450 14α-demethylase. *Antimicrobial Agents and Chemotherapy*, *47*(2), 577-581.

Mansour, M., Feicht, E. A., Behechti, A., Schramm, K. W., & Kettrup, A. (1999). Determination photostability of selected agrochemicals in water and soil. *Chemosphere*, *39*(4), 575-585.

Marais, J. (1994). Sauvignon Blanc cultivar aroma- a review. *South African Journal of Enology and Viticulture*, *15*(2), 41.

Martínez, Á. T., Speranza, M., Ruiz-Dueñas, F. J., Ferreira, P., Camarero, S., Guillén, F., Martínez, M. J., Gutiérrez, A., Río Andrade, J. C. D. (2005). Biodegradation of lignocellulosics: microbial, chemical, and enzymatic aspects of the fungal attack of lignin. *International Biology*, *8*, 195-204.

Masai, E., Sasaki, M., Minakawa, Y., Abe, T., Sonoki, T., Miyauchi, K., Katayama, Y., Fukuda, M. (2004). A novel tetrahydrofolate-dependent *O*-demethylase gene is essential for growth of *Sphingomonas paucimobilis* SYK-6 with syringate. *Journal of Bacteriology*, *186*(9), 2757-2765.

Masai, E., Katayama, Y., & Fukuda, M. (2007). Genetic and biochemical investigations on bacterial catabolic pathways for lignin-derived aromatic compounds. *Bioscience, Biotechnology, and Biochemistry*, *71*(1), 1-15.

Masai, E., Kamimura, N., Kasai, D., Oguchi, A., Ankai, A., Fukui, S., Takahashi, M., Yashiro, I., Sasaki, h., Harada, T., Nakamura, S., Katano, Y., Narita-Yamada, S., Nakazawa, H., Hara, H., Katayama, Y., Fukuda, M., Yamazaki, S., Fujita, N. (2012). Complete genome sequence of *Sphingobium* sp. strain SYK-6, a degrader of lignin-derived biaryls and monoaryls. *Journal of Bacteriology*. *194*(2). 534-535.

Mason, J. R., & Cammack, R. (1992). The electron-transport proteins of hydroxylating bacterial dioxygenases. *Annual Review of Microbiology*, *46*(1), 277-305.

Masuda, M., Satsuma, K., & Sato, K. (2012). An environmental fate study of methoxychlor using water-sediment model system. *Bioscience, Biotechnology, and Biochemistry*, *76*(1), 73-77.

Mateo, J. J., & Di Stefano, R. (1997). Description of the β-glucosidase activity of wine yeasts. *Food Microbiology*, *14*(6), 583-591.

Mateo, J. J., Peris, L., Ibañez, C., & Maicas, S. (2011). Characterization of glycolytic activities from non-*Saccharomyces* yeasts isolated from Bobal musts. *Journal of Industrial Microbiology & Biotechnology*, *38*(2), 347-354.

Matsuyama, A., Arai, R., Yashiroda, Y., Shirai, A., Kamata, A., Sekido, S., Kobayashi, Y., Hashimoto, A., Hamamota, M., Hiraoka, Y., Horinouchi, S., Yoshida, M. (2006). ORFeome cloning and global analysis of protein localization in the fission yeast *Schizosaccharomyces pombe*. *Nature Biotechnology*, *24*(7), 841-847.

Mattey, M., Harle, E. M. (1976). Aerobic metabolism of pyrazine compounds by a *Pseudomonas* species. *Biochemical Society Transactions*. *4*(3), 492-494.

Matthews, B. W. (1993). Structural and genetic analysis of protein stability. *Annual Review of Biochemistry*, *62*(1), 139-160.

Mayr, C. M., Geue, J. P., Holt, H. E., Pearson, W. P., Jeffery, D. W., & Francis, I. L. (2014). Characterization of the key aroma compounds in Shiraz wine by quantitation, aroma reconstitution, and omission studies. *Journal of Agricultural and Food Chemistry*, *62*(20), 4528–4536.

Mazzafera, P. (2002). Degradation of caffeine by microorganisms and potential use of decaffeinated coffee husk and pulp in animal feeding. *Scientia Agricola*, *59*(4), 815-821.

Mazzafera, P. (2004). Catabolism of caffeine in plants and microorganisms. *Frontiers Bioscience*, *9*, 1348-1359.

Mbuyane, L. L., de Kock, M., Bauer, F. F., & Divol, B. (2018). *Torulaspora delbrueckii* produces high levels of C5 and C6 polyols during wine fermentations. *FEMS Yeast Research*, *18*(7), foy084.

McCullum, E. O., Williams, B. A., Zhang, J., & Chaput, J. C. (2010). Random mutagenesis by error-prone PCR. In *In vitro Mutagenesis Protocols* (pp. 103-109). Humana Press, Totowa, NJ.

McLean, K. J., Leys, D., & Munro, A. W. (2015). Microbial cytochromes P450. In *Cytochrome P450* (pp. 261-407). Springer, Boston.

Measday, V., & Hieter, P. (2002). Synthetic dosage lethality. In *Methods in Enzymology* (pp. 316-326). Academic Press, Cambridge, US.

Mellado, E., Diaz-Guerra, T. M., Cuenca-Estrella, M., & Rodriguez-Tudela, J. L. (2001). Identification of two different 14-α sterol demethylase-related genes (*cyp51A* and *cyp51B*) in *Aspergillus fumigatus* and other *Aspergillus* species. *Journal of Clinical Microbiology*, *39*(7), 2431-2438.

Mendez-Costabel, M. P., Wilkinson, K. L., Bastian, S. E. P., Jordans, C., McCarthy, M., Ford, C. M., & Dokoozlian, N. (2014). Effect of winter rainfall on yield components and fruit green aromas of *Vitis vinifera* L. *cv*. Merlot in California. *Australian Journal of Grape and Wine Research*, *20*(1), 100-110.

Mendez-Costabel, M. P., Wilkinson, K. L., Bastian, S. E., McCarthy, M., Ford, C. M., & Dokoozlian, N. (2013). Seasonal and regional variation of green aroma compounds in commercial vineyards of *Vitis vinifera* L. Merlot in California. *American Journal of Enology and Viticulture*, *64*(4), 430-436.

Merín, M. G., & de Ambrosini, V. I. M. (2018). Kinetic and metabolic behaviour of the pectinolytic strain *Aureobasidium pullulans* GM-R-22 during pre-fermentative cold maceration and its effect on red wine quality. *International Journal of Food Microbiology*, *285*, 18-26.

Merín, M. G., Martín, M. C., Rantsiou, K., Cocolin, L., & de Ambrosini, V. I. M. (2015). Characterization of pectinase activity for enology from yeasts occurring in Argentine Bonarda grape. *Brazilian Journal of Microbiology*, *46*(3), 815-823.

Michaels, G. B., & Lewis, D. L. (1985). Sorption and toxicity of azo and triphenylmethane dyes to aquatic microbial populations. *Environmental Toxicology and Chemistry: An International Journal*, *4*(1), 45-50.

Middelhoven, W. J. (1993). Catabolism of benzene compounds by ascomycetous and basidiomycetous yeasts and yeastlike fungi. *Antonie van Leeuwenhoek*, *63*(2), 125-144.

Middelhoven, W. J. (1997). Identity and biodegradative abilities of yeasts isolated from plants growing in an arid climate. *Antonie van Leeuwenhoek*, *72*(2), 81-89.

Mihara, S., & Masuda, H. (1988). Structure-odor relationships for disubstituted pyrazines. *Journal of Agricultural and Food Chemistry*, *36*(6), 1242-1247.

Miller, G. H. (2019). Whiskey Science: A Condensed Distillation. Springer, Cham, Switzerland.

MillerIII, A., Scanlan, R. A., Lee, J. S., Libbey, L. M., & Morgan, M. E. (1973). Volatile compounds produced in sterile fish muscle (*Sebastes melanops*) by *Pseudomonas perolens*. *Applied Microbiology, 25*(2), 257-261.

Miyazawa, M., Ando, H., Okuno, Y., & Araki, H. (2004). Biotransformation of isoflavones by *Aspergillus niger*, as biocatalyst. *Journal of Molecular Catalysis B: Enzymatic*, *27*(2-3), 91-95.

Miyazawa, M., Takahashi, K., & Araki, H. (2006). Biotransformation of isoflavones by *Aspergillus niger* as biocatalyst. *Journal of Chemical Technology & Biotechnology: International Research in Process, Environmental & Clean Technology*, *81*(4), 674-678.

Mizunoe, Y., Wai, S. N., Takade, A., & Yoshida, S. I. (1999). Restoration of culturability of starvation-stressed and low-temperature-stressed *Escherichia coli* O157 cells by using H_2O_2-degrading compounds. *Archives of Microbiology*, *172*(1), 63-67.

Mondolfi, A. P., Stavropoulos, C., Gelanew, T., Loucas, E., Alvarez, A. P., Benaim, G., Polsky, B., Schoenian, G., Sordillo, E. M. (2011). Successful treatment of old world cutaneous leishmaniasis caused by *Leishmania infantum* with posaconazole. *Antimicrobial Agents and Chemotherapy*, *55*(4), 1774-1776.

Monk, B. C., Tomasiak, T. M., Keniya, M. V., Huschmann, F. U., Tyndall, J. D., O'Connell, J. D., Cannon, R. D., McDonald, J. G., Rodriguez, A., Finer-Moore, J. S., Stroud, R. M. (2014). Architecture of a single membrane spanning cytochrome P450 suggests constraints

that orient the catalytic domain relative to a bilayer. *Proceedings of the National Academy of Sciences*, *111*(10), 3865-3870.

Moore, J. C., & Arnold, F. H. (1996). Directed evolution of a *para*-nitrobenzyl esterase for aqueous-organic solvents. *Nature Biotechnology*, *14*(4), 458-467.

Moran, M. A., Buchan, A., González, J. M., Heidelberg, J. F., Whitman, W. B., Kiene, R. P., Henriksen, J. R., King, G. M., Belas, R., Fuqua, cl., Brinkac, L., Lewis, M., Johri, S., Weaver, B., Pai, G., Eisen, J. A., Rahe, E., Sheldon, W. M., Ye, W., Miller, T. R., Carlton, J., Rasko, D. A., Paulsen, I. T., Ren, Q., Daugherty, S. C., Deboy, R. T., Dodson, R. J., Durkin, A. S. Madupu, R., Nelson, W. C., Sullivan, S. AL., Rosovitz, M. J., Haft, D. H., Selengut, J., Ward, N. (2004). Genome sequence of *Silicibacter pomeroyi* reveals adaptations to the marine environment. *Nature*, *432*(7019), 910-913.

Morawski, B., Segura, A., & Ornston, L. N. (2000). Substrate Range and Genetic Analysis of *Acinetobacter* Vanillate Demethylase. *Journal of Bacteriology*, *182*(5), 1383-1389.

Moreira, N., De Pinho, P. G., Santos, C., & Vasconcelos, I. (2010). Volatile sulphur compounds composition of monovarietal white wines. *Food Chemistry*, *123*(4), 1198-1203.

Moreira, N., Mendes, F., de Pinho, P. G., Hogg, T., & Vasconcelos, I. (2008). Heavy sulphur compounds, higher alcohols and esters production profile of *Hanseniaspora uvarum* and *Hanseniaspora guilliermondii* grown as pure and mixed cultures in grape must. *International Journal of Food Microbiology*, *124*(3), 231-238.

Moreno, J. J., Millán, C., Ortega, J. M., & Medina, M. (1991). Analytical differentiation of wine fermentations using pure and mixed yeast cultures. *Journal of Industrial Microbiology*, *7*(3), 181-189.

Morvan, X., Mouvet, C., Baran, N., & Gutierrez, A. (2006). Pesticides in the groundwater of a spring draining a sandy aquifer: temporal variability of concentrations and fluxes. *Journal of Contaminant Hydrology*, *87*(3-4), 176-190.

Moyano, L., Zea, L., Moreno, J., & Medina, M. (2002). Analytical study of aromatic series in sherry wines subjected to biological aging. *Journal of Agricultural and Food Chemistry*, *50*(25), 7356–7361.

Muir, D. C., & Yarechewski, A. L. (1984). Degradation of methoxychlor in sediments under various redox conditions. *Journal of Environmental Science & Health Part B*, *19*(3), 271-295.

Müller, E., Fahlbusch, K., Walther, R., & Gottschalk, G. (1981). Formation of *N*, *N*-dimethylglycine, acetic acid, and butyric acid from betaine by *Eubacterium limosum*. *Applied and Environmental Microbiology*, *42*(3), 439-445.

Müller, R., & Rappert, S. (2010). Pyrazines: occurrence, formation and biodegradation. *Applied Microbiology and Biotechnology*, *85*(5), 1315-1320.

Müller, W., Weber, H., Meyer, F., & Weissmann, C. (1978). Site-directed mutagenesis in DNA: Generation of point mutations in cloned β globin complementary DNA at the positions corresponding to amino acids 121 to 123. *Journal of Molecular Biology*, *124*(2), 343-358.

Murray, K. E., & Whitfield, F. B. (1975). The occurrence of 3-alkyl-2-methoxypyrazines in raw vegetables. *Journal of the Science of Food and Agriculture*, *26*(7), 973-986.

Nakatsu, C. H., Straus, N. A., & Wyndham, R. C. (1995). The nucleotide sequence of the Tn5271 3-chlorobenzoate 3, 4-dioxygenase genes (*cbaAB*) unites the class IA oxygenases in a single lineage. *Microbiology*, *141*(2), 485-495.

Nierman, W. C., Pain, A., Anderson, M. J., Wortman, J. R., Kim, H. S., Arroyo, J., Berriman, M., Abe, K., Archer, D. B., Bermejo, C., Bennett, J., Bowyer, P., Chen, D., Collins, M., Coulsen, R., Davies, R., Dyer, P. S., Farman, M., Fedorova, N., Fedorova, N., Feldblyum, T. V., Fischer, R., Fosker, N., Fraser, A., García, J. L., García, M. J., Denning, D. W. (2005). Genomic sequence of the pathogenic and allergenic filamentous fungus *Aspergillus fumigatus*. *Nature*, *438*(7071), 1151-1156.

Niewmierzycka, A., & Clarke, S. (1999). *S*-adenosylmethionine-dependent methylation in *Saccharomyces cerevisiae* identification of a novel protein arginine methyltransferase. *Journal of Biological Chemistry*, *274*(2), 814-824.

Nishikawa, S., Sonoki, T., Kasahara, T., Obi, T., Kubota, S., Kawai, S., Morohoshi, N., Katayama, Y. (1998). Cloning and sequencing of the *Sphingomonas* (*Pseudomonas*) *paucimobilis* gene essential for the *O*-demethylation of vanillate and syringate. *Applied and Environmental Microbiology*, *64*(3), 836-842.

Noble, A. C., Elliott-Fisk, D. L., & Allen, M. S. (1995). Vegetative flavor and methoxypyrazines in Cabernet Sauvignon. In *Fruit Flavors: Biogenesis, Characterization, and Authentication* (*pp* 226-233). ACS symposium series, US.

Nursten, H. E., & Sheen, M. R. (1974). Volatile flavour components of cooked potato. *Journal of the Science of Food and Agriculture*, *25*(6), 643-663.

Okuno, Y., & Miyazawa, M. (2004). Biotransformation of nobiletin by *Aspergillus niger* and the antimutagenic activity of a metabolite, 4'-hydroxy-5, 6, 7, 8, 3'-pentamethoxyflavone. *Journal of Natural Products*, *67*(11), 1876-1878.

Okuno, Y., & Miyazawa, M. (2006). Microbial *O*-demethylation of sinesetin and antimutagenic activity of the metabolite. *Journal of Chemical Technology & Biotechnology: International Research in Process, Environmental & Clean Technology*, *81*(1), 29-33.

Oliver, J. D. (2000). The public health significance of viable but nonculturable bacteria. In *Nonculturable Microorganisms in the Environment* (pp. 277-300). Springer, Boston, MA.

O'Neill, K. R., Jones, S. H., & Grimes, D. J. (1992). Seasonal incidence of *Vibrio vulnificus* in the Great Bay estuary of New Hampshire and Maine. *Applied and Environmental Microbiology*, *58*(10), 3257-3262.

Oren, A. (1990). Formation and breakdown of glycine betaine and trimethylamine in hypersaline environments. *Antonie van Leeuwenhoek*, *58*(4), 291-298.

Padilla, B., Gil, J. V., & Manzanares, P. (2018). Challenges of the non-conventional yeast *Wickerhamomyces anomalus* in winemaking. *Fermentation*, *4*(3), 68.

Parapouli, M., Hatziloukas, E., Drainas, C., & Perisynakis, A. (2010). The effect of Debina grapevine indigenous yeast strains of *Metschnikowia* and *Saccharomyces* on wine flavour. *Journal of Industrial Microbiology & Biotechnology*, *37*(1), 85.

Paul, L., Ferguson, D. J., & Krzycki, J. A. (2000). The trimethylamine methyltransferase gene and multiple dimethylamine methyltransferase genes of *Methanosarcina barkeri* contain in-frame and read-through amber codons. *Journal of Bacteriology*, *182*(9), 2520-2529.

Pavel, E. G., Martins, L. J., Ellis Jr, W. R., & Solomon, E. I. (1994). Magnetic circular dichroism studies of exogenous ligand and substrate binding to the non-heme ferrous active site in phthalate dioxygenase. *Chemistry & Biology*, *1*(3), 173-183.

Peinado, R. A., Moreno, J., Bueno, J. E., Moreno, J. A., & Mauricio, J. C. (2004). Comparative study of aromatic compounds in two young white wines subjected to pre-fermentative cryomaceration. *Food Chemistry*, *84*(4), 585–590.

Pereira, C. S., Marques, J. F., & San Romao, M. V. (2000). Cork taint in wine: scientific knowledge and public perception - a critical review. *Critical Reviews in Microbiology*, *26*(3), 147-162.

Pérès, F., Florin, D., Grollier, T., Feurtet-Mazel, A., Coste, M., Ribeyre, F., Ricard, M., Boudou, A. (1996). Effects of the phenylurea herbicide isoproturon on periphytic diatom communities in freshwater indoor microcosms. *Environmental Pollution*, *94*(2), 141-152.

Perry, C., De los Santos, E. L., Alkhalaf, L. M., & Challis, G. L. (2018). Rieske non-heme iron-dependent oxygenases catalyse diverse reactions in natural product biosynthesis. *Natural Product Reports*, *35*(7), 622-632.

Pettersen, E. F., Goddard, T. D., Huang, C. C., Couch, G. S., Greenblatt, D. M., Meng, E. C., & Ferrin, T. E. (2004). UCSF Chimera - a visualization system for exploratory research and analysis. *Journal of Computational Chemistry*, *25*(13), 1605-1612.

Phillips, D. A., Sande, E. S., Vriezen, J. A. C., de Bruijn, F. J., Le Rudulier, D., & Joseph, C. M. (1998). A new genetic locus in *Sinorhizobium meliloti* is involved in stachydrine utilization. *Applied and Environmental Microbiology*, *64*(10), 3954-3960.

Pickering, G., Inglis, D., Botezatu, A., Beh, A., Humes, E., & Brindle, I. (2014). New approaches to removing alkyl-methoxypyrazines from grape juice and wine. *Scientific Bulletin. Series F. Biotechnologies*, *18*, 130-134.

Pickering, G., Lin, J., Reynolds, A., Soleas, G., & Riesen, R. (2006). The evaluation of remedial treatments for wine affected by *Harmonia axyridis*. *International Journal of Food Science & Technology*, *41*(1), 77-86.

Pickering, G. J., Spink, M., Kotseridis, Y., Inglis, D., Brindle, I. D., Sears, M., & Beh, A. L. (2008). Yeast strain affects 3-isopropyl-2-methoxypyrazine concentration and sensory

profile in Cabernet Sauvignon wine. *Australian Journal of Grape and Wine Research*, *14*(3), 230-237.

Pickering, G. J., Spink, M., Kotseridis, Y., Brindle, I. D., Sears, M., & Inglis, D. (2008). Morbidity of *Harmonia axyridis* mediates ladybug taint in red wine.

Picking, J. W., Behrman, E. J., Zhang, L., & Krzycki, J. A. (2019). MtpB, a member of the MttB superfamily from the human intestinal acetogen *Eubacterium limosum*, catalyzes proline betaine demethylation. *Journal of Biological Chemistry*, *294*(37), 13697-13707.

Pietila, M. P., Vohra, P. K., Sanyal, B., Wengenack, N. L., Raghavakaimal, S., & Thomas Jr, C. F. (2006). Cloning and characterization of CYP51 from *Mycobacterium avium*. *American Journal of Respiratory Cell and Molecular Biology*, *35*(2), 236-242.

Pinazo, M. J., Espinosa, G., Gállego, M., López-Chejade, P. L., Urbina, J. A., & Gascón, J. (2010). Successful treatment with posaconazole of a patient with chronic Chagas disease and systemic lupus erythematosus. *The American Journal of Tropical Medicine and Hygiene*, *82*(4), 583-587.

Podust, L. M., Poulos, T. L., & Waterman, M. R. (2001a). Crystal structure of cytochrome P450 14α-sterol demethylase (CYP51) from *Mycobacterium tuberculosis* in complex with azole inhibitors. *Proceedings of the National Academy of Sciences*, *98*(6), 3068-3073.

Podust, L. M., Stojan, J., Poulos, T. L., & Waterman, M. R. (2001b). Substrate recognition sites in 14α-sterol demethylase from comparative analysis of amino acid sequences and X-ray structure of *Mycobacterium tuberculosis* CYP51. *Journal of Inorganic Biochemistry*, *87*(4), 227-235.

Podust, L. M., Yermalitskaya, L. V., Lepesheva, G. I., Podust, V. N., Dalmasso, E. A., & Waterman, M. R. (2004). Estriol bound and ligand-free structures of sterol 14α-demethylase. *Structure*, *12*(11), 1937-1945.

Podust, L. M., von Kries, J. P., Eddine, A. N., Kim, Y., Yermalitskaya, L. V., Kuehne, R., Ouellet, H., Warrier, T., Altekös ter, M., Lee, J.-S., Rademann, J., Oschkinat, H., Kaufmann, S. H. E., Waterman, M. R. (2007). Small-molecule scaffolds for CYP51 inhibitors identified by high-throughput screening and defined by X-ray crystallography. *Antimicrobial Agents and Chemotherapy*, *51*(11), 3915-3923.

Pometto III, A. L., Sutherland, J. B., & Crawford, D. L. (1981). *Streptomyces setonii*: catabolism of vanillic acid via guaiacol and catechol. *Canadian Journal of Microbiology*, *27*(6), 636-638.

Pontius, J., Richelle, J., & Wodak, S. J. (1996). Deviations from standard atomic volumes as a quality measure for protein crystal structures. *Journal of Molecular Biology*, *264*(1), 121-136.

Pramanik, S. K., Bhattacharyya, J., Dutta, S., Dey, P. K., & Bhattacharyya, A. (2006). Persistence of Acetamiprid in/on Mustard (*Brassica juncea* L.). *Bulletin of Environmental Contamination & Toxicology*, *76*(2).

Prelich, G. (2012). Gene overexpression: uses, mechanisms, and interpretation. *Genetics*, *190*(3), 841-854.

Pretorius, I. S., Van der Westhuizen, T. J., & Augustyn, O. P. H. (1999). Yeast biodiversity in vineyards and wineries and its importance to the South African wine industry. A review. *South African Journal of Enology and Viticulture*, *20*(2), 61-70.

Priefert, H., Rabenhorst, J., & Steinbüchel, A. (1997). Molecular characterization of genes of *Pseudomonas* sp. strain HR199 involved in bioconversion of vanillin to protocatechuate. *Journal of Bacteriology*, *179*(8), 2595-2607.

Puspita, I. D., Kamagata, Y., Tanaka, M., Asano, K., & Nakatsu, C. H. (2012). Are uncultivated bacteria really uncultivable? *Microbes and Environments*, *27(*4*),* 356-366.

Radler, F., & Schütz, H. (1982). Glycerol production of various strains of *Saccharomyces*. *American Journal of Enology and Viticulture*, *33*(1), 36-40.

Rajchl, A., Cizkova, H., Voldrich, M., Lukesova, D., Panovska, Z. (2009). Methoxypyrazines in Sauvignon Blanc wines, detection of addition of artificial aroma. *Czech Journal of Food Sciences*, *27*(4), 259-266.

Rajini, K. S., Aparna, P., Sasikala, C., & Ramana, C. V. (2011). Microbial metabolism of pyrazines. *Critical Reviews in Microbiology*, *37*(2), 99-112.

Ram, V. J., Sethi, A., Nath, M., & Pratap, R. (2019). *The Chemistry of Heterocycles: Nomenclature and Chemistry of Three to Five Membered Heterocycles*. Elsevier, Amsterdam, Netherlands.

Rankine, B. C. (1972). Influence of yeast strain and malo-lactic fermentation on composition and quality of table wines. *American Journal of Enology and Viticulture*, *23*(4), 152-158.

Rankine, B. C., Pocock, K. F. (1970). Alkalimetric determination of sulphur dioxide in wine. *The Australian Wine Brewing and Spirit Review*, *88*(8): 40, 42, 44.

Rappert, S., Botsch, K. C., Nagorny, S., Francke, W., & Müller, R. (2006). Degradation of 2, 3-diethyl-5-methylpyrazine by a newly discovered bacterium, *Mycobacterium* sp. strain DM-11. *Applied and Environmental Microbiology*, *72*(2), 1437-1444.

Rappert, S., Li, R., Kokova, M., Antholz, M., Nagorny, S., Francke, W., & Müller, R. (2007). Degradation of 2, 5-dimethylpyrazine by *Rhodococcus erythropolis* strain DP-45 isolated from a waste gas treatment plant of a fishmeal processing company. *Biodegradation*, *18*(5), 585-596.

Rappert, S., & Müller, R. (2005). Microbial degradation of selected odorous substances. *Waste Management*, *25*(9), 940-954.

Rasila, T. S., Pajunen, M. I., & Savilahti, H. (2009). Critical evaluation of random mutagenesis by error-prone polymerase chain reaction protocols, *Escherichia coli* mutator strain, and hydroxylamine treatment. *Analytical Biochemistry*, *388*(1), 71-80.

Reetz, M. T., Carballeira, J. D., & Vogel, A. (2006). Iterative saturation mutagenesis on the basis of B factors as a strategy for increasing protein thermostability. *Angewandte Chemie*, *118*(46), 7909-7915.

Reetz, M. T., & Carballeira, J. D. (2007). Iterative saturation mutagenesis (ISM) for rapid directed evolution of functional enzymes. *Nature Protocols*, *2*(4), 891.

Reetz, M. T., Prasad, S., Carballeira, J. D., Gumulya, Y., & Bocola, M. (2010). Iterative saturation mutagenesis accelerates laboratory evolution of enzyme stereoselectivity: rigorous comparison with traditional methods. *Journal of the American Chemical Society*, *132*(26), 9144-9152.

Reisch, C. R., Moran, M. A., & Whitman, W. B. (2008). Dimethylsulfoniopropionate-dependent demethylase (DmdA) from *Pelagibacter ubique* and *Silicibacter pomeroyi*. *Journal of Bacteriology*, *190*(24), 8018-8024.

Reisch, C. R., Stoudemayer, M. J., Varaljay, V. A., Amster, I. J., Moran, M. A., & Whitman, W. B. (2011). Novel pathway for assimilation of dimethylsulphoniopropionate widespread in marine bacteria. *Nature*, *473*(7346), 208-211.

Reisch, C. R., Crabb, W. M., Gifford, S. M., Teng, Q., Stoudemayer, M. J., Moran, M. A., & Whitman, W. B. (2013). Metabolism of dimethylsulphoniopropionate by *Ruegeria pomeroyi* DSS-3. *Molecular Microbiology*, *89*(4), 774-791.

Reisky, L., Büchsenschütz, H. C., Engel, J., Song, T., Schweder, T., Hehemann, J. H., & Bornscheuer, U. T. (2018). Oxidative demethylation of algal carbohydrates by cytochrome P450 monooxygenases. *Nature Chemical Biology*, *14*(4), 342-344.

Renault, P., Miot-Sertier, C., Marullo, P., Hernández-Orte, P., Lagarrigue, L., Lonvaud-Funel, A., & Bely, M. (2009). Genetic characterization and phenotypic variability in *Torulaspora delbrueckii* species: potential applications in the wine industry. *International Journal of Food Microbiology*, *134*(3), 201-210.

Retnadhas, S., & Gummadi, S. N. (2018). Identification and characterization of oxidoreductase component (NdmD) of methylxanthine oxygenase system in *Pseudomonas* sp. NCIM 5235. *Applied Microbiology and Biotechnology*, *102*(18), 7913-7926.

Resnick, S. M., Lee, K., & Gibson, D. T. (1996). Diverse reactions catalyzed by naphthalene dioxygenase from *Pseudomonas* sp strain NCIB 9816. *Journal of Industrial Microbiology*, *17*(5-6), 438-457.

Reynolds, C. R., Islam, S. A., & Sternberg, M. J. (2018). EzMol: a web server wizard for the rapid visualization and image production of protein and nucleic acid structures. *Journal of Molecular Biology*, *430*(15), 2244-2248.

Ribéreau-Gayon, P., Dubourdieu, D., Donèche, B., & Lonvaud, A. (Eds.). (2006). *Handbook of Enology, Volume 1: The Microbiology of Wine and Vinifications* (Vol. 1). John Wiley & Sons, US.

Rivers, A. R., Smith, C. B., & Moran, M. A. (2014). An updated genome annotation for the model marine bacterium *Ruegeria pomeroyi* DSS-3. *Standards in Genomic Sciences*, *9*(1), 11.

Robb, C. S., Reisky, L., Bornscheuer, U. T., & Hehemann, J. H. (2018). Specificity and mechanism of carbohydrate demethylation by cytochrome P450 monooxygenases. *Biochemical Journal*, *475*(23), 3875-3886.

Robert, L. D., Rydel, T. J., Storek, M. J., Sturman, E. J., Moshiri, F., Bartlett, R. K., Brown, G. R., Eilers, R. J., Dart, C., Qi, Y., Flasinski, S., Franklin, S. J. (2009). Dicamba

monooxygenase: structural insights into a dynamic Rieske oxygenase that catalyzes an exocyclic monooxygenation. *Journal of Molecular Biology*, *392*(2), 481-497.

Robin, J., Gueroult, M., Cheikhrouhou, R., Guicherd, M., Borsenberger, V., Marty, A., & Bordes, F. (2019). Identification of a crucial amino acid implicated in the hydroxylation/desaturation ratio of CpFAH12 bifunctional hydroxylase. *Biotechnology and Bioengineering*, *116*(10), 2451-2462.

Robinson, A. L., Ebeler, S. E., Heymann, H., Boss, P. K., Solomon, P. S., & Trengove, R. D. (2009). Interactions between wine volatile compounds and grape and wine matrix components influence aroma compound headspace partitioning. *Journal of Agricultural and Food Chemistry*, *57*(21), 10313-10322.

Rodríguez, M. E., Lopes, C. A., Barbagelata, R. J., Barda, N. B., & Caballero, A. C. (2010). Influence of *Candida pulcherrima* Patagonian strain on alcoholic fermentation behaviour and wine aroma. *International Journal of Food Microbiology*, *138*(1-2), 19-25.

Roh, C., Seo, S. H., Choi, K. Y., Cha, M., Pandey, B. P., Kim, J. H., Park, J. -S., Kim, D. H., Chang, I. S., Kim, B. G. (2009). Regioselective hydroxylation of isoflavones by *Streptomyces avermitilis* MA-4680. *Journal of Bioscience and Bioengineering*, *108*(1), 41-46.

Rojas, V., Gil, J. V., Piñaga, F., & Manzanares, P. (2003). Acetate ester formation in wine by mixed cultures in laboratory fermentations. *International Journal of Food Microbiology*, *86*(1-2), 181-188.

Roncoroni, M., Santiago, M., Hooks, D. O., Moroney, S., Harsch, M. J., Lee, S. A., Richards, K. D., Nicolau, L., Gardner, R. C. (2011). The yeast IRC7 gene encodes a *β*-lyase responsible for production of the varietal thiol 4-mercapto-4-methylpentan-2-one in wine. *Food Microbiology*, *28*(5), 926-935.

Rondon, M. R., Goodman, R. M., & Handelsman, J. (1999). The Earth's bounty: assessing and accessing soil microbial diversity. *Trends in Biotechnology*, *17*(10), 403-409.

Rosi, I., Vinella, M., & Domizio, P. (1994). Characterization of *β*-glucosidase activity in yeasts of oenological origin. *Journal of Applied Bacteriology*, *77*(5), 519-527.

Roujou de Boubée, D. R., Cumsille, A. M., Pons, M., & Dubourdieu, D. (2002). Location of 2-methoxy-3-isobutylpyrazine in Cabernet Sauvignon grape bunches and its extractability during vinification. *American Journal of Enology and Viticulture*, *53*(1), 1-5.

Roujou de Boubée, D., Van Leeuwen, C., & Dubourdieu, D. (2000). Organoleptic impact of 2-methoxy-3-isobutylpyrazine on red Bordeaux and Loire wines. Effect of environmental conditions on concentrations in grapes during ripening. *Journal of Agricultural and Food Chemistry*, *48*(10), 4830-4834.

Roujou de Boubée, D. (2003). Research on 2-methoxy-3-isobutylpyrazine in grapes and wine. *Academie Amorim, Bordeaux*.

Roy, A., Kucukural, A., & Zhang, Y. (2010). I-TASSER: a unified platform for automated protein structure and function prediction. *Nature Protocols*, *5*(4), 725-738.

Ryona, I., Leclerc, S., & Sacks, G. L. (2010). Correlation of 3-isobutyl-2-methoxypyrazine to 3-isobutyl-2-hydroxypyrazine during maturation of bell pepper (*Capsicum annuum*) and wine grapes (*Vitis vinifera*). *Journal of Agricultural and Food Chemistry*, *58*(17), 9723-9730.

Ryona, I., Pan, B. S., Intrigliolo, D. S., Lakso, A. N., & Sacks, G. L. (2008). Effects of cluster light exposure on 3-isobutyl-2-methoxypyrazine accumulation and degradation patterns in red wine grapes (*Vitis vinifera* L. *cv*. Cabernet Franc). *Journal of Agricultural and Food Chemistry*, *56*(22), 10838-10846.

Ryona, I., Reinhardt, J., & Sacks, G. L. (2012). Treatment of grape juice or must with silicone reduces 3-alkyl-2-methoxypyrazine concentrations in resulting wines without altering fermentation volatiles. *Food Research International*, *47*(1), 70-79.

Sala, C., Busto, O., Guasch, J., & Zamora, F. (2004). Influence of vine training and sunlight exposure on the 3-alkyl-2-methoxypyrazines content in musts and wines from the *Vitis vinifera* variety Cabernet Sauvignon. *Journal of Agricultural and Food Chemistry*, *52*(11), 3492-3497.

Sala, C., Busto, O., Guasch, J., & Zamora, F. (2005). Contents of 3-alkyl-2-methoxypyrazines in musts and wines from *Vitis vinifera* variety Cabernet Sauvignon: influence of irrigation and plantation density. *Journal of the Science of Food and Agriculture, 85* (7), 1131-1136.

Sala, C., Mestres, M., Marti, M. P., Busto, O., & Guasch, J. (2002). Headspace solid-phase microextraction analysis of 3-alkyl-2-methoxypyrazines in wines. *Journal of Chromatography A, 953* (1-2), 1-6.

Sadoudi, M., Rousseaux, S., David, V., Alexandre, H., & Tourdot-Maréchal, R. (2017). *Metschnikowia pulcherrima* influences the expression of genes involved in PDH bypass and glyceropyruvic fermentation in *Saccharomyces cerevisiae*. *Frontiers in Microbiology*, *8*, 1137.

Sadoudi, M., Tourdot-Maréchal, R., Rousseaux, S., Steyer, D., Gallardo-Chacón, J. J., Ballester, J., Vichi, S., Guérin-Schneider, R., Caixach, J., Alexandre, H. (2012). Yeast–yeast interactions revealed by aromatic profile analysis of Sauvignon Blanc wine fermented by single or co-culture of non-*Saccharomyces* and *Saccharomyces* yeasts. *Food Microbiology*, *32*(2), 243-253.

Sanchez-Gonzalez, M., & Rosazza, J. P. N. (2004). Microbial transformations of chalcones: hydroxylation, *O*-demethylation, and cyclization to flavanones. *Journal of Natural Products*, *67*(4), 553-558.

Santos, I. S., Ponte, B. M., Boonme, P., Silva, A. M., & Souto, E. B. (2013). Nanoencapsulation of polyphenols for protective effect against colon–rectal cancer. *Biotechnology Advances*, *31*(5), 514-523.

Sarnaik, S., & Kanekar, P. (1999). Biodegradation of methyl violet by *Pseudomonas mendocina* MCM B-402. *Applied Microbiology and Biotechnology*, *52*(2), 251-254.

Satsuma, K., Masuda, M., & Sato, K. (2012). *O*-Demethylation and successive oxidative dechlorination of methoxychlor by *Bradyrhizobium* sp. strain 17-4, isolated from river sediment. *Applied and Environmental Microbiology*, *78*(15), 5313-5319.

Scanes, K. T., Hohrnann, S., & Prior, B. A. (1998). Glycerol production by the yeast *Saccharomyces cerevisiae* and its relevance to wine: a review. *South African Journal of Enology and Viticulture*, *19*(1), 17-24.

Schmid, A., Dordick, J. S., Hauer, B., Kiener, A., Wubbolts, M., & Witholt, B. (2001). Industrial biocatalysis today and tomorrow. *Nature*, *409*(6817), 258-268.

Schmidlin, L., Poutaraud, A., Claudel, P., Mestre, P., Prado, E., Santos-Rosa, M., Wiedemann-Merdinoglu, S., Karst, F., Merdinoglu, D., & Hugueney, P. (2008). A stress-inducible resveratrol *O*-methyltransferase involved in the biosynthesis of pterostilbene in grapevine. *Plant Physiology*, *148*(3), 1630-1639.

Schnekenburger, M., Dicato, M., & Diederich, M. (2014). Plant-derived epigenetic modulators for cancer treatment and prevention. *Biotechnology Advances*, *32*(6), 1123-1132.

Schuller, D. J., Reisch, C. R., Moran, M. A., Whitman, W. B., & Lanzilotta, W. N. (2012). Structures of dimethylsulfoniopropionate-dependent demethylase from the marine organism *Pelagabacter ubique*. *Protein Science*, *21*(2), 289-298.

Schweigert, N., Zehnder, A. J., & Eggen, R. I. (2001). Chemical properties of catechols and their molecular modes of toxic action in cells, from microorganisms to mammals: minireview. *Environmental Microbiology*, *3*(2), 81-91.

Segura, A., Bünz, P. V., D'Argenio, D. A., & Ornston, L. N. (1999). Genetic Analysis of a chromosomal region containing *vanA* and *vanB*, genes required for conversion of either ferulate or vanillate to protocatechuate in *Acinetobacter*. *Journal of Bacteriology*, *181*(11), 3494-3504.

Seifert, R. M., Buttery, R. G., Guadagni, D. G., Black, D. R., & Harris, J. G. (1970). Synthesis of some 2-methoxy-3-alkylpyrazines with strong bell pepper-like odors. *Journal of Agricultural and Food Chemistry*, *18*(2), 246-249.

Shao, Y. H., Guo, L. Z., Zhang, Y. Q., Yu, H., Zhao, B. S., Pang, H. Q., & Lu, W. D. (2018). Glycine betaine monooxygenase, an unusual Rieske-type oxygenase system, catalyzes the oxidative *N*-demethylation of glycine betaine in *Chromohalobacter salexigens* DSM 3043. *Applied and Environmental Microbiology*, *84*(13).

Shen, C., Shan, T., Zhao, W., Ou, C., Li, L., Liu, X., Liu, J., Yu, B. (2019a). Regio-and enantioselective *O*-demethylation of tetrahydroprotoberberines by cytochrome P450 enzyme system from *Streptomyces griseus* ATCC 13273. *Applied Microbiology and Biotechnology*, *103*(2), 761-776.

Shen, C., Zhao, W., Liu, X., & Liu, J. (2019b). Enzyme-catalyzed regio-selective demethylation of papaverine by CYP105D1. *Biotechnology Letters*, *41*(1), 171-180.

Sidhu, D., Lund, J., Kotseridis, Y., & Saucier, C. (2015). Methoxypyrazine analysis and influence of viticultural and enological procedures on their levels in grapes, musts, and wines. *Critical Reviews in Food Science and Nutrition*, *55*(4), 485-502.

Sinha, N. K., & Haimes, M. D. (1981). Molecular mechanisms of substitution mutagenesis. An experimental test of the Watson-Crick and topal-fresco models of base mispairings. *Journal of Biological Chemistry*, *256*(20), 10671-10683.

Siriwardena, A. H., Tian, F., Noble, S., & Prestegard, J. H. (2002). A straightforward NMR-spectroscopy-based method for rapid library screening. *Angewandte Chemie International Edition*, *41*(18), 3454-3457.

Smith, A. (2002). Effects of caffeine on human behavior. *Food and Chemical Toxicology*, *40*(9), 1243-1255.

Smith, V., & Rosazza. P., (1974). Microbial models of mammalian metabolism. Aromatic hydroxylation. *Archives of Biochemistry and Biophysics, 161*(2), 551-558.

Smith, R. V., & Rosazza, J. P. (1975). Microbial models of mammalian metabolism. *Journal of Pharmaceutical Sciences*, *64*(11), 1737-1759.

Soden, A., Francis, I. L., Oakey, H., & Henschke, P. A. (2000). Effects of co-fermentation with *Candida stellata* and *Saccharomyces cerevisiae* on the aroma and composition of Chardonnay wine. *Australian Journal of Grape and Wine Research*, *6*(1), 21-30.

Solís-González, C. J., Domínguez-Malfavón, L., Vargas-Suárez, M., Gaytán, I., Cevallos, M. Á., Lozano, L., Cruz-Gómez, M. J., Loza-Tavera, H. (2018). Novel metabolic pathway for *N*-methylpyrrolidone degradation in *Alicycliphilus* sp. strain BQ1. *Applied and Environmental Microbiology*, *84*(1).

Sonoki, T., Obi, T., Kubota, S., Higashi, M., Masai, E., & Katayama, Y. (2000). Coexistence of two different *O*-demethylation systems in lignin metabolism by *Sphingomonas paucimobilis* SYK-6: cloning and sequencing of the lignin biphenyl-specific *O*-demethylase (LigX) gene. *Applied and Environmental Microbiology*, *66*(5), 2125-2132.

Sonoki, T., Otsuka, Y., Ikeda, S., Masai, E., Kajita, S., & Katayama, Y. (2002). Tetrahydrofolate-dependent vanillate and syringate *O*-demethylation links tightly to one-carbon metabolic pathway associated with amino acid synthesis and DNA methylation in the lignin metabolism of *Sphingomonas paucimobilis* SYK-6. *Journal of Wood Science*, *48*(5), 434-439.

Stanier, R. Y. (1942). Agar-decomposing strains of the *Actinomyces coelicolor* species-group. *Journal of Bacteriology*, *44*(5), 555.

Stefels, J. (2000). Physiological aspects of the production and conversion of DMSP in marine algae and higher plants. *Journal of Sea Research*, *43*(3-4), 183-197.

Stevens, J. T., & Sumner, D. D. (1991). In *Handbook of pesticide toxicology* (pp .1317-1408). Academic Press, Cambridge, US.

Stocking, A. J., Deeb, R. A., Flores, A. E., Stringfellow, W., Talley, J., Brownell, R., & Kavanaugh, M. C. (2000). Bioremediation of MTBE: a review from a practical perspective. *Biodegradation*, *11*(2-3), 187-201.

Stupp, H. D. (2007). Remediation technologies and costs for cleaning MTBE contaminated groundwater. In *Fuel oxygenates* (pp. 249-273). Springer, Berlin, Heidelberg.

Summers, R. M., Louie, T. M., Yu, C. L., Gakhar, L., Louie, K. C., & Subramanian, M. (2012). Novel, highly specific *N*-demethylases enable bacteria to live on caffeine and related purine alkaloids. *Journal of Bacteriology*, *194*(8), 2041-2049.

Summers, R. M., Seffernick, J. L., Quandt, E. M., Yu, C. L., Barrick, J. E., & Subramanian, M. V. (2013). Caffeine junkie: an unprecedented glutathione *S*-transferase-dependent oxygenase required for caffeine degradation by *Pseudomonas putida* CBB5. *Journal of Bacteriology*, *195*(17), 3933-3939.

Sun, J., Steindler, L., Thrash, J. C., Halsey, K. H., Smith, D. P., Carter, A. E., Landry, Z. C., Giovannoni, S. J. (2011a). One carbon metabolism in SAR11 pelagic marine bacteria. *PloS One*, *6*(8), e23973.

Sun, J. Q., Huang, X., Chen, Q. L., Liang, B., Qiu, J. G., Ali, S. W., & Li, S. P. (2009). Isolation and characterization of three *Sphingobium* sp. strains capable of degrading isoproturon and cloning of the catechol 1, 2-dioxygenase gene from these strains. *World Journal of Microbiology and Biotechnology*, *25*(2), 259-268.

Sun, X., Wang, J., Feng, D., Ma, Z., & Li, H. (2011b). PdCYP51B, a new putative sterol 14α-demethylase gene of *Penicillium digitatum* involved in resistance to imazalil and other fungicides inhibiting ergosterol synthesis. *Applied Microbiology and Biotechnology*, *91*(4), 1107.

Sunda, W. K. D. J., Kieber, D. J., Kiene, R. P., & Huntsman, S. (2002). An antioxidant function for DMSP and DMS in marine algae. *Nature*, *418*(6895), 317-320.

Sutherland, J. B. (1986). Demethylation of veratrole by cytochrome P450 in *Streptomyces setonii*. *Applied and Environmental Microbiology*, *52*(1), 98-100.

Swiegers, J. H., Bartowsky, E. J., Henschke, P. A., & Pretorius, I. S. (2005). Yeast and bacterial modulation of wine aroma and flavour. *Australian Journal of Grape and Wine Research*, *11*(2), 139–173.

Sylvestre, J., Chautard, H., Cedrone, F., & Delcourt, M. (2006). Directed evolution of biocatalysts. *Organic Process Research & Development*, *10*(3), 562-571.

Takken, H. J., Van der Linde, L. M., Boelens, M., & Van Dort, J. M. (1975). Olfactive properties of a number of polysubstituted pyrazines. *Journal of Agricultural and Food Chemistry*, *23*(4), 638-642.

Thanbichler, M., Iniesta, A. A., & Shapiro, L. (2007). A comprehensive set of plasmids for vanillate-and xylose-inducible gene expression in *Caulobacter crescentus*. *Nucleic Acids Research*, *35*(20), e137-e137.

Tian, J. H., Pourcher, A. M., Bouchez, T., Gelhaye, E., & Peu, P. (2014). Occurrence of lignin degradation genotypes and phenotypes among prokaryotes. *Applied Microbiology and Biotechnology*, *98*(23), 9527-9544.

Tinschert, A., Tschech, A., Heinzmann, K., & Kiener, A. (2000). Novel regioselective hydroxylations of pyridine carboxylic acids at position C2 and pyrazine carboxylic acids at position C3. *Applied Microbiology and Biotechnology*, *53*(2), 185-195.

Todd, B. L., Stewart, E. V., Burg, J. S., Hughes, A. L., & Espenshade, P. J. (2006). Sterol regulatory element binding protein is a principal regulator of anaerobic gene expression in fission yeast. *Molecular and Cellular Biology*, *26*(7), 2817-2831.

Todd, J. D., Curson, A. R., Sullivan, M. J., Kirkwood, M., & Johnston, A. W. (2012). The *Ruegeria pomeroyi acuI* gene has a role in DMSP catabolism and resembles *yhdH* of *E. coli* and other bacteria in conferring resistance to acrylate. *PloS One*, *7*(4), e35947.

Tominaga, T., Masneuf-Pomarède, I., & Dubourdieu, D. (1995). A S-cysteine conjugate, precursor of aroma of white Sauvignon. *Oeno One*, *29*(4), 227-232.

Tominaga, T., Peyrot des Gachons, C., & Dubourdieu, D. (1998). A New Type of Flavor Precursors in *Vitis vinifera* L. *cv*. Sauvignon Blanc: S-Cysteine Conjugates. *Journal of Agricultural and Food Chemistry*, *46*(12), 5215-5219.

Treloar, J. D., & Howell, G. S. (2006). Influence of yeast and malolactic bacteria strain choice on 3-isobutyl-2-methoxypyrazine concentration in Cabernet Sauvignon and Franc

wines. In *Wine Making Workshop, Vegetable & Farm Market EXPO, Great Lakes Fruit, Grand Rapids, MI, USA: <http://www.glexpo.com/abstracts/2006abstracts/WineMaking2006.pdf.*

Tristezza, M., Tufariello, M., Capozzi, V., Spano, G., Mita, G., & Grieco, F. (2016). The oenological potential of *Hanseniaspora uvarum* in simultaneous and sequential co-fermentation with *Saccharomyces cerevisiae* for industrial wine production. *Frontiers in Microbiology*, *7*, 670.

Trojanowski, J., Haider, K., & Sundman, V. (1977). Decomposition of 14 C-labelled lignin and phenols by a *Nocardia* sp. *Archives of Microbiology*, *114*(2), 149-153.

Tsang, H. T., Batie, C. J., Ballou, D. P., & Penner-Hahn, J. E. (1989). X-ray absorption spectroscopy of the [2-iron-2-sulfur] Rieske cluster in *Pseudomonas cepacia* phthalate dioxygenase. Determination of core dimensions and iron ligation. *Biochemistry*, *28*(18), 7233-7240.

Uchida, A., Ogawa, M., Yoshida, T., & Nagasawa, T. (2003). Quinolinate dehydrogenase and 6-hydroxyquinolinate decarboxylase involved in the conversion of quinolinic acid to 6-hydroxypicolinic acid by *Alcaligenes* sp. strain UK21. *Archives of Microbiology*, *180*(2), 81-87.

Urbina, J. A., Payares, G., Molina, J., Sanoja, C., Liendo, A., Lazardi, K., Piras, M. M., Piras, R., Perez, N., Wincker, P., Ryley, J. F. (1996). Cure of short-and long-term experimental Chagas' disease using D0870. *Science*, *273*(5277), 969-971.

Urbina, J. A., Payares, G., Contreras, L. M., Liendo, A., Sanoja, C., Molina, J., Piras, M., Piras, R., Perez, N., Wincker, P., Loebenberg, D. (1998). Antiproliferative effects and mechanism of action of SCH 56592 against *Trypanosoma* (*Schizotrypanum*) *cruzi*: *in vitro* and *in vivo* studies. *Antimicrobial Agents and Chemotherapy*, *42*(7), 1771-1777.

Vallarino, J. G., Gainza-Cortés, F., Verdugo-Alegría, C., González, E., & Moreno, Y. M. (2014). Abiotic stresses differentially affect the expression of *O*-methyltransferase genes related to methoxypyrazine biosynthesis in seeded and parthenocarpic fruits of *Vitis vinifera* (L.). *Food Chemistry*, *154*, 117-126.

Vallarino, J. G., López-Cortés, X. A., Dunlevy, J. D., Boss, P. K., González-Nilo, F. D., & Moreno, Y. M. (2011). Biosynthesis of methoxypyrazines: elucidating the structural/functional relationship of two *Vitis vinifera O*-methyltransferases capable of

catalyzing the putative final step of the biosynthesis of 3-alkyl-2-methoxypyrazine. *Journal of Agricultural and Food Chemistry*, *59*(13), 7310-7316.

van Breda, V., Jolly, N., & van Wyk, J. (2013). Characterisation of commercial and natural *Torulaspora delbrueckii* wine yeast strains. *International Journal of Food Microbiology*, *163*(2-3), 80-88.

van der Walt, J. P., & van Kerken, A. E. (1959). The wine yeasts of the Cape. *Antonie van Leeuwenhoek*, *25*(1), 449-457.

Van Nistelrooy, J. G. M., Van den Brink, J. M., Van Kan, J. A. L., Van Gorcom, R. F. M., & De Waard, M. A. (1996). Isolation and molecular characterisation of the gene encoding eburicol 14α-demethylase (CYP51) from *Penicillium italicum*. *Molecular and General Genetics MGG*, *250*(6), 725-733.

Varela, C., Siebert, T., Cozzolino, D., Rose, L., McLean, H., & Henschke, P. A. (2009). Discovering a chemical basis for differentiating wines made by fermentation with 'wild' indigenous and inoculated yeasts: role of yeast volatile compounds. *Australian Journal of Grape and Wine Research*, *15*(3), 238-248.

Vasundhara, T. S., & Parihar, D. B. (1980). Studies in pyrazines formed in roasted spices*:* *Coriandrum sativum*, *Cuminum cyminum* and *Trigonella foenum-graecum*. *Food/Nahrung*, *24*(7), 645-651.

Vejarano, R. (2018). *Saccharomycodes ludwigii*, control and potential uses in winemaking processes. *Fermentation*, *4*(3), 71.

Venkatesagowda, B. (2019). Enzymatic demethylation of lignin for potential biobased polymer applications. *Fungal Biology Reviews*, *33*(3-4), 190-224.

Venkateswarlu, K., & Kelly, S. L. (1997). Stereoselective interaction of SCH 39304, a triazole, with sterol 14 alpha-demethylase of *Aspergillus fumigatus*. *The Journal of Antimicrobial Chemotherapy*, *39*(5), 597-601.

Venturi, V., Zennaro, F., Degrassi, G., Okeke, B. C., & Bruschi, C. V. (1998). Genetics of ferulic acid bioconversion to protocatechuic acid in plant-growth-promoting *Pseudomonas putida* WCS358. *Microbiology*, *144*(4), 965-973.

Vernin, G., & Vernin, G. (1982). Heterocyclic aroma compounds in foods: occurrence and organoleptic properties. *Chemistry of Heterocyclic Compounds in Flavours and Aromas*, 92-97.

Vieböck, F., & Brecher, C. (1930). Eine neue Methode zur massanlytischen Bestimmung deer Methoxyl- und Athoxylgruppe II. Mikro-Analyse. *Ber Dtsch Chem Ges*, 63, 3207-3210。

Vieböck, F., & Schwappach, A. (1930). Eine neue Methode zur maßanalytischen Bestimmung der Methoxyl-und Äthoxylgruppe. *Berichte der deutschen chemischen Gesellschaft (A and B Series)*, *63*(10), 2818-2823.

Vila-Costa, M., Simó, R., Harada, H., Gasol, J. M., Slezak, D., & Kiene, R. P. (2006). Dimethylsulfoniopropionate uptake by marine phytoplankton. *Science*, *314*(5799), 652-654.

Villamor, R. R., Evans, M. A., Mattinson, D. S., & Ross, C. F. (2013). Effects of ethanol, tannin and fructose on the headspace concentration and potential sensory significance of odorants in a model wine. *Food Research International*, *50*(1), 38-45.

Wang, J., Capone, D. L., Wilkinson, K. L., & Jeffery, D. W. (2016). Chemical and sensory profiles of rosé wines from Australia. *Food Chemistry*, *196*, 682-693.

Wang, J., Hirai, H., & Kawagishi, H. (2012). Biotransformation of acetamiprid by the white-rot fungus *Phanerochaete sordida* YK-624. *Applied Microbiology and Biotechnology*, *93*(2), 831-835.

Wang, X., Li, B., Herman, P. L., & Weeks, D. P. (1997). A Three-Component Enzyme System Catalyzes the *O*-Demethylation of the Herbicide Dicamba in *Pseudomonas maltophilia* DI-6. *Applied and Environmental Microbiology*, *63*(4), 1623-1626.

Wass, M. N., Kelley, L. A., & Sternberg, M. J. (2010). 3DLigandSite: predicting ligand-binding sites using similar structures. *Nucleic Acids Research*, *38*(suppl_2), W469-W473.

Wegkamp, A., Teusink, B., De Vos, W. M., & Smid, E. J. (2010). Development of a minimal growth medium for *Lactobacillus plantarum*. *Letters in Applied Microbiology*, *50*(1), 57-64.

White, P. A., & Rasmussen, J. B. (1998). The genotoxic hazards of domestic wastes in surface waters. *Mutation Research/Reviews in Mutation Research*, *410*(3), 223-236.

Whitehouse, L. W., Lodge, B. A., & Thomas, B. H. (1987). Metabolic disposition of pyrazinamide in the rat: identification of a novel *in vivo* metabolite common to both rat and human. *Biopharmaceutics & Drug Disposition*, *8*(4), 307-318.

Wieser, M., Heinzmann, K., & Kiener, A. (1997). Bioconversion of 2-cyanopyrazine to 5-hydroxypyrazine-2-carboxylic acid with *Agrobacterium* sp. DSM 6336. *Applied Microbiology and Biotechnology*, *48*(2), 174-176.

Wilson, D. S., & Keefe, A. D. (2000). Random mutagenesis by PCR. *Current Protocols in Molecular Biology*, *51*(1), 8-3.

Winterton, N. (2000). Chlorine: the only green element–towards a wider acceptance of its role in natural cycles. *Green Chemistry*, *2*(5), 173-225.

Wood, V., Gwilliam, R., Rajandream, M. A., Lyne, M., Lyne, R., Stewart, A., Sgouros, J., Peat, N., Hayles, J., Baker, S., Basham, D., Bowman, S., Brooks, K., Brown, D., Brown, S., Chillingworth, T., Churcher, C., Collins, M., Connor, R., Cronin, A., Davis, P., Feltwell, T., Fraser, A., Gentles, S., Goble, A., Hamlin, N., Harris, D., Hidalgo, J., Hodgson, G., Holroyd, S., Nurse, P. (2002). The genome sequence of *Schizosaccharomyces pombe*. *Nature*, *415*(6874), 871-880.

Woolfolk, C. A. (1975). Metabolism of *N*-methylpurines by a *Pseudomonas putida* strain isolated by enrichment on caffeine as the sole source of carbon and nitrogen. *Journal of Bacteriology*, *123*(3), 1088-1106.

Woolfson, A., & Rothschild, M. (1990). Speculating about pyrazines. *Proceedings of the Royal Society of London B: Biological Sciences*, *242*(1304), 113-119.

Wu, X., Tian, Z., Jiang, X., Zhang, Q., & Wang, L. (2018). Enhancement in catalytic activity of *Aspergillus niger* XynB by selective site-directed mutagenesis of active site amino acids. *Applied Microbiology and Biotechnology*, *102*(1), 249-260.

Xi, W., Fang, B., Zhao, Q., Jiao, B., & Zhou, Z. (2014). Flavonoid composition and antioxidant activities of Chinese local pummelo (*Citrus grandis Osbeck*.) varieties. *Food Chemistry*, *161*, 230-238.

Xiao, J., Muzashvili, T. S., & Georgiev, M. I. (2014). Advances in the biotechnological glycosylation of valuable flavonoids. *Biotechnology Advances*, *32*(6), 1145–1156.

Xiao, J. B., & Högger, P. (2015). Dietary polyphenols and type 2 diabetes: current insights and future perspectives. *Current Medicinal Chemistry*, *22*(1), 23-38.

Xiao, J., Ni, X., Kai, G., & Chen, X. (2015). Advance in dietary polyphenols as aldose reductases inhibitors: structure-activity relationship aspect. *Critical Reviews in Food Science and Nutrition*, *55*(1), 16-31.

Xu, K. Z., Wang, H. R., Wang, Y. J., Xia, J., Ma, H., Cai, Y. J., Liao, X. R., Guan, Z. B. (2019a). Enhancement in catalytic activity of CotA-laccase from *Bacillus pumilus* W3 via site-directed mutagenesis. *Journal of Bioscience and Bioengineering*.

Xu, W., Peng, J., Zhang, W., Zhang, T., Guang, C., & Mu, W. (2019b). Enhancement of the *Brenneria* sp. levansucrase thermostability by site-directed mutagenesis at Glu404 located at the "-TEAP-" residue motif. *Journal of Biotechnology*, *290*, 1-9.

Yamamoto, T., Moriwaki, Y., Takahashi, S., Hada, T., & Higashino, K. (1987). *In vitro* conversion of pyrazinamide into 5-hydroxypyrazinamide and that of pyrazinoic acid into 5-hydroxypyrazinoic acid by xanthine oxidase from human liver. *Biochemical Pharmacology*, *36*(19), 3317-3318.

Yang, J., Roy, A., & Zhang, Y. (2013a). Protein–ligand binding site recognition using complementary binding-specific substructure comparison and sequence profile alignment. *Bioinformatics*, *29*(20), 2588-2595.

Yang, J., Roy, A., & Zhang, Y. (2013b). BioLiP: a semi-manually curated database for biologically relevant ligand–protein interactions. *Nucleic Acids Research*, *41*(D1), D1096-D1103.

Yang, J., Yan, R., Roy, A., Xu, D., Poisson, J., & Zhang, Y. (2015). The I-TASSER Suite: protein structure and function prediction. *Nature Methods*, *12*(1), 7-8.

Yang, J., & Zhang, Y. (2015). I-TASSER server: new development for protein structure and function predictions. *Nucleic Acids Research*, *43*(W1), W174-W181.

Yao, L., Jia, X., Zhao, J., Cao, Q., Xie, X., Yu, L., He, J., Tao, Q. (2015). Degradation of the herbicide dicamba by two *Sphingomonads* via different *O*-demethylation mechanisms. *International Biodeterioration & Biodegradation*, *104*, 324-332.

Yao, L., Yu, L. L., Zhang, J. J., Xie, X. T., Tao, Q., Yan, X., Hong, Q., Qiu, J. G., Ding, D. R. (2016). A tetrahydrofolate-dependent methyltransferase catalyzing the demethylation of dicamba in *Sphingomonas* sp. strain Ndbn-20. *Applied and Environmental Microbiology*, *82*(18), 5621-5630.

Yao, S., Chen, L., Yang, Z., Yao, L., Zhu, J., Qiu, J., Wang, G., He, J. (2019). The properties of 5-methyltetrahydrofolate dehydrogenase (MetF1) and its role in the tetrahydrofolate-dependent dicamba demethylation system in *Rhizorhabdus dicambivorans* Ndbn-20. *Journal of Bacteriology*, *201*(17), e00096-19.

Yatome, C., Yamada, S., Ogawa, T., & Matsui, M. (1993). Degradation of crystal violet by *Nocardia corallina*. *Applied Microbiology and Biotechnology*, *38*(4), 565-569.

Yoch, D. C. (2002). Dimethylsulfoniopropionate: its sources, role in the marine food web, and biological degradation to dimethylsulfide. *Applied and Environmental Microbiology*, *68*(12), 5804-5815.

Youngster, L. K., Somsamak, P., & Häggblom, M. M. (2008). Effects of co-substrates and inhibitors on the anaerobic *O*-demethylation of methyl *tert*-butyl ether (MTBE). *Applied Microbiology and Biotechnology*, *80*(6), 1113-1120.

Yuan, J. H., Goehl, T. J., Murrill, E., Moore, R., Clark, J., Hong, L., & Irwin, R. (1993). Toxicokinetics of pentachloroanisole in F344 rats and B6C3F1 mice. *Xenobiotica*, *23*(4), 427-438.

Zeisel, S. (1885). Über ein Verfahren zum quantitativen Nachweise von Methoxyl. *Monatshefte für Chemie und verwandte Teile anderer Wissenschaften*, *6*(1), 989-997.

Zeisel S, Fanto R (1902) Neues Verfahren zur Bestimmung des Glycerins. Z Landw Vers-Wes Ost 5:729-745

Zeisel, S., & Fanto, R. (1903). Bestimmung des Rohglycerins im Weine mittelst der "Jodidmethode". *Zeitschrift für analytische Chemie*, *42*(9-10), 549-578.

Zezula, J., & Hudlicky, T. (2005). Recent progress in the synthesis of morphine alkaloids. *Synlett*, *2005*(03), 388-405.

Zha, D., Eipper, A., & Reetz, M. T. (2003). Assembly of designed oligonucleotides as an efficient method for gene recombination: a new tool in directed evolution. *ChemBioChem*, *4*(1), 34-39.

Zhang, B. Q., Luan, Y., Duan, C. Q., & Yan, G. L. (2018). Use of *Torulaspora delbrueckii* co-fermentation with two *Saccharomyces cerevisiae* strains with different aromatic characteristic to improve the diversity of red wine aroma profile. *Frontiers in Microbiology*, *9*, 606.

Zhang, H. Z., Gan, L. L., Wang, H., & Zhou, C. H. (2017). New progress in azole compounds as antimicrobial agents. *Mini Reviews in Medicinal Chemistry*, *17*(2), 122-166.

Zhang, J., Li, L., Lv, Q., Yan, L., Wang, Y., & Jiang, Y. (2019). The fungal CYP51s: Their functions, structures, related drug resistance, and inhibitors. *Frontiers in Microbiology*, *10*, 691.

Zhao, H., Giver, L., Shao, Z., Affholter, J. A., & Arnold, F. H. (1998). Molecular evolution by staggered extension process (StEP) *in vitro* recombination. *Nature Biotechnology*, *16*(3), 258-261.

Zhao, H., & Arnold, F. H. (1999). Directed evolution converts subtilisin E into a functional equivalent of thermitase. *Protein Engineering*, *12*(1), 47-53.

Zott, K., Thibon, C., Bely, M., Lonvaud-Funel, A., Dubourdieu, D., & Masneuf-Pomarede, I. (2011). The grape must non-*Saccharomyces* microbial community: impact on volatile thiol release. *International Journal of Food Microbiology*, *151*(2), 210-215.

Zubieta, C., He, X. Z., Dixon, R. A., & Noel, J. P. (2001). Structures of two natural product methyltransferases reveal the basis for substrate specificity in plant *O*-methyltransferases. *Nature Structural Biology, 8*(3), 271.

Zubieta, C., Kota, P., Ferrer, J. L., Dixon, R. A., & Noel, J. P. (2002). Structural basis for the modulation of lignin monomer methylation by caffeic acid/5-hydroxyferulic acid 3/5-*O*-methyltransferase. *The Plant Cell*, *14*(6), 1265-1277.